Investigation on the production of secondary metabolites from anoxygenic phototrophic bacteria.

Dissertation

Zur Erlangung des Doktorgrades

der Mathematisch-Naturwissenschaftlichen Fakultät

der Christian-Albrechts-Universität zu Kiel

Vorgelegt von

Min Sun

Kiel 2015

Referent: Prof. Dr. Johannes F. Imhoff

Korreferentin: Prof. Dr. Ute Hentschel-Humeida

Tag der mündlichen Prüfung: 19.02.2016

Zum Druck genehmigt: Ja

gez. Prof. Dr. Johannes F. Imhoff

This present work was carried out at the GEOMAR Helmholtz Centre for Ocean Research Kiel Christian-Albrechts-University of Kiel from August 2011 to August 2015 under the supervision of Prof. Dr. Johannes F. Imhoff.

Scientific contribution

All the strains used in this studied were offered by Prof. Dr. Johannes F. Imhoff. *Allochromatium vinosum* strain MT86 was isolated and identified by Dr. Marcus Tank. All bioassays of crude extracts, fractions and pure compounds were done by Arlette Wenzel-Storjohann (Marine Natural Products, GEOMAR). NMR measurement was performed at the Otto-Diels Institute of Organic Chemistry (Christian-Albrechts University of Kiel) and NMR data analysis was analysis by the assistance of Dr. Bin Wu (Zhejiang University, China) and Prof. Dr. Alex Zeeck (BioViotica Naturstoffe GmbH, Götingen). Prof. Dr. Alex Zeeck did the TLC and IR, CD, and polarimetry measurements.

All other experiments were done by Min Sun under supervision of Prof. Dr. Johannes F. Imhoff at GEOMAR Marine Microbiology Department.

Erklärung

Hiermit erkläre ich, dass ich die vorliegende Arbeit unter Einhaltung der Regeln guter wissenschaftlicher Praxis der Deutschen Forschungsgesellschaft verfasst habe, und dass sie nach Form und Inhalt meine eigene Arbeit ist. Außer den angegebenen Quellen und Hilfsmitteln wurden keine weiteren verwendet. Sie wurde keiner anderen Stelle im Rahmen eines Prüfungsverfahrens vorgelegt. Dies ist mein erstes und bisher einziges Promotionsverfahren.

Min Sun

Kiel, den 15. 12. 2015

Table of contents

List of Figures

List of Tables

Abbreviations

%	percent
°C	degree Celsius
µl	micro liter
µm	micro meter
$[\alpha]_D^{25}$	specific rotatory power; sodium D-line (589 nm); 25 °C
aa	amino acid
A	adenylation
AAPB	aerobic anoxygenic phototrophic bacteria
Abb.	abbreviation
AchE	acetylcholinesterase
Acc.-No	accession number
ACN	acetonitrile
ACP	acyl carrier protein
ADC	antibody drug conjugate
antiSMASH	Antibiotics & Secondary Metabolite Analysis SHell
APB	anoxygenic phototrophic bacteria
AT	acyl transferase
ATP	adenosine triphosphate
Bs	*Bacillus subtillis*
Bchl	bacteriochlorophyll
BLASTn	Nucleotide Basic Local Alignment Search Tool
bp	base pairs
Ca	*Candida albicans*
ca.	circa
$CaCl_2$	calcium chloride
calcd.	calculated
CD	circular dichroism
CO_2	carbon dioxide
CoA	coenzyme A
COSY	correlation spectroscopy
CYC	cyclase
d	common difference
d	doublet
DAD	diode-array-detector
dd	doublet of doublets
ddd	doublet of doublet of doublets
ddH_2O	double-distilled Water
ddt	doublet of doublet of triplets
demin. water	demineralized water
DEPT	distortionless enhancement by polarization transfer
DH	dehydratase
DMSO	dimethyl sulfoxide
DNA	desoxyribonucleic acid
DNPs	Dictionary of Natural Products
DSMZ	Deutsche Sammlung von Microorganismen und Zellkulturen, German collection of microorganisms and cell cultures
dt	doublet of triplets
Ec	*Escherichia coli*
e. g.	exampli gratia (Latin), for example
EDTA	ethylene diamine tetraacetate
EDTA-Na_2	ethylene diamine tetraacetate-Na_2
EGFR	epidermal growth factor receptor

ENPP3	ectonucleotide pyrophosphatase/phosphodiesterase family member 3
ER	enoyl reductase
ESI	electrospray ionisation
ESIMS	electrospray ionization mass spectrometry
ETBR	endothelin B receptor
EtOAc	ethyl acetate
EtOH	ethanol
FDA	Food and Drug Administration
GCC	guanylyl cyclase C
GNSB	green nonsulfur bacteria
GPNMB	glycoprotein nonmetastatic B
GSB	green sulfur bacteria
GSK-3β	glykogensynthase-kinase 3
HMBC	heteronuclear multiple bond correlation
HPLC	high performance liquid chromatography
HPLC-DAD/MS	HPLC-diode array detection-mass spectrometry
HRESI-MS	high resolution electron spray ionization mass spectra
HSQC	heteronuclear single quantum cohenrence
Hz	Hertz
IC_{50}	half maximal inhibitory concentration
IR	infrared spectroscopy
J	spin-spin coupling constant
JGI	DOE Joint Genome Institute
JNK	c-Jun N-terminal protein kinases
KR	ketoreductase
KS	ketosynthase
LIV-1	zinc transporter SLC39A6
m	meter
m	multiplet
max	maxima
MeOD	methanol with D element
MeOH	methanol
mg	milligram
MHz	megahertz
Milli-Q water	deionized water was purified by Milli-Q system
mM	mill molar
MMAE	monomethyl auristatin E
MMAF	monomethyl auristatin F
MNPs	marine natural products
MRSA	methicillin-resistant *Staphylococcus aureus*
MS	mass spectrometry
MW	molecular weight
NA	not available
NaPi2b	sodium-dependent phosphate transport protein 2b
NCBI	National Center for Biotechnology Information
NITE	National Institute of Technology and Evaluation
nm	nano meter
NMR	nuclear magnetic resonance
NOESY	nuclear overhouser enhancement spectroscopy
NPs	natural products
NRPS	nonribosomal peptide synthetase
nt	nucleotide
OD_{600}	optical density at 600 nm
PBS	phosphate buffered saline

PCR	polymerase chain reaction
Pf medium	Pfennig's medium
PKS	polyketide synthase
PNSB	purple nonsulfur bacteria
ppm	parts per million
PSB	purple sulfur bacteria
PSMA	prostate-specific membrane antigen
PTFE	polytetrafluoroethylene
RAC1	Ras-related C3 botulinum toxin substrate 1
RDP-II	the Ribosomal Database Project II
RP	reversed phase
rpm	rotation per minute
Rt	retention time
sh	shoulder
Sl	*Staphylococcus lentus*
SCUBA	self-contained underwater breathing apparatus
SLITRK6	SLIT and NTRK-like protein 6
sp.	species
STEAP1	anti-six transmembrane epithelial antigen of the prostate 1
T	temperature
td	triplet of doublets
TE	thioesterase
TBE	Tris-Borat-EDTA
TLC	thin layer chromatograph
TSB	tryptic soy broth
UV	ultraviolet
V	volt
Xc	*Xanthomonas campestris*
δ	NMR chemical shift [ppm]

Chemicals used in this study

Formula/name	**IUPA name**	**Company**
$(CH_3COO)_2Mg \cdot 4H_2O$	Magnesium acetate tetrahydrate; Mg-acetate	Merck
$C_2H_3NaO_2$	Sodium acetate; Na-acetate	Roth
$C_3H_3NaO_3$	Pyruvic acid sodium salt; Na-pyruvate	Roth
$C_{63}H_{88}O_{14}N_{14}PCo$	Vitamin B_{12}	Merck
$C_6H_7NaO_6$	Na-ascorbate L(+)-ascorbic acid sodium salt	Fluka
$CaCl_2 \cdot 2H_2O$	Calcium chloride dihydrate	Merck
CH_3CH_2OH	Ethanol 99 %	Walter CMP
CH_3CN	Acetonitril (HPLC gradient grade)	VWR Prolabo
$CH_3COOCH_2CH_3$	Ethyl acetate	Roth
CH_3COONH_4	Ammonium acetate	Roth
$CoCl_2 \cdot 6H_2O$	Cobalt(II) chloride hexahydrate	Merck
$CuCl_2 \cdot 2H_2O$	Copper(II) chloride dihydrate	Merck
EDTA/$C_{10}H_{16}N_2O_8$	Ethylene diamine tetraacetate	Merck
EDTA-Na_2	Ethylene diamine tetraacetate-Na_2	Roth
$FeCl_2 \cdot 4H_2O$	Iron(II) chloride tetrahydrate	Sigma
$FeSO_4 \cdot 7H_2O$	Iron(II) sulfate heptahydrate, ferrous sulfate	Sigma
H_3BO_3	Trihydroxidoboron, Boric acid	Roth
KCl	Potassium chloride	Merck
KH_2PO_4	Potassium dihydrogen phosphate	Merck
Methanol/ CH_3OH	HPLC gradient grade	Roth
Methanol-d_4/ CD_3OD	99.8 Atom % D	Roth
$MgCl_2 \cdot 6H_2O$	Magnesium chloride hexahydrate	Roth
$MgSO_4 \cdot 7H_2O$	Magnesium sulfate heptahydrate	Merck
$MnCl_2 \cdot 7H_2O$	Manganese(II) chloride heptahydrate	Merck
$Na_2MoO_4 \cdot 2H_2O$	Sodium molybdate	Merck
$Na_2S \cdot 9H_2O$	Sodium sulfide nonahydrate	Sigma
$Na_2S_2O_3 \cdot 5H_2O$	Sodium thiosulfate pentahydrate	Merck
Na_2SO_4	Sodium sulfate anhydrous	Roth
NaCl	Sodium chloride	Roth
$NaHCO_3$	Sodium bicarbonate	Sigma-Aldrich
$NH_4C_2H_3O_2$	Ammonium acetate, NH_4-Acetate	Roth
NH_4Cl	Ammonium chloride	Merck
$NiCl_2 \cdot 6H_2O$	Nickel(II) chloride	Sigma
Tris/$C_4H_{11}NO_3$	2-Amino-2-hydroxymethyl-propane-1,3-diol	Roth
$ZnCl_2$	Zinc chloride	Merck

1 INTRODUCTION

1.1 Natural products

1.1.1 Definition

Natural products are a huge and diverse group of chemical compounds produced by living creatures from nature (Porter, 1913) (http://www.thefreedictionary.com/natural+product). They can be extracted from plants and animals, from cells or tissues, from microorganisms (bacteria, fungi) or their excreted metabolites (Strobel and Daisy, 2003) and may have notable biological activity for using as phamaceuticals.

Natural products include flavonoids, alkaloids (quinine, ephedrine, chelerythrine etc.), polysaccharides, volatiles oils, quinonoids, terpenoids, waxes, coumarins, saponins, cardiac glycosides from plants, but also monosaccharides, oligosaccharides, polysaccharides, phenylpropanoids, amino acids (L-glutamic acid, L-lysine), antibiotics (streptomycin), pigments (cytochrome C), polypeptides, vitamins, organic acids, phenols, lactones, steroids, tannins, and other naturally occurring chemicals from microorganisms and their fermentation broths. About 50% of the drugs introduced into the market in the last 20 years were traced back to natural products or derivatives thereof. Several reviews and reports have discussed this significant role of natural products in drug discovery (Newman *et al.*, 2000; Newman *et al.*, 2003; Chin *et al.*, 2006; Koehn and Carter, 2005; Paterson and Anderson, 2005).

1.1.2 Category

In the field of organic chemistry, natural products can be defined into primary metabolites and secondary metabolites. Primary metabolites are deemed essential to the survival of organism in maintaining basic metabolic pathways that are required for life. They are associated with significant cellular functions such as nutrient assimilation, energy production, and growth/development and propagation. Primary metabolites include carbohydrates, lipids, amino acids (Kliebenstein, 2004; Karlovsky, 2008), and nucleic acids which are typically produced during the active growth phase.

Many primary metabolites and fermentation products are used in industrial microbiology for large-scale fermentation production like beer and wine, amino acids including L-glutamate and L-lysine, citric acid that are used in mass marketing production as ingredients in food production and pharmaceutical and cosmetic industries.

Secondary metabolites have an extrinsic function that in particular affects other organisms. Secondary metabolites are organic compounds in many cases formed at the end of stationary phase of growth. In contrast to primary metabolites, secondary metabolites are small molecules that are dispensable and not required for sustaining life. However, they increase the competitiveness of the producer within its environment with the ability of biochemical and signal transduction pathways modulations. Secondary

metabolites have a broad range of functions. These include pheromones (act as social signalling molecules), communication molecules, and competitive biological weapons (repellents, venoms, toxins etc.).

A restrictive definition limiting natural products to secondary metabolites is commonly used within the fields of medicinal chemistry and pharmacognosy. These metabolites can be used in industrial microbiology to obtain amino acids, develop vaccines and antibiotics, and isolate chemicals necessary for organic synthesis. General structural classes of secondary metabolites include alkaloids, phenylpropanoids, polyketides, and terpenoids. Examples of important secondary metabolites are antibiotics such as the antibiotic bacitracin (Figure 1-1), which is synthesized in nature by a nonribosomal peptide synthetase and the antimicrobial erythromycin (Figure 1-2), which derived from *Saccharopolyspora erythraea*.

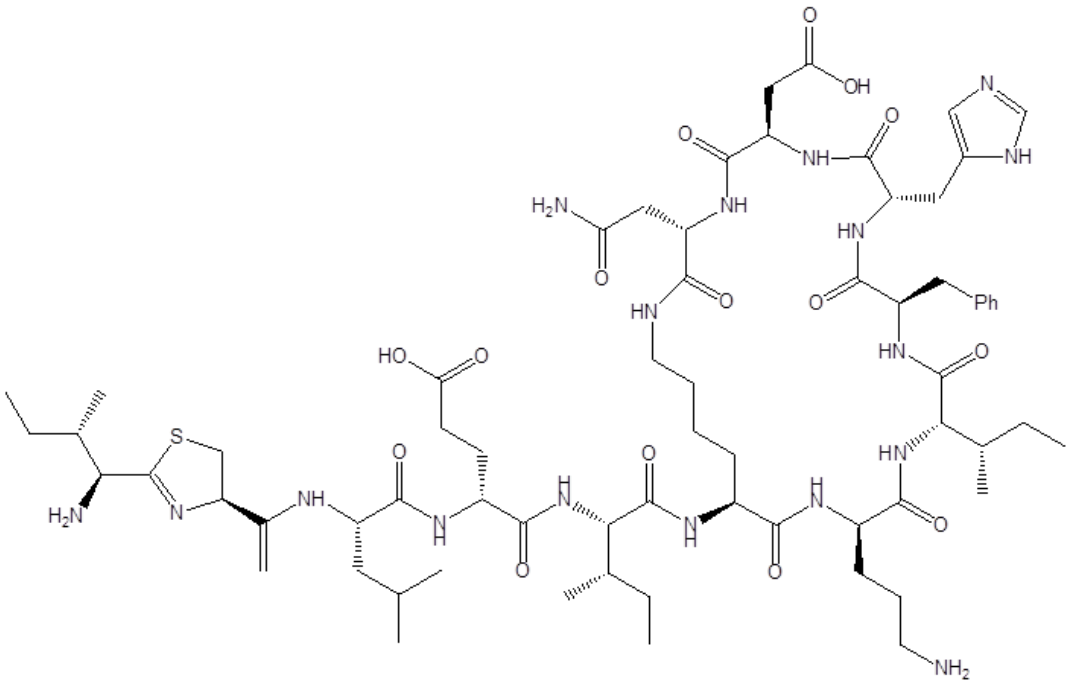

Figure 1-1. Structure of bacitracin.

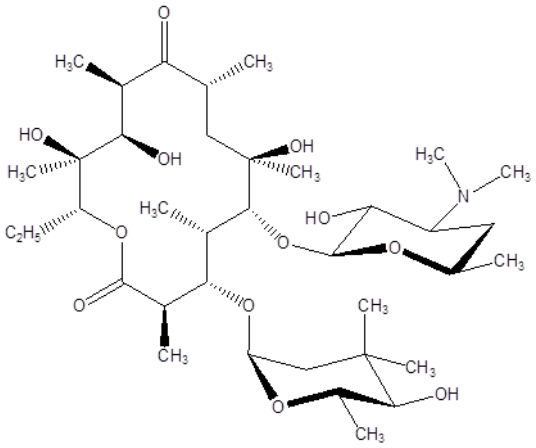

Figure 1-2. Structure of erythromycin.

Until the early 20th century, treatments of infections were based primarily on traditional folklore medicine. Such mixtures with antimicrobial properties that were used in treatments of infections were described over 2000 years ago. In the ancient Egyptian and ancient Greek cultures (Lindblad, 2008), specially selected molds and plant materials and their extracts were used to treat infections (Wainwright, 1989; Shah, 2011; Forrest, 1982).

In 1928, Alexander Fleming, a Scottish microbiologist, identified a compound derived from the fungus *Penicillium chrysogenum* and demonstrated its antibacterial activity (Newman *et al.*, 2000). He named the compound penicillin. Later in 1942, Howard Florey and Ernst Boris Chain succeeded in purifying the first antibiotic of the penicillin class, penicillin G (Figure 1-3 and Figure 1-4). Penicillin displayed potent antibacterial activity against a wide range of bacteria and had low toxicity in humans. Further, Dorothy Crowfoot Hodgkin determined the chemical structure in 1945. For the successful development of penicillin, as a therapeutic drug in clinic application, Ernst Chain and Howard Florey and Alexander Fleming shared the 1945 Nobel Prize in Medicine.

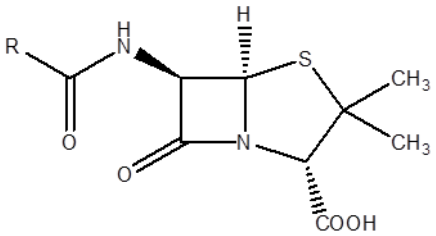

Figure 1-3. Structure of penicillin.

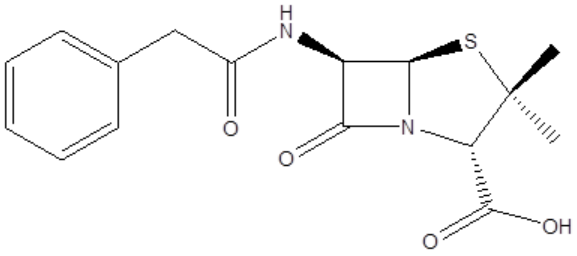

Figure 1-4. Structure of penicillin G.

Another example of a successful antibiotic drug is streptomycin which is derived from *Actinomyces griseus* (later changed the name to *Streptomyces griseus* in 1943) isolated by Selman Waksman's group from soil and water samples (Schatz *et al.*, 1944). It is an important antibiotic agent to treat a variety of infectious diseases. Selman Waksman was awarded the 1952 Nobel Prize in physiology or medicine for the discovery of streptomycin as the first antibiotic effective against tuberculosis.

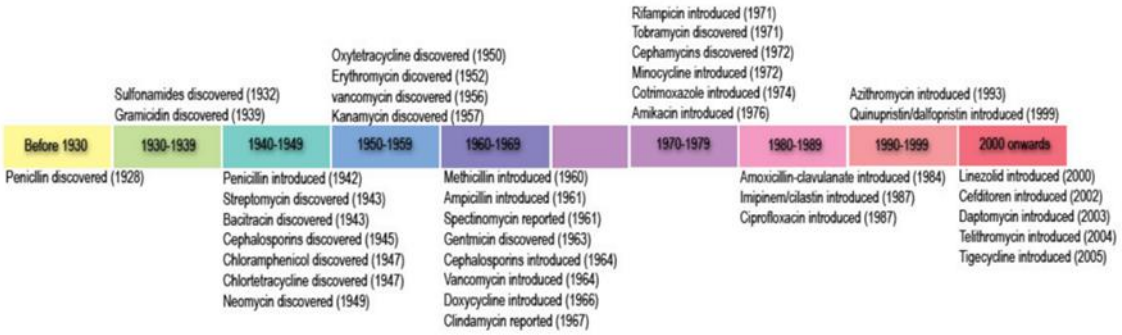

From: http://amrls.cvm.msu.edu/pharmacology/historical-perspectives/the-golden-age-of-antibacterials

Figure 1-5. The history of the golden age of antibiotics.

The serendipitous discovery and subsequent clinical successes of penicillin and streptomycin prompted a large-scale search for other microorganisms that might produce pharmacologically active natural products with anti-infective properties. The following decade are known as the 'Golden Age of Antibiotics' (Figure 1-5), the time period from the 1940s to the 1970s in which most of the modern drugs were discovered.

About 200,000 natural compounds are currently known until 2005 (Tulp and Bohlin, 2005). The chemical diversity of natural compounds represents a basis for their use in drug therapy. Some show antibacterial activities (β-lactams, aminoglycosides), antifungal activities (lipopeptides, non-lipoeptides), antimalarial (nucleoside analogues, HIV protease inhibitors), and some are enzyme inhibitors which can be used to treat cardiovascular (the β-adrenergic amines, cholesterol lowering

agents, angiotensin converting enzyme inhibitors (ACE inhibitors), pain and central nervous system (the opiates, the conotoxins, the epibatidines).

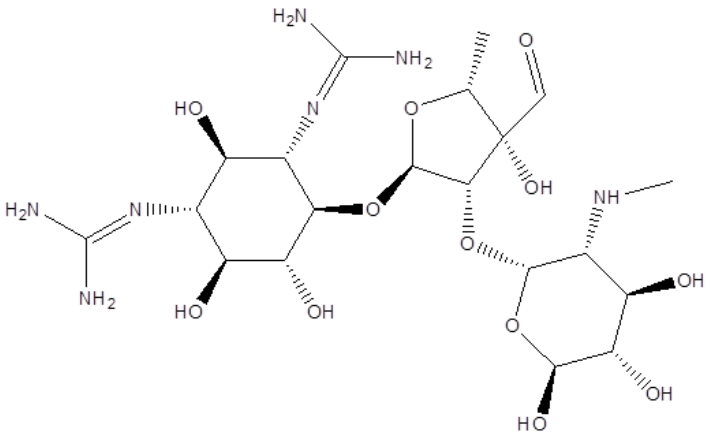

Figure 1-6. The structure of streptomycin.

About 50% of the drugs introduced into the market during the last 20 years are derived directly or indirectly from natural products (Vuorela *et al.*, 2004). Even a high percentage of pharmaceuticals are products of synthetic chemistry, natural products have by no means forfeited their importance as a source of new drugs. During the period from 1981 to 2006, 68% of anti-infectives and 63% of drugs used in cancer treatment were derived from natural products (Newman and Cragg, 2007).

1.2 Marine natural products

Secondary metabolites, in limited consideration, are thought to have specific functions in interrelationships between microorganisms and are produced under specific environmental conditions. Throughout the long time period of human history, traditional pharmacognosy mainly focused on the investigation and identification of medically important plants and animals in the terrestrial environment. Due to the increasing infectious resistance, available treatments for many diseases became limited. In addition, diseases caused by viral pathogens have demonstrated the need for new medicines. Today, many scientists focus the research for new drugs to the oceans. The oceans cover more than 70% of the earth's surface and have more biological and chemical diversity and higher probability of yielding natural products with unprecedented carbon skeletons than that in terrestrial environments.

Marine sources may contain over 80% of the world's animal species (Chakraborty *et al.*, 2009) and account for 90% of biomass of the earth's total biomass. Since the organisms first appeared in the sea over 3.5 billion years ago, they developed numerous mechanisms to survive various harsh conditions in marine environments such as high salinity, extreme high or low temperatures, high pressure,

different levels of aeration and radiation in layers and harsh conditions in the depth of the ocean (Jimeno *et al.*, 2004; Skropeta, 2008). Therefore, the diversity of marine microorganism is very high and the ocean is considered as a treasure box containing lots of hidden biological, pharmacological active natural products. This consideration has initiated great interest in the marine organisms and in particular in marine natural products recently. Our current understanding on marine life in general and marine microbial life in special is rather limited (less 1% of marine microorganisms are known to date) and marine natural products chemistry is still young, dating back only to the 1950s. In the early days, marine natural products discovery mainly focussed on most conspicuous and easily collected organisms. Chemists turned to the marine microorganisms with the development of open circuit self-contained underwater breathing apparatus (SCUBA) in the 1940s. Today, more than 22,000 marine metabolites have been isolated and structurally characterized (Gerwick and Fenner, 2013).

In the early 1950s arabinose nucleosides (spongouridine and spongothymidine) from a Caribbean sponge were discovered and later due to their potent activities used for the development of anticancer drugs by Bergmann (Buss and Butler, 2010). The drug discovery starts its focus to marine natural products chemistry in the 1970s. By 1974, two marine-derived natural products (cytarabin, Ara-C and vidarabine, Ara-A) were part of the pharmacopeia used to treat human disease (Mayer *et al.*, 2010b). Almost 30 years later, another novel marine-derived natural product, ziconotide (Prialt®) gained approval and become part of the pharmacopeia for the treatment of severe pain. In 2007, Yondelis® has received European approval for the treatment of soft tissue sarcoma (STS) and for ovarian carcinoma (in 2009).

At present, most marine natural products are either sterols, terpenes, saponins, unsaturated fatty acids, polysaccharides and glycosides, macrolides, polyether compounds, enzymes or peptides which have shown promise in treating cancer, pain, inflammation, allergies, and viral infections (Newman and Cragg, 2004; Newman and Cragg, 2012).

In the last 60 years, marine natural products have become fascinating targets for searching lead compounds in the purpose of clinical development (Cooper, 2004; Bhadury *et al.*, 2006; Bull and Stach, 2007; Williams, 2009; Jones *et al.*, 2009; Gulder and Moore, 2009; Mayer *et al.*, 2011; Mayer *et al.*, 2010a; Villa and Gerwick, 2010; Waters *et al.*, 2010). There are several databases of natural compounds from marine sources. For example, 42 950 natural products were identified from marine microorganisms which possess highly interesting pharmaceutical properties by September of 2014 from the database of AntiBase 2014 (Laatsch, 2014). 35 000 natural compounds were selected in marine chemistry of the Chapman & Hall/CRC Dictionary of Marine Natural Products database (untill November 2015).

However, only few marine natural products have been advanced to pharmaceuticals and achieved full commercial application. From 2003-2013, 10 599 natural products were isolated and identified from

marine environment and hundreds of new natural compounds are found from marine organisms per year, especially over 1 000 new compounds are discovered every year since 2008 (Hu *et al.*, 2015) (http://marinepharmacology.midwestern.edu/clinPipeline.htm). Nevertheless, only 39 compounds (until August 2015) account for a small percentage of these have been tested for pharmaceutical potential as following (in clinical used or in preclinical phases).

There are now six drugs approved by the Food and Drug Administration (FDA), namely cephalosporin C (brentuximab vedotin, SGN-35, Adcetris®), cytarabine (Ara-C, Cytosar-U®, Depocyt®), eribulin mesylate (E7389, Halaven®), omega-3-acid ethyl esters (Lovaza®), ziconotide (Prialt®), and vidarabine (Vira-A®), one EU registered drug trabectedin (ET-743, Yondelis®), and 32 natural products or derivatives in different phases of the clinical pipeline. In addition, a large number of marine natural products (http://marinepharmacology.midwestern.edu/clinPipeline.htm) are in the preclinical pipeline. More detailed information of marine natural compounds is shown in Table 1-1. From a global perspective the marine pharmaceutical pipeline remains very active, and now has sufficient momentum to deliver several additional compounds to the marketplace in the near future (Mayer *et al.*, 2010a).

Although the percentage of marine natural products that can be expected to be promoted into a drug is very low (1 out of 331), it is highly likely that an increasing number of marine bioactive compounds will be approved for the treatment of human diseases (Haefner, 2003; Nastrucci *et al.*, 2012; Liu *et al.*, 2012).

Many different marine organisms have been explored for bioactive compounds such as vertebrate animals (e.g. fish, sharks and snakes), invertebrates (e.g. sponges, coelenterates, tunicates, echinoderms, corals, algae, mollusks and bryozoans), as well as microorganisms (bacteria and fungi) (Chakraborty *et al.*, 2009).

In symbiotic relationship with e.g. sponges and tunicates, bacteria could be the actual producers of some of the metabolic products (Piel, 2004). Recently, attention turned to marine microorganisms that had previously escaped cultivation and examination, such as marine cyanobacteria, actinobacteria and fungi. Marine microorganisms will certainly be of particular interest in the future especially due to their ability to produce new valuable bioactive compounds with different pharmacological activities (Salomon *et al.*, 2004).

There are many compounds produced by marine bacteria, mostly come from cyanobacteira, however, salinosporamide A (NPI-0052, marizomib) with cytotoxic activity trials was isolated from the marine actinobacterium *Salinispora tropica* (Feling *et al.*, 2003; Niewerth *et al.*, 2014).

Reports on marine natural products with anticancer, antibacterial activities, and effects against other infectious diseases are discussed in various reviews (Molinski *et al.*, 2009; Newman *et al.*, 2000;

Newman and Cragg, 2012; Newman and Cragg, 2014; Munro *et al.*, 1999; Haefner, 2003; Gerwick and Moore, 2012; Mayer *et al.*, 2010a; Mayer *et al.*, 2013).

Table 1-1. Some marine natural products isolated from microorganisms.

Compound name	Trade-mark	Marine organism	Activity	Chemical class	Molecular targets	Reference	Clinical status
Brentuximab vedotin (SGN-35)	Adcetris®	Mollusk/cyanobacterium	anticancer	ADC(MMAE)	CD30 & microtubules	Katz *et al.* (2011)	FDA-approved
ABT-414 EGFRvIII-MMAF	NA	Mollusk/cyanobacterium	anticancer	ADC(MMAF)	EGFR & microtubules	Phillips *et al.* (2013)	II
Glembatumumab Vedotin (CDX-011)	NA	Mollusk/cyanobacterium	anticancer	ADC (MMAE)	GPNMB & microtubules	Naumovski and Junutula (2010)	II
PSMA-ADC	NA	Mollusk/cyanobacterium	anticancer	ADC (MMAE)	PSMA & microtubules	Petrylak *et al.* (2014)	II
DNIB0600A	NA	Mollusk/cyanobacterium	anticancer	ADC (MMAE)	NaPi2b & microtubules	Lin *et al.* (2014)	I/II
Pinatuzumab vedotin (DCDT-2980S)	NA	Mollusk/cyanobacterium	anticancer	ADC (MMAE)	CD22 & microtubules	Pfeifer *et al.* (2015)	I/II
Polatuzumab vedotin (DCDS-4501A)	NA	Mollusk/cyanobacterium	anticancer	ADC (MMAE)	CD79b & microtubules	Pfeifer *et al.* (2015)	I/II
AGS-16C3F	NA	Mollusk/cyanobacterium	anticancer	ADC (MMAE)	ENPP3 & microtubules	Thompson *et al.* (2015)	I
ASG-67E	NA	Mollusk/cyanobacterium	anticancer	ADC (MMAE)	CD37 & microtubules	Pereira *et al.* (2015)	I
ASG-15ME	NA	Mollusk/cyanobacterium	anticancer	ADC (MMAE)	SLITRK6 & microtubules	Jain *et al.* (2015)	I
ASG-22ME	NA	Mollusk/cyanobacterium	anticancer	ADC (MMAE)	Nectin-4 & microtubules	Jain *et al.* (2015)	I
DEDN6526A	NA	Mollusk/cyanobacterium	anticancer	ADC (MMAE)	ETBR & microtubules	Infante *et al.* (2014)	I
DMUC5754A	NA	Mollusk/cyanobacterium	anticancer	ADC (MMAE)	Mucin 16 & microtubules	Liu *et al.* (2013)	I
DSTP3086S	NA	Mollusk/cyanobacterium	anticancer	ADC (MMAE)	STEAP1 & microtubules	Danila *et al.* (2014)	I

HuMax®-TF-ADC	NA	Mollusk/cyanobacterium	anticancer	ADC (MMAE)	Tissue Factor & microtubules	Newman and Cragg (2014)	I
Marizomib (NPI-0052; Salinosporamide A)	NA	Bacterium	anticancer	Beta-lactone-gamma lactam	20S proteasome	Feling *et al.* (2003)	I
MLN-0264	NA	Mollusk/cyanobacterium	anticancer	ADC (MMAE)	GCC & microtubules	Jain *et al.* (2015)	I
SGN-CD19A	NA	Mollusk/cyanobacterium	anticancer	ADC (MMAE)	CD19 & microtubules	Jain *et al.* (2015)	I
SGN-LIV1A	NA	Mollusk/cyanobacterium	anticancer	ADC (MMAE)	LIV-1 & microtubules	Jain *et al.* (2015)	I
PM00104	Zalypsis®	Mollusk	anticancer	Alkaloid	DNA-binding	Guirouilh-Barbat *et al.* (2009)	II
Soblidotin (TZT 1027)	NA	Bacterium	anticancer	peptide	microtubule & monosodium glutamate-induced tubulin polymerization	Natsume *et al.* (2000)	III

ADC: Antibody Drug Conjugate; **CD**: Cluster of Differentiation; **EGFR**: Epidermal Growth Factor Receptor; **ENPP3**: Ectonucleotide Pyrophosphatase/Phosphodiesterase Family Member 3; **ETBR**: Endothelin B Receptor; **FDA**: Food and Drug Administration; **GCC**: Guanylyl Cyclase C; **GPNMB**: Glycoprotein nonmetastatic B; **LIV-1**: Zinc transporter SLC39A6; **NA**: Not Available; **NaPi2b**: Sodium-Dependent Phosphate Transport Protein 2b; **PSMA**: Prostate-Specific Membrane Antigen; **SLITRK6**: SLIT and NTRK-like protein 6; **STEAP1**: Anti-Six Transmembrane Epithelial Antigen of the Prostate 1

1.3 Methods of natural products screening

Natural products become one of the most important sources for lead compounds in drug discovery. Most biologically active natural compounds are secondary metabolites with very complex structures. The compounds usually have to be extracted from the natural source by complex processes including the isolation, identification, structure elucidation and characterization of the chemical substances produced by living organisms.

In traditional drug discovery, if the lead compound or active compound is present in a mixture of other compounds from a natural source, it has to be purified and isolated. The elucidation of the chemical structure is critical to identify the compounds. Potential bioactive compounds were extracted by different solvents and structure elucidated with the help of the technologies that have become widely used in the pharmaceutical industry, such as high-performance liquid chromatography coupled with diode array detection and mass spectrometry (HPLC-DAD/MS) for the analytical screening. Semi-preparative high-performance liquid chromatography (semi-preparative HPLC) is often used to separate the individual chemicals, and nuclear magnetic resonance (NMR) spectra are used to obtain structural information of novel compounds showing interesting bioactivity. These methods allow purification and characterization of secondary metabolites from natural sources.

For detecting the secondary metabolite pathways for natural products synthesis, genetic approaches are promising tools. The genome analysis of marine microorganisms facilitates the use of specific genes for biotechnological applications such as the production of new drugs. Part of known natural products are derived from nonribosomal peptides and polyketides (Donadio *et al.*, 2007) which are biosynthesized by nonribosomal peptide synthetase (NRPSs) and polyketide synthases (PKSs), respectively. PKs and NRPs are the key enzymes in the regulation of secondary metabolite biosynthesis of polyketides and nonribosomal peptides, respectively.

1.3.1 Polyketides

Polyketides (PKs) are produced by bacteria, fungi, plants and animals and represent a large and important class of secondary metabolites with diverse biological activities and pharmacological properties They are an important source of naturally occurring small molecules used for chemotherapy (Koehn and Carter, 2005) and structurally classified into four major groups: aromatics (e.g., doxorubicin and tetracycline), macrolides (e.g., erythromycin and rapamycin), polyethers (e.g., monensin and salinomycin), and polyenes (e.g., amphotericin and candicidin) (Shen, 2000). For example, rapamycin (immunosuppressant), erythromycin (antibiotic), lovastatin (anticholesterol drug), and epothilone B (anticancer drug), avermectin (antihelmintic agent) can be produced industrially (Wawrik *et al.*, 2005).

The common feature of polyketides natural products is that they are biosynthesized by repeated addition of small building blocks to form a linear chain. The polyketide chains, which are catalyzed by large enzyme complexes, polyketide synthases (PKSs), are frequently further modified into bioactive natural products.

PKSs are a family of large multienzyme protein complexes that consists of multiple active domains organized into modules. PKSs are divided into three classes: type I PKSs are multifunctional proteins consisting of processive or iterative multidomains for individual enzyme activities and have been found in bacteria, fungi and plants; type II PKSs are aggregates of mono-functional discrete proteins which are involved in the biosynthesis of aromatic natural products (e. g., actinorhodin, tetracenomycin and doxorubicin) only in bacteria so far; and type III PKSs are always responsible for the synthesis of small aromatic molecules in plants and bacteria without having a phosphopantetheinyl (P-pant) arm.

Many of the polyketide synthase pathways have not yet been characterized (Castoe *et al.*, 2007; Ridley *et al.*, 2008). However, the key chain-building step of polyketide biosynthesis is a decarboxylative condensation of extender units with the growing polyketide chain that is analogous to the well-understood chain elongation process (a Claisen condensation) of fatty acid biosynthesis (catalyzed by fatty acid synthases, FASs) (Khosla *et al.*, 1999; Jenke-Kodama *et al.*, 2005).

The synthesis of a polyketide requires multidomains that can be organized in modules. Each module is responsible for the construction of a carbon-carbon bond. There is a loading module in most PKSs for obtaining the starter unit at the front of module 1. The loading module of type I PKS normally starts with the acyltransferase (AT) domain. The AT-domain is responsible for loading of starter, extender and intermediates bound to the enzymatic machinery.

Acyl carrier protein (ACP) domains are dependent on a post-translational modification to function. This modification is the attachment of a 4'-phosphopantetheine cofactor to a conserved serine residue. Therefore the substrates are covalently attached to the growing polyketide via a thioester bond with an SH group on the 4'-phosphopantetheine (4'PP) cofactor. The extension of polyketide is catalyzed by β-keto-acyl-synthase (KS) between the growing poly-β-ketone intermediates and ACP. The growing acyl chain can be further modified with β-keto reductase (KR, responsible for the first reduction to alcohol functionality), enoyl reductase (ER, catalyzes the final reduction to full saturation) or dehydratase (DH, responsible for eliminating water to give an unsaturated thioester) domains before finally being released from the enzyme complex via a thioesterase domain (TE, responsible for unloading the product at the end of the last module). These type I and II polyketides are synthesized via the step-wise condensation. In the case of modular type I PKSs, it includes iterative PKSs, which reuse domains in a cyclic fashion, and modular PKSs, which contain a sequence of discrete modules and do not repeat domains. This type I PKSs include non-reducing PKSs (NR-PKS), the products of

which are true polyketides, the practically reducing PKSs (PR-PKS), and fully reducing PKSs (FR-PKSs) which are fatty acid derivatives.

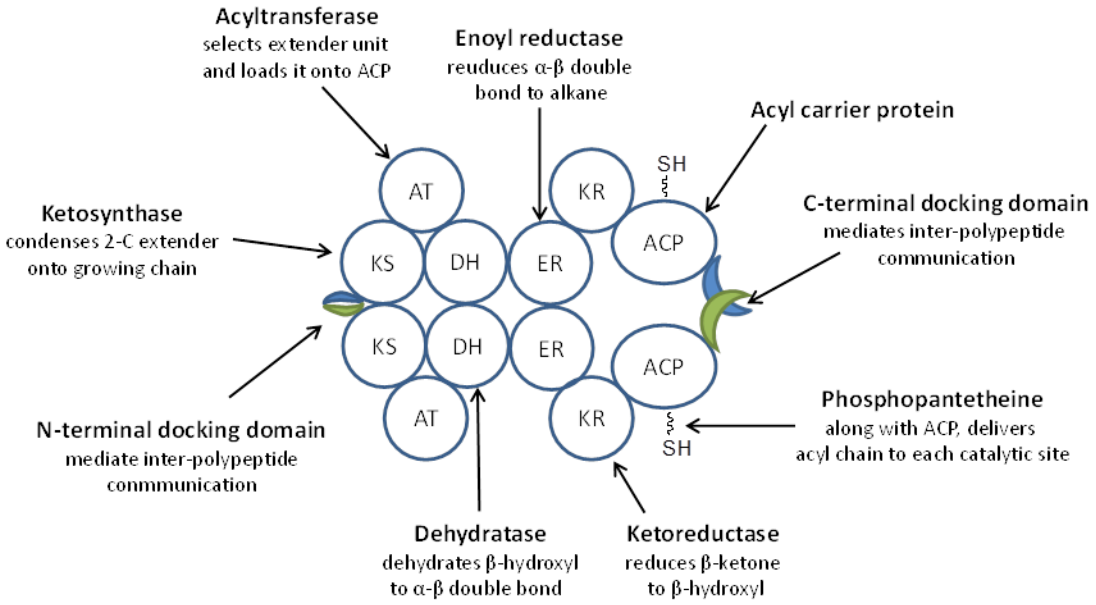

An individual domains in a full type I polyketide synthase extension module. Homodimeric contacts are made in the N-terminal docking, ketosynghase, dehydratase, enoyl recuctase, and C-terminal docking domains (Tonia J. Buchholz *et al.*, 2009).

Figure 1-7. Conventional modular type I PKS paradigm.

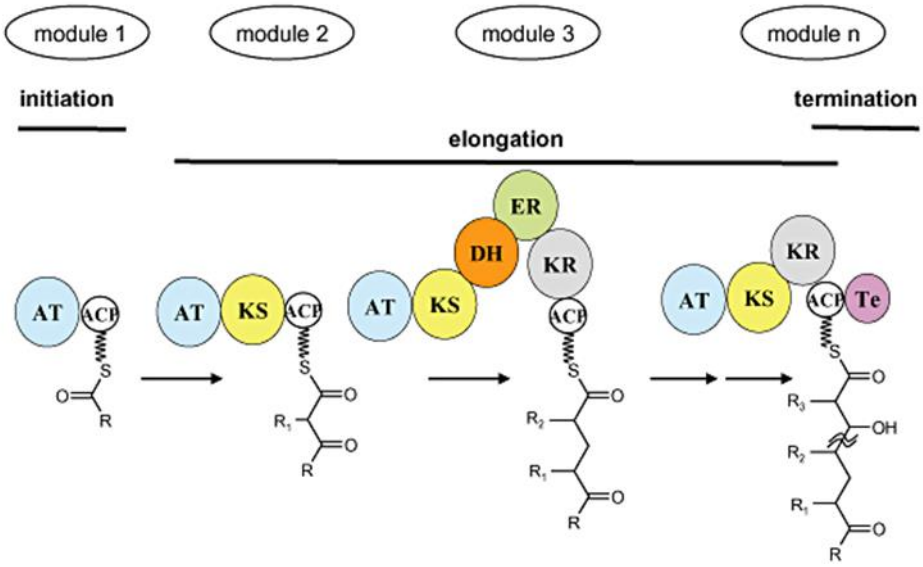

Figure from Siezen and Khayatt (2008)

Figure 1-8. Basic steps during polyketide synthesis.

Type II PKS systems are aggregates of monofunctional proteins. They produce a linear polypeptide by the action of an iteratively used keto-synthase (KS) domain with an SH group on a cysteine side-chain, and make the unmodified aromatic polyketide together with chain length factor (CLF), aromatase (ARO), cyclase (CYC).

Type III polyketide synthases (PKSs) have been found in bacteria, fungi and plant. Type III PKS systems which do not use ACP domains are simple homodimers of KSs which catalyze the condensation of two β-keto fatty acyl CoAs to several molecules of extender substrate onto a starter substrate via iterative decarboxylative Claisen condensation reactions (Katsuyama and Ohnishi, 2012; Hashimoto et al., 2014). Many compounds produced by microbial type III PKSs have significant biological functions or important pharmaceutical activities.

Several polyketide antibiotics, antifungals, cytostatics, anticholesteremic, antiparasitics, coccidiostats, animal growth promoters and natural insecticides are now in commercial use.

1.3.2 Nonribosomal peptides

Many microorganisms have evolved an unusual way of producing secondary peptide metabolites, using a nonribosomal peptides biosynthesis, which is differ from the ribosomal pathway. Non-ribosomal peptides (NRPs) are produced by a large number of bacteria, fungi, and lower eukaryotes.

The biological functions of most nonribosomal peptides are unknown; however, for some of them an essential function has been identified. For example, the well-studied penicillin produced by *Penicillum notatum* is a weapon against nutrient competitors, and the siderophore bacillibactin helps its producer *Bacillus subtilis* to acquire iron and thereby prevent iron starvation (Schoenafinger and Marahiel, 2009).Nonribosomal peptides (NRPs) are a diverse class of cyclic and branched linear peptide secondary metabolites. They are synthesized by mega-enzymes nonribosomal peptide synthetases (NRPSs) which compose a unique class of multidomain enzymes capable of producing peptides with various functions, such as cytostatic, immunosuppressive, antibacterial, or antitumor properties. The mechanisms of NRPSs are a kind of assembly line of template-directed, nucleic-acid-independent modules. Each module takes up one specific amino acid and each one of NRPS can produce only one type of nonribosomal peptide (Weber and Marahiel, 2001).

Modules can be subdivided into initiation and elongation modules (Finking and Marahiel, 2004). These modules catalyse at least the steps of substrate activation, covalent binding, and peptide bond formation of nonribosomal peptide synthesis.

Before peptide formation occur, the building blocks (amino acids) to be condensed need to be recognized and activated. The adenylation (A) domain is capable of substrate recognition and formation of the corresponding acyl-adenylate-monophosphate by consumption of ATP. Thus, the

peptidyl carrier protein (PCP) domain (~90 amino acid residues, counterpart to the ACP in PKS and FAS) acts as a thioester through covalent fixation to keeping the reaction intermediates bound to the enzymatic machinery. PCP domains are post-translational modified to function via the attachment of a 4'-phosphopantetheine cofactor to a conserved serine residue. Thus, amino acids are covalently attached to PCP domains via a thioester. After such an acylation, the PCP domain directs the substrate toward the next processing condensation (C) domain (~450 aa). The C domain catalyses the formation of peptide bonds between an activated aminoacyl bound intermediate and a peptidyl-bound intermediates of two adjacent module. The growing peptide chain is handed over from one module to the next until it reaches the PCP-domain of the final module, in which a transesterification (TE) domain (~250 aa) promotes the liberation of the assembled peptide from the synthetase.

The basic set of domains within a module can be edited and/or extended by optional modification domains, including domains for substrate epimerization, N-methylation, and oxidation, methylation, reduction domains, and heterocyclic ring formation. Cyclization of amino acids against the peptide "backbone" is often performed, resulting in further oxidized or reduced oxazolines and thiazolines. In addition to the essential domains, a number of tailoring enzymes act in the maturation of the NRPS-products.

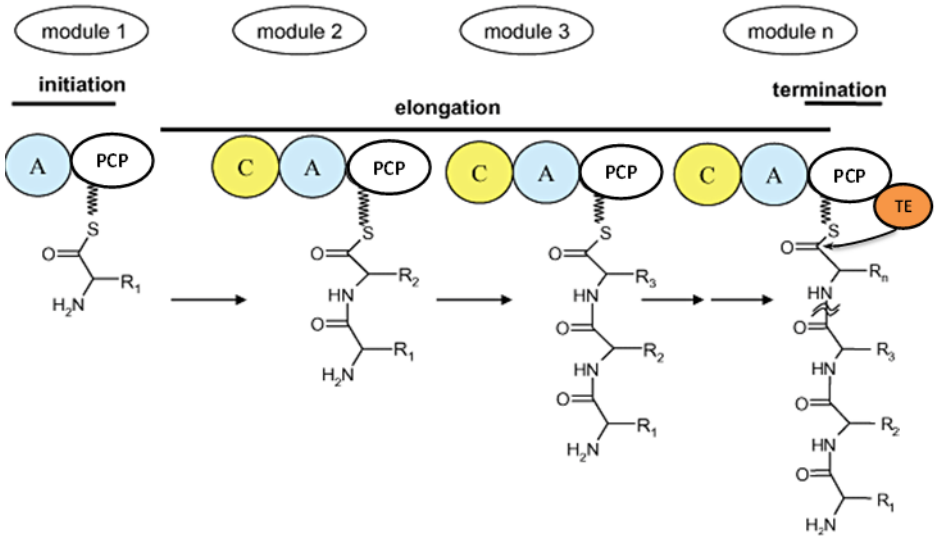

Figure modified from Siezen and Khayatt (2008).

Figure 1-9. Basic steps during nonribosomal peptide synthesis.

Although NRPSs, PKSs, and fatty acid synthases (FASs) are related in their biosynthetic logic, the existence of NRPS-PKS hybrids led to the assumption that at least the PKS part of the protein should dimerize. The NRPS part of the protein, however, was thought to retain a monomeric architecture.

NRPs are a very diverse family of natural products with an extremely broad range of biological activities and pharmacological properties. They are often toxins, siderophores, or pigments. Non-ribosomal peptide antibiotics, cytostatics, and immunosuppressants are in commercial use.

1.3.3 Phenanzines

Another important compound class are the phenazines, which have been paid attention and which represent promising secondary metabolites and possible drug candidates (Arbiser and Moschella, 1995). More than 100 biologically active (antibacterial, antifungal, antiviral, antitumor) phenazines from natural origin are known till now, and they are synthesized mainly by *Pseudomonas* and *Streptomyces* species (McDonald *et al.*, 2001).

Phenazine ($C_{12}H_8N_2$ or $C_6H_4N_2C_6H_4$, structure is seen in Figure 1-10) is a dibenzo annulated pyrazine and has been used as the original substance of many dyestuffs (e.g. toluene red, indulines and safranines).

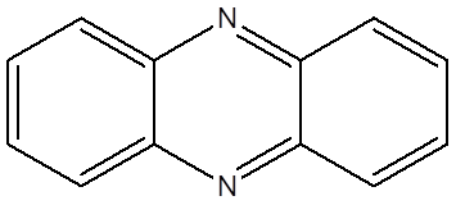

Figure 1-10. The structure of phenazine.

Bacteria such as *Pseudomonas* spp. and *Streptomyces* spp. can produce phenazine products, which can be implicated in the virulence and competitive fitness of the producing organism. For instance, the phenazine pyocyanin produced by *Pseudomonas aeruginosa* contributes to its ability to colonize the lungs of cystic fibrosis patients (McDonald *et al.*, 2001).

At the point subsequent to chorismic acid in the shikimic acid biosynthesis pathway, the specific biosynthesis of phenazines starts. Two molecules of chorismate-derived intermediates are then brought together to form the basic phenazine scaffold. Sequential modifications then lead to a variety of phenazines with different biological activities.

The genetic ability of phenazine biosynthesis was verified by analyzing the metabolite pattern of PCR-positive strains via HPLC-UV/MS (Schneemann *et al.*, 2011). The PCR based screening approach for the identification of phenazine producing bacteria was demonstrated by the transformation from chorismate to 2-amino-2-deoxyisochorismic acid (ADIC), which is necessary for the formation of the core structure of phenazines and is catalyzed by the enzyme PhzE. Sequences of *phz*E were used to design one universal primer system and to analyze the ability of bacteria to produce phenazine. The

application of the *phz*E primer system is a promising tool to indicate the presence of the phenazine biosynthetic pathway in various groups of bacteria including marine *Actinobacteria*.

1.3.4 Terpenes

Terpenes are a large and diverse class of organic compounds, produced mainly by a variety of plants, particularly conifers (Webster, 2006). They are often strong-smelling and may protect the plants that produce them by deterring herbivores and by attracting predators and parasites of herbivores (Martin *et al.*, 2003). Many terpenes are aromatic hydrocarbons and thus may have had a protective function (Pichersky *et al.*, 2006). They are the major components of resins, and of turpentine produced from the resins. In addition to their roles as end-products in many organisms, terpenes are major biosynthetic building blocks within nearly every living creature. Steroids, for example, are derivatives of the triterpene squalene.

Terpenes and terpenoids are the primary constituents of the essential oils of many types of plants and flowers. Essential oils are used widely as natural flavour additives for food, as fragrances in perfumery, and in medicine and alternative medicines such as aromatherapy. Synthetic variations and derivatives of natural terpenes and terpenoids also greatly expand the variety of aromas used in perfumery and flavours used in food additives. Vitamin A is a terpene.

Isoprene (C_5H_8, Figure 1-11) is the basic unit from which terpenes derive biosynthetically. The molecular formulae of terpenes are multiples of isoprene, $(C_5H_8)n$, and the value of n is the number of linked isoprene units. They may be linked together 'head to tail' to form linear chains or arranged to form rings.

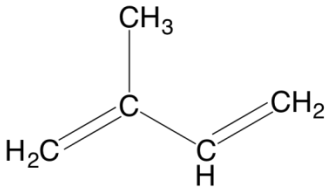

Figure 1-11. The structure of isoprene.

Isopentenyl pyrophosphate (IPP, Figure 1-12) and dimethylallyl pyrophosphate (DMAPP, Figure 1-13) are the components in activated forms in the biosynthetic pathway while isoprene itself does not undergo the process. IPP can be formed by HMG-CoA reductase pathway and 2-Methyl-D-Erythritol-4-phosphate pathway (MEP pathway) which start from acetyl-CoA and C5-sugars, respectively. In both pathways, IPP is isomerized to DMAPP by the enzyme isopentenyl pyrophosphate isomerase.

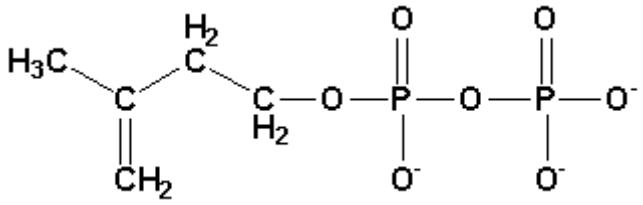

Figure 1-12. The structure of isopentenyl pyrophosphate (IPP).

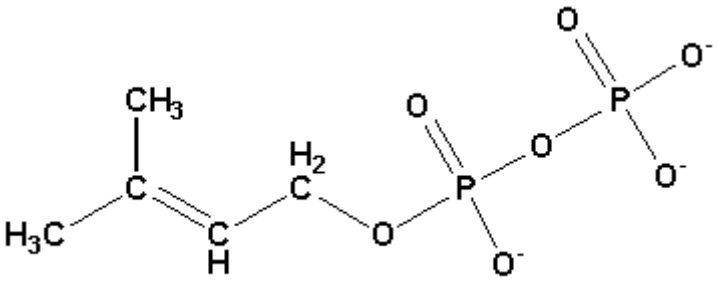

Figure 1-13. The structure of dimethylallyl pyrophosphate (DMAPP).

Isoprene units are synthesized by terpene synthase to chains and the resulting terpenes are classified by the number of basic units in the molecule, such as hemiterpenes, moniterpenes $(C_5H_8)_2$, sesquiterpenes $(C_5H_8)_3$, diterpenes $(C_5H_8)_4$, sesterterpenes$(C_5H_8)_5$, triterpenes $(C_5H_8)_6$, and sesquarterpenes $(C_5H_8)_7$, tetraterpenes $(C_5H_8)_8$, and polyterpenes (C_5H_8)n.

A range of terpenes have been identified as high-value chemicals in food, cosmetic, pharmaceutical and biotechnology industries (Thimmappa *et al.*, 2014; Augustin *et al.*, 2011).

Chemical synthesis of terpenes can be problematic because of their complex structure, and plants produce very small amounts of these valuable chemicals, making it difficult, time consuming and expensive to extract them directly from plants. Scientists are working to identify the key enzymes and pathways that produce terpenes in plants.

Once genes for the synthetic pathway of a specific terpene have been identified, synthetic biology techniques could be used to make high levels of this terpene, using plants or microorganisms (e.g. yeast) as "factories". This could mean cheaper and more sustainable production of economically and medicinally important terpenes. For example, the effective anti-malarial terpene artemisinin, from the plant *Artemisia annual*, can now be produced in yeast (Paddon and Keasling, 2014).

1.3.5 Updating tools for exploration of diversities of natural compounds

Various genome-based strategies together with traditional bioassay-based methods promote the exploration of natural compounds. However, Glöckner and Joint (2010) pointed out that the success of

the genome-based methods is largely dependent on the accuracy of bioinformatic analysis. Researchers are now developing various bioinformatic tools such as antiSMASH 3.0 (Weber *et al.*, 2015), ClustScan (Starcevic *et al.*, 2008), NP searcher (Li *et al.*, 2009), SBSPKS (Anand *et al.*, 2010) for the analysis of PKS or NRPS modular sequences and structure predictions.

On the other hand, new tools in the detection of natural products are continuously being developed to explore the chemical diversity of microbial natural products, such as the imaging mass spectrometry (IMS) tools (Esquenazi *et al.*, 2008), the PrISM (Proteomic Investigation of Secondary Metabolism) approach (Bumpus *et al.*, 2009) and single-cell genomics approaches (Siegl *et al.*, 2011). All these updated bioinformatics tools and detection tools can be combined to facilitate new marine natural products in the future.

1.4 Anoxygenic phototrophic bacteria

Anoxygenic phototrophic bacteria (APB) that are capable of anaerobic anoxygenic photosynthesis are referred to as anaerobic anoxygenic phototrophic bacteria, in contrast to those that are aerobic bacteria contain Bchl and perform anoxygenic photosynthesis under aerobic conditions which are called the aerobic anoxygenic phototrophic bacteria (AAPBs) (Yurkov and Beatty, 1998).

APBs perform anoxygenic photosynthesis without oxygen production and convert the light energy to ATP. APBs are widely distributed in nature and play an important role in carbon dioxide assimilation and nitrogen fixation. Anoxic conditions are required for photosynthesis, and these bacteria cannot thrive in oxygenated environments (Proctor, 1997).

Most characteristically, they can oxidize sulfide and other reducing agent as electron donor (Imhoff, 2008) that is different from the mechanisms in plants (Bryant and Frigaard, 2006) or cyanobacteria (water as electron donor).

Based on phenotypic characteristics and phylogenetic relationships, anaerobic anoxygenic phototrophic bacteria are divided into five major groups of the purple sulfur bacteria (PSB, Gammaproteobacteria), purple nonsulfur bacteria (PNSB, Alpha- and Betaproteobacteria), green sulfur bacteria (GSB, Chlorobiaceae), green nonsulfur bacteria (GNSB, Chloroflexaceae) and green heliobacteria Heliobacteriaceae (Sattley and Madigan, 2014).

1.4.1 Purple bacteria

Anoxygenic phototrophic purple bacteria are Proteobacteria and representatives of the Gammaproteobacteria (Chromatiaceae and Ectothiorhodospiraceae), Alphaproteobcteria ("*Rhodo-spirillum* and relatives") and Betaproteobacteria (Woese *et al.*, 1984; Woese, 1987). They are

pigmented with bacteriochlorophyll *a* or *b*, together with various carotenoids, which give them distinct colors ranging between purple, red, brown, and orange.

Anoxygenic phototrophic bacteria are generally found in illuminated anoxygenic parts of fresh and seawater habitats and also in marine habitats, sulfur hot springs, soda and salt lake, and intertidal microbial mats. They typically develop in all kinds of low or no oxygen tensions aquatic habitats that are reached by sunlight. Reduced sulfur compounds (H_2S, elemental sulfur, and thiosulfate) are important electron donors of the phototrophic sulfur bacteria. The ability to carry out light-dependent bacteriochlorophyll mediated energy transfer processes is a common property of phototrophic purple bacteria, cyanobacteria, Chlorobiaceae, "Chloroflexaceae", and heliobacteria.

Phylogenetically, the purple sulfur bacteria (PSB) are classified into two families within the Gammaproteobacteria, Chromatiaceae and Ectothiorhodospiraceae on the basis of fundamental phenotypic and phylogenetic differences (Imhoff *et al.*, 1984). The purple sulfur bacteria contain Bchl *a* and *b*, and all components of the photosynthetic apparatus are located in the intracellular membrane.

The family Chromatiaceae are Gram-negative, contain internal photosynthetic membranes and typically are characterized by accumulation of sulfur globules within the cell (Imhoff *et al.*, 1984). With a few exception (e.g. *Thiococcus pfennigii*), the intracellular membrane system is of the vesicular type. During aerobic dark growth, elemental sulfur may support respiration and serve as electron donor for chemolithotrophic growth, and under anoxic conditions in the light, all species are capable of photolith autotrophic growth with sulfide or S^0 as electron donor (Imhoff, 2014). In contrast, the family of Ectothiorhodospiraceae (Imhoff *et al.*, 1984) form sulfur globules outside the cells and contain lamellar intracellular membrane systems.

Anoxygenic phototrophic purple nonsulfur bacteria（PNSB）represent by far the most diverse group of the phototrophic purple bacteria (Imhoff and Trüper, 1989) and preferentially grow under photoheterotrophic conditions (Imhoff, 2003). Most of the PNSB are representatives of the Alphaproteobacteria (''*Rhodospirillum* and relatives'', aerobic bacteriochlorophyll-containing bacteria), but a distinct group of species belongs to the Betaproteobacteria.

1.4.2 Green bacteria

The green sulfur bacteria (GSB), represented by the family Chlorobiaceae, are obligately anaerobic photoautotrophic bacteria. They are non-motile (except *Chloroherpeton thalassium* which may glide (Bryant and Frigaard, 2006) and occur in spheres, rods, and spirals and contain bacteriochlorophyll (BChl) *a*, *c*, *d*, or *e* in light-harvesting complexes.

GNSB (phylum Chloroflexi) are Gram-negative (*Oscillochloris chrysea* is an exception because they stain Gram-positive). They are aerobic thermophilic phototrophs using oxygen and can grow well in

high temperatures (Garrity and Holt, 2001). They can form flexible filaments with gliding motility, and also called filamentous anoxygenic phototrophic bacteria (FAP). Most of them do not have gas vesicles and include bacteriochlorophylls *c*, or *d*, with small amounts of chlorophyll *a* and carotenoids (gamma- and beta-carotene). The most conspicuous representatives are the green- or orange-colored thermophilic bacteria which form dense microbial mats in hot springs (Overmann, 2008). The genera *Chloroflexus*, *Chloronema*, *Heliothrix*, and *Oscillochloris* constitute the green nonsulfur bacteria group (GNSB) according to Bergey's Manual of Systematic Bacteriology (Garrity and Holt, 2001), and one new genus of *Roseiflexus* was included (Hanada *et al.*, 2002).

1.4.3 Heliobacteriaceae

The cells of family Heliobacteriaceae are rod-shaped to short filaments or spirillum-shaped cells. They are anoxygenic phototrophic bacteria, but differ from others by their unique light harvesting and reaction center pigment Bchl *g* and carotenoids (Asao and Madigan, 2009). Bchl *g* confers to the cells a near infrared absorption maximum at 788 nm, which is unique among photosynthetic organisms (Gest and Favinger, 1983). The known species of Heliobacteriaceae all grow photoheterotrophically and are strict anaerobes. Gas vesicles are not present.

1.4.4 Aerobic anoxygenic phototrophic bacteria (AAPBs)

Aerobic anoxygenic phototrophic bacteria (AAPBs) are Alphaproteobacteria and Gamma-proteobacteria and they comprise a considerable number of species. AAPBs are photoheterotrophic bacteria that exist in a variety of aquatic environments. They are obligate aerobes (require oxygen for growth) and can capture energy from light by anoxygenic photosynthesis, but are unable to utilize carbon dioxide as their primary carbon source. One remarkable aspect of these bacteria unlike other similar bacteria is the inability of utilize bacteriochlorophyll (BChl) for anaerobic growth. The only bacteriochlorophyll pigment that exists in AAPB is BChl *a* (Yurkov and Beatty, 1998). However, anaerobic phototrophic bacteria, on the contrary, contain a number of different bacteriochlorophylls: *a*, *b*, *c*, *d*, *e*, and *g.*

AAPB are usually pink or orange in color when isolated from water. All species of AAPB produce large amounts of carotenoid pigments. The color of each species is due to the presence of carotenoids, giving peaks in the blue and green absorption spectra.

1.5 Aims of this study

The biomass turnover of marine photosynthetic microorganisms is about 700 times faster than that of terrestrial higher plants. Thus, marine photosynthetic organisms contribute significantly to total primary productivity ($55 \cdot 10^9$ t dry weight·year^{-1}, or 44% of the global primary production) (Overmann and Garcia-Pichel, 2013). The dominant primary producers are halophilic and halotolerant algae,

cyanobacteria, and anoxygenic phototrophic bacteria (Thiel *et al.*, 2010). The role of anoxygenic phototrophic bacteria's contribution to the global primary production is low, for example, phototrophic sulfur bacteria altogether contribute only 4% to global primary production (Whittaker and Likens, 1975). However in certain aquatic environments, APB are important primary producers which can contribute up to 83% of the primary production (Van Gemerden and Mas, 1995). As far as we know, there is rare research about bioactive compounds of anoxygenic phototrophic bacteria. This work studied the bioactive compounds associated with the bacterium *Allochromatium vinosum* MT86 by using cultivation-dependent and molecular-based approaches.

1) **Optimal parameters for cultivation of *Allochromatium vinosum* strain MT86.**

From Dr. Marcus Tank's previous work, one anoxygenic phototrophic purple sulfur bacterium with antibiotic potential was found. Strain MT86 was isolated from a marine sandy rock pool near Trivendrum, southwest coast in the Indian Ocean (sample station CH3) by Dr. Marcus Tank in 2009 and was identified as *Allochromatium* species. It was taxonomically characterized and its 16S rRNA gene sequence was 97% similar to the type strain of *Allochromatium vinosum* DSM 180^T, which is a species of the Chromatiaceae.

The biotechnological potential of anoxygenic phototrophic bacteria was addressed by different methods. The cultivation media and conditions have great impact on the searching of the chemicals; therefore, much effort (culture-based development, tests of fermentation parameters, salt tolerance and so on) were made to screening for bioactive compounds of *A. vinosum* strain MT86.

2) **Screening and identification of the bioactive compounds from *A. vinosum* strain MT86.**

Dr. Marcus Tank identified antimicrobial activities in crude extracts of *A. vinosum* strain MT86, and therefore, identification of the antimicrobial activity and structure analysis of bioactive compounds produced by *A.* strain MT86 was one of the main purposes of this study.

3) **Screening for antimicrobial (and other bio-) activity of extracts from other phototrophic bacteria.**

Another three selected microorganisms were screened for antimicrobial compounds following the same methods as used for *A. vinosum* strain MT86.

4) **Screening for functional genes of natural product metabolic pathways (*pks*, *nrps*, and *phz*E).**

A total of ten selected strains were screened for *pks* I, *pks* II, *nrps*, and *phz*E genes by PCR amplification. Sequences of fragments were submitted to NCBI for BLASTn and functional genes can give metabolite information.

5) Genome evaluation of phototrophic bacteria by antiSMASH.

The whole genome sequences of 62 phototrophic bacteria were downloaded from NCBI database and analyzed online by antiSMASH for secondary metabolites. In comparison with interesting clusters of secondary metabolites and similar compounds, further potential of bioactive compounds of phototrophic bacteria was predicted.

2 MATERIALS AND METHODS

2.1 Preparation of the medium

The Pfennigs medium was prepared by the method of Eichler and Pfennig (1988), a defined medium for freshwater and marine *Chromatium* and *Allochromatium* species (Pfennig, 1965; Pfennig and Trüper, 1981; Pfennig and Trüper, 1992).

The medium was prepared in a 5-liter Erlenmeyer flask bottle (see Figure 2-1) with four openings at the top. Two openings were connected to tubings: 1) a short, gas inlet tube with a sterile cotton filter and 2) an outlet tube near the bottom at central part of the vessel for the medium, at the other end, a silicon rubber tube with a pinchcock and a bell for aseptic dispensing of the medium into bottles. The other two openings had gas-tight screw caps. One of these openings was for the addition of sterile solutions and the other served as a gas outlet. The medium was dispensed aseptically into sterile 100 ml, 500 ml or 1000 ml bottles with metal screw caps containing autoclavable rubber seals.

The Pfennig's medium was composed as follow:

Solution 1 (basic medium in 5 L):		
	demin. water	4900 ml
	KH_2PO_4	1.70 g
	$NHCl_4$	1.70 g
	$MgSO_4 \cdot 7H_2O$	1.25 g
	$CaCl_2 \cdot 2H_2O$	1.25 g
	KCl	1.70 g
Solution 2:	Vitamin B_{12}	5 ml
Solution 3:	SL-12	5 ml
Solution 4:	$NaHCO_3$	7.5 g in 100 ml demin. water.
Solution 5:	$Na_2S \cdot 9H_2O$	2.0 g in 20 ml demin. water.

Solution 2 of vitamin B_{12} was prepared by 2 mg vitamin B_{12} in 100 ml demin water, and then filtered by a 0.2 μm filter to the sterile tubes and stored at 4°C.

Solution 3, trace element solution SL-12 (Pfennig and Trüper, 1992) included the following ingredients: 3.0 g EDTA-Na_2, 1.1 g $FeSO_4 \cdot 7H_2O$, 300 mg H_3BO_3, 190 mg $CoCl_2 \cdot 6H_2O$, 50 mg $MnCl_2 \cdot 7H_2O$, 42 mg $ZnCl_2$, 24 mg $NiCl_2 \cdot 6H_2O$,18 mg $Na_2MoO_4 \cdot 2H_2O$, and 2 mg $CuCl_2 \cdot 2H_2O$ dissolved in 1 L demin. water in order. The pH was adjusted to 2-3 with HCl. SL-12 was stored at 4°C. When adding to 5 L basic medium (solution 1) of Pf medium, 5 ml was added sterilized by a 0.2 μm filter.

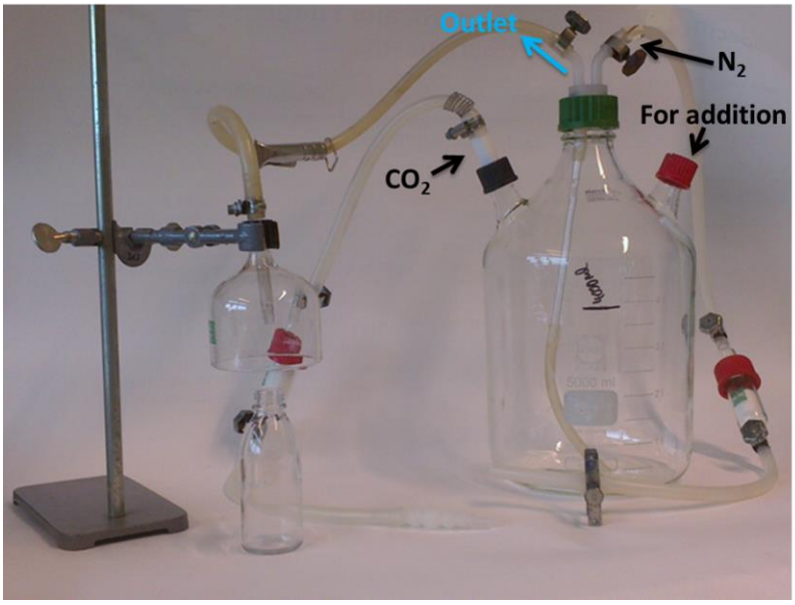

Figure 2-1. The apparatus for preparation of Pfenning medium.

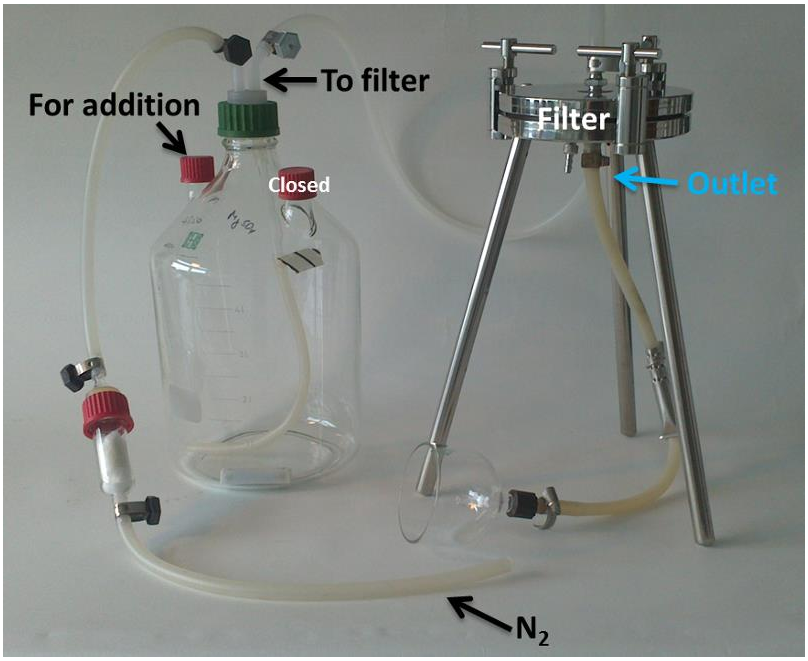

Figure 2-2. The apparatus for preparation of AT medium.

Solution 4 was a 7.5% $NaHCO_3$ solution that contained 7.5 g $NaHCO_3$ in 100 ml demin. water. After saturated with CO_2, the solution was autoclaved under CO_2 atmosphere in a tightly closed bottle.

Solution 5 was a 10% $Na_2S \cdot 9H_2O$ solution (2.0 g $Na_2S \cdot 9H_2O$ in 20 ml demin. water) prepared in a screwed-cap bottle. After replacement of the air by N_2, the bottle is tightly closed and autoclaved under an N_2 atmosphere.

Chemicals of the solution one were dissolved in the order given. Solution one was autoclaved for 45 min at 121°C in the 5-liter bottle, together with a Teflon-coated magnetic stir bar. After the medium had been autoclaved and cooled to room temperature under an atmosphere of N_2 with a positive pressure of 0.05-0.1 atm, the cold medium was saturated with CO_2 by magnetic stirring for 30 min under CO_2 atmosphere of 0.05-0.1 atm (100 mbar).

The sterile solutions 2 through 5 were added aseptically through one of the screw-cap openings while access of air was prevented by continuous flushing with N_2 while the medium was magnetically stirred.

After combining and carefully mixing solutions 1 through 5, the pH of the medium was adjusted to pH 7.2 by stirring under an atmosphere of CO_2 (0.5 bar pressure) for approximately 40 min (if the pH required for 6.8, longer time of stirring under CO_2 gas was needed). The medium was then immediately dispensed aseptically under pressure of N_2 (0.05-0.1 atm) into sterile 100 ml, 500 ml, or 1 L bottles with metal screw caps containing autoclavable rubber seals. A small, pea-sized air bubble was left in each bottle to accommodate possible pressure changes. The tightly sealed screw-cap bottles can be stored for several weeks to a month in the dark. During the first 24 hours, some trace metal (mainly iron) sulfides of the medium precipitate in the form of fine black particles. No other sediment should arise in the otherwise clear medium.

Additionally, sulfide solution was necessary for purple sulfur bacteria during the growth. It contained 7 g $Na_2S \cdot 9H_2O$ and 2.65 g Na_2CO_3 dissolved in 250 ml demin. water. The pH of the sulfide solution was adjusted by CO_2 gas to 7.2-7.8.

Salt solution included 58 g NaCl and 8 g $MgCl_2 \cdot 6H_2O$ dissolved in 200 ml demin. water in a srewed-cap bottle. The solution was autoclaved and stored at room temperature.

Salt solution:

demin. water	200 ml
NaCl	58 g
$MgCl_2 \cdot 6H_2O$	8 g

The basic Pf medium was modified for the growth of *A. vinosum* strain MT86 by replacing $MgSO_4 \cdot 7H_2O$ by $MgCl_2 \cdot 6H_2O$ and by addition of thiosulfate and acetate.

The salt solution was according to (Imhoff, 2014) was used to adjust the salt concentration of the medium to determine the salt optimum of *A. vinosum* strain MT86 (1% salt = 3 ml salt solution into 100 ml modified Pf medium).

Solution 1 (basic medium in 5 L):

demin. water	4900 ml
KH_2PO_4	1.70 g
$NHCl_4$	1.70 g
$MgCl_2 \cdot 6H_2O$	2.06 g
$CaCl_2 \cdot 2H_2O$	1.25 g
KCl	1.70 g
Thiosulfate	5.00 g
$NH_4 \cdot$Acetate	1.25 g
Mg·Acetate	1.25 g

The AT medium for cultivation of purple nonsulfur bacteria was prepared in a 5 L Erlenmeyer flask. The two side openings of flask were closed by two silicon rubber stoppers with an inlet for gas and an outlet near the bottom with a screw-cap glass tube (the same one as Pf medium). One of the stoppers was closed during the medium preparation and anther one was used for adding other solutions. A silicon rubber tube interlinked the outlet to a filter, and another silicon rubber tube from filter outlet connected with a pinchcock and a bell for aseptic distribution of the medium into bottles (see Figure 2-2). The defined basal medium and additional solutions had the following composition:

Solution 2 of $NaHCO_3$ was saturated with CO_2 and autoclaved under a CO_2 atmosphere. The yeast extract solution was autoclaved too.

Solution 3 of Na-ascorbate (L (+)-Ascorbic acid sodium salt/$C_6H_7NaO_6$) was freshly prepared before adding to the flask. 2.5 g of Na-ascorbate was dissolved in 50 ml demin. water and added to the basal medium by 0.2 µm filter.

Solution 4, vitamin A (Imhoff, 2006) contained 10 mg biotin, 35 mg niacin amide, 30 mg thiamine dichloride, 20 mg *p*-aminobenzoic acid, 10 mg pyridoxal hydrochloride, 10 mg calcium pantothenate, and 5 mg vitamin B_{12} in 100 ml demin. water. Solution 4 was filtered by a 0.2 µm filter to the sterile tubes and stored at 4°C.

Solution 1: (basic medium in 5 L):	
demin. water	4700 ml
KH_2PO_4	5.0 g
$MgCl_2 \cdot 6H_2O$	2.5 g
$CaCl_2 \cdot 2H_2O$	0.5 g
$NHCl_4$	5.0 g
Na_2SO_4	3.5 g
$Na(C_2H_3O_2)$	5.0 g
$C_3H_3NaO_3$	5.0 g
NaCl	5.0 g
Solution 2:	
$NaHCO_3$	15 g in 200 ml demin. water.
Yeast extract	2.5 g in 50 ml demin. water.
Solution 3:	
L(+)-Ascorbic acid sodium salt/$C_6H_7NaO_6$	2.5 g in 50 ml demin. water.
Solution 4: Vitamin solution A	5 ml
Solution 5: SLA	5 ml

Solution 5 of sulfate-free trace element solution SLA (Imhoff, 2006) contained 1.8 g $FeCl_2 \cdot 4H_2O$, 250 mg $CoCl_2 \cdot 6H_2O$, 10 mg $NiCl_2 \cdot 6H_2O$, 10 mg $CuCl_2 \cdot 2H_2O$, 70 mg $MnCl_2 \cdot 7H_2O$, 100 mg $ZnCl_2$, 500 mg H_3BO_3, 30 mg $Na_2MoO_4 \cdot 2H_2O$ dissolve in 800 ml demin. water in order. The pH of the medium was adjusted to 1.0 with 1 M HCl demin. water to 1000 ml. SLA solution was stored at 4°C. When adding to 5 L basic medium (solution 1) of AT medium, 5 ml of sterilized solution SLA was added by a 0.2 μm filter.

After the medium had been autoclaved and cooled under an atmosphere of N_2, the five additional components were added in order aseptically while the medium was magnetically stirred and the access of air was prevented by continuous flushing with the gas of N_2.

The bottle of the AT medium with additions was tightened to the filter and both of the side openings were closed. The N_2 was opened firstly and then the clips were opened from gas side to other. The medium was then immediately dispensed aseptically under pressure of N_2 (0.05-0.1 atm) into sterile 100 ml, 500 ml, or 1 L bottles with metal screw caps containing autoclavable rubber seals. A small, pea-sized air bubble was left in each bottle to accommodate possible pressure changes.

2.2 Bacterial strains

All the information (*i.e.* taxonomic classification, type strains of genus, media for cultivation) of strains is given in Table 2-1.

Table 2-1. Strains' information.

No. strain	Media	Class	Group	Family	(Type) strains of genus
5212^{T}	Pf, 2% S, pH 7.2+Ac	Gammaproteobacteria	PSB	Chromatiaceae	*Marichromatium gracile* DSM 203 ^{T} (DSM203 ^{T} = =BN5210 ^{T})
5410^{T}*	Pf, 0% S, pH 7.2+Thio	Gammaproteobacteria	PSB	Chromatiaceae	*Thiocystis violascens* DSM 198 ^{T} (DSM198 ^{T} =BN 5410 ^{T})
5110 ^{T}	Pf, 0% S, pH 7.2	Gammaproteobacteria	PSB	Chromatiaceae	*Allochromatium vinosum* DSM 180 ^{T} (DSM 180 ^{T} = BN 5110 ^{T})
2310	Pf, 0% S, pH 6.8+Ac	Chlorobia	GSB	Chlorobiaceae	*Chlorobium limicola*
2410	Pf, 1% S, pH 6.8	Chlorobia	GSB	Chlorobiaceae	*Prosthecochloris aestuarii*
2360	Pf, 0% S, pH 6.8	Chlorobia	GSB	Chlorobiaceae	*Chlorobium phaeobacteroides*
120/1	AT	Alphaproteobacteria	PNSB	Bradzrhiyobiaceae	*Rhodopseudomonas palustris*
182	AT	Alphaproteobacteria	PNSB	Rhodobacteraceae	*Rhodobacter capsulatus*
151	AT	Betaproteobacteria	PNSB	Comamonadaceae	*Rubrivivax gelatinosus*
MT86	Pf, 0% S, pH 7.2+Ac+Thio	Gammaproteobacteria	PSB	Chromatiaceae	*Allochromatium vinosum* MT86

PSB: Purple sulfur bacteria; PNSB: Purple nonsulfur bacteria; GSB: Green sulfur bacteria; GNSB: Green nonsulfur bacteria
Thio: Thiosulfate solution; Ac: Actate solution; S: salt solution; T: Typical strain
*: Strain 5410 was identified to *Thiocystis violascens*, later in my study, 16S rRNA BLASTn result showed different.

2.3 Cultivation experiments

An overview of the cultivation experiment of *A. vinosum* strain MT86 is seen in flowchart of Figure 2-3.

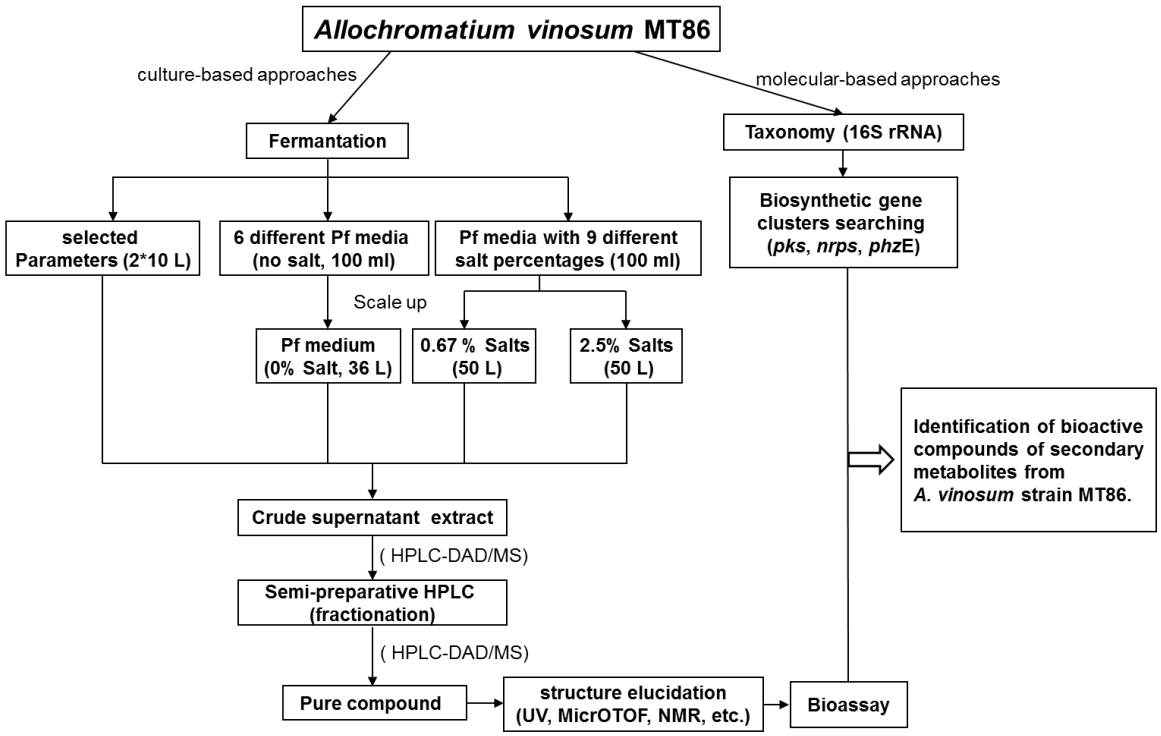

Figure 2-3. The flowchart of *A. vinosum* strain MT86.

2.3.1 Optimization of the growth condition for the cultivation of *A. vinosum* MT86

The *A.vinosum* strain MT86 was grown in liquid culture (100 ml or 1000 ml screw cap bottles) using freshly prepared Pf medium (no salt solution included) or Pf medium with salt solution (0%-3.33%).

A new fresh 100 ml Pf media was inoculated with a 5 ml of *A. vinosum* MT86 culture. The inoculated bottle was stored in the dark condition for 2 hours, then placed under the light of a tungsten lamp (ca. 1000 lux), and incubated at 28°C until turbidity was visible. Sulfide solution was added every two days until the bacteria grow well via microscopic observation, such as the state of movement, sulfur globules within the cells and the size of the cells. Afterwards, a 1 L fresh Pf medium was inoculated with the preculture mentioned above, and incubated under the same conditions. Finally, when the color of the broth became dark red and the bacteria grew well, new ten 1 L bottles (5% of each bottle) were inoculated with the aim to get enough biomass to analyze the produced compounds. Three times 10 L cultures of strain MT86 were incubated and grown at 28°C for 14 days before extraction according to the paragraph 2.4.1, on page 33.

2.3.2 Media for screening of optimal cultivation condition

A. vinosum strain MT86 was cultivated using several modifications of Pf medium. All changed parameters are shown in Table 2-2. Because thiosulfate and acetate were added into the basic medium, no more sulfide solution was needed during growth. All bottles of *A. vinosum* MT86 grew at 28°C and 1000 lux light intensity.

Table 2-2. Changed parameters of Pf media.

	New parameters	Old parameters
Basic medium	$MgCl_2 \cdot 6H_2O$	$MgSO_4 \cdot 7H_2O$
	Thiosulfate	/
	Acetate	/
Sulfide	New crystal	Old sulfide
Trace element solution	SLA	SL-12
Preparation	no N_2 gas	N_2 gas
Pre-culture	liquid N_2 vial	4°C stored culture
Additional sulfide solution	/	added every 2 days

/: not used

Table 2-3. The protocol of incubation of *A. vinosum* strain MT86 in different Pf media and control media.

No. of bottles	Name of medium	Volume
1	Pf ($MgSO_4$) + Thiosulfate	100 ml
2	Pf ($MgSO_4$) + Thiosulfate + Acetate	100 ml
3	Pf ($MgCl_2$) + Thiosulfate	100 ml
4	Pf ($MgCl_2$) + Thiosulfate + Acetate	100 ml
5	Pf ($MgSO_4$)	100 ml
6	Pf ($MgCl_2$)	100 ml
7	Control of Pf ($MgSO_4$)	100 ml
8	Control of Pf ($MgCl_2$)	100 ml
9	Control of Pf ($MgCl_2$) without Sulfide	100 ml
10	Control of Pf ($MgCl_2$) without Sulfide	1 L

After 10 days of incubation, the cultures and corresponding controls of Pf medium (Table 2-3) media were extracted using ethyl acetate and analyzed by HPLC-DAD/MS and used for bioassays.

2.3.3 Scale up to a 36 L culture volume of *A. vinosum* strain MT86

The extracts were analyzed and Pf medium amended with 1% thiosulfate and 1% acetate-solution (NH_4-acetate/Mg-acetate, 2.5 g each/100 ml) was the best stable incubation condition for *A. vinosum*

strain MT86. Scale up to a 36 L (36 bottles of 1 L Pf medium) approach was preformed using this optimal condition.

36 L Pfennig´s medium with 5% bacteria (50 ml preculture per 1 L Pf medium) was inoculated. All the bottles were stored in the dark condition for 2 hours, then placed under the light of a tungsten lamp (ca. 1000 lux), and incubated at 28°C for 11 days. 36 L of culture broth was extracted by ethyl acetate. The crude supernatant extract for HPLC-DAD/MS was prepared by the method as described in paragraph 2.4.1, on page 33.

2.3.4 Salt tolerance of *A. vinosum* strain MT86

According to Bergey's Manual of Systematic Bacteriology (Imhoff, 2005b), the mesophilic freshwater bacterium *A. vinosum* showed an optimal growth at 25-35°C and pH 7.0-7.3 (range pH 6.5-7.6). There were no distinct requirements for salt of the mesophilic bacterium, except for strains that originate from the marine and brackish water environment and may tolerate or require low concentrations of NaCl. *A. vinosum* was enriched at high sulfide concentrations (3-4 mM), at high light intensities of more than 1000 lux and at incubations temperature of 20-30°C. Some interesting results were shown by Dr. Marcus Tank (2010) about the salt concentration for phenotypes related to *Allochromatium vinosum*. They obviously tolerated elevated salt concentrations and can compete even at hypersaline conditions, which contrasted to the properties known from the genus *Allochromatium*. Previous work was based on the properties of the genus *Allochromatium*. Therefore, for experiments on the first screening and optimal cultivation conditions, Pf medium without salt solution was used for cultivation. If these bacteria can tolerate salt, the addition of salt might stimulate the secondary metabolites of *A. vinosum* strain MT86.

2.3.4.1 100 ml Pf medium approach

In order to study the influence of salt concentration to the compounds production, different salt concentrations (0%, 0.33%, 0.67%, 1%, 1.67%, 2.33%, 2.5%, 2.67%, and 3.33%) were used (see in Table 2-4).

Table 2-4. Growth parameters for cultivation at different salt concentrations.

Salt concentration	0%, 0.33%, 0.67%, 1%, 1.67%		2.33%, 2.5%, 2.67%, 3.33%	
Incubation time	7 days	10 days	15 days	20 days*
Culture volume	100 ml			
Mg^{2+}	$MgCl_2 \cdot 6H_2O$			
Thiosulfate & acetate	1% thiosulfate, 1% acetate			
Light intensity	1000 lux			
Temperature	28-30°C			

*: Culture broth at 2.67% salts after 20 days was contaminated.

2.3.4.2 Scale up to a 50 L approach using optimized Pf medium

From the former part of screening, the crude supernatant extract of culture grown at 0.67% salt after 10 days showed the maximum numbers of peaks from the HPLC-DAD/MS chromatogram and crude supernatant extract from culture grown at 2.33% salts after 15 days showed another series of UV absorption peaks. Thus, 0.67% and 2.5% salts of Pf media were chosen for scaling up for cultivation and extraction. The Pf medium with $MgCl_2 \cdot 6H_2O$, 1% thiosulfate solution, and 1% acetate solution were incubated at 1000 lux, 28-30°C.

Table 2-5. Growth parameters for 50 L cultivation at different salt concentrations.

Parameters	Value of each parameter	
Salt	0.67%	2.5%
Incubation time	10 days	15 days
Culture volume	50 L	50 L
Extraction volume	45 L	50 L

2.4 Chemical screening and structure identification

The culture broth of *A. vinosum* strain MT86 was centrifuged to separate the cell biomass and liquid supernatant. HPLC-DAD/MS and semi-preparative HPLC were used to set first insights into the presence of compounds in the crude extracts. Using the semi-preparative HPLC, most peaks seen from the analytical HPLC chromatogram were separated and used for biological activity tests. Selected fractions which showed bioactivity were purified and their chemical structure was analysed by different methods (MS, NMR).

2.4.1 Extraction procedures

The culture broth was centrifuged to separate cell biomass and supernatant. These two parts were extracted in different approaches to determine whether the compounds exist in the cells or are secreted into the medium.

2.4.1.1 Separation of cells and supernatant by centrifugation

Centrifugation steps were done as follows:

1) The centrifuge tubes were weighted before and after centrifugation. The broth was centrifuged in 500 mL centrifuge tubes at 10,000 rpm × 15 min, 4°C. For 100 ml culture broth, 50 ml centrifugation tubes were used at 4670 rpm × 20 min, 4°C.

2) Upper supernatant was collected in new blue-screw glass bottles and the cell pellets were left in the bottle with the next centrifugation.

3) For the cell part, 250 ml of MeOH was added to each centrifugation tube and homogenized by use the Ultraturrax for 1 min.

4) All extraction tubes were kept in the darkness overnight at 4°C until further treatment.

2.4.1.2 Extraction of the supernatant/control medium and evaporation

The supernatant was extracted in a 2 L separation funnel as follow:

1) 500 ml/100 ml supernatant was transferred into a 2000 ml/500 ml separatory funnel and the same volume (1:1) of ethyl acetate (EtOAC) was added.

2) The separatory funnel was shaken for 1 min and the phases were allowed to separate.

3) The lower water phase was discarded.

4) 100 ml demin. water was added to wash the ethyl acetate phase. The funnel was shaken again and after phase separation, the lower water phase was discarded.

5) The upper phase was collected and filtered through a 1PS paper phase separator (GE Health Waterman™, 180 mm), a high-grade filter paper impregnated with a stabilized silicone that renders it hydrophobic, retaining the aqueous phase and any solid impurities and passing the solvent phase through.

6) EtOAc was evaporated using a rotational evaporator at the 40°C water bath with 200 mbar.

7) The round-bottom flasks were weighed before and after evaporation to get the dry weight of the total supernatant extract.

8) MeOH was added to the dry crude supernatant extract and the dissolved extract was transferred to a brown bottle for storage at 4°C.

For control experiment, Pf medium was extracted directly by ethyl acetate without centrifugation steps.

2.4.1.3 Extraction of the cell pellets and evaporation

After centrifugation of a 500 ml culture, 100 ml MeOH was added to the cell pellets for extraction. The solvent suspension is kept in the darkness overnight and further extraction steps were performed as following described.

1) The cell suspension of a 100 ml culture was evaporated to dryness.

2) A suitable volume of MeOH (1-5 ml) was added to the dried cells and cell extract.

3) 500 ml demin. water was added and the sonic bath was used to wash the flask for several times.

4) 500 ml above dissolved extract was taken to the separator funnel.

5) 500 ml of EtOAc was added to the cell/methanol suspension, and the mixture was shaken for extraction. After phases' separation, the lower water phase was discarded and the upper solvent phase was collected.

6) 100 mL demin. water was added to wash the ethyl acetate phase. The mixture was shaken and after phase separation, the lower water phase was discarded and the upper solvent phase was collected.

7) A 1 PS paper phase separator was used to retain the aqueous phase and any solid impurities.

8) The round-bottom flasks were weighed before and after evaporation to get the dry weight of the crude cell extract.

9) MeOH was added to the dry crude cell extract and the dissolved extract was transferred to a brown bottle for storage at 4°C.

For cells from 100 ml cultures, the volume of solvents used for extraction was one-fifth of the values shown above.

2.4.2 Analytical HPLC-DAD/MS

All crude extracts were analyzed by HPLC-DAD/MS. The HPLC samples were prepared as following described.

1) 0.3 ml extracts were taken by a syringe and filtered (0.25µm) into a HPLC weighed vial.

2) The extracts were evaporated to dryness in a flow of nitrogen gas generator LCMS 30-0 (Domnick Hunter) until dry. The vials were weighed after evaporation of the solvent.

3) MeOH was added to adjust the concentration for injection into HPLC to 1.0 mg/ml.

4) Pf medium extract was chosen as negative control and MeOH was as solvent control.

The analytical HPLC was performed using a system comprised of a Hitachi Elite LaChrom system; it contains the autosampler L2200 injection port (Rheodyne LLC, Rohnert Park, CA, USA), organizer, diode array detector L 2450 (DAD), the column oven L 2300, and a L2130 pump (Hitachi Ltd. Tokyo, Japan). The crude extracts were subjected to HPLC-DAD/MS using a reversed phase C18 column (100 × 3.00 mm, Phenomenex Onyx Monolithic) with solvent A (0.1% formic acid in 100%

acetonitrile) and solvent B (0.1% formic acid in 100% miliQ H_2O) with the gradients shown in Table 2-6.

Table 2-6. The solvent gradients for analytical HPLC using a flow of 2 ml/min.

Time	Gradient	
	A	B
0 min	95%	5%
4 min	40%	60%
6 min	0%	100%

Solvent A: 0.1% formic acid in 100% acetonitrile;
Solvent B: 0.1% formic acid in 100% miliQ H_2O.

By using of an ESI-ion trap detector (Esquire 400, Bruker Daltonics) along with LaChrom system, the samples were measured with positive and/or negative ionization (Esquire 4000, Bruker Daltonics). The mass spectra and UV chromatograms of the extracts were analyzed by using of Bruker Daltonics-Compass Analysis 4.0 and Compass Hystar Post Processing software respectively. Molecular weight, UV maxima and biological sources were used for identification of the compounds by using of dictionary of natural products DNPs (Chapman, 2012).

2.4.3 Fractionation of crude supernatant extract by semi-preparative HPLC

All samples were dissolved in MeOH and filtered through 0.2µm PTFE syringe filters before applying to analytical HPLC and semi-preparative HPLC.

Semi-preparative HPLC was performed using a VWR Hitachi Elite LaChrom HPLC system. This system consisted of a C18 column (110A AXIA, 100 × 50.00 mm, Phenomenex Gemini) or polar column (4 µl Polar-RP 80A, 250 × 21.20 mm, Phenomenex Synergi), a L-2200 autosampler, a fraction collector (Foxy Jr. ISCO), a L-7150 pump, and an L-2450 diode array detector (DAD). Solvents A (0.1% formic acid in 100% acetonitrile) and B (0.1% formic acid in 100% miliQ H_2O) were used as solvents for semi-preparative HPLC.

Specific gradient (Table 2-7) of solvent A and solvent B were applied to this semi-preparative HPLC system for fractionation. Hitachi HPLC system separated the compounds or fractions by monitoring UV absorption between at 200 to 550 nm wavelengths. The injection concentration was 100 mg/ml, and injection volume was 300-900 µl. Finally, fractions were collected.

Semi-preparative HPLC programs for 1st (10 L) and 2nd & 3rd (totally 20 L: 10 L + 10 L) extracts were identical. However, there were differences in the collection methods (according to time or UV absorption).

Table 2-7. The gradient used for semi-preparative HPLC of the extract from the 36 L culture of *A. vinosum* strain MT86.

Time	Gradient		Flow/ml
	A	B	
0 min	90%	10%	5
0.5 min	80%	20%	10
26 min	0%	100%	15
30 min	0%	100%	15

Solvent A: 0.1% formic acid in 100% acetonitrile;
Solvent B: 0.1% formic acid in 100% miliQ H_2O.

The injection of 1st extracts of *A. vinosum* strain MT86 was 900 µl and fractions were collected according to time. The whole separation time of the preparation run was 24 minutes and every minute a fraction was collected. Because the first two fractions were mixed together, they were combined to one fraction. In total, 23 fractions were obtained.

The combined 2nd & 3rd crude extracts were fractionated according to UV absorption. An injection volume of 900 µl was applied for four times. All fractions showing a clear UV signal were manually collected. Finally, 10 fractions were obtained, and fraction tube nine (named F9) was mixed from the semi-preparative HPLC chromatogram.

The solvents were removed by rotation in vacuum. Then, fractions were resuspended in methanol, which was evaporated by nitrogen flow at 40°C and stored at 4°C. The purification of the fractions was checked by analytical HPLC-DAD/MS.

In comparison of the two different methods of collection, UV signal dependent fractionation was a better way to obtain pure fractions. Later all samples (crude supernatant extracts of 36 L, 45 L and 50 L) were fractionated by UV absorption manually and with a modified gradient program (Table 2-8).

Table 2-8. Modified gradient used for semi-preparative HPLC of the 36 L, 45 L and 50 L *A. vinosum* strain MT86 supernatant extracts.

Time	Gradient		Flow/ml
	A	B	
0 min	80%	20%	5
0.5 min	80%	20%	10
26 min	0%	100%	10
30 min	0%	100%	10

Solvent A: 0.1% formic acid in 100% acetonitrile;
Solvent B: 0.1% formic acid in 100% miliQ H_2O.

2.4.4 Screening of crude cell extract (TLC)

Crude cell extracts were performed by thin layer chromatography (TLC). The crude cell extracts (MeOH as solvent) were filtered (the filtered fraction) and the residue was treated with acetone. The acetone-dissolved compounds were separated by filtration (acetone-extract fraction) and the residue was extracted with methyl dichloride if the undissolved material was left. The methyl dichloride extract was filtered again (methyl dichloride extract fraction) and separated according to Prof. Dr. A. Zeeck (personal communication).

2.4.5 Antimicrobial activities screening

The crude extracts and fractions were assayed for their antimicrobial activity by cell based assays. The test organisms used are listed in Table 2-9.

Antimicrobial activity tests against *Bacillus subtilis*, *Staphylococcus aureus*, *Staphylococcus lentus*, *Propionibacterium acnes* (representatives of Gram-positive bacteria) and *Escherichia coli*, *Pseudomonas syringe*, *Xanthomonas campestris*, *Erwinia amylovora*, and *Ralstonia solanacearum* (representative of Gram-negative bacteria) were performed as described by Schneemann *et al.* (2010), Silber *et al.* (2013), Alfano and Collmer (1996), Mitchell and Teh (2005), and Yin *et al.* (2004). A phytopathogenic *Septoria tritici*, dermatophyte *Trichophyton rubrum*, *Candida albicans*, and *Candida glabrata* were employed for antifungal tests according to Jansen *et al.* (2013). Four enzymes, acetylcholinesterase (AchE), glycogen synthase kinase 3β (GSK-3β), phosphodiesterase 4 (PDE-4β2) and protein-tyrosine-phosphatase (PTP) were used for enzyme inhibition assays.

The acetylcholinesterase (AchE) is an enzyme to cleave the neurotransmitter acetylcholine. It is used as a target for the treatment of Alzheimer's disease (Bolognesi *et al.*, 2008). Inhibitory activity against AchE and the human pathogenic yeast *C. albicans* were performed according to Ohlendorf *et al.* (2012).

The enzyme glycogen synthase kinase 3β (GSK-3β) is a key regulator of many signal transduction pathways. The therapeutic benefits of glycogen synthase kinase inhibitors was in the treatment of type II diabetes, neurological diseases and cancer (Martinez *et al.*, 2002). The assay was performed according to Baki *et al.* (2007).

Phosphodiesterase 4 (PDE-4β2) forms second messengers such as cyclic andenosin monophosphat (cAMP) and cyclic guanosine monophosphate (cGMP), and PDE-4β2 inhibitors were applied for treatment of depression and Alzheimer's disease (Houslay and Adams, 2003). The inhibitory activity against PDE-4β2 were determined according to Schulz *et al.* (2011).

The test for protein tyrosine phosphatase (PTP) was implemented following to Helaly *et al.* (2009).

Table 2-9. Microbial strains and enzymes used for the bioactivity assay.

	Strains*	**Abbreviation**	**DSMZ No.**
Gram-positive bacteria	*Bacillus subtilis*	*Bs*	DSM 347
	Staphylococcus aureus	MRSA	DSM 18827
	Staphylococcus lentus	*Sl*	DSM20352.
	Propionibacterium acnes	*Pa*	DSM 1897
Gram-negative bacteria	*Escherichia coli*	*Ec*	DSM 498
	Pseudomonas syringae	*Ps*	DSM 10604
	Xanthomonas campestris	*Xc*	DSM 3586
	Erwinia amylovora	*Ea*	DSM 30165
	Ralstonia solanacearum	*Rs*	DSM 9544
Yeast and fungi	*Candida albicans*	*Ca*	DSM 1386
	Septoria tritici	*Sep*	/
	Trichophyton rubrum	*Tru*	/
	Candida glabrata	*Cg*	DSM 6425
Enzymes	Acetylcholinesterase	AchE	/
	Glycogen synthase kinase 3β	GSK-3β	/
	Phosphodiesterase 4	PDE-4β2	/
	Protein-tyrosin-phosphatase	PTP	/

*All obtained from DSMZ (Braunschweig, Germany); /: no DSMZ number.

The crude extracts and fractions were added to the wells (10 µl) in a 96-well microtiter plate for inhibitory bioassay and pure substances were dissolved in dimethyl sulfoxide (DMSO) and added to a concentration of 100 µM for antibacterial and antifungal activity, and to 10 µM for enzymatic assays for IC_{50}. The pure substances were pipetted in a 96-well microtiter plate and the solvent evaporated in vacuum. All media used for bioassay tests are shown in Table 2-10.

The test samples (crude extracts, fractions, or substances) were pipetted to the wells in a 96-well microtiter plate (two wells for every sample), and positive control (chloramphenicol solution), negative control (wells without extract or positive control, just bacteria cells), and blank value (just medium) were set. The microplate was placed into a centrifugal evaporator to eliminate solvent in order to have a dry microplate with the substances.

The respective indicator organisms were cultured overnight in corresponding medium (TSB medium and M186/3 media were used for bacteria and yeast cultivation, respectively), and diluted with medium to a final optical density (OD_{600}) of 0.01 for *B. subtilis* and *S. lentus*, and 0.02 for *X. campestris*.

Table 2-10. Media and solutions used for bioactivity tests.

Medium name	Composition
TSB medium	1.2% tryptic soy broth 0.5% NaCl
M186/3 medium	0.1% yeast extract 0.1% malt extract 0.17% peptone from soybeans 0.33% glucose
Resazurin solution	0.2 mg ml^{-1} phosphate-buffered saline
Positive control	10 µM chloramphenicol for bacteria 10 µM nystatin for the yeast
Negative control	blank/no compound

To the dry microplate, 200 µl of the diluted test organism was added into each well and incubated for 5 h, 37°C, 200 rpm (*B. subtilis* and *S. lentus*), or for 6 h, 28°C, 200 rpm (*X. campestris*). 10 µl resazurin solution was added to each well, and the microplate was incubated for 5-60 min (37°C, 120 rpm) until color changed. To evaluate cell viability, the reduction of resazurin to resorufin was assessed by measuring the absorbance at 600 nm (600 nm was a modified wavelength; the reference absorbance was 690 nm). The resulting values were compared with a positive and a negative control (100% growth = 0% inhibition) on the same plate. The calculation of the inhibition of the extracts (in %) was carried out over the rule of proportion. If the accurate mass of substance was known, the IC_{50} value can be calculated.

2.4.6 NMR analysis

Fractions which showed high purity (a single UV signal or > 90%) were analyzed by different NMR methods, such as ^{1}H NMR, and ^{13}C NMR.

^{1}H and ^{13}C NMR spectra were recorded on a Bruker DRX 500 (600 and 150 MHz) with tetramethylsilane (TMS) as the internal standard. Methanol-d_4 (MeOD) (residual peaks are δ_H 3.31 ppm, and δ_C 49.0 ppm) was used as the solvent in ^{1}H NMR and ^{13}C NMR. Coupling constants (*J*) were given in Hz. NMR measurements were performed at the Otto-Diels-Institute of Organic Chemistry (Christian-Albrechts University of Kiel, Prof. Dr. Frank Sönnichsen). MestReNova was used for spectra analysis (Version 9.0.1, 2014, Mestrelab Research S. L., Santiago de Compostela, Spain).

2.4.7 TOF-MS

Measurements of high-resolution mass spectra were performed on a benchtop time-of flight spectrometer (TOF-MS, Agilent 6210 TOF LC/MS Spectrometer) with positive and negative ESI by

Dr. Bin Wu at Zhejiang University (Hangzhou, China) and Prof. Dr. Axel Zeeck at BioViotica Naturstoffe GmbH (Göttingen, Germany).

2.5 Other strains of phototrophic bacteria

From the established global sampling collection of anaerobic photosynthetic bacteria, three potential antimicrobial purple nonsulfur bacteria (*Rhodopseudomonas palustris* strain 120/1, *Rhodobacter capsulatus* strain 182, *Rubrivivax gelatinosus* strain 151) were chosen for products research and analysis.

2.5.1 First screening of selected strains

Firstly, 500 ml of each strain was incubated and the supernatants were extracted as the same method as strain MT86. The incubation parameters are given in Table 2-11. All strains were grown in 500 ml AT medium with 1% inoculation preculture. The bacteria were grown at 1000 lux, 28°C for 7 days and then extracted with ethyl acetate. Crude extracts were used for bioassays.

Moreover, for optimal growth determination, these three strains were incubated under the same parameters as above for 7 d and 10 d in 100 ml bottle with AT medium. Extraction, HPLC analysis, and bioassay tests were performed by the same methods as previous described (paragraph 2.4, on page 33).

Table 2-11. Growth conditions of strains 120/1, 151, and 182.

Parameters	Values
Incubation time	7 d
Basic medium	AT
Volum of medium	500 ml
Inoculation percentage	1%
Light intensity	1000 lux
Temperature	28°C

2.5.2 Scale up of cultivation of *Rubrivivax gelatinosus* strain 151 and fractionation the crude extract by semi-preparative HPLC

Rubrivivax gelatinosus 151 was chosen for 20 L scale up approach because the HPLC results showed that there were interesting compounds at Rt 5.0 to Rt 6.5 min. Extraction, HPLC analysis, and semi-preparative HPLC were performed by the same methods as previous used for *A. vinosum* strain MT86 (paragraph 2.4, on page 33).

2.6 Molecular screening

Molecular screening contains the DNA extraction, PCR amplification, sequencing and BLASTn analysis of selected phototrophic bacteria. For whole genome sequences analysis, antiSMASH was used for secondary metabolites screening.

2.6.1 DNA extraction

The DNA extraction of strains was performed by two different kits, Biofilm® DNA Isolation Kit was used for fresh culture samples and DNeasy® Blood & Tissue Kit was used for both fresh culture samples and frozen samples (stored at -20°C) as recommended by the manufacture.

2.6.2 PCR and sequencing

PCR amplification of the 16S rRNA, *pks* I, *pks* II, *nrps* and *phz*E genes were performed using modified primer sets based on primers previously published. The primer sequences are seen in Table 2-12.

16S rRNA gene sequences were amplified using the primers 27F and 1492R PCR and amplificates were sequenced with the primers 342f, 790f and 543r. The 16S rRNA gene sequence was submitted to the GenBank database for BLASTn similarity analysis. Sequencing of the *pks* I, *pks* II, *nrps*, and *phz*E gene fragments were assembled by using their pairs of PCR primers, respectively. Amplification of *pks* I, *pks* II, *nrps*, and *phz*E were used to screen the potential of secondary metabolite biosynthesis on the molecular level. The PCR systems and programs are shown in Table 2-13, Table 2-14, Table 2-15, Table 2-16, and Table 2-17.

Table 2-12. Primers used in this study.

Primers		Sequence	Expected fragment length	References
16S rRNA	27F	5'- AGAGTTTGATCMTGGCTCAG-3'	1500 nt	Brosius *et al.* (1978)
	1492R	5'- TACGGYTACCTTGTTACGACTT-3'		Suzuki and Giovannoni (1996)
	342f	5'-TACGGGAGGCAGCAG-3'		Stackebrandt and Goodfellow (1991)
	790 f	5'-GATACCCTGGTAGTCC-3'		Muyzer *et al.* (1993)
	543 r	5'-ATTACCGCGGCTGCTGG-3'		Muyzer *et al.* (1993)
pks I	K1F	5´TSAAGTCSAACATCGGBCA3´	1200-1400 nt	Ayuso-Sacido and Genilloud (2005)
	M6R	5´CGCAGGTTSCSGTACCAGTA3´		
pks II	945f	5´TSG CST GCT TCG AYG SA TC3´	600-613 nt	Metsä-Ketelä *et al.* (1999)
	945r	5´TGG AAN CCG CCG AAB CCG CT3´		
nrps	A2f	5´AAG GCN GGC GSB GCS TAY STG CC 3´	300 nt	Doekel and Marahiel (2001)
	A3r	5´TTG GGB IKB CCG GTS GIN CCS GAG GTG 3´		
*phz*E	*phz*Ef	5´-GAAGGCGCCAACTTCGTYATCAA-3´	450 nt	Schneemann *et al.* (2011)
	*phz*Er	5´-GCCYTCGATGAAGTACTCGGTGTG-3´		

Table 2-13. PCR system of 16S rRNA and program.

PCR system	(25 µl)	PCR Program		
ddH_2O	3.0 µl	95°C	5 min	
27F (10 pmol/µl)	1.0 µl	95°C	30 sec	
1492R (10 pmol/µl)	1.0 µl	55°C	2 min	
2 × DreamTaq Green Mastermix	12.5 µl	72°C	4 min	to 2) 35×
DMSO	2.5 µl	72°C	10 min	
Template	5.0 µl	10°C	∞	

Negative control was 5.0 µl ddH_2O as template.

Table 2-14. PCR system of *pks* I and program.

PCR system	(25 µl)	PCR Program		
ddH_2O	3.0 µl	95°C	5 min	
K1F (10 pmol/µl)	1.0 µl	95°C	30 sec	
M6R (10 pmol/µl)	1.0 µl	55°C	2 min	
2 × DreamTaq Green Mastermix	12.5 µl	72°C	4 min	to 2) 35×
DMSO	2.5 µl	72°C	10 min	
Template	5.0 µl	10°C	∞	

Positive control for *pks* I was 1.5 µl *Streptomyces clavuligerus* DSM 738 and 3.5 µl ddH_2O, and negative control was 5.0 µl ddH_2O as template.

Table 2-15. PCR system of *pks* II and program.

PCR system	(25 µl)	PCR Program		
ddH_2O	3.0 µl	95°C	5 min	
945f (50 pmol/µl)	1.0 µl	95°C	30 sec	
945r (50 pmol/µl)	1.0 µl	55°C	2 min	
2 × DreamTaq Green Mastermix	12.5 µl	72°C	4 min	to 2) 35×
DMSO	2.5 µl	72°C	10 min	
Template	5.0 µl	10°C	∞	

Positive control for *pks* II was 5 µl *Streptomyces achromogenes* DSM 40789, and negative control was 5.0 µl ddH_2O as template.

Table 2-16. PCR system of *nrps* and program.

PCR system	(25 µl)	PCR Program		
ddH_2O	5.5 µl	95°C	2 min	
A2f (10 pmol/µl)	1.0 µl	95°C	1 min	
A3r (10 pmol/µl)	1.0 µl	68°C	1 min	
2 × DreamTaq Green Mastermix	12.5 µl	72°C	2 min	to 2) 39×
Template	5.0 µl	72°C	7 min	
		10°C	∞	

Positive control for *nrps* was 1.5 µl *Pseudomonas* sp. DSM 50117 and 3.5 µl ddH_2O, and negative control was 5.0 µl ddH_2O as template.

Table 2-17. PCR system of *phz*E and program.

PCR system	(25 µl)	PCR Program		
ddH_2O	5.5 µl	95°C	2 min	
*phz*E f (10 pmol/µl)	1.0 µl	95°C	1 min	
*phz*E r (10 pmol/µl)	1.0 µl	68°C	1 min	
2 × DreamTaq Green Mastermix	12.5 µl	72°C	2 min	to 2) 39×
Template	5.0 µl	72°C	7 min	
		10°C	∞	

Positive control for *phz*E was 1.5 µl *Pseudomonas* sp. DSM 50117 and 3.5 µl ddH_2O, and negative control was 5.0 µl ddH_2O as template.

2.6.3 Gel electrophoresis

1.0% 1×TBE agarose gel (1.0 g agarose dissolved in 100 ml TBE solution with SYBR® safe staining for *pks* I, *pks* II, and *phz*E, GelGreen™ staining for *nrps*) was prepared and the gel electrophoresis was performed at 130 V for 30 min for detection or 80 min for gel purification. The ingredients of 1 × TBE solution (pH 8.0) were 121.14 g Tris, 51.32 g boric acid, and 3.72 g EDTA.

The marker for *pks* I, and *pks* II was 8 µl Marker X and for *nrps* was 3 µl GeneRuler™ 100 bp DNA Ladder Plus. Both markers were used for *phz*E.

2.6.4 Purification

The DNA bands of the PCR amplification were cut from the TBE agarose gel and purified using UltraClean® 15 DNA Purification Kit (extracting DNA from a TBE agarose gel) according to the manufacture.

2.6.5 BLASTn analyses

Sequencing was performed at the Institut für Klinische Molekularbiologie (Christian-Albrechts University of Kiel) using the BigDye Terminator v1.1 Sequencing Kit (Applied Biosystems, USA) in a 3730-DNA-Analyzer (Applied Biosystems, USA) as specified by the manufacturer. Sequences were edited by ChromasPro (ChromasPro version 1.7.6, 2012, Technelysium Pty Ltd, South Brisbane, Queensland, Australia), and deposited in the NCBI database for BLASTn research (http://blast.ncbi.nlm.nih.gov/Blast.cgi?PROGRAM=blastn&PAGE_TYPE=BlastSearch&LINK_LOC=blasthome).

Isolates were identified using 16S rRNA gene sequencing combined with BLASTn analysis. The established *pks* I, *pks* II, *nrps*, and *phz*E sequences were deposited in NCBI databases and used for BLASTn analyses with available genome information on secondary metabolite biosynthesis genes.

2.7 Genome evaluation of phototrophic bacteria from databases

As far as known, phototrophic bacteria were not paid much attention in secondary metabolites research. Except the traditional natural compounds screening and isolation, the completely genome-based molecular screening was a useful way to predetermine the potential of bioactive compounds of these bacteria. Completed sequences or accession numbers were obtained from GenBank databases (ftp site or *Genome* searching). Automated gene prediction and functional annotation was performed by antiSMASH for detecting biosynthetic clusters of secondary metabolites in the genomes of phototrophic bacteria.

A complete overview of all available genome sequence from the phototrophic bacteria can be seen in Table 2-18.

Table 2-18. Overview of 62 genera belonging to anerobic anoxygenic phototrophic bacteria, genome sequences are available of taxa in bold.

Class	Order	Family	Abb.	Genus	*
Gamma-proteobacteria (phototrophic purple sulfur bacteria, PSB)	Chromatiales	Chromatiaceae	*Chr*	*Chromatium*	
			Alc	***Allochromatium***	1
			Hch	*Halochromatium*	
			Isc	*Isochromatium*	
			Lpb	*Lamprobacter*	
			Lpc	*Lamprocystis* (previous name *Pfennigia*)	
			Mch	***Marichromatium***	1
			Rbc	*Rhabdochromatium***	
			Tch	*Thermochromatium*	
			Tac	*Thioalkalicoccus*	
			Tca	*Thiocapsa*	
			Tco	*Thiococcus*	
			Tcs	***Thiocystis***	1
			Tdc	*Thiodictyon*	
			Tfc	***Thioflavicoccus***	1
			Thc	*Thiohalocapsa*	
			Tlp	*Thiolamprovum*	
			Tpd	*Thiopedia*	
			Trc	*Thiorhodococcus*	
			Trv	*Thiorhodovibrio*	
			Tsp	*Thiospirillum*	
			Tba	*Thiobaca****	
			Tpc	*Thiophaeococcus****	
		Ectothiorhodospiraceae	*Ect*	*Ectothiorhodospira*	
			Hlr	***Halorhodospira***	1
			Trs	*Thiorhodospira*	
Alpha-proteobacteria (purple nonsulfur bacteria, PNSB)	I. Rhodospirillales	I. Rhodospirillaceae	*Rsp*	***I. Rhodospirillum***	4
			Phs	*V. Phaeospirillum*	
			Rcs	*VI. Rhodocista*	
			Rsa	*VII. Rhodospira*	
			Rhv	*VIII. Rhodovibrio*	
			Ros	*IX. Roseospira*	
			Rss	*X. Roseospirillum*	
		II. Acetobacteraceae	*Rpi*	*XI. Rhodopila*	
	III. Rhodobacterales	I. Rhodobacteraceae	*Rba*	***I. Rhodobacter***	5
			Rbc	*XIII. Rhodobaca*	
			Rvu	*XIV. Rhodovulum*	
			Rts	*XXVI. Rhodothalassium*	
	VI. Rhizobiales	X. Rhodobiaceae	*Rbi*	*I. Rhodobium*	
		VIII. Hyphomicrobiaceae	*Blc*	*VII. Blastochloris*	
			Rmi	***XVI. Rhodomicrobium***	1
			Rpl	*XVII. Rhodoplanes*	
		VII. Bradyrhizobiaceae	*Rbl*	*VIII. Rhodoblastus*	
			Rps	***IX. Rhodopseudomonas***	7
Beta-	I. Burkholderiales	IV. Comamonadaceae	*Rfx*	*IX. Rhodoferax*	

proteobacteria (purple nonsulfur bacteria, PNSB)			*Rvi*	***XV. Rubrivivax***	1
	VI. Rhodocyclales	I. Rhodocyclaceae	*Rcy*	*I. Rhodocyclus*	
Green sulfur bacteria (GSB)	Phylum: Chlorobi Class I: Chlorobia Subclass I: Order I: Chlorobiales Family I: Chlorobiaceae **Green Sulfur Bacteria**		*Chl*	***I. Chlorobium***	**7**
			Anc	*II. Ancalochloris*	
			Chp	***III. Chloroherpeton***	**1**
			Pld	***IV. Pelodictyon*****	**1**
			Ptc	***V. Prosthecochloris***	**1**
			Cba	***Chlorobaculum******	**1**
Green nonsulfur bacteria (GNSB) (Filamentous anoxygenic phototrophic bacteria)	Phylum: Chloroflexi Class I: Chloroflexi Order I: Chloroflexales Family I: Chloroflexaceae		*Cfl*	***Chloroflexus***	**3**
			Cln	*Chloronema*	
			Htr	*Heliothrix*	
			Osc	*Oscillochloris*	
			Rof	***Roseiflexus***	**2**
Heliobacteria	Phylum: Firmicutes Class I: Clostridia Order I: Clostridiales Family VI: Heliobacteriaceae		*Hbt*	***Heliobacterium***	**1**
			Hba	*Heliobacillus*	
			Hph	*Heliophilum*	
			Hrs	*Heliorestis*	
Sum				62/**18**	**32**

*: Number of strains which genome sequence available;

**: There are two species of *Pelodictyon*, and one of them has changed the name to *Chlorobium luteolum* DSM 273;

***: The strains are new ones after Bergey's Manual of Systematic Bacteriology (2nd Edition).

Total 62 genera were known belonging to anaerobic anoxygenic phototrophic bacteria (Table 2-18), including purple sulfur bacteria (PSB), purple nonsulfur bacteria (PNSB), green sulfur bacteria (GSB), green nonsulfur bacteria (GNSB), and heliobacteria. Number of species for a genus ranged from one to eight. Among them, there are 32 genome sequences available for 18 genera.

18 specific species for which a genome sequence was available were summarized in Table 2-19. Those whole genome sequences or NCBI reference accession numbers were uploaded to online antiSMASH for secondary metabolites prediction screening. The results were collected and analyzed compare with the PCR amplification of ten strains' *pks* I, *pks* II, *nrps*, and *phz*E results.

Table 2-19. Summarized overview of the strains which genome sequences were available.

Class	Order	Family	Genera	Species	Submitter	BioProject	Length (Mb)	Acc.-No.
Gamma-proteobacteria (phototrophic purple sulfur bacteria, PSB)	Chromatiales	Chromatiaceae	*Allochromatium*	*A.vinosum* DSM 180^T	JGI	PRJNA46083	3.53	NC_013851.1
			Marichromatium	*M. purpuratum* 984	JGI	PRJNA72575 PRJNA224116 PRJNA62513	3.78	NZ_CP007031.1
			Thiocystis	*T. biolascens* DSM 198	JGI	PRJNA74025 PRJNA60641	5.02	NC_018012.1
			Thioflavicoccus	*T. mobilis 8321*	JGI	PRJNA184343 PRJNA60883	4.05	NC_019940.1
		Ectothiorhodo-spiracea	*Halorhodospira*	*H. halophile SL1*	JGI	PRJNA58473, PRJNA15767	2.68	NC_008789.1
Alphaproteobaceria (purple nonsulfur bacteria, PNSB)	Rhodospirillales	Rhodospirill-aceae	*Rhodospirillum*	*R. centenum* SW	TGen	PRJNA58805 PRJNA18307	4.36	NC_011420.2
				R. rubrum ATCC11170	JGI	PRJNA57655 PRJNA58	4.35	NC_007643.1
				R. photometricum DSM122	CNRS	PRJEA81611, 159003	3.88	NC_017059.1
				R. rubrum F11	Gonzaga University	PRJNA162149 PRJNA67413	4.35	NC_017584.1
	Rhodobacterales	Rhodobacter-aceae	*Rhodobacter*	*R. capsulatus* SB1003	University Chicago	PRJNA47509, PRJNA55	3.74	NC_014034.1
				R. sphaeroides 2.4.1	JGI	PRJNA57653, PRJNA56	3.19	NC_007493.2
				R. sphaeroides ATCC 17025	JGI	PRJNA58451, PRJNA15755	3.22	NC_009428.1
				R. sphaeroides ATCC 17029	JGI	PRJNA58449, PRJNA15754	3.15	NC_009049.1
				R. sphaeroides KD131	GenoTech corp.	PRJNA59277, PRJNA31111		NC_011960.1
	Rhizobiales	Hyphomicrobi-aceae	*Rhodomicrobium*	*R. vannielii* ATCC 17100	JGI	PRJNA38253, 43247	4.01	NC_014664.1

		Bradyrhizobi-aceae	*Rhodopseudo-monas*	*R. palustris* CGA009	JGI	PRJNA62901 PRJNA57	5.46	NC_005296.1
				R. palustris DX-1	JGI	PRJNA43327, PRJNA38503	5.4	NC_014834.1
				R. palustris HaA2	JGI	PRJNA58439, PRJNA15747	5.33	NC_007778.1
				R. palustris BisB5	JGI	PRJNA58441, PRJNA15749	4.89	NC_007958.1
				R. palustris BisB18	JGI	PRJNA58443, PRJNA15750	5.51	NC_007925.1
				R. palustris BisA53	JGI.	PRJNA58445, PRJNA15751	5.51	NC_008435.1
				R. palustris TIE-1	JGI	PRJNA58995, PRJNA20167	5.74	NC_011004.1
Betaproteobacteria (purple nonsulfur bacteria, PNSB)	Burkholderiales	Comamonad-aceae	*Rubrivivax*	*R. gelatinosus* IL144	NITE	PRJNA158163, PRJNA62703	5.04	NC_017075.1
Green sulfur bacteria (GSB)	Chlorobiales	Chlorobiaceae	*Chlorobium*	*C. phaeovibrioides* DSM 265	JGI	PRJNA12607 PRJNA58129	1.97	NC_009337.1
				C. phaeobacteroides DSM 266	JGI	PRJNA58133, PRJNA12609	3.13	NC_008639.1
				C. limicola DSM 245	JGI	PRJNA12606, 58127	2.76	NC_010803.1
				C. tepidum TLS	TIGR	PRJNA57897, PRJNA302	2.15	NC_002932.3
				C. chlorochromatii CaD3	JGI	PRJNA13921, 58375	2.57	NC_007514.1
				C. luteolum DSM 273	JGI	PRJNA13012, 58175	2.36	NC_007512.1
				C. phaeobacteroides BS1	JGI	PRJNA58131, PRJNA12608	2.74	NC_010831.1
			Pelodictyon	*P. phaeoclathratiforme* BU-1	JGI	PRJNA13011, 58173	3.02	NC_011060.1

			Prosthecochloris	*P. aestuarii* DSM 271	JGI	PRJNA12749, 58151	2.51	NC_011059.1
			Chloroherpeton	*C. thalassium* ATCC35110	JGI	PRJNA29215, 59187	3.29	NC_011026.1
			Chlorobaculum	*C. parvum* NCIB 8327	JGI	PRJNA29213, 59185	2.29	NC_011027.1
			Chloroflexus	*C.aggregans* DSM 9485	JGI	PRJNA16708, 58621	4.68	NC_011831.1
				Chloroflexus. sp. Y-400-fl	JGI	PRJNA59085, PRJNA21119	5.27	NC_012032.1
				C. aurantiacus J-10-f1	JGI	PRJNA57657 PRJNA59	5.26	NC_010175.1
Green nonsulfur bacteria (GNSB)	Chloroflexales	Chloroflex-aceae	*Roseiflexus*	*R. castenholzii* DSM 13941	JGI	PRJNA13462, 58287	5.72	NC_009767.1
				Roseiflexus RS-1	JGI	PRJNA58523, PRJNA16190	5.8	NC_009523.1
heliobacteria	Clostridiales	Heliobacteri-aceae	*Heliobacterium*	*H. modesticaldum* Ice1	Arizona State University	PRJNA13427, 58279	3.08	NC_010337.2

NITE: National Institute of Technology and Evaluation; JGI: DOE Joint Genome Institute

3 RESULTS

3.1 First screening of *A. vinosum* strain MT86

According to the previous experiments from Dr. Marcus Tank, Pf medium without salt solution was used for cultivation of *A. vinosum* MT86 at 1000 lux and 28°C for 10-17 days. A total of 30 L of cultures were grown in 1 L bottles (three times of 10 L). The cultures were extracted (10 L each in 1st, 2nd and 3rd extraction) for screening of secondary metabolites from *A. vinosum* MT86 and the combined 2nd & 3rd extracts were analyzed (see paragraph 2.4, on page 33).

Single cells of *A. vinosum* strain MT86 were colorless, but the color of growing culture was firstly pink to dark red (Figure 3-1). The microscopic observation showed that cells were rod shaped, 2 × 2.5-6 µm and occasionally longer. Globules of S^0 were evenly distributed within some of the cells, and some cells were motile and dividing.

Figure 3-1. Cultures and microscopic observation of *A. vinosum* strain MT86.

3.1.1 Metabolite profiles of *A. vinosum* MT86

The ethyl acetate extracted supernatant extract and methanol extracted cell extract were used for analytical HPLC analysis.

The amount of all extracts was shown in Table 3-1 and their color was shown in Figure 3-3. The results of HPLC analyses were shown in Figure 3-2. The extraction results of the second 10 L culture showed the lowest amount of wet cells but highest amount of dried supernatant (64 mg). All three extraction of the culture supernatant yielded a total of 110 mg dried extract, which were used for fractionation of the components. The 1st supernatant extract was further fractionated by the semi-preparative HPLC by per minute and the combined 2nd and 3rd supernatant extracts were fractionated manually by semi-preparative HPLC by using the UV absorption to separately fractionate peaks. The HPLC-DAD/MS chromatograms and colors of supernatant extract and cell extract are shown in Table 3-1 and Figure 3-2.

Table 3-1. The amounts of extracts of *A. vinosum* MT86.

	1st (10 L)	2nd (10 L)	3rd (10 L)
Incubation time	14 d	16 d	17 d
Wet cells	28.218 g	23.296 g	25.919 g
Dried supernatant extract	27 mg	64 mg	18.7 mg
Dried cell extract	4.973 g	6.402 g	7.8313 g

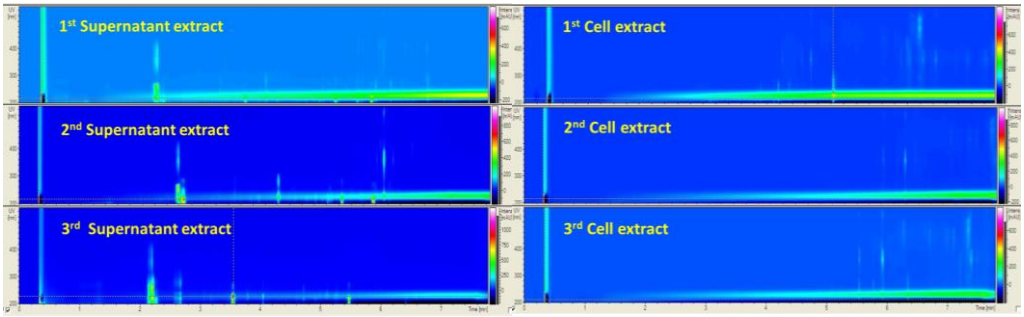

Figure 3-2. HPLC chromatograms of three extractions of *A. vinosum* MT86.

In extracts from the culture supernatants, 8 to 11 UV absorption peaks can be seen, and the UV absorptions between Rt 2-3 min looked identical. The methanolic cell extracts showed dark green color due to the presence of large amounts of pigments and this also can be seen in the HPLC-DAD/MS chromatograms (after Rt 4 min). The chromatograms showed several pigments of UV absorption at 300-500 nm wavelength after Rt 5.5 min which correspond to the UV_{max} absorption wavelength of bacteriochlorophyll *a* (375, 590, 805, and 830-911 nm in the whole cells, and 358, 578, and 771 nm in acetone extracts) and carotenoids. Because large amount of pigments in the cell extracts, no matter which solvents were used for extraction, only analytical HPLC-DAD/MS chromatograms were obtained. For the same reason, HPLC separation was made only with extracts of the culture supernatants in the following.

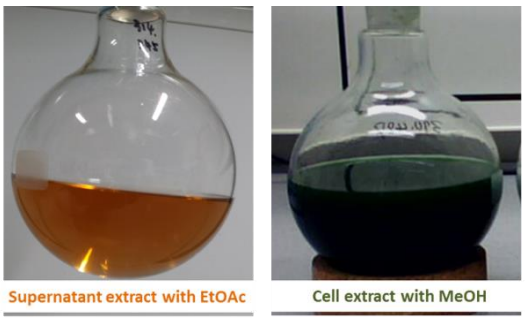

Figure 3-3. The color of extracts from culture supernatant and cell extracts of *A. vinosum* MT86.

3.1.2 Fractionation of supernatant extracts by semi-preparative HPLC

The 1st 10 L extract was fractionated by per minute. The whole duration of the preparation was 24 minutes and 24 fractions were achieved technically. For the operation reason, the first two fractions were combined automatically, thus, 23 fractions were obtained for further analysis. There was no or very weak UV absorption of the 23 fractions according to the analytical HPLC chromatograms (data are not shown).

The extract of 20 L supernatant culture (2nd & 3rd extract) was fractionated by per UV absorption and 10 fractions were obtained, named P1 to P10 (0.3 mg of P1, 0.7 mg of P2, 0.2 mg of P3, 0.6 mg of P4, 1.0 mg of P5, 0.6 mg of P6, 0.5 mg of P7, 0.2 mg of P8, and 0.2 mg of P10). Semi-preparative HPLC chromatogram of crude supernatant extract is shown in Figure 3-4. Analytical HPLC-DAD/MS chromatograms of each fraction (data are not shown) showed that fraction P9 was not pure. There were at least three UV peaks which were not easily separated and the amount was not enough for a second fractionation. Except fractions P9 (not pure) and P5 (one main absorption and another weak one), there was only one main UV absorption of other eight fractions.

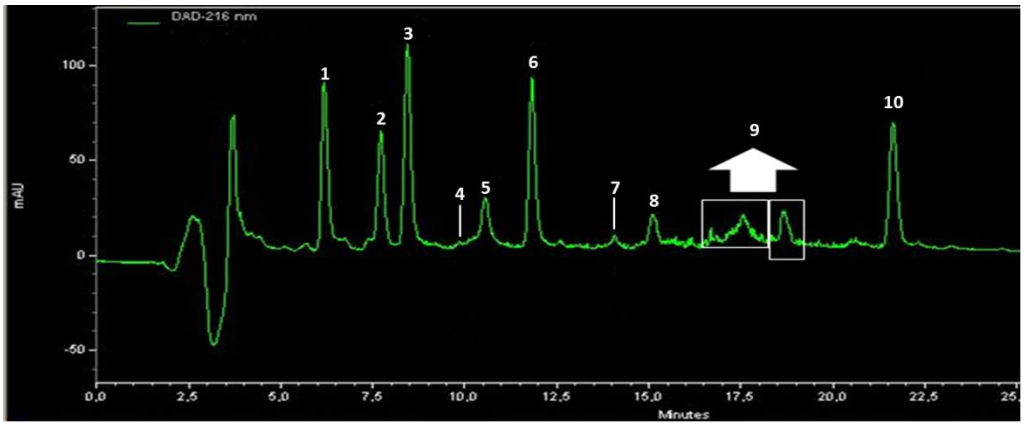

Figure 3-4. The semi-preparative HPLC chromatogram of crude supernatant extract of 2nd & 3rd combined 20 L culture.

3.1.3 NMR analysis of the fractions from the 20 L supernatant extract

Although fractions P1, P3, P8 and P10 were pure according to analytical HPLC-DAD/MS chromatograms and were used for ^{1}H NMR analysis, not sufficient material was available for further studies (^{13}C NMR *etc.*). Information of these four fractions is shown in Table 3-2. P10 was the most interesting fraction after comparison with databases and used for further NMR experiments such as ^{13}C NMR, ^{1}H-^{1}H COSY and HSQC (NMR chromatograms are identical to those of F13 and are not shown). Due to the limited amount of the purified substance, more supernatant extract was necessary for metabolites analysis.

Table 3-2. NMR experiments of four fractions isolated from 20 L supernatant extract of *A. vinosum* MT86.

Peak No.	Amount	m/z	Dissolve solvent	^{1}H-NMR	^{1}H-COSY	^{13}C-HSQC
P1	0.3 mg	243, 279	MeOD	×	/	/
P3	0.2 mg	152	MeOD	×	/	/
P8	0.2 mg	182	MeOD	×	/	/
P10	**0.2 mg**	nd	MeOD	×	×	×

nd: not determined; ×: analysis was performed; /: the amount was not enough and not interesting for further analysis.

3.1.4 Bioactivity of crude supernatant and cell extracts from the 20 L culture

The results of bioassay tests of controls, supernatant and cell extracts are shown in Table 3-3. The different extractions revealed some differences in inhibition of the test strains. In addition to *X. campestris*, the supernatant and cell extracts showed good to moderate activity against *B. subtilis*, *S. lentus*, and *C. albicans*, which indicated that bioactive substances exist in the crude extracts.

For the tests against *X. campestris*, nearly all the samples showed inhibition, but also Pf medium showed 98% inhibition. The basis of inhibition by the medium extract is not known and this extract may not represent a good reference point because the inhibitory activity may be consumed by the cells during growth and not be present in the culture extract.

Most of the tests did not show bioactivity, probably because the concentration of substances was too low to affect the microorganisms. Production of more biomass was necessary for further tests of bioactivity.

The 23 fractions from the 1st 10 L culture supernatant extract were used for bioactivity tests with four microorganisms of *B. subtilis*, *S. lentus*, *X. campestris* and *C. albicans*. All concentrations of the assays were too low to be calculated and the fractions showed low or no activities.

Table 3-3. The results of bioassay tests of controls, supernatant and cell extracts*.

Extracts	Inhibition (%)			
	Bacillus subtilis	***Staphylococcus lentus***	***Xanthomonas campestris***	***Candida albicans***
1st_Supernatant	23	37	90	45
1st_Cell	84	51	95	92
2nd_Supernatant	99	84	83	-
2nd_Cell	-	-	25	-
3rd_Supernatant	-	25	48	-
3rd_Cell	98	-	86	-
Pf media	67	23	98	-

*: The bioassay concentration of all extracts was 476 µg/ml.

Note: The results of the bioassays are defined as follows: ⩾ 80% inhibition: very good activity; < 80% and ⩾ 60% inhibition: moderate activity; < 60% and > 30% inhibition: low activity; ⩽ 30% inhibition & -: no activity.

Table 3-4. The bioactivity tests of 10 fractions from the 2nd and 3rd supernatant extracts.

Extract/ Fractions	Concentration* (µg/ml)	Inhibition (%)								
		Bs	***Sl***	***Ec***	**MRSA**	***Xc***	***Pa***	***Ca***	***Sep***	***Tru***
20 L-Sup	/	-	-	-	-	-	-	-	-	20
P1	/	-	-	-	-	-	-	-	-	-
P2	476	-	-	-	-	-	-	-	-	-
P3	762	-	-	-	-	-	-	-	-	-
P4	38	-	-	-	-	-	-	-	-	-
P5	/	-	-	-	-	-	-	-	-	-
P6	/	95	82	-	85	93	-	85	92	100
P7	/	-	-	-	-	-	-	-	-	-
P8	/	-	-	-	-	-	-	-	-	-
P9	19.05	-	-	-	-	-	-	-	-	-
P10	57.14	89	80	-	80	65	62	-	-	31

1.***Bs***: *Bacillus subtilis*, ***Sl***: *Staphylococcus lentus*, ***Ec***: *Escherichia coli*, **MRSA**: methicillin-resistant *Staphylococcus aureus*, ***Xc***: *Xanthomonas campestris*, ***Pa***: *Propionibacterium acnes*, ***Ca***: *Candida albicans*, ***Sep***: *Septoria tritici*, ***Tru***: *Trichophyton rubrum;* **Sup:** supernatant;
2. Note: The results of the bioassays are defined as follows: ⩾ 80% inhibition: very good activity; < 80% and ⩾ 60% inhibition: moderate activity; < 60% and > 30% inhibition: low activity; ⩽ 30% inhibition & -: no activity. *: assay concentration.

The 10 fractions obtained from the 2nd & 3rd 20 L supernatant extracts were used for bioassays with nine microorganisms. As shown in Table 3-4, only P6 and P10 indicated bioactivities. In comparison with analytical HPLC data and DNP database, P10 appeared of interest because no hits were found in databases and the bioactivities showed good results. Only fractions P6 and P10 showed good inhibition of several test strains. According to analysis of analytical HPLC chromatograms and NMR chromatograms, fraction P10 was almost pure and identified to be a bioactive compound produced by *A. vinosum* strain MT86.

3.2 Optimization of the growth conditions and culture of 36 L of *A. vinosum* strain MT86.

During the first screening of *A. vinosum* strain MT86, methods for preparation and cultivation conditions were used according to the Bergey's Manual of Systematic Bacteriology (Imhoff, 2005a). As mentioned above, the optimization of the growth conditions of *A. vinosum* MT86 for production of secondary metabolites was necessary. The components of the medium and incubation parameters were modified and the biomass production was analyzed in 100 ml culture bottles. In addition, a scale up to 36 L cultures in modified Pf medium was performed to obtain more supernatant extract for the analysis of bioactive compounds.

3.2.1 Media for screening of optimal cultivation conditions

A. vinosum MT86 was grown in six different media (paragraph 2.3.2, on page 31) in order to achieve the best conditions for the production of metabolites.

The amounts of extracts of six different media and four controls of Pf media are shown in Table 3-5. Accordingly, the highest amounts of wet cells (437.2 mg and 406.8 mg) were obtained from Pf medium No. 2 and 4 (Pf medium with thiosulfate and acetate), compared to less than 300 mg with other media. The amounts of dried supernatants were within a range from 2 to 7 mg in different media. Pf media with thiosulfate and/or acetate were extracted much more than Pf medium without supplements.

The photos (Figure 3-5) of the cultures and extracts of *A. vinosum* MT86 indicate that the best growth and the most intensively colored extracts were obtained in Pf medium with thiosulfate and acetate. The color of the cultures (and thereby the pigments content) can be used as an indicator for growth of *A. vinosum* MT86. The lack of obvious difference in the content of dried extracts could be due to the small volume (100 ml) used.

The HPLC-DAD/MS chromatograms of the extracts are shown in Figure 3-6 and Figure 3-7. The extract of the culture supernatant using Pf medium with $MgCl_2$ showed the highest number of peaks according to UV absorption. This indicated that production of secondary metabolites in Pf medium with $MgCl_2$ is better than with $MgSO_4$. Considering that cultures with Pf media containing thiosulfate and acetate are easier to handle, because feeding with sulfide solution is not necessary. Thus, Pf medium with $MgCl_2$, thiosulfate and acetate was considered as the best condition for cultivation of *A. vinosum* MT86.

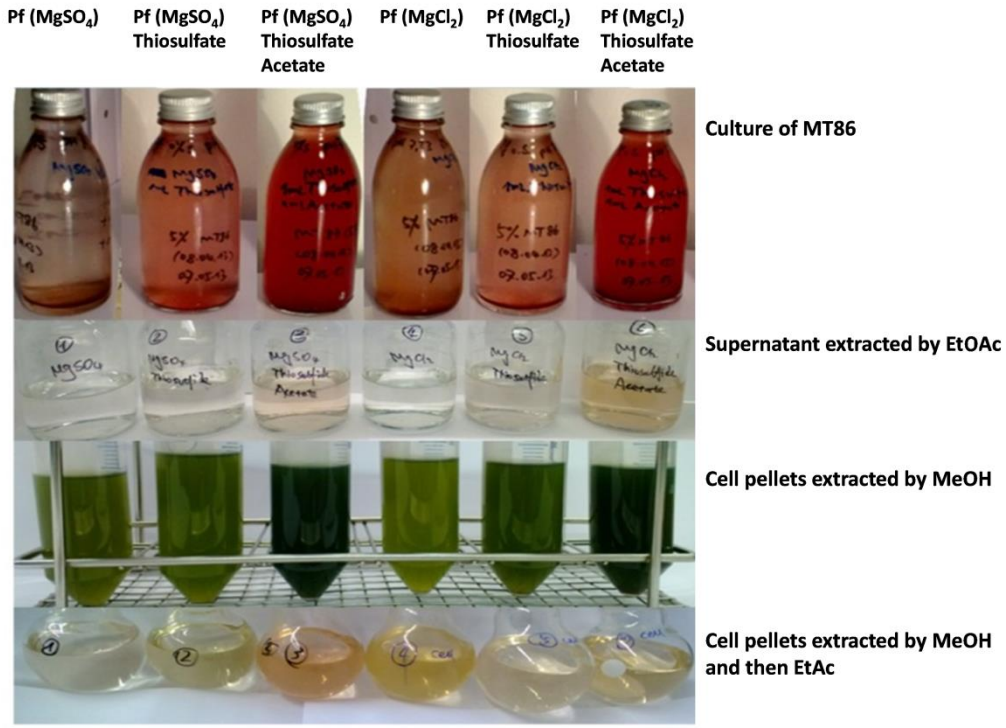

Figure 3-5. Photos of cultures and extracts of *A. vinosum* MT86 in different media.

Table 3-5. Extraction of *A. vinosum* MT86 in 6 different modifications and 4 controls of Pf media.

	1	2	3	4	5	6	CK	CK	CK	CK
Medium	Pf ($MgSO_4$) Thiosulfate	Pf ($MgSO_4$) Thiosulfate Acetate	Pf ($MgCl_2$) Thiosulfate	Pf ($MgCl_2$) Thiosulfate Acetate	Pf ($MgSO_4$)*	Pf ($MgCl_2$)*	Pf ($MgSO_4$)	Pf ($MgCl_2$)	Pf($MgCl_2$) no Sulfide	Pf($MgCl_2$) no Sulfide
Volume	100 ml	100 ml	100 ml	100 ml	100 ml	100 ml	100 ml	100 ml	100 ml	1 L
Incubation time	10 days	10 days	10 days	10 days	*10 days	*10 days	/	/	/	/
Wet Cell	258.2 mg	437.2 mg	271.5 mg	406.8 mg	289 mg	243 mg	/	/	/	/
Dried Cell	7 mg	6 mg	7 mg	5 mg	5 mg	6 mg	/	/	/	/
Dried supernatant	7 mg	7 mg	5 mg	4 mg	2 mg	2 mg	-	-	-	-
Volume of MeOH	2 ml	2 ml	2 ml	2 ml	2 ml	2 ml	2 ml	2 ml	2 ml	2 ml

*Addition of 1 % sulfide solution every 2 days.
All cultures grown at 28°C, 500 lux in Pf medium
/ : no results
-: amount is too low to calculate

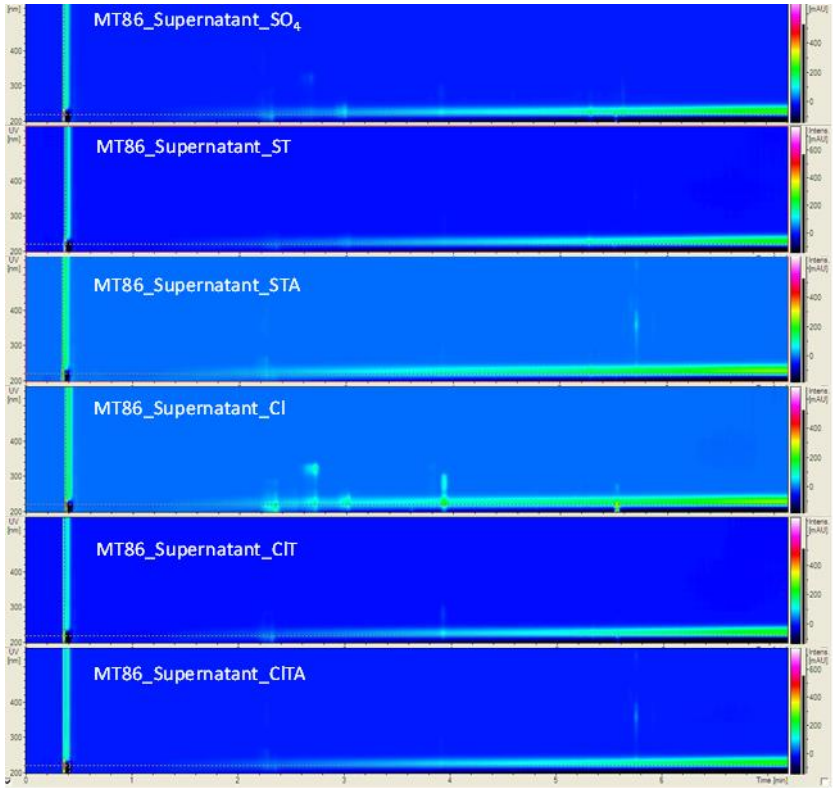

Figure 3-6. HPLC chromatograms of six different supernatant extracts.

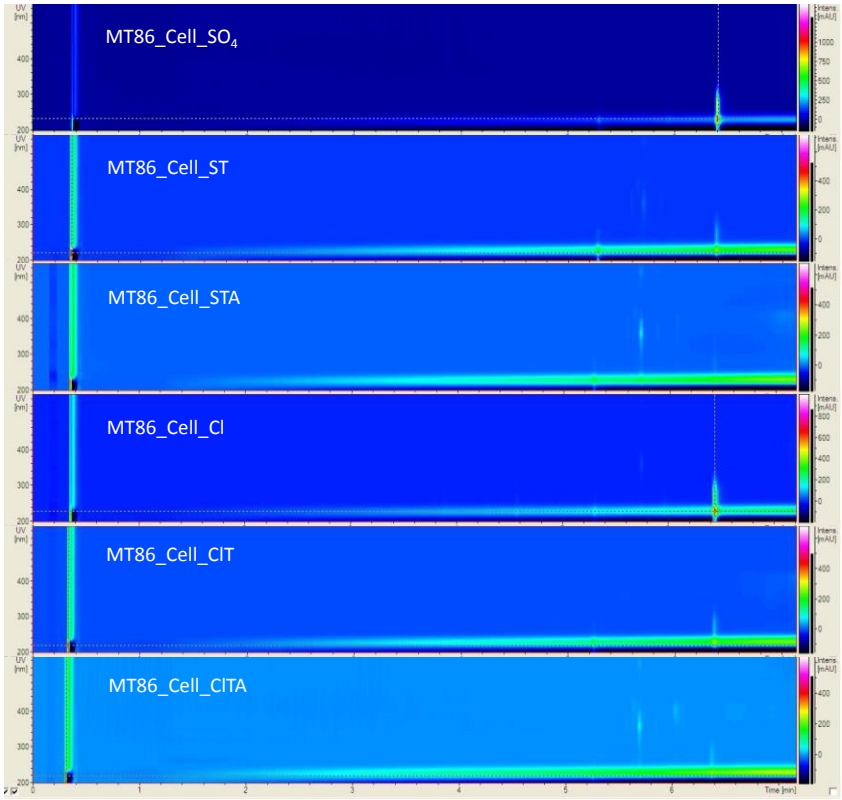

Figure 3-7. HPLC chromatograms of six different cell extracts.

Table 3-6. Bioassay tests with extracts of *A. vinosum* MT86 grown in 100 ml flasks in 6 different media.

Crude extracts	Concentration* (µg/ml)	Inhibition (%)								
		Bs	***Sl***	***Ec***	**MRSA**	***Xc***	***Pa***	***Ca***	***Sep***	***Tru***
MT86-Sup-$MgSO_4$	476	35	-	-	63	-	-	-	-	-
MT86-Sup-ST	455	-	-	-	69	-	-	-	-	23
MT86-Sup-STA	476	-	-	-	-	-	-	-	-	-
MT86-Sup-$MgCl_2$	476	-	-	-	-	-	-	-	-	-
MT86-Sup-ClT	455	22	-	-	-	-	-	-	-	-
MT86-Sup-ClTA	452	-	-	-	-	-	-	-	-	-
MT86-Cell-$MgSO_4$	476	-	-	-	-	-	-	-	-	29
MT86-Cell-ST	476	74	-	-	-	-	-	-	22	89
MT86-Cell-STA	476	68	-	-	-	-	-	-	-	97
MT86-Cell-$MgCl_2$	476	74	-	-	-	-	-	-	32	96
MT86-Cell-ClT	476	68	-	-	-	-	-	-	-	100
MT86-Cell-ClTA	476	66	-	-	-	-	-	21	-	99
Pf-100ml-$MgSO_4$	433	33	-	-	-	49	-	-	96	90
Pf-100ml-$MgCl_2$	476	40	-	-	25	45	-	-	100	100
Pf-1L-no sulfide	476	31	-	-	31	74	-	-	-	79

1. ***Bs***: *Bacillus subtilis*, ***Sl***: *Staphylococcus lentus*, ***Ec***: *Escherichia coli*, **MRSA**: methicillin-resistant *Staphylococcus aureus*, ***Xc***: *Xanthomonas campestris*, ***Pa***:*Propionibacterium acnes*, ***Ca***: *Candida albicans*, ***Sep***: *Septoria tritici*, ***Tru***: *Trichophyton rubrum*;

2. **-Sup**: Crude medium extract from *A. vinosum* MT86 culture which was incubated with Pf medium ($MgSO_4$); **-Cell**: Crude cell extract from MT86 which was incubated with Pf medium ($MgSO_4$); **-$MgSO_4$**: Pf (**$MgSO_4$**); **-ST**: Pf (Mg**S**O_4) + **T**hiosulfide; **-STA**: Pf (Mg**S**O_4) + **T**hiosulfide + **A**cetate; -$MgCl_2$: Pf (**$MgCl_2$**); **-ClT**: Pf (Mg**Cl**$_2$) + **T**hiosulfide; **-ClTA**: Pf (Mg**Cl**$_2$) + **T**hiosulfide+**A**cetate;

3. Note: The results of the bioassays are defined as follows: ⩾ 80% inhibition: very good activity; < 80% and ⩾ 60% inhibition: moderate activity; < 60% and > 30% inhibition: low activity; ⩽ 30% inhibition &-: no activity. *: assay concentration.

All supernatant and cell extracts were tested for bioactivity with nine test microorganisms. Some of the test strains, for example *Bacillus*, *Trichophyton* and *Xanthomonas*, are more sensitive to compounds than others are. The results are seen in Table 3-6. Bioactive tests with extracts of uninoculated Pf media with $MgSO_4$, $MgCl_2$ and without sulfide to *X. campestris* showed low and moderate activity (49%, 45%, and 74%), and high inhibition to *S. tritici* (96%, 100% in the presence of sulfide) and *T. rubrum* (90%, 100%, and 79%), respectively. There is no explanation for this inhibition and the sensitivity of these strains to extracts of the Pf medium itself.

It was interesting that five cell extracts showed moderate activity (< 80% and ⩾ 60% inhibition), but all six supernatant extracts showed no inhibition to *T. rubrum*, whereas the uninoculated medium

extracts did. A reason for this effect could be that the strain used the inhibitory components of the Pf medium, but the cells apparently did not secrete bioactive metabolites.

In the bioassay tests to *B. subtilis*, five cell extracts showed moderate activity (< 80% and ⩾ 60% inhibition) while supernatant extracts of all cultures showed no inhibition of *B. subtilis*. Apparently, no or only low amount of secondary metabolites are produced under the tested conditions/media.

From this comparison of six different Pf media, the modification shown in Table 3-7 was chosen for the following studies on metabolite production by *A. vinosum* MT86.

Table 3-7. Basic Pf medium for *A. vinosum* strain MT86.

Ingredients	5 L
H_2O	4900 ml
KH_2PO_4	1.70 g
$NHCl_4$	1.70 g
$MgCl_2 \cdot 6H_2O$	2.05 g
$CaCl_2 \cdot 2H_2O$	1.25 g
KCl	1.70 g
Thiosulfate	5.0 g
$NH_4 \cdot$Acetate	6.25 g
Mg·Acetate	6.25 g

Additional solutions for 5 L Pf medium:
B12: 5 ml, SLA: 5 ml, $NaHCO_3$: 7.5 g /100 ml, Na_2S: 2.0 g/20 ml

3.2.2 Scale up to a 36 L volume culture of *A. vinosum* MT86

In order to obtain sufficient supernatant extract for tests and structure elucidation of bioactive compounds from *A. vinosum* strain MT86, a total of 36 L culture was grown in this modification of Pf medium (Table 3-7).

3.2.2.1 Cultivation, Extraction and HPLC-DAD/MS analysis

After 11 days of incubation, the 36 L culture broth was extracted. The amount of extracts is shown in Table 3-8. The HPLC-DAD/MS chromatogram showed at least 11 UV absorption peaks (data are not shown).

Table 3-8. The amount of extract from a 36 L culture of *A. vinosum* strain MT86.

	4^{th} (36L)
Incubation time	11 d
Wet Cell deposit	124.0549 g
Dried supernatant extract	283 mg

The amount of the dried cell extract could not be determined, because it could not be completely dried.

3.2.2.2 Fractionation by semi-preparative HPLC of the 36 L crude supernatant extract

After the supernatant extract was concentrated to 100 mg/ml, semi-preparative HPLC was used for fractionation following the UV absorption. Finally, 17 fractions (named F1-F17, Figure 3-8) were obtained.

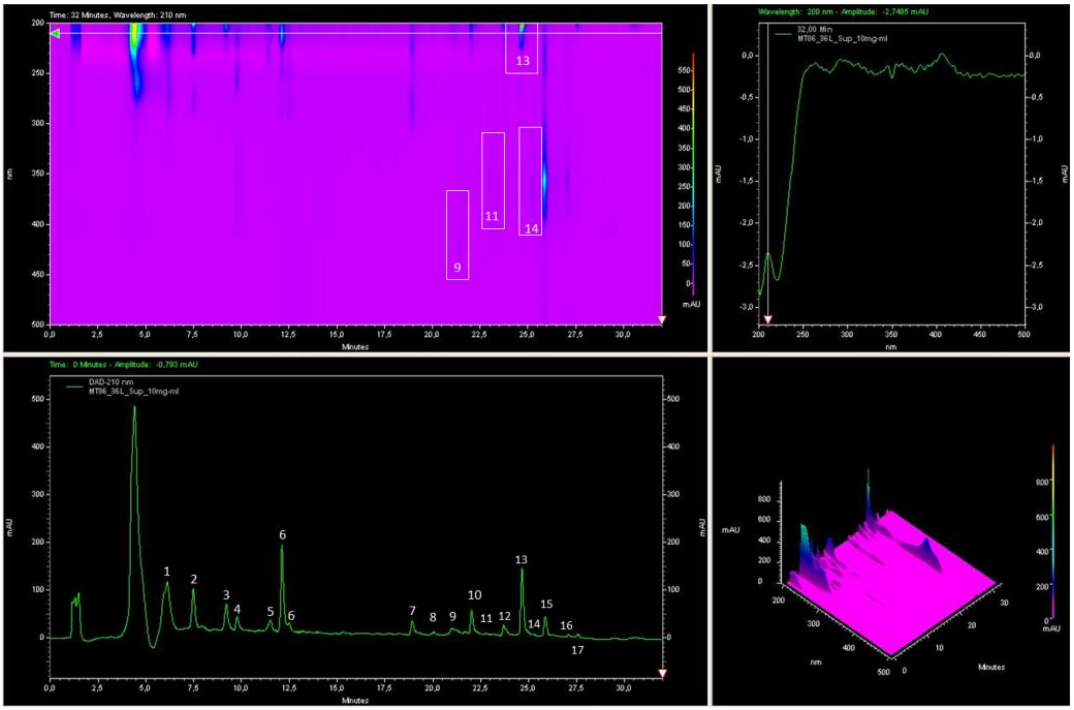

Figure 3-8. Semi-preparative HPLC chromatogram of supernatant extract of 36 L culture broth of *A. vinosum* strain MT86.

These fractions were evaporated to dry and dissolved in MeOH to a concentration of 1 mg/ml. Analytical HPLC-DAD/MS was performed to check the purity and determine m/z of each fraction (data are not shown).

3.2.2.3 NMR analysis and TOF-MS analysis

From the analytical HPLC-DAD/MS analysis (data are not shown), three (F4, F13, and F15) of seventeen fractions were considered as pure compounds and ^{1}H NMR analysis was performed with these fractions (Table 3-9). With fraction F4, only ^{1}H NMR analysis could be made because the amount was insufficient for further analysis. Fraction F15 was a pigment and was not of interest for bioactive screening.

Only fraction F13 was pure and available in sufficient amount (1.1 mg) to perform more detailed NMR analysis. The HPLC-DAD/MS chromatogram of F13 is seen in Figure 3-9, and ^{1}H-NMR, ^{1}H-^{1}H COSY, ^{1}H-^{13}C HMBC, and ^{1}H-^{13}C HSQC were identical to those shown in Figure 3-26, Figure 3-28, Figure 3-29 and Figure 3-30.

Table 3-9. NMR analysis of compounds from 36 L supernatant extract.

No.	Amount	Dissolve solvent	^{1}H-NMR	^{1}H-^{1}H COSY	^{1}H-^{13}C HSQC	^{1}H-^{13}C HMBC
F4	0.4 mg	MeOD	×			
F13	1.1 mg	MeOD	×	×	×	×
F15	2.8 mg	MeOD	×			

×: analysis was performed; /: the amount was not enough and not interesting for further analysis.

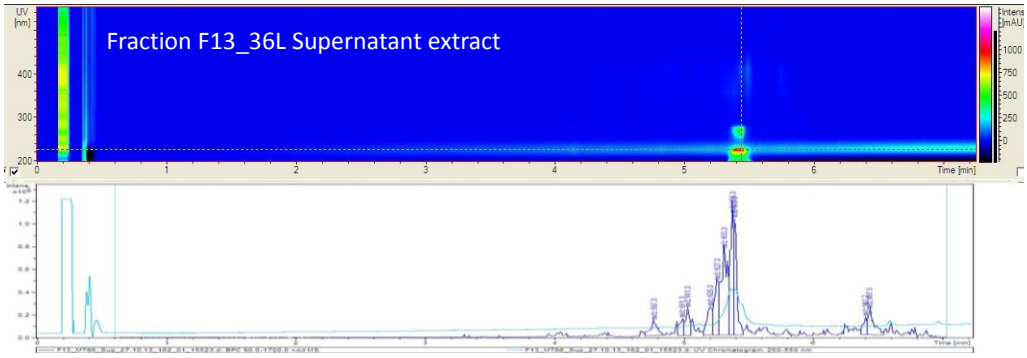

Figure 3-9. HPLC-DAD/MS chromatogram of fraction F13 isolated from *A. vinosum* MT86.

Table 3-10. The cultivation parameters for extraction of compound P10/F13.

Parameters		20 L	36 L
Medium (Pf)	Salt concentration	0%	0%
	Thiosulfate	0%	1%
	Acetate	0%	1%
	Mg^{2+}	$MgSO_4 \cdot 7H_2O$	$MgCl_2 \cdot 6H_2O$
	Trace Element solution	SL-12	SLA
Adding sulfide solution		1%, every 2 days	/
Inoculation time		in twice (16 d+17 d)	in once (11 d)
Inoculation present (%)		5%	5%
Light intensity (lux)		1000	1000
Temperature (°C)		28-30	28-30
Dried weight of supernatant crude extract		64 mg+18.7 mg = 82.7 mg	283 mg (oil-gel like)

/: not used

From the NMR data together with the analytical HPLC-DAD/MS analysis, compound F13 was the same as the previous fraction P10 isolated from 20 L supernatant extract. It was interesting that F13 and P10 were isolated from different Pf media and incubated under different cultivation conditions (Table 3-10). It is concluded that F13 was produced as a secondary metabolite of *A. vinosum* strain

MT86 under different conditions and F13 was identical to the P10 from a previous preparation. Later in the following, the compound name F13 is used (F13 = P10).

3.3 Salt tolerance of *A. vinosum* MT86

Some strains of *Allochromatium* originate from marine and brackish water habitats and may tolerate or require low concentrations of salt. Therefore, the response of *A. vinosum* strain MT86 to low salt concentrations was tested. As shown in Figure 3-10, strain MT86 in Pf media with different salt concentrations grew in different speed as indicated by the color development in the cultures. After 5 days of cultivation, *A. vinosum* strain MT86 grew faster in the medium (0%-1.67% salts) than those at higher salt concentrations (2.33%-3.33%). Best growth was obtained at up to 1.67% salts.

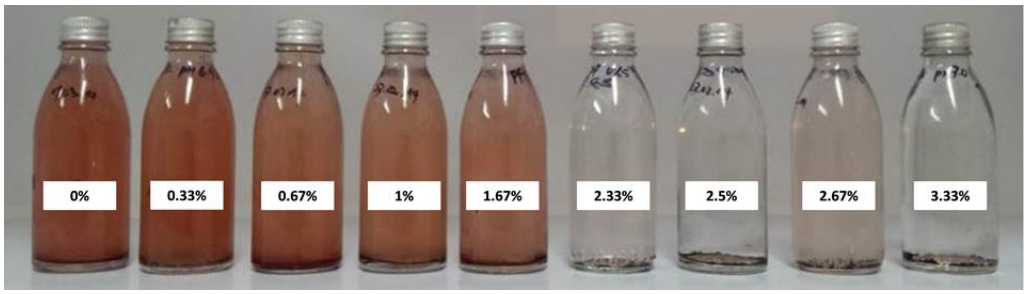

Figure 3-10. Cultivation of MT86 in of different salt concentrations after 5 days.

The cultures grown at salt concentrations of 0%, 0.33%, 0.67%, 1%, and 1.67% were extracted after 7 and 10 days. Cultures grown at higher salt concentrations of 2.33%, 2.5%, 2.67%, and 3.33% were extracted after 15 and 20 days.

3.3.1 Comparison of culture broths with 0%, 0.33%, 0.67%, 1%, and 1.67% salts

The cultures of *A. vinosum* strain MT86 grown in salt concentrations from 0% to 1.67% salts were compared after cultivation times of 7 and 10 days.

3.3.1.1 Comparison of 7 d's and 10 d's crude extracts (0%, 0.33%, 0.67%, 1%, and 1.67% salts)

The HPLC chromatograms of extracts obtained after 7 and 10 days' incubation are shown in Figure 3-11 and Figure 3-12. 22 distinct UV absorption peaks were visible and assigned to peak numbers 1 to 22. Detailed information of UV absorption and m/z or mass analysis is shown in Table 3-11.

From these HPLC chromatograms, there were all numbers of UV absorption peaks (peak 1 to peak 22) in the extract of culture broth grown at 1% salts for 7 days.

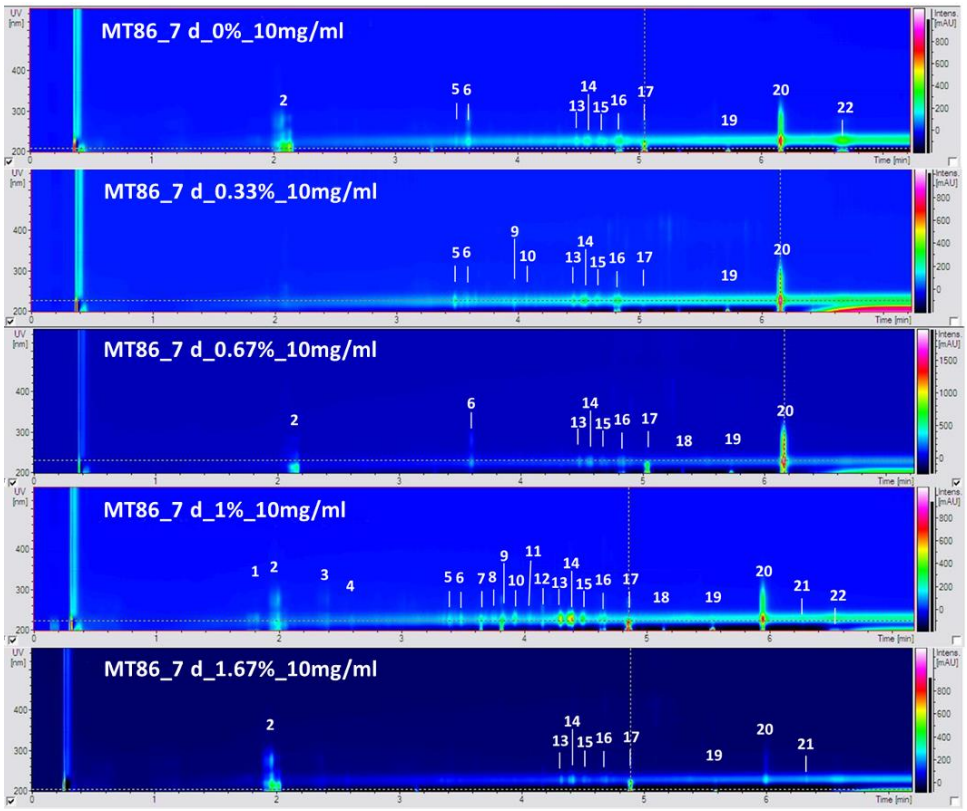

Figure 3-11. Comparison of chromatograms of extracts from *A. vinosum* strain MT86 grown at salt concentrations from 0-1.67% salts for 7 days.

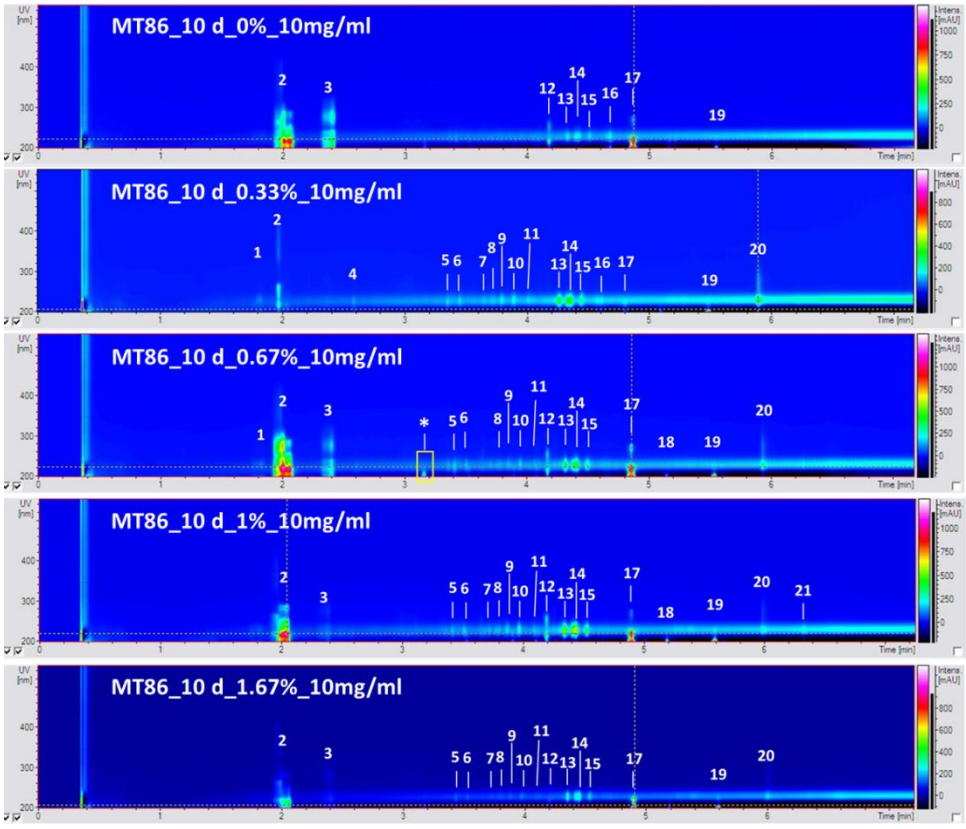

Figure 3-12. Comparison of chromatograms of extracts from *A. vinosum* strain MT86 grown at salt concentrations from 0-1.67% salts for 10 days.

Table 3-11. UV and m/z information of each peak of extracts from cultures grown for 7 and 10 days.

Peak No.	Rt/min	UV/nm	m/z	7 d					10 d				
				0%	1%	2%	3%	5%	0%	1%	2%	3%	5%
1	1.83	228	183				+			+	+		
2	1.99	218 , sh238, 274	196	+		+	+	+	+	+	+	+	+
3	2.40	222, 275	mass 213 (+Na, +K), m/z 402				+		+		+	+	+
4	2.60	226	/				+			+	**		
5	3.39	226	293	+	+		+			+	+	+	+
6	3.49	226	/	+	+	+	+			+	+	+	+
7	3.65	227, 280	297				+			+		+	+
8	3.75	226	/				+			+	+	+	+
9	3.82	224, 275	/		+		+			+	+	+	+
10	3.92	229	279		+		+			+	+	+	+
11	4.05	227	279				+			+	+	+	+
12	4.15	220, sh228, sh255, 296	279				+		+		+	+	+
13	4.30	227	295	+	+	+	+	+	+	+	+	+	+
14	4.39	227	295	+	+	+	+	+	+	+	+	+	+
15	4.48	227	/	+	+	+	+	+	+	+	+	+	+
16	4.66	227, 275, 277	279	+	+	+	+	+	+	+			
17	4.85	220, 267, 276	253	+	+	+	+	+	+	+	+	+	+
18	5.14	227	267			+	+				+	+	
19	5.53	227	281*	+	+	+	+	+	+	+	+	+	+
20	5.95	227, sh264	mass: 749/705/ 661/ 617/ 573/529	+	+	+	+	+		+	+	+	+
21	6.27	228	/				+	+				+	
22	6.52	228	/	+			+						

+: peak presents in this position; Blank: no peak presents /: from the mass chromatography, the intensity is too low to consider and/or there is no accurate m/z information; mass: there is no distinct evidence to make sure the m/z, so the mass number is the number which shows directly from mass chromatogram.*: m/z=281, this compound always present and is not in consider**: additional peak is in Rt 3.15 min of 10 days, 2% salt concentration, which m/z is 224.

3.3.1.2 Comparison of extracts after growth at 1% salts for 7 and 10 days.

The extract of cultures grown at 1% salts for 7 days showed 22 UV absorption peaks and was used as a reference for comparison with the other growth conditions.

Comparison of the chromatograms showed that peaks 1, 4, 16 and 22 were present after 7 days, but disappeared after 10 days of cultivation (Figure 3-13). However, the main peaks (peak 2, 5-21) were present under both conditions. In addition, the intensity of peak 2 (Rt 1.99 min, UV 218, sh238, and 274 nm, m/z 196) was higher in the extract after 10 days. In contrast, the intensity of peak 20 (Rt 5.95 min, UV 227, sh264 nm, mass 749, 705, 661, 617, 573, and 529) decreased from 7 to 10 days of incubation. The extract after 10 days was more interesting in regard to UV absorbing peaks.

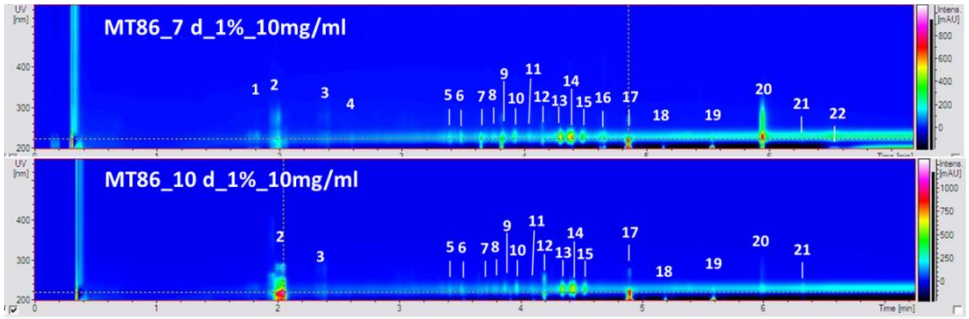

Figure 3-13. Comparison of extracts from *A. vinosum* MT86 grown at 1% salts for 7 and 10 days.

3.3.1.3 Comparison of extracts of cultures grown at 0.67% and 1% salts for 10 days

Peaks 2, 3, 5-6, and 8-10 were present in extracts of cultures grown at 0.67% and 1% salts (Figure 3-14). Peak 1 was found in the extract from the culture grown at 0.67% salts only. While peaks 7 and 21 were found in cultures grown at 1% salts only, an additional peak (peak *, Rt 3.15 min, UV 226 nm, m/z 224) was found in the culture grown at 0.67% salts.

Because m/z 281 (peak 19) was present in all chromatograms, it is considered as a contamination and can be ignored. From HPLC chromatograms of extracts from cultures grown for 10 days, peak 20 showed lower intensity than others did. An additional peak at Rt 3.15 min of extract from culture at 0.67% salts after 10 days was the only peak presented obviously.

Incubation of *A. vinosum* strain MT86 at 0.67% salts concentration after 10 days is the preferred cultivation condition if compared with salt concentration up to 1.67% (≤ 1.67%).

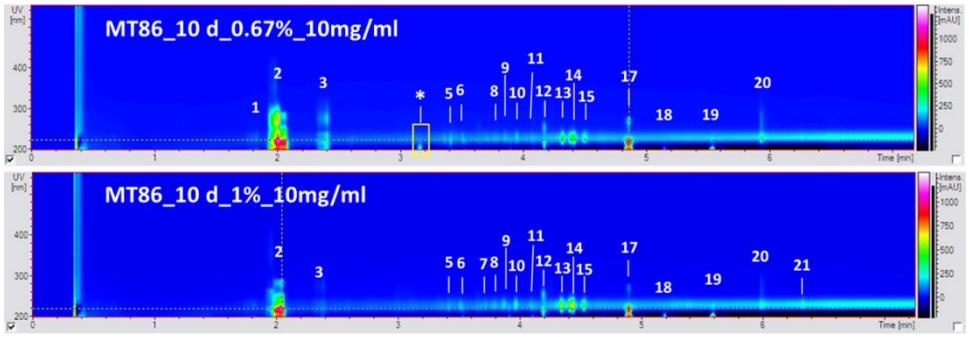

Figure 3-14. Comparison of extracts from cultures of *A. vinosum* MT86 grown at 0.67% and 1% salts.

3.3.2 Comparison of culture broths with 2.33%, 2.5%, 2.67%, and 3.33 % salts

Because the metabolite profiles of cultures grown at salt concentrations of 2.33% and higher were clearly different from those grown up to 1.67% salts, different numbers were used for a first identification of the peaks. The peaks in these chromatograms were assigned peak numbers 1' to 18'.

3.3.2.1 Comparison of crude extracts after 15 and 20 days (with 2.33%, 2.5%, 2.67%, and 3.33 % salts)

The HPLC chromatograms of extracts in total 18 peaks can be pointed out (Figure 3-15, and Figure 3-16).

A total of 18 peaks were present in extracts from cultures grown at 2.5% salts for 15 days' incubation. Under these conditions, the intensity of peaks 1' and 2' were lower than those in extracts from cultures grown at 2.33% salts for 15 days and at 2.67% salts for 15 days. Peaks 6', 7' (Rt 4.41 min, UV 227 nm, mass 296; same as peak 14), 14', and 18' (Rt 5.95min, UV 228 nm, sh262 nm, mass 749/705/ 661/ 617/ 573/529; same as peak 20) showed highest intensity in the extract from the culture grown at 2.5% salts for 15 days. Furthermore, peak 9' only existed in the extract from the culture at 2.5% salts for 15 days.

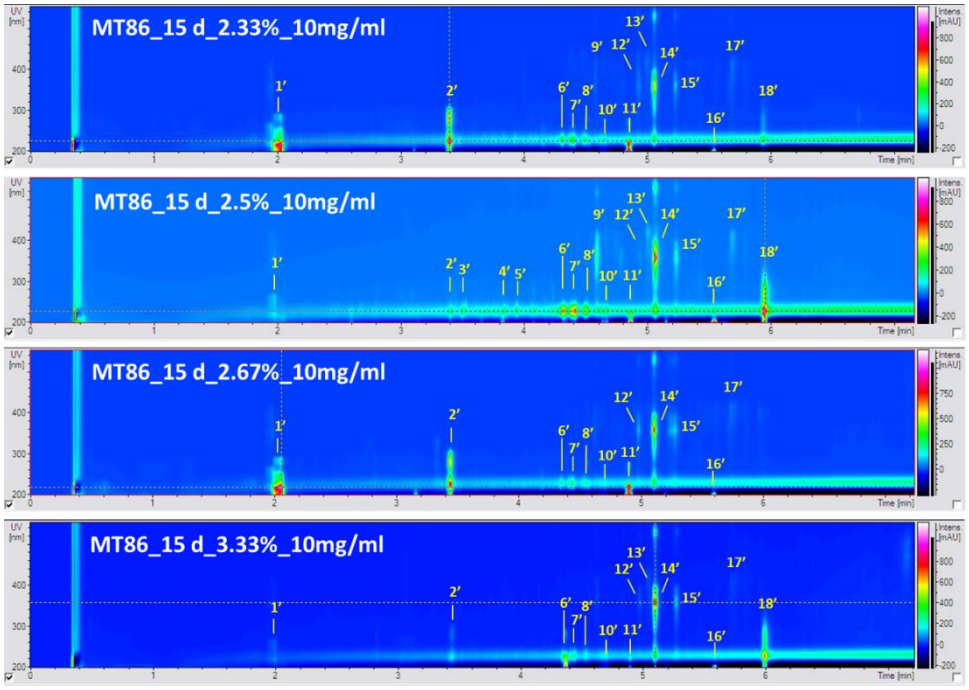

Figure 3-15. Comparison of extracts from cultures of *A. vinosum* MT86 grown at salt concentrations of 2.33%, 2.5%, 2.67%, and 3.33 % for 15 days.

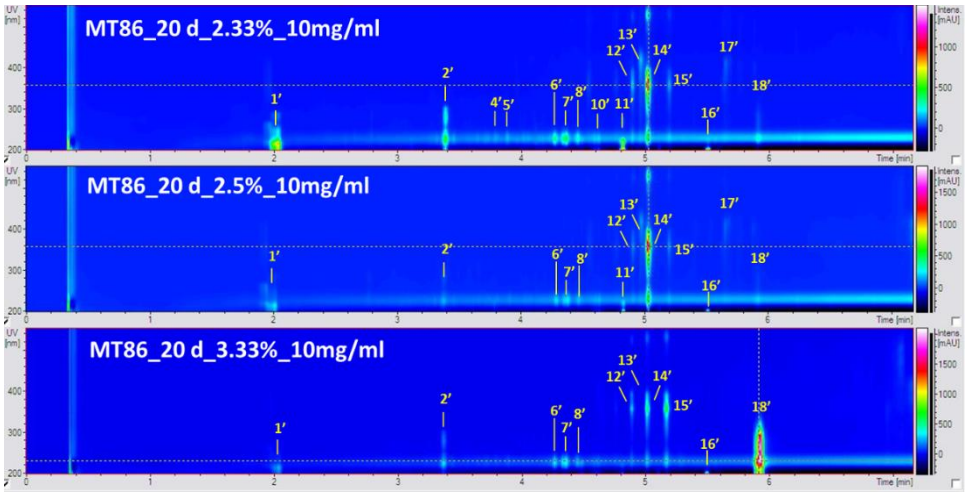

Figure 3-16. Comparison of extracts from cultures of *A. vinosum* MT86 grown at salt concentrations of 2.33%, 2.5%, 2.67%, and 3.33 % for 20 days.

Table 3-12. UV_{max} and m/z information of peaks of extracts from cultures of *A. vinosum* MT86 grown for 15 and 20 days.

Peak No.	Rt/min	UV/nm	m/z	15 d				20 d		
				7%	7.5%	8%	10%	7%	7.5%	10%
1'	1.98	220, 261, 348	170	+	+	+	+	+	+	+
2'	3.4	225	293	+	+	+	+	+	+	+
3'	3.5	227	728		+					
4'	3.84	227	291		+			+		
5'	3.94	228	451		+			+		
6'	4.32	227	mass 296	+	+	+	+	+	+	+
7'	4.41	227	mass 296	+	+	+	+	+	+	+
8'	4.50	228	610	+	+	+	+	+	+	+
9'	4.58	227, 346, 350, sh410, 513	mass 280	+	+					
10'	4.67	227	/	+	+	+	+	+		
11'	4.86	221	253	+	+	+	+	+	+	
12'	4.93	228	610	+	+	+	+	+	+	+
13'	5.01	418	610	+	+		+	+	+	+
14'	5.06	230	279	+	+	+	+	+	+	+
15'	5.23	228, 356, sh388, 526	255	+	+	+	+	+	+	+
16'	5.54	227	281	+	+	+	+	+	+	+
17'	5.69	413	880	+	+	+	+	+	+	
18'	5.95	228, sh262	mass: 749/705/ 661/ 617/ 573/529	+	+		+	+	+	

+: peak presents in this position; Blank: no peak presents; /: from the mass chromatography, the intensity is too low to consider and/or there is no accurate m/z information; mass: there is no distinct evidence to make sure the m/z, so the mass number is the number which shows directly from mass chromatogram.

3.3.2.2 Comparison of extracts of cultures grown at 2.5% salts for 15 and 20 days.

Because the extract from the culture grown at 2.5% salts for 15 days showed all 18 UV absorption peaks, it was used as a reference HPLC chromatogram for comparison with the other HPLC chromatograms of other extracts. The comparison of different time of cultivation was included.

The comparison of the HPLC chromatograms of extracts is shown in Figure 3-17. Peaks 3' 4', 5', 9', and 10' disappeared in the extract from the culture grown at 2.5% salts for 20 days if compared with the extract for 15 days. Other peaks in the extract from cultures grown at 2.5% salts showed lower intensity for 20 days than for 15 days.

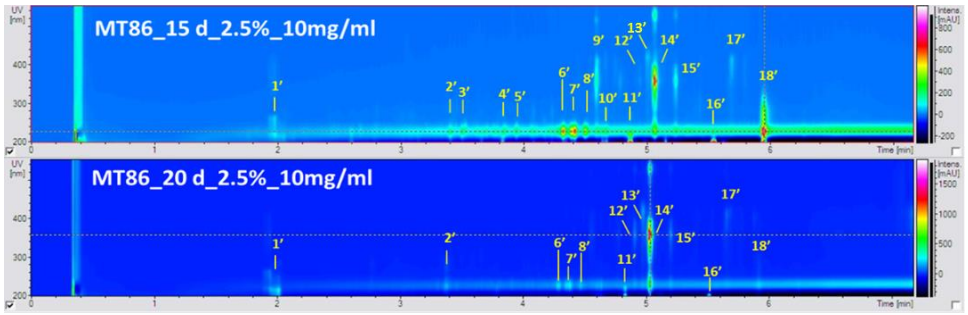

Figure 3-17. Comparison of extracts from cultures of *A. vinosum* MT86 grown at 2.5% salts for 15 and 20 days.

During the growth experiments with different salt concentrations, it was shown that *A. vinosum* strain MT86 tolerated higher salt concentrations up to 3.33%, but did grow slowly. Some interesting peaks were seen in the chromatograms. According to UV-absorption, cells grown at 2.5 % salts for 15 days produced several interesting peaks. Peaks 6', 7', 8' were identical to peaks 13, 14, and 15 of cultures grown at 0.67% (10 days). Peaks 9', 14', 15', and 17' maybe pigments according to the absorption wavelength. Peak 18' had the same Rt as peak 20, but had a different m/z (mass 573 or m/z: 528).

Extract from culture of strain MT86 grown at 2.5% salts for 15 days were the most interesting.

3.3.3 Bioactivity tests of crude extracts from controls Pf media and from cultures grown at different salt concentrations.

Bioassays were performed with four test microorganisms and the results are shown in Table 3-13. As a control, Pf media with different salt concentrations were extracted with the same method as culture broth. Some of the medium extracts showed inhibition of *B. subtilis*. Culture extracts after 7 days grown at 0.33%, 0.67%, and 1% salts showed moderate to high inhibition of *B. subtilis*.

Table 3-13. Inhibition of test strains by different extracts of *A. vinosum* strain MT86.

Samples		Concentration* (µg/ml)	*Bs*	MRSA	*Xc*	*Tru*
Control	Pf_0%	476	-	-	-	69
	Pf_0.33%	429	-	-	-	93
	Pf_0.67%	47.62	85	-	-	60
	Pf_1%	476	52	-	-	83
	Pf_1.67%	95.24	-	-	-	78
	Pf_2.33%	429	-	-	-	74
	Pf_2.5%	476	82	-	-	66
	Pf_2.67%	429	-	-	-	69
	Pf_3.33%	333	23	-	-	72
7 d	MT86_0%	476	-	-	-	99
	MT86_0.33%	476	77	-	26	100
	MT86_0.67%	476	96	-	32	100
	MT86_1%	476	100	-	43	100
	MT86_1.67%	476	-	-	-	100
10 d	MT86_0%	476	-	-	-	69
	MT86_0.33%	476	-	-	-	100
	MT86_0.67%	476	-	-	-	91
	MT86_1%	476	-	-	-	81
	MT86_1.67%	476	-	-	-	92
15 d	MT86_2.33%	476	-	24	-	100
	MT86_2.5%	476	-	-	-	100
	MT86_2.67%	476	-	33	-	41
	MT86_3.33%	476	-	-	-	100
20 d	MT86_2.33%	476	-	-	-	100
	MT86_2.5%	476	-	-	-	100
	MT86_3.33%	476	42	-	-	100

1. ***Bs***: *Bacillus subtilis*, **MRSA**: methicillin-resistant *Staphylococcus aureus*, ***Xc***: *Xanthomonas campestris*, ***Tru***: *Trichophyton rubrum*;
2. Note: The results of the bioassays are defined as follows: ⩾ 80% inhibition: very good activity; < 80% and ⩾ 60% inhibition: moderate activity; < 60% and > 30% inhibition: low activity; ⩽ 30% inhibition &-: no activity. *: assay concentration.

All extracts including the control Pf medium extracts did not inhibit MRSA but showed moderate to high inhibition of the fungus *T. rubrum*. Extracts from cultures grown at 0.33%, 0.67% and 1% salts (for 7 days) showed no or very low inhibition of *X. campestris*, but moderate (77%) to high (96%, and 100%) inhibition of *B. subtilis*.

3.3.4 Scale up of cultures to a 50 L volume at two salt concentrations

Pfennig media with 0.67% and 2.5% salts were identified as the best conditions for secondary metabolite production of *A. vinosum* MT86. Therefore, 50 L cultures were grown both at 0.67% salts (10 days) and at 2.5% salts (15 days), respectively. The supernatant of both cultures were extracted with ethyl acetate (EtOAc) and cell deposits were extracted by MeOH, acetone, and dichloromethane for TLC analysis. The incubation parameters of *A. vinosum* MT86 are shown in Table 3-14.

Table 3-14. Incubation parameters for scale up experiments.

Salts	**0.67%**	**2.5%**
Incubation time	10 days	15 days
Culture volume	50 L	50 L
Extract volume	45 L	50 L
Mg^{2+}	$MgCl_2 \cdot 6H_2O$	
Thiosulfate & acetate	1% thiosulfate, 1% acetate	
Light intensity	1000 lux	
Temperature	28-30°C	

3.3.4.1 Cultures grown at 0.67% salts

After 10 days' incubation, 45 L of the cultures (five bottles of media were broken) were extracted. 318 mg dried supernatant extract was obtained and then dissolved in MeOH. The HPLC chromatogram is shown in Figure 3-18. Fractionation was performed by semi-preparative HPLC, and 18 fractions were obtained (see in Figure-19). Detailed information on the peaks is contained in Table 3-15.

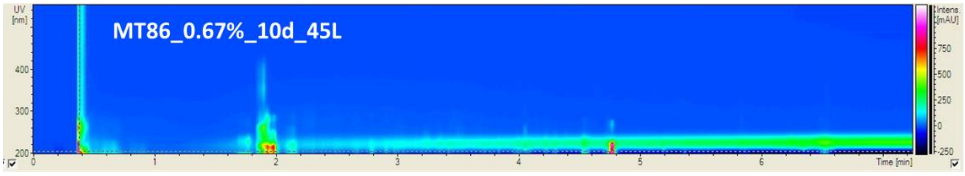

Figure 3-18. HPLC chromatogram of supernatant extract from 45 L culture of *A. vinosum* MT86 grown at 0.67% salts for 10 days.

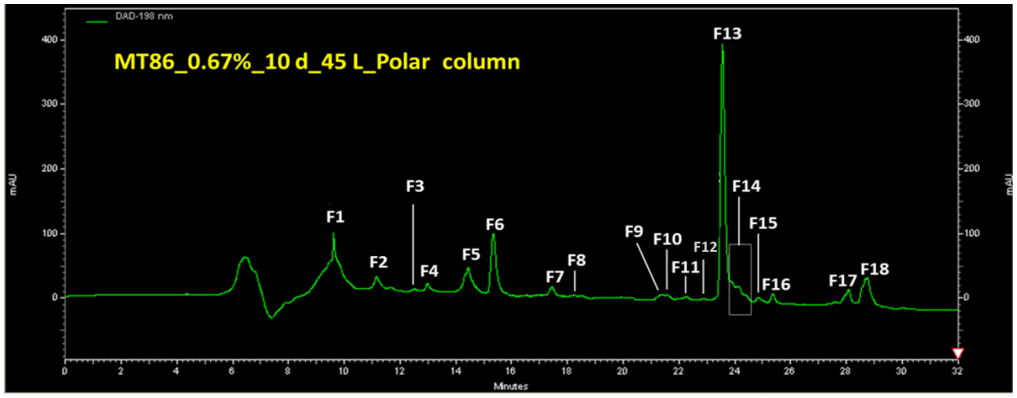

Figure 3-19. Semi-preparative HPLC chromatogram of supernatant extract from 45 L culture of *A. vinosum* strain MT86 grown at 0.67% salts.

From the chromatogram of analytical HPLC-DAD/MS and in comparison with the Dictionary of Natural Products, seven fractions F3, F4, F5, F6, F11, F13, and F17 were selected for NMR analyses. With the exception of F3 (only ^{1}H NMR), these fractions were analyzed by ^{1}H NMR, ^{13}C NMR, HMBC, HSQC, DEPT, and NOESY. Fraction F13 was identical to the same compound F13/P10 from previous analyses (paragraph 3.1.3 on page 54, and paragraph 3.2.2.3 on page 62) by comparison of the UV_{max}, mass, and NMR data. The analytical HPLC chromatogram of F13 is shown in Figure 3-20.

.

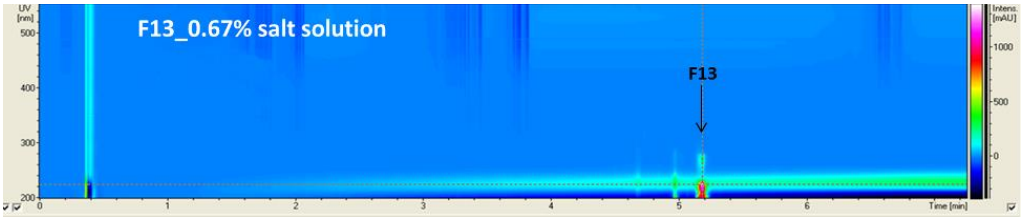

Figure 3-20. HPLC chromatogram of compound F13 isolated from 45 L culture grown at 0.67% salts.

Table 3-15. Detailed information on fractions of extract from 45 L culture broths of *A. vinosum* MT86 grown at 0.67% salts.

Com.	Weight (mg)	Rt of UV_{max} (min)	Mass information (Rt/min)		MW	DNP	HRESIMS & Formula	NMR					
			Pos.	Neg.				^{1}H	^{13}C	HMBC	HSQC	DEPT	NOESY
F1	2.0	/	/	/	/	-	-	-	-	-	-	-	-
F2	0.6	/	/	/	/	-	-	-	-	-	-	-	-
F3	0.2	Rt 2.40	Rt2.3, m/z 266	Rt 2.3, m/z 264	265	36 hits	-	+	-	-	-	-	-
F4	0.5	Rt 2.24	Rt 2.2, m/z 243	Rt 2.2, m/z 240	241/242	37 hits	-	+	+	+	+	+	+
F5	1.7	Rt 2.07	/	/	/	/	-	+	+	+	+	+	+
F6	1.4	Rt2.26 Rt 2.31	Rt2.2, m/z 197.9, m/z 151.9	Rt 2.2, m/z 149.7	/	/	-	+	+	+	+	+	+
F7	0.4	Rt 2.08	/	/	/	/	-	-	-	-	-	-	-
F8	-	not pure	/	/	/	/	-	-	-	-	-	-	-
F9	-	not pure	/	/	/	/	-	-	-	-	-	-	-
F10	-	not pure	/	/	/	/	-	-	-	-	-	-	-
F11	0.4	Rt 4.43	Rt 2.2, m/z 243	Rt 2.2, m/z 241	242	519 hits	-	+	+	+	+	+	+
F12	0	/	/	/	/	-	-	-	-	-	-	-	-
F13	5.2	Rt 4.61 Rt 4.89	Rt 5.1, m/z 623 (m/z 173, m/z 301)	Rt 5.1, m/z 621	622?	93 hits	-	+	+	+	+	+	+
F14	3.5	not pure	/	/	/	-	-	-	-	-	-	-	-
F15	1.2	not pure	/	/	/	-	-	-	-	-	-	-	-
F16	1.5	not pure	/	/	/	-	-	-	-	-	-	-	-
F17	1.4	Rt 3.59	Rt 5.1, m/z 627	Rt 5.1, m/z 625	626	70 hits	-	+	+	+	+	+	+
F18	3.3	Rt 3.63	not pure	/	/	-	/	-	-	-	-	-	-

/: not sure; -: no experiments; +: experiments done.

The accurate mass of compound F13 was obtained by the high-resolution mass detection (TOF and micrOTOF). The accurate mass of F13 can be seen in Figure 3-21. The positive method showed the m/z $[M+H]^+$ was 301.1 and the negative method showed the m/z $[M-H]^-$ was 299.2. Thus, the accurate mass of F13 is MW 300.

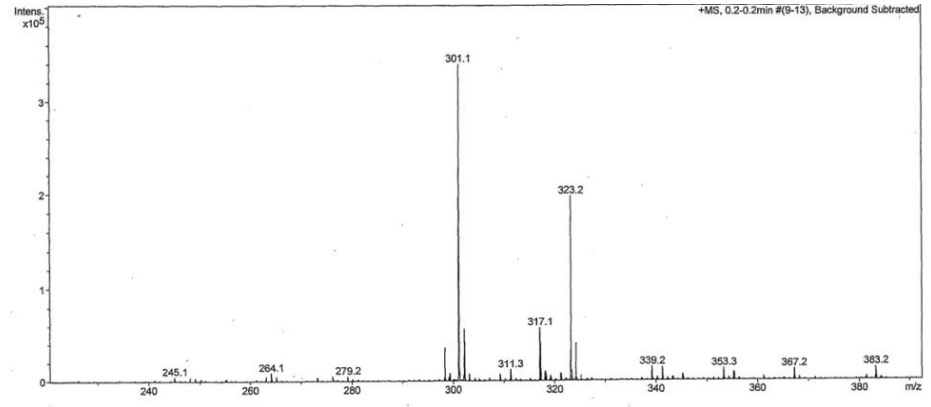

(a)

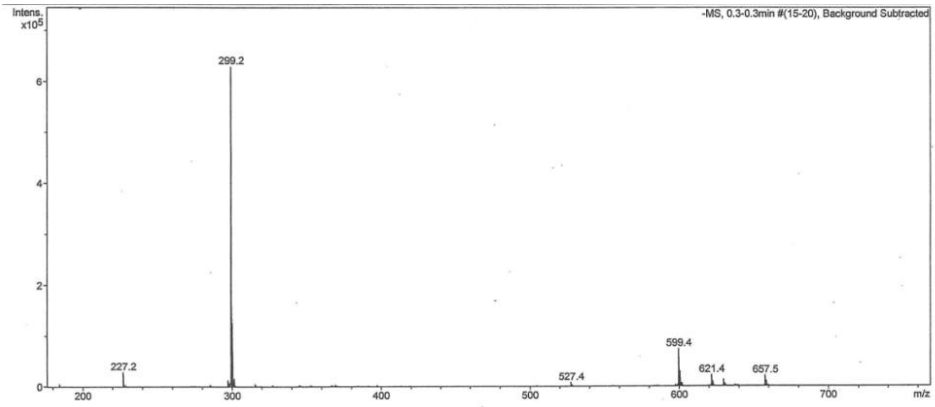

(b)

Figure 3-21. Mass spectrum of compound F13 isolated from culture extract grown at 0.67% salts with (a) positive method and (b) negative method.

3.3.4.2 Cultures grown at 2.5% salts

After 15 days' incubation, 50 L culture broths were extracted. 570 mg dried supernatant extract was obtained and then dissolved in MeOH. The HPLC chromatogram is shown in Figure 3-22. The semi-preparative HPLC chromatograms with two different columns are shown in Figure 3-23 and Figure 3-24. The 18 fractions of a reverse-phase C18 column (2/3 crude supernatant extract) are named C1 to C18 and those from a polar column (1/3 crude supernatant extract) are named P1 to P18.

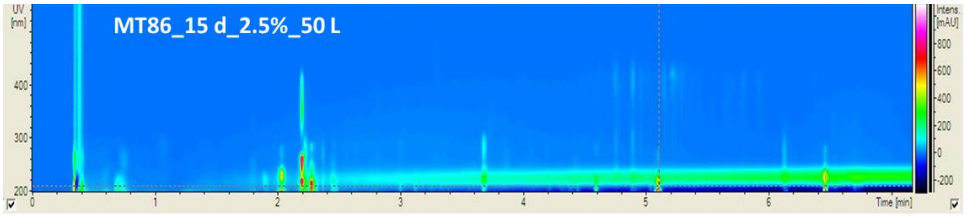

Figure 3-22. HPLC chromatogram of extracts from 50 L supernatant culture broth of *A. vinosum* strain MT86 grown at 2.5% salts for 15 days.

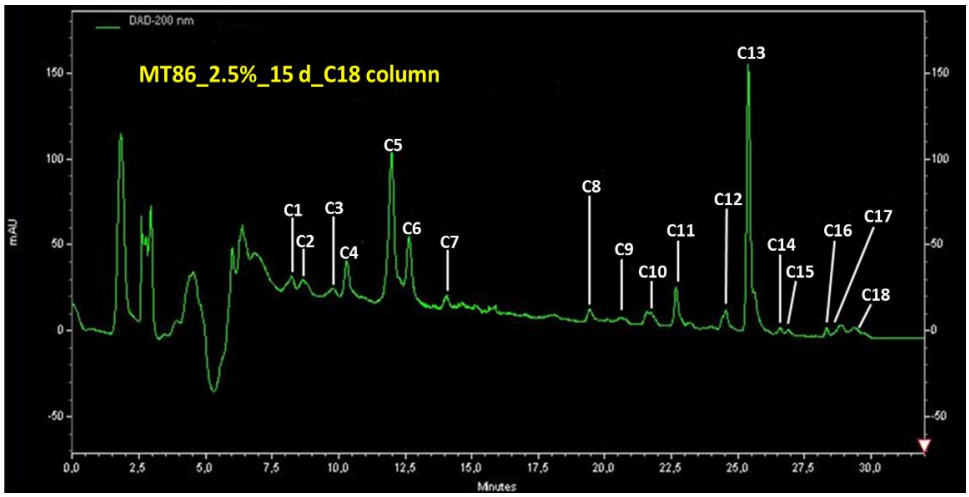

Figure 3-23. Semi-preparative HPLC (C18 column) chromatogram of supernatant extract from 50 L culture of *A. vinosum* MT86 at 2.5% salts for 15 days.

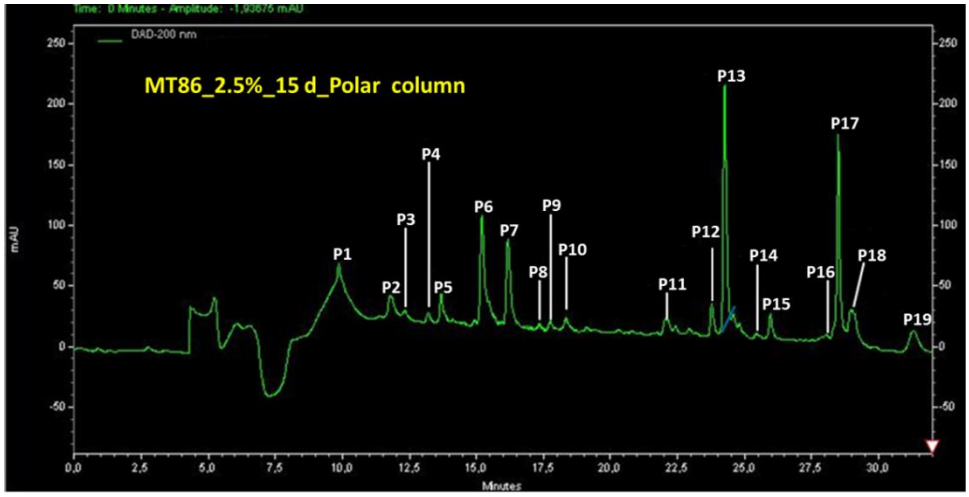

Figure 3-24. Semi-preparative HPLC (polar column) chromatogram of supernatant extract from 50 L culture of *A. vinosum* MT86 at 2.5 salts for 15 days.

The comparison of semi-preparative HPLC chromatograms showed the most significant differences after Rt 28 min, with the intensity of P17 being higher than C17, and no corresponding compound to P19 was detected. P13 and C13 showed almost the same Rt and shape. These indicated that the polar column was a better method for fractionation than C18 column.

The comparison of semi-preparative HPLC chromatograms of extracts from culture of *A. vinosum* MT86 grown at 0.67% salts for 10 days and at 2.5% salts for 15 days, which were separated on the same polar column, showed one additional UV absorption peak around Rt 32 min (P19) in the later chromatogram (culture at 2.5% salts). In addition, peaks P6 and P7 (ca. 100 mAU) were separated better without overlapping and P17 (180 mAU) showed much higher intensity in extract from the culture grown at 2.5% salts than F17 (20 mAU) in that from cultures grown at 0.67% salts.The most important feature of these three semi-preparative chromatograms (Figure 3-19, Figure 3-23 and Figure 3-14) was that the obvious UV absorption peaks, namely F13, C13 and P13, existed with highest intensity than all other peaks. Their identity was approved by NMR spectra. The intensity of F13 was 400 mAU which was higher than the intensity of C13 (160 mAU) and P13 (220 mAU). This indicated that F13 was the compound that can be reproduced under different cultivation conditions and columns used for fractionation. However, according to the comparison of cultivation time and fractionation methods, incubation at 0.67% salts concentration after 10 days was the best conditions for isolation of compound F13.

Table 3-16. Comparison of fractions from different cultures of *A. vinosum* strain MT86.

0.67% Salts (Polar)	amount	real mass	2.5% Salts (C18)	amount	real mass	2.5% Salts (Polar)	amount	real mass	Note
F1	2.0 mg	not pure	**C1**	-	no UV	**P1**	0.6 mg	not pure	
F2	0.6 mg	not pure	**C2**	3.8 mg	not pure	**P2**	-	no	
F3	0.2 mg	265	**C3**	-	UV pure, 397 not pure enough	**P3**	-	643? 671?	
F4	0.5 mg	241? 242?	**C4**	1.3 mg	not pure (one strong, one weak) pos m/z 243, 266 neg m/z 240.9, 263	**P4**	-	265	probably they are the same
F5	1.7 mg	not pure	**C5**	0.3 mg	not pure	**P5**	-	not pure	
F6	1.4 mg	not pure	**C6**	-	not pure	**P6**	-	no	
F7	0.4 mg	not pure	**C7**	-	no UV	**P7**	-	no	
F8	-	not pure	**C8**	-	too weak UV	**P8**	-	no	
F9	-	not pure	**C9**	-	UV pure, m/z not pure	**P9**	-	no	
F10	-	not pure	**C10**	0.7 mg	UV pure, neg pure m/z277 pos m/z>3 peaks	**P10**	-	no	
F11	0.4 mg	142	**C11**	-	not pure	**P11**	0.4 mg	UV pure, m/z no	
F12	0 mg	not pure	**C12**	0.9 mg	UV pure, m/z not pure	**P12**	-	not pure	
F13	5.2 mg	622 oil-like	**C13**	0.6 mg	>2 UV neg m/z 621 pos m/z 173	**P13**	0.7 mg	622	F13 = C13 = P13 (= P10 from 20 L)
F14	3.5 mg	not pure	**C14**	-	not pure	**P14**	0.5 mg	no UV	
F15	1.2 mg	not pure	**C15**	-	not pure	**P15**	0.2	not pure	
F16	1.5 mg	not pure	**C16**	-	not pure	**P16**	-	UV pure, m/z no	
F17	1.4 mg	626	**C17**	-	not pure	**P17**	0.8 mg	UV pure, m/z no	
F18	3.3 mg	not pure	**C18**	-	not pure	**P18**	0	not pure	

3.3.5 NMR analysis of compound F13 from 0.67% salts concentration

NMR chromatograms of ^{1}H NMR (Figure 3-26), ^{13}C NMR and DEPT (Figure 3-27), ^{1}H-^{1}H COSY (Figure 3-28), ^{1}H-^{13}C HMBC (Figure 3-29), ^{1}H-^{13}C HSQC (Figure 3-30) and NOESY (Figure 3-31) of compound F13 were obtained with the substance purified from the crude supernatant extract of a 45 L *A. vinosum* MT86 cultures grown at 0.67% salts for 10 day. The NMR spectroscopic data information is shown in Table 3-17 and Table 3-18. The ESI mass spectra (positive and negative ions) provided that the molecular weight was 300 and molecular formula was $C_{20}H_{28}O_2$. The predicted formula and the mass from the HPLC were corresponding well. The formula indicated the presence of seven degrees of unsaturation.

The ^{1}H NMR spectra gave the H atom information. *J* values of δ7.14, δ6.95, and δ6.84 indicated that there were three aromatic-H, which were corresponding to a trisubstituted phenyl ring. *J* values of δ2.85 and δ2.78 indicated the presence of three aliphatic-H.

The ^{13}C-NMR in connection with the DEPT and HSQC measurement gave 20 C atoms information. The C atom of δ183.45 was an acid carboxyl C, δ150-125 signals showed six aromatic-C (according to a phenyl group), and δ46.67-17.24 signals indicated 12 aliphatic-C, among them were 4 CH_3, 5 CH_2, 2 CH and a quaternary C.

According to the NMR analyses, structure information was obtained. There were three ring units in compound F13. The ^{13}C NMR and DEPT spectrum showed that this compound had 20 carbons (Table 3-18). The ^{1}H spectrum showed there were 28 H protons which corresponding to the results of HSQC and DEPT. The structure of F13 was obtained as shown in Figure 3-25.

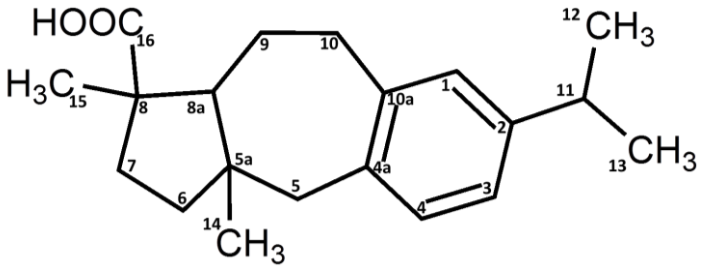

Figure 3-25. Structure of compound F13 repurified from combined fractions of F13, P13 and C13.

Table 3-17. ^{1}H NMR (600 MHz, MeOD), ^{1}H-^{1}H COSY and ^{1}H-^{13}C HMBC correlation for compound F13.

No.	δ_H /ppm	δ_H type, *J*/Hz	No. of H proton	^{1}H-^{1}H COSY (δ_H/ppm)	HSQC	δ_C, type	HMBC
1	7.14	d, 8.2	1	6.95	125.20	CH	C-4
2	6.95	dd, 8.2, 1.9	1		124.83	CH	C-3
3	6.84	d, 1.9	1		127.75	CH	C-1
5	2.85	ddd, 54.02, 8.2, 3.5	2	1.84, 1.53	31.23	CH_2	C-10
6	2.78	hept, 7.0	1		34.86	CH	C-11
7	2.33	dt, 13.3, 3.2	2	1.43,	39.51	CH_2	C-5
8	2.17	m	1		46.67	CH	C-8a
9	1.83	m	2	1.65	38.15	CH_2	C-7
10	1.64	m	2	1.83	19.77	CH_2	C-6
11	1.52	ddt, 13.0, 5.7, 2.3	2	1.83	22.90	CH_2	C-9
12	1.43	td, 12.7, 4.3	1				
13	1.26	d, 20.6	3		17.24	CH_3	C-17
14	1.20	m	9				C-14, C-12, C-15
	Sum of H proton		28				

d = doublet, dd = doublet of doublets, ddt = doublet of doublet of triplets, ddd = doublet of doublet of doublets, dt = doublet of triplets, m = multiplet, td = triplet of doublets, hept = heptet.

Table 3-18. ^{13}C NMR (150 MHz, MeOD) spectroscopic data for F13.

No. of C	δ_C/ppm	C-Atom	H-Atom	δ_H/ppm	Position
1	183.45	COOH	1	1.25	C16
2	148.34	C	-	-	C-4a
3	146.83	C	-	-	C-2
4	135.78	C	-	-	C-10a
5	127.75	CH	1	6.84	C-1
6	125.20	CH	1	7.14	C-4
7	124.83	CH	1	6.95	C-3
8	48.41	C	-	-	C-8
9	46.67	CH	1	2.18	C-8a
10	39.51	CH_2	2	2.33/1.43	C-5
11	38.15	CH_2	2	1.83/1.65	C-7
12	38.07	C	-	-	C-5a
13	34.86	CH	1	2.78	C-11
14	31.23	CH_2	2	2.85	C-10
15	25.55	CH_3	3	1.20	C-14
16	24.49	CH_3	3	1.20	C-12
17	24.49	CH_3	3	1.20	C-13
18	22.90	CH_2	2	1.83/1.52	C-9
19	19.77	CH_2	2	1.83/1.70	C-6
20	17.24	CH_3	3	1.25	C-15
Total		20 C	28 H		

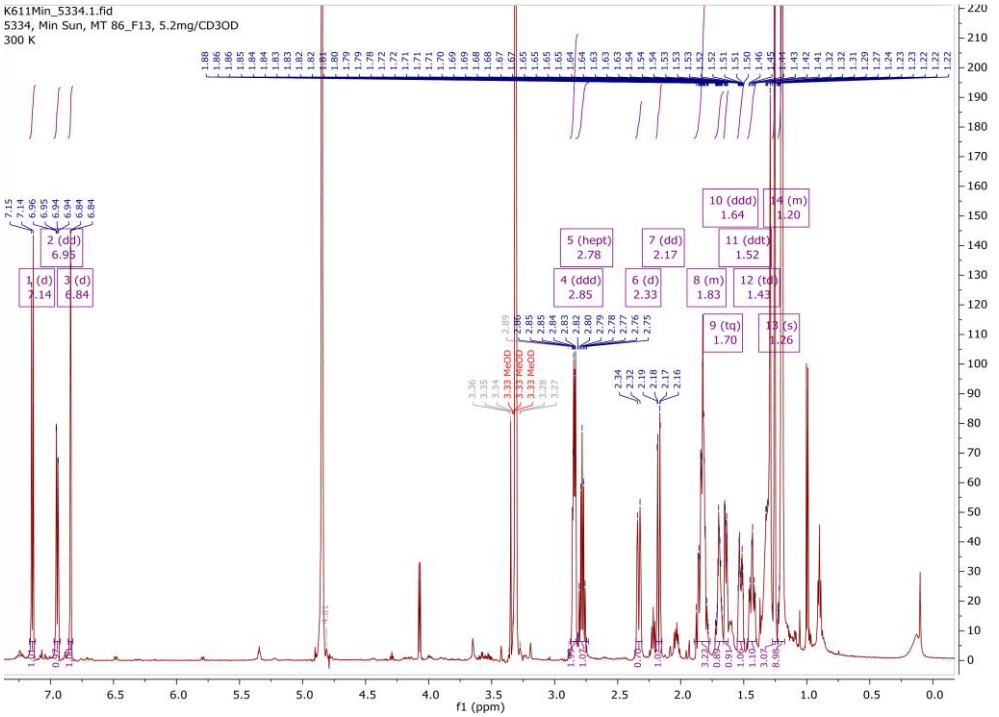

Figure 3-26. ^{1}H NMR chromatogram of compound F13.

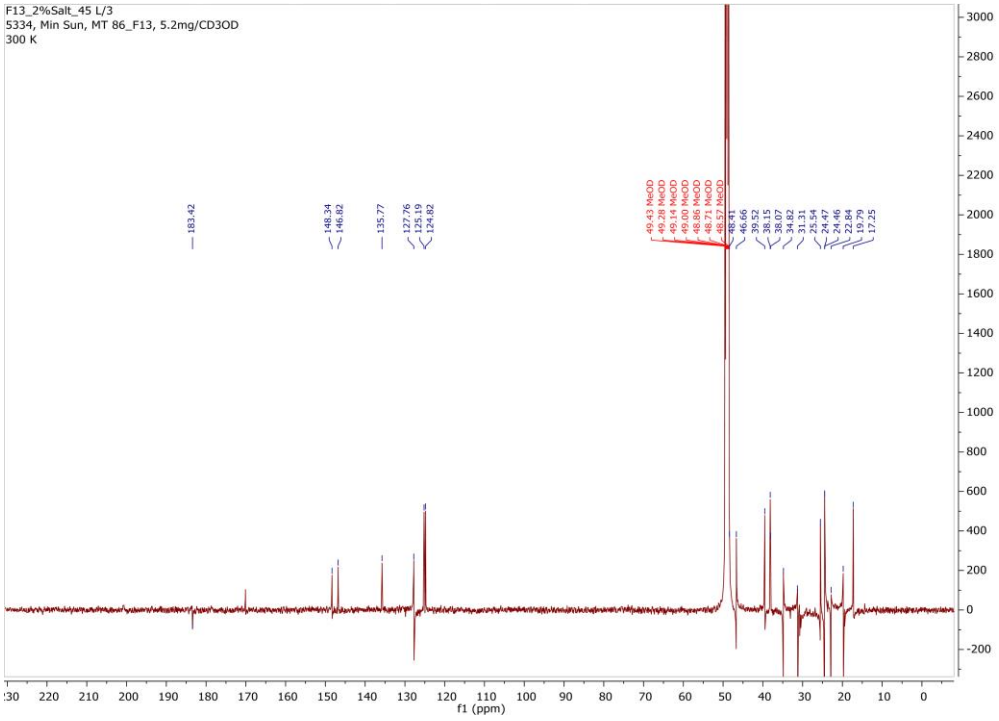

Figure 3-27. ^{13}C NMR and DEPT chromatogram of compound F13.

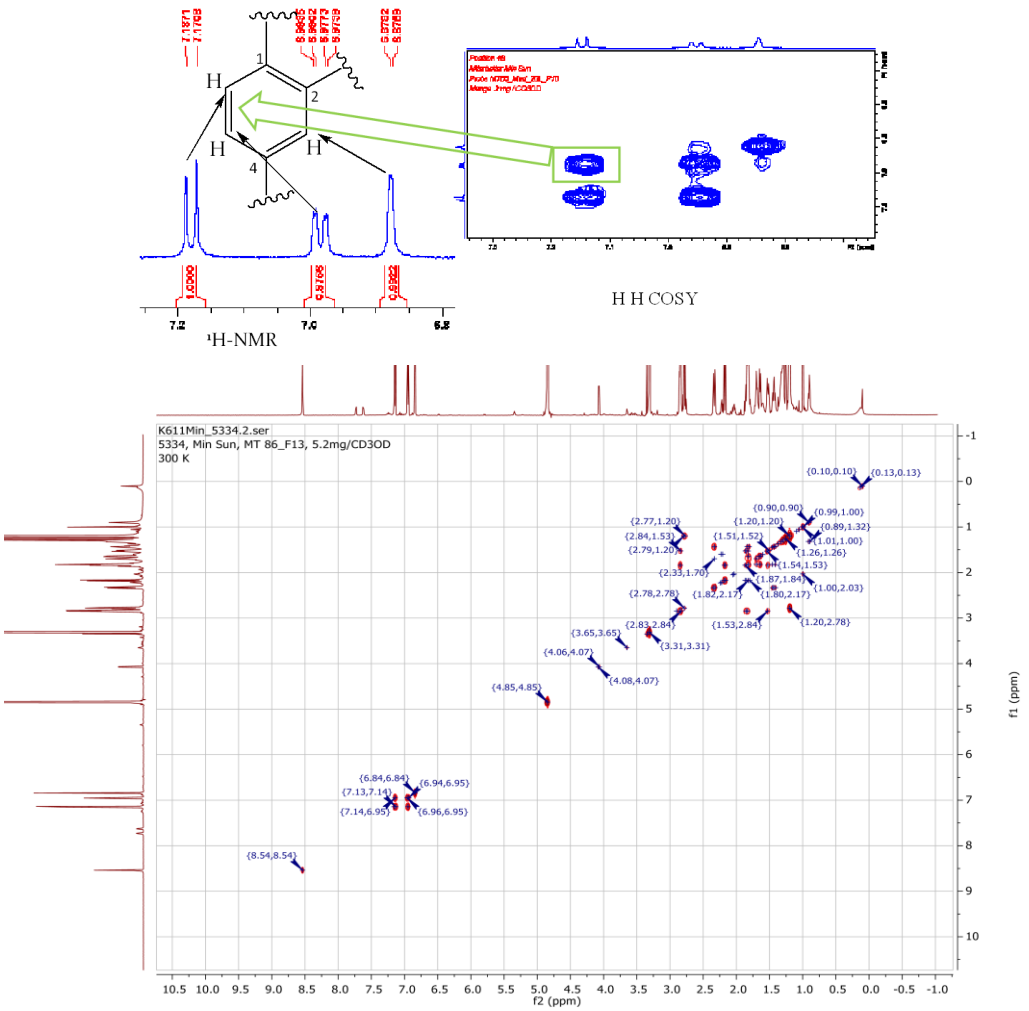

Figure 3-28. ^{1}H-^{1}H COSY chromatograms of compound F13.

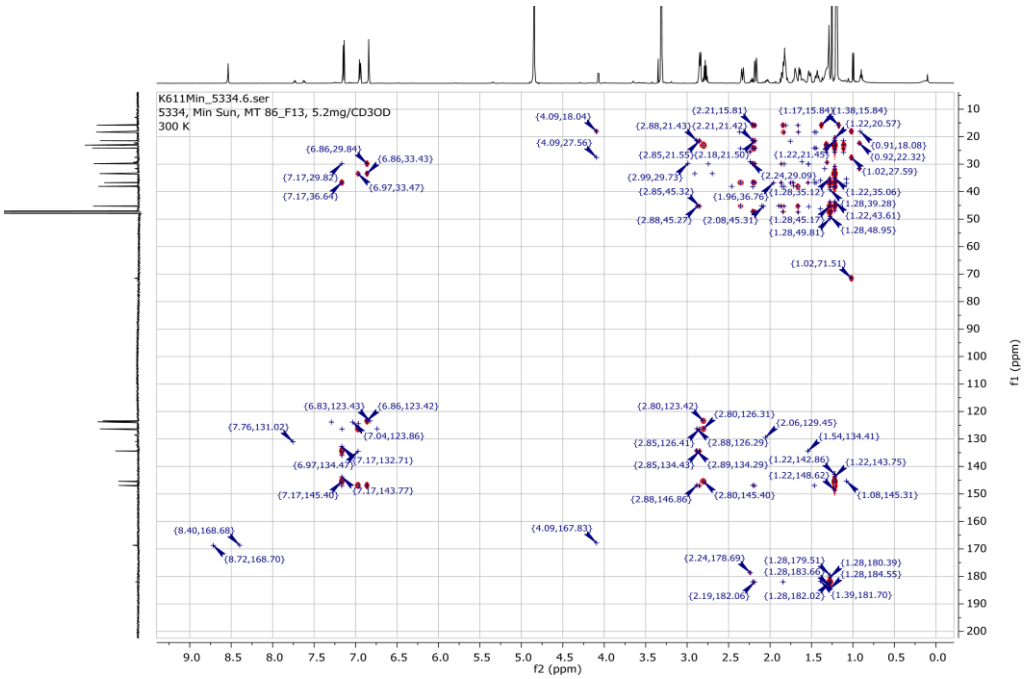

Figure 3-29. ^{1}H-^{13}C HMBC chromatogram of compound F13.

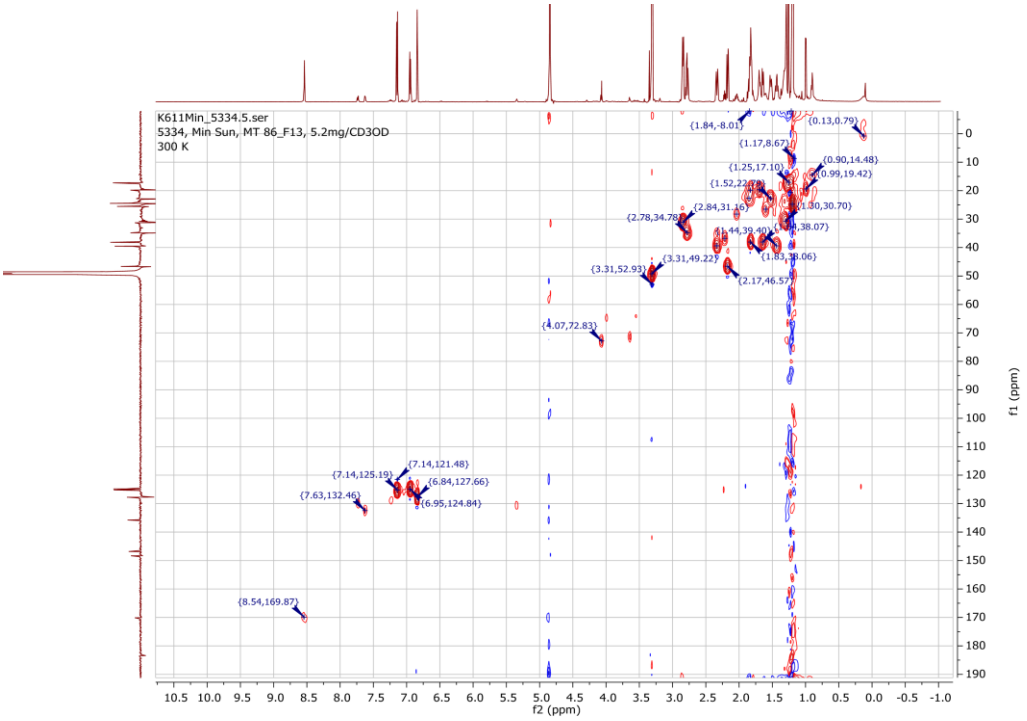

Figure 3-30. ^{1}H-^{13}C HSQC chromatogram of compound F13.

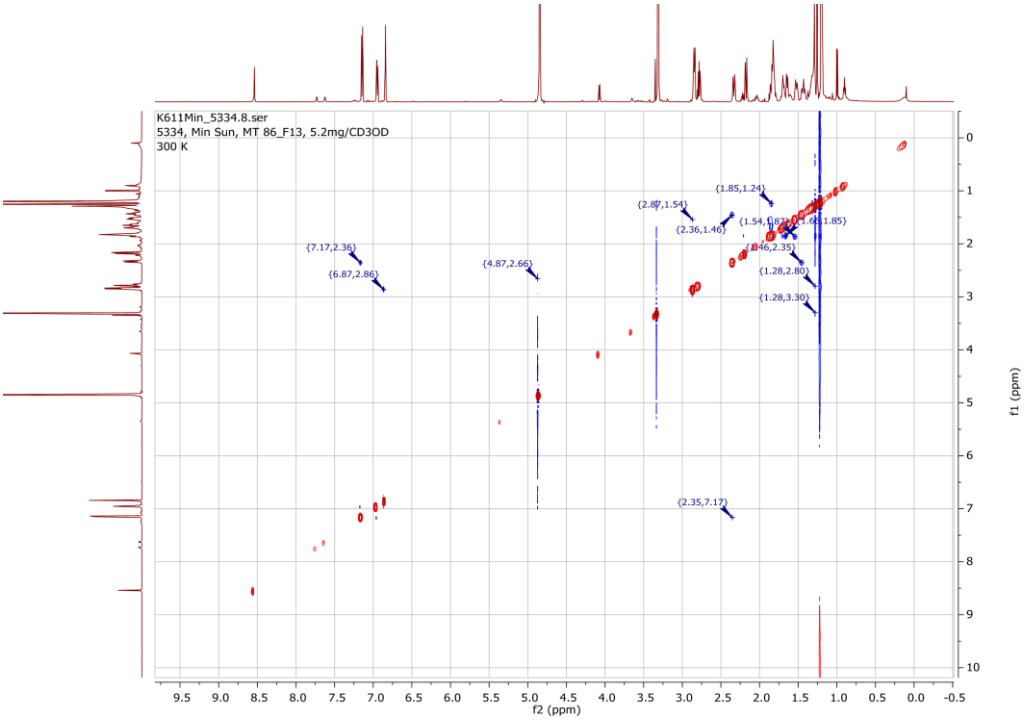

Figure 3-31. NOESY chromatogram of compound F13.

3.3.6 Bioactivity tests of fractions from cultures grown at 0.67% salts

Seven fractions (F3, F4, F11, and F17, including the impure F5, F6 and F18) and pure compound F13 were selected for antibacterial, antifungal, and enzyme activities. Seven antibacterial tests, one antifungal test, and four enzymes inhibition tests were performed.

The IC_{50} values for compound F13 in tests with *B. subtilis*, *S. lentus*, and AchE were 70.5 µM (± 2.9), 57.0 µM (± 3.3), and >10 µM, respectively. The seven fractions showed no antibacterial and antifungal inhibition. However, it was very interesting that the fraction F5 and F18 showed inhibition of AchE with IC_{50} of 3.95 µM (± 1.9) and IC_{50} of 8.91 µM (± 3.28), respectively. Other fractions and compound F13 showed low inhibition of AchE (IC_{50} valuce of > 10µM). There were no bioactivities against the other three enzymes.

Table 3-19. Bioactivities of fractions from *A. vinosum* strain MT86.

	Antibacterial									Antifungal	Enzyme				
Fractions/ compounds	*B. subtilis* 100 µM (%)	*B. subtilis* IC_{50}	*S. lentus* 100 µM (%)	*S. lentus* IC_{50}	*E. coli* 100 µM (%)	*P. syringae* 100 µM (%)	*X. campestris* 100 µM (%)	*E. amylovora* 100 µM (%)	*R. solanacearum* 100 µM (%)	*C. glabrata* 100 µM (%)	AchE 10 µM (%)	AchE IC_{50}	GSK 10 µM (%)	PDE-4β2 10 µM (%)	PTP 10 µM (%)
MT86_F3	-	-	-	-	-	-	-	-	-	-	49	> 10 µM	-	-	-
MT86_F4	-	-	-	-	-	-	-	-	-	-	46	> 10 µM	-	-	-
MT86_F5*	-	-	-	-	-	-	-	-	-	-	86	3.95 µM (± 1.9)	-	-	-
MT86_F6*	-	-	-	-	-	-	-	-	-	-	-	> 10 µM	-	-	-
MT86_F11	-	-	-	-	-	-	24	-	-	-	-	> 10 µM	-	-	-
MT86_F13	100	70.5 µM (± 2.9)	100	57.0 µM (± 3.3)	27	-	-	-	-	-	-	> 10 µM	-	-	-
MT86_F17	-	-	-	-	-	-	-	-	-	-	33	> 10 µM	-	-	-
MT86_F18*	-	-	-	-	-	-	-	-	-	-	83	8.91 µM (±3.28)	-	-	-

1. ***B. subtilis***: *Bacillus subtilis*, ***S. lentus***: methicillin-resistant *Staphylococcus lentus*, ***E. coli***: *Escherichia coli*, **MRSA**: *Staphylococcus aureus*, ***X campestris***: *Xanthomonas campestris*, ***P. syringae*****:** *Pseudomonas syringae*; ***R. solanacearum***: *Ralstonia solanacearum*; ***C. glabrata***: *Candida glabrata*; **AchE:** acetylcholinesterase**, GSK:** glycogen synthase kinase, **PDE-4β2**: phosphodiesterase 4, PTP: protein-tyrosine-phosphatase.

2. Note: The results of the bioassays are defined as follows: ⩾ 80% inhibition: very good activity; < 80% and ⩾ 60% inhibition: moderate activity; < 60% and > 30% inhibition: low activity; ⩽ 30% inhibition &-: no activity. 3. *: fraction was not pure

3.3.7 Screening of crude cell extract for compound F13 by TLC

TLC was carried out on precoated silica gel 60 F_{254} plates (0.25 mm, Merck); spots were visualized by spraying with anisaldehyde in 10% H_2SO_4 solution followed by heating.

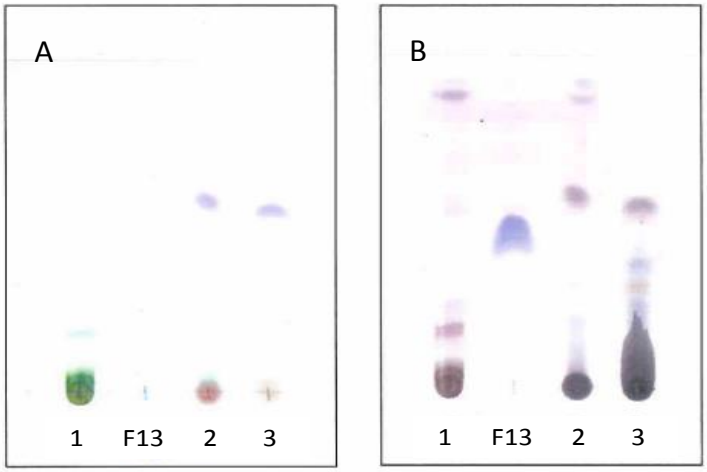

A: TLC chromatogram before staining;
B: TLC chromatogram of extracts after spraying with 10% H_2SO_4 solution followed by heating.
1: MeOH-extract; F13: compound F13; 2: Acetone-extract; 3: dichloromethane-extract

Figure 3-32. The TLC chromatograms of compound F13 and cell extracts.

The TLC chromatogram (Figure 3-32) shows that the spot of compound F13 was not present in any of the cell extracts, no matter what kind of solvent was used for extraction.

3.4 Properties of compound F13 from *A. vinosum*. MT86

Compounds F13 isolated from supernatant extract of a 45 L culture grown at 0.67% salts for 10 days, P13, and C13 isolated from supernatant extract of a 50 L culture grown at 2.33% salts for 15 days (fractionated by polar and C18 reverse columns) were collected for purification to obtain substance of sufficient purity for structure elucidation (purification and elucidation of IR, CD and polarimetry are not shown, personal communication to Prof. Dr. A. Zeeck) .

There were 12 apparent absorption peaks from IR spectrum of F13 (Figure 3-33 and Table 3-20). Absorption at 1698 cm^{-1} was significant which indicates the presence of a carboxyl group (CO-stretching vibration).

The CD spectrum (Figure 3-34) showed a signal at 220 nm wavelength. The CD effects were not significant.

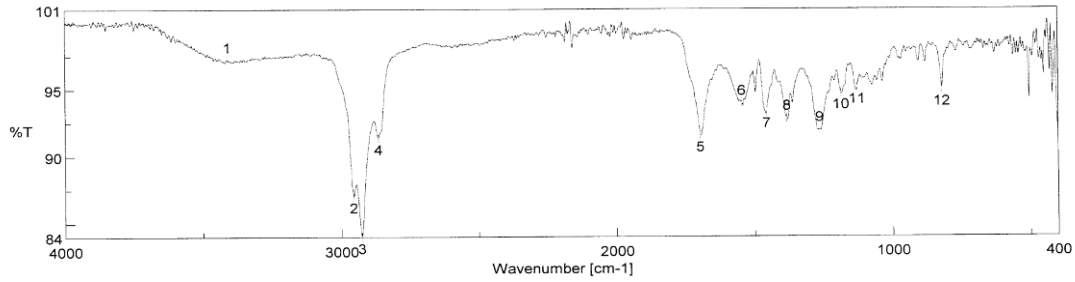

Figure 3-33. IR spectrum of compound F13 from *A. vinosum* MT86.

Table 3-20. The results of peak picking from the IR spectrum of compound F13.

No.	Position/cm^{-1}	Intensity	Identification of absorption peaks
1	3412.42	97.2348	
2	29.55.38	87.0512	
3	2926.45	84.0294	
4	2865.7	91.3928	
5	1698.02	91.549	Carboxyl group (CO-stretching vibration)
6	1546.63	93.9369	
7	1456.96	93.316	
8	1382.71	92.8089	
9	1265.07	91.9499	
10	1187.94	94.7089	
11	1129.12	95.1132	
12	820.563	94.9275	

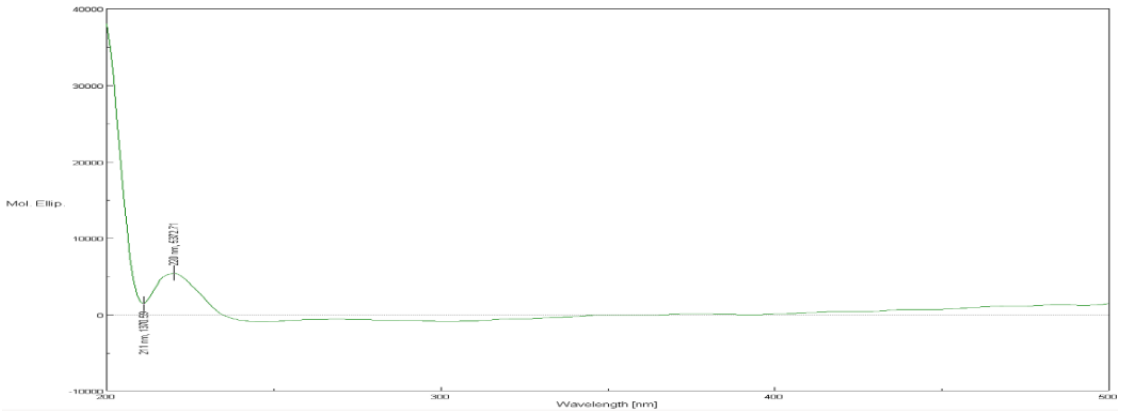

Figure 3-34. The CD spectrum of compound F13.

F13 was isolated as a yellowish oil-like compound that gave a pseudomolecular ion $[M+H]^+$ at *m/z* 301, $[M+Na]^+$ at *m/z* 323, $[M-H]^-$ at *m/z* 299 in the HRESIMS, indicating the molecular formula $C_{20}H_{27}O_2$

(299.2017) (calcd. for $C_{20}H_{28}NaO_2$, 323.1982) (7° of unsaturation). The IR spectrum of F13 showed IR (neat) V_{max} 3412.42 cm-1 a broadband at 1698.02 cm^{-1}, consistent with the presence of carboxyl group (CO-stretching vibration). The optical rotation $[\alpha]_D^{25}$ of compound F13 was + 42 (MeOH), and no effect from CD spectrum showed that CD effects were not significant.

Compound F13 (Table 3-21) is the first antibiotic substance (an aromatic tricyclic diterpenoid) isolated from anoxygenic phototrophic bacteria, although the measured activities were moderate. IC_{50} values for F13 against *Bacillus subtilis*, and *Staphylococcus lentus* were 70.5 µM (± 2.9) and 57.0 µM (± 3.3), respectively.

Table 3-21. Summary of structural features of F13.

Compound name	**F13**
Isolated from	*Allochromatium vinosum* strain. MT86, supernatant extract
MW	300
Formula	$C_{20}H_{28}O_2$
UV maxima (nm)	225, 268, sh271, 275/276
$[\alpha]_D^{25}$	+ 42°

3.5 Metabolite profiles of other phototrophic bacteria

Purple nonsufur bacteria (PNSB) *Rhodopseudomonas palustris* strain 120/1, *Rhodobacter capsulatus* strain 182, and *Rubrivivax gelatinosus* strain 151 were selected for secondary metabolites screening. The first screening of these three strains was performed in 500 ml AT medium and antibiotic activities were tested against nine microorganisms. The second screening of them was performed in 100 ml AT medium to compare the UV absorption peaks.

3.5.1 First screening of strains 120/1, 182, and 151

From the HPLC chromatograms (Figure 3-35), there are some UV absorption peaks (200 to 540 nm) from Rt 4.8 min to Rt 6.2 min in the crude extracts of all three strains. These peaks are correlated to pigments from these bacteria. The results of bioassay tests to nine organisms are seen in Table 3-22. There is no inhibition of extracts from these three strains of *E. coli*, *X. campestris*, *P. acnes*, and *C. albicans*. The extract of strain 120/1 showed no activity against *T. rubrum*, low activities to *B. subtilis* (50%), MRSA (39%) and *S.tritici* (35%) but moderate activity against *S. lentus* (72%). The extract of strain 182 showed no activities against *B. subtilis* (23%), *S. tritici* (21%), low activity against MRSA (38%), moderate activity against *T. rubrum* (67%) and good activity against *S. lentus* (81%). The extract of strain 151 showed low activities against *B. subtilis* (34%), MRSA (42%), and *T. rubrum* (53%) but very good activities against *S. lentus* (82%) and *S. tritici* (80%), the later organism was only inhibited very well by the extract of strain 151.

The HPLC chromatograms (Figure 3-35) showed that strain 151 has the highest number of UV peaks and the crude culture extract of strain 151 showed moderate to very good inhibitions of several test microorganisms (Table 3-22).

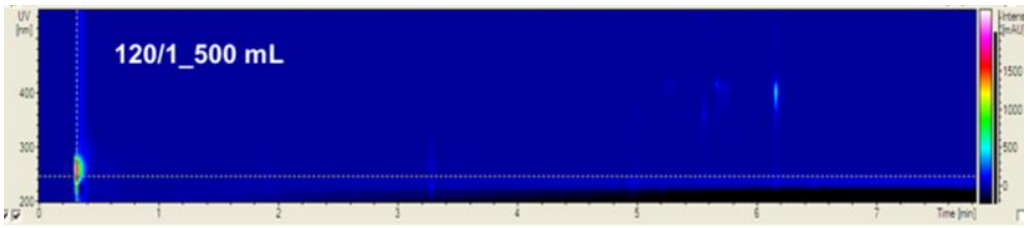

(a)

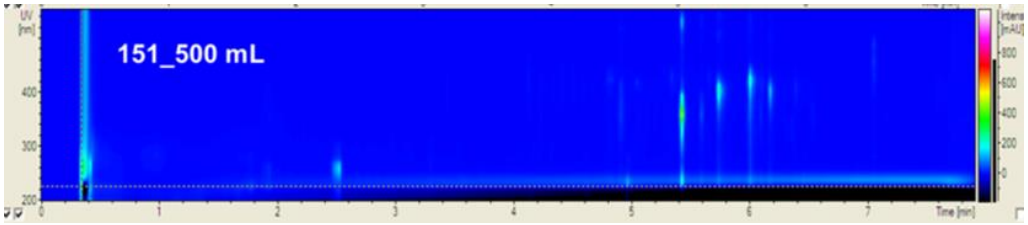

(b)

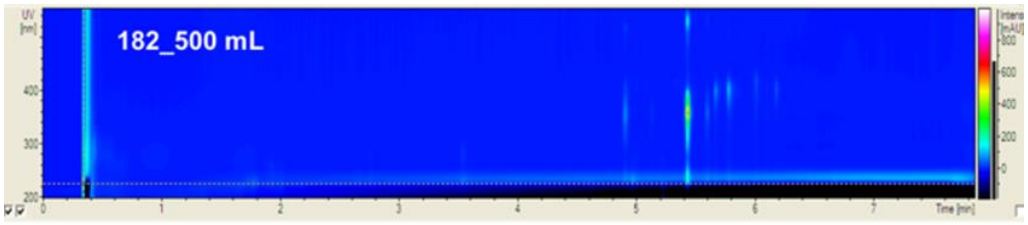

(c)

Figure 3-35. HPLC-DAD/MS results of strains 120/1, 182 and 151.

Table 3-22. Bioassay results of extracts from *Rhodopseudomonas palustris* 120/1, *Rhodobacter capsulatus* 182, and *Rubrivivax gelatinosus* 151.

Crude extracts	Inhibitions								
	Bs	***Sl***	***Ec***	**MRSA**	***Xc***	***Pa***	***Ca***	***Sep***	***Tru***
120/1-500ml	50	72	-	39	-	-	-	35	-
182-500ml	23	81	-	38	-	-	-	21	67
151-500ml	34	82	-	42	-	-	-	80	53

1. **Bs**: *Bacillus subtilis*, **Sl**: *Staphylococcus lentus*, **Ec**: *Escherichia coli*, **MRSA**: *Staphylococcus aureus*, **Xc**: *Xanthomonas campestris*, **Pa**:*Propionibacterium acnes*, **Ca**: *Candida albicans*, **Sep**: *Septoria tritici*, **Tru**: *Trichophyton rubrum*. *: assay concentration was 476 µg/ml;

2. Note: The results of the bioassays are defined as follows: ⩾ 80% inhibition: very good activity; < 80% and ⩾ 60% inhibition: moderate activity; < 60% and > 30% inhibition: low activity; ⩽ 30% inhibition & -: no activity.

3.5.2 Screening of culture broth in a 100 ml volume

Rhodopseudomonas palustris strain 120/1, *Rhodobacter capsulatus* strain 182, and *Rubrivivax gelatinosus* strain 151 were inoculated in 100 ml AT medium for comparison of metabolite profiles according to UV absorption and mass.

The HPLC-DAD/MS chromatograms of extracts obtained after 7 and 10 days' incubation showed 24 distinct peaks of strain 120/1 (Figure 3-36), 25 peaks of strain 182 (Figure 3-37), and 20 peaks of strain 151 (Figure 3-38).

3.5.2.1 Screening of crude extract of *Rhodopseudomonas palustris* strain 120/1 grown for 7 and 10 days

The HPLC chromatograms are shown in Figure 3-36. 24 UV absorption peaks (p1-p24) are present (UV_{max} and mass information is in Table 3-23).

Peak p22 (UV maximum at 228 nm and m/z 821, belonging to an arithmetic progression from m/z 865 to m/z 425, common difference is 44) found in the HPLC chromatogram of extract from culture grown for 10 days was absent in the extract from culture grown for 7 days.

There was not much difference between the extracts from cultures grown for different incubation time (7 and 10 days). Peaks p1, p2, p3, p21 and p24 in extracts of cultures grown for 7 and 10 days showed small difference in UV absorption (some shoulder UV absorption), but had the same MW (or obvious m/z, arithmetic progression) in mass spectra. Peak p6 showed the same UV absorption but different MW in extracts from cultures after 7 and 10 days. Peak p5 had m/z 294 in extract obtained after 7 days, but m/z 295 (MW 294) in extract obtained after 10 days. In consideration of the intensity of UV absorption, peaks p11-p19 of extract from culture grown for 10 days showed higher intensity than for 7 days. Comparison of p22, p23 and p24 revealed that these peaks belonged to a serial arithmetic progression from m/z 865 to 425, with the common difference (*d* value) of 44. 10 days of cultivation of *Rhodopseudomonas palustris* strain120/1 was better than 7 days.

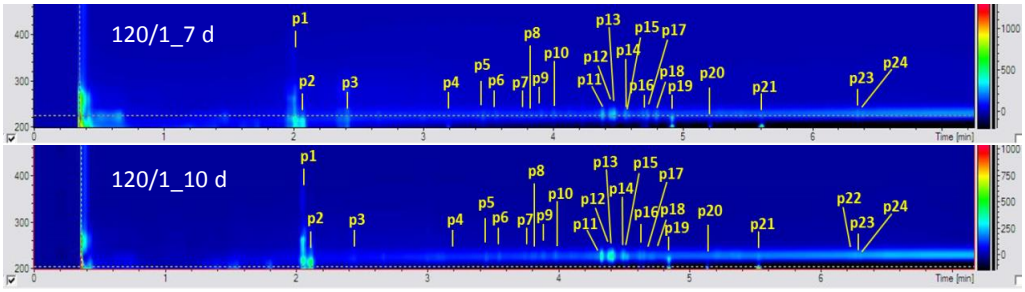

Figure 3-36. HPLC chromatograms of extracts from 100 ml supernatant culture broth of *Rhodopseudomonas palustris* strain 120/1 grwon for 7 and 10 days.

Table 3-23. Comparison of extracts from cultures of strain 120/1 grown for 7 and 10 days.

120/1	7 d			10 d		
Peak	**Rt/min**	**UV_{max} /nm**	**MW or m/z**	**Rt/min**	**UV_{max} /nm**	**MW or m/z**
p1	2.01	220 nm, 460 mAU 263 nm, 257 mAU sh282nm, 150 mAU	170	2.05	220 nm, 461 mAU sh 240 nm, 304 mAU 262 nm, 373 mAU sh 271 nm, 200 mAU 356 nm, 85 mAU	170
p2	2.07	214 nm, 411 mAU 220 nm, 340 mAU 282 nm. 57 mAU	170	2.11	214 nm, 514 mAU 220 nm, 431 mAU sh 247 nm, 142 mAU 287 nm, 59 mAU	170
p3	2.42	220 nm, 249 mAU sh 237 nm, 178 mAU 277 nm, 139 mAU	/	2.44	222 nm, 120 mAU 275 nm, 49 mAU	/
p4	3.2	226 nm, 133 mAU	224	3.2	226 nm, 121 mAU	224
p5	3.47	222 nm, 171 mAU	m/z 294	3.45	220 nm, 166 mAU	294
p6	3.56	226 nm, 167 mAU	293	3.55	226 nm, 167 mAU	m/z 551
p7	3.76	226 nm, 153 mAU	297	3.74	226 nm, 154 mAU	297
p8	3.83	226 nm, 150 mAU	/	3.80	226 nm, 155 mAU	/
p9	3.91	227 nm, 167 mAU	m/z 310	3.88	227 nm, 172 mAU	m/z 310
p10	4.01	227 nm, 186 mAU	279	4.01	227 nm, 161 mAU	279
p11	4.38	227 nm, 332 mAU	295	4.39	227 nm, 364 mAU	295
p12	4.45	227 nm, 312 mAU	295	4.41	227 nm, 432 mAU	295
p13	4.47	227 nm, 364 mAU	295	4.49	227 nm, 283 mAU	295
p14	4.56	226 nm, 250 mAU	295	4.52	226 nm, 252 mAU	295
p15	sh 4.59	226 nm, 187 mAU	297	4.62	227 nm, 215 mAU	297
p16	4.69	227 nm, 205 mAU	m/z 280	4.65	227 nm, 213 mAU	m/z 280
p17	4.73	227 nm, 234 mAU	362	4.70	227 nm, 196 mAU	362
p18	4.80	227 nm, 267 mAU	227	4.72	227 nm, 192 mAU	227
p19	4.92	221 nm, 336 mAU	253	4.84	221 nm, 306 mAU	253
p20	5.21	228 nm, 164 mAU	267	5.21	228 nm, 204 mAU	267
p21	5.61	227 nm, 202 mAU	281	5.60	sh 219 nm, 102 mAU 227 nm, 200 mAU	281
p22	-	-	-	6.22	228 nm, 228 mAU	865- 425, *d*=44
p23	6.35	227 nm, 243 mAU	865-425, *d*=44	6.26	228 nm, 241 mAU	865- 425, *d*=44
p24	6.39	227 nm, 236 mAU	865-425, *d*=44	6.30	sh 219 nm, 106 mAU 228 nm, 235 mAU	865- 425, *d*=44

-: not existed; /: not sure

3.5.2.2 Screening of crude extract of *Rhodobacter capsulatus* strain 182 grown for 7 and 10 days

The HPLC chromatograms of extracts from cultures of strain 182 after 7 and 10 days are shown in Figure 3-37, in which 25 distinct peaks (named c1 to c25) are present (UV_{max} and mass information in Table 3-24).

Eight peaks (c5-c11, c17) were absent in extract from culture grown for 7 days compared to extract for 10 days. However, two other peaks (c15', MW 796 and c16', MW 521) appeared next to their neighbors c15 (MW 796) and c16 (MW 521) only in extract from culture grown for 7 days.

Peak c23 belonged to an arithmetic progression, which began from m/z 837 to m/z 441, and the common difference (*d*) was 44. Peaks of c24 and c25 (same UV_{max} absorption and m/z) belonged to another arithmetic progression (m/z 865 to m/z 425, *d* = 44) which was the same arithmetic progression as p22, p23 and p24 in the extracts from cultures of strain 120/1.

From the previous analyses, cultivation for 10 days of *Rhodobacter capsulatus* strain 182 was better than that for 7 days.

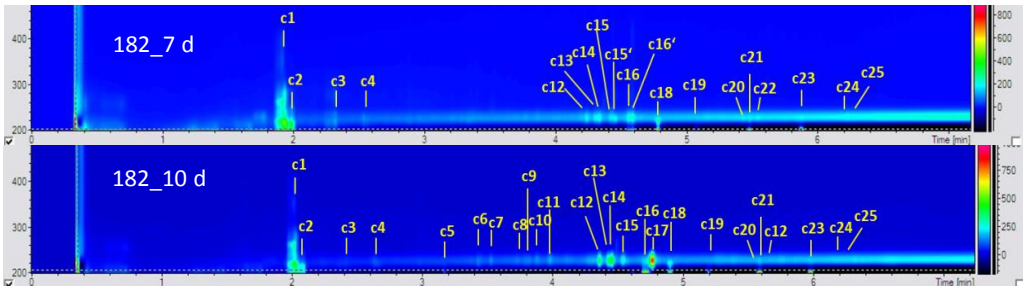

Figure 3-37. HPLC chromatogram of extracts from 100 ml supernatant culture broth of *Rhodobacter capsulatus* strain 182 grown for 7 and 10 days.

Table 3-24. Comparison of extracts from cultures of strain 182 grown for 7 and 10 days.

Peak	7 d			10 d		
	Rt/min	**UV_{max} /nm**	**MW or m/z**	**Rt/min**	**UV_{max} /nm**	**MW or m/z**
c1	1.93	217 nm, 496 mAU 240 nm, 250 mAU 265 nm, 235 mAU	170	2.02	220 nm, 473 mAU 241 nm, 287 mAU 262 nm, 332 mAU	170
c2	1.99	214 nm, 404 mAU	170	2.08	213 nm, 300 mAU 286 nm, 30 mAU	170
c3	2.32	222 nm, 124 mAU 236 nm, 91 mAU 276 nm, 60 mAU	/	2.42	222 nm, 85 mAU 276 nm, 24 mAU	/
c4	2.54	226 nm, 108 mAU	280	2.64	225 nm, 113 mAU	280
c5	-	-	-	3.17	226 nm, 99 mAU	/
c6	-	-	-	3.43	222 nm, 146 mAU	452
c7	-	-	-	3.53	226 nm, 155 mAU	477
c8	-	-	-	3.73	226 nm,142 mAU	553
c9	-	-	-	3.82	226 nm, 145 mAU	553
c10	-	-	-	3.88	228 nm,162 mAU	538
c11	-	-	-	3.98	228 nm, 192 mAU	m/z 292
c12	4.24	227 nm, 212 mAU	710	4.36	227 nm, 425 mAU	710
c13	4.31	227 nm, 206 mAU	295	4.43	227 nm, 391 mAU	295
c14	4.33	227 nm, 232 mAU	295	4.45	227 nm, 480 mAU	295
c15	4.43	227 nm, 194 mAU	796	4.54	227 nm, 294 mAU	796
c15'	4.46	227 nm, 215 mAU	796	-	-	-
c16	4.56	227 nm, 237 mAU	521	4.70	225 nm, 215 mAU	521
c16'	4.59	227 nm, 256 mAU	521	-	-	-
c17	-	-	-	4.76	228 nm, 888 mAU	m/z 279
c18	4.78	221 nm, 313 mAU	227	4.90	221 nm, 333 mAU	227
c19	5.08	228 nm, 161 mAU	279	5.20	228 nm, 170 mAU	279
c20	5.43	228 nm, 194 mAU	255	5.53	228 nm, 200 mAU	255
c21	5.48	228 nm, 197 mAU	281	5.59	228 nm, 213 mAU	281
c22	5.55	228 nm, 205 mAU	281	5.67	228 nm, 200 mAU	281
c23	5.87	228 nm, 202 mAU	837-441, *d*=44	5.98	228 nm, 214 mAU	837-441, *d*=44
c24	6.23	228 nm, 222 mAU	865-425, *d*=44	6.33	228 nm, 235 mAU	865-425, *d*=44
c25	6.27	228 nm, 217 mAU	865-425, *d*=44	6.37	228 nm, 230 mAU	865-425, *d*=44

-: not existed; /: not sure

3.5.2.3 Screening of crude extract of *Rubrivivax gelatinosus* strain 151 grown for 7 and 10 days

HPLC chromatograms of extracts from cultures of strain 151 after 7 and 10 days are shown in Figure 3-38, and 23 distinct UV absorption peaks (g1 to g20, and gA, gB, gC) were identified.

Peaks g3, g5 and g15 were absent in extract from the culture grown for 10 days compared to that for 7 days, however, extra peaks of gA, gB and gC appeared in the extract from the culture grown for 10 days.

According to Table 3-25, peaks g1, g2 and g4 showed different intensity of UV absorption and MW (or m/z). Peak g12 showed different intensity of UV absorption but same m/z value. Peaks g13 and g14 in 7 d gave same UV_{max} (228 nm) and m/z 883, however, g13 and g14 in extract from culture grown for 10 days showed UV_{max} of 227 nm and m/z 298.

The extra UV absorption peaks gB and gC belonged to an arithmetic progression (start from m/z 837 to m/z 441, d = 44). In addition, this arithmetic progression was the same one as c23's arithmetic progression in *Rhodobacter capsulatus* strain 182. In *Rhodopseudomonas palustris* strain 120/1, there was not such a progression.

Peak g20 belonged to one arithmetic progression (m/z 864 to m/z 425, d = 44) which was same as c24 and c25 in *Rhodobacter capsulatus* strain 182, and p22, p23 and p24 in *Rhodopseudomonas palustris* strain 120/1.

Because interesting extra UV absorption peaks (gA, gB, and gC) were present in extracts from cultures of *Rubrivivax gelatinosus* strain 151 grown for 10 days, this was the better conditions for cultivation of the strain.

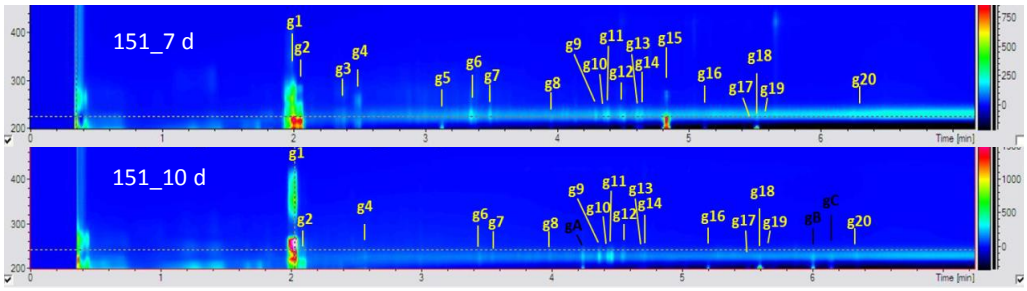

Figure 3-38. HPLC chromatogram of extracts from supernatant cultures of *Rubrivivax gelatinosus* strain 151 grown for 7 and 10 days.

Table 3-25. Comparison of extracts from cultures of strain 151 grown for 7 and 10 days.

Peak	7 d			10 d		
	Rt/min	**UV_{max} /nm**	**MW or m/z**	**Rt/min**	**UV_{max} /nm**	**MW or m/z**
g1	2.00	220 nm, 983 mAU sh240 nm, 536 mAU 266 nm, 468 mAU sh280 nm, 449 mAU	170	2.03	223 nm, 1541 mAU 241-262 nm, 2000 mAU 345 nm, 868 mAU sh 389 nm, 678 mAU	m/z 243 (+Na)
g2	2.05	217 nm, 946 mAU 220 nm, 898 mAU 246 nm, 322 mAU 280 nm, 146 mAU 287 nm, 143 mAU	170	sh2.1	214 nm, 503 mAU	m/z 243 (+Na)
g3	2.38	223 nm, 130 mAU sh 234 nm, 100 mAU 275 nm, 60 mAU	/	-	-	-
g4	2.50	215 nm, 133 mAU 220 nm, 127 mAU 257 nm, 131 mAU	668	2.57	227 nm, 184 mAU	/
g5	3.13	226 nm, 132 mAU	224	-	-	-
g6	3.34	227 nm, 247 mAU	/	3.45	222 nm, 205 mAU	/
g7	3.49	227 nm, 199 mAU	/	3.54	226 nm, 191 mAU	/
g8	3.95	225 nm, 150 mAU	538	3.99	227 nm, 187 mAU	538
gA	-	-	-	4.24	227 nm, 289 mAU	m/z 280
g9	4.29	228 nm, 185 mAU	m/z 296	4.37	227 nm, 342 mAU	m/z 296
g10	sh 4.36	228 nm, 196 mAU	m/z 296	4.43	227 nm, 327mAU	m/z296
g11	4.38	228 nm, 220 mAU	m/z 296	4.46	227 nm, 388 mAU	m/z296
g12	4.50	226 nm, 227 mAU 280 nm, 33 mAU 421 nm, 26 mAU	m/z 296	4.55	228 nm, 263 mAU	m/z 296
g13	4.61	228 nm, 208 mAU	m/z 883	4.68	227 nm, 193 mAU	m/z 298
g14	4.64	228 nm, 200 mAU	m/z 883	4.71	227 nm, 211 mAU	m/z 298
g15	4.83	222 nm, 974 mAU 269 nm, 120 mAU 276 nm, 117 mAU	227	-	-	-
g16	5.12	228 nm, 164 mAU	279	5.20	227 nm, 175 mAU	279
g17	5.47	228 nm, 185 mAU	m/z 256	5.56	228 nm, 201 mAU	m/z 256
g18	5.51	228 nm, 196 mAU	281	5.60	227 nm, 221 mAU	281
g19	5.58	228 nm, 192 mAU	281	5.67	228 nm, 202 mAU	281
gB	-	-	-	6.01	227 nm, 266 mAU	837-441, *d*=44
gC	-	-	-	6.15	227 nm, 244 mAU	837-441, *d*=44
g20	6.25	228 nm,230 mAU	865-425, *d*=44	6.34	228 nm, 263 mAU	865-425, *d*=44

-: not existed; /: not sure

3.5.3 Scale up of cultures of *Rubrivivax gelatinosus* strain 151 to a 20 L volume

Comparison of the HPLC chromatograms and bioassays, extract from the culture broth of *Rubrivivax gelatinosus* strain 151 was more interesting than compared to extracts from *Rhodopseudomonas palustris* strain 120/1 and *Rhodobacter capsulatus* strain 182. An additional aspect is the analysis of the whole genome of *Rubrivivax gelatinosus* IL144 from antiSMASH screening. The potential bioactive synthesis gene cluster of terpenes and T1pks-other cluster (very poor similarity to a zainomycin biosynthetic cluster) can be found.

Therefore, 20 L cultures were grown at 1000 lux light and 28°C anaerobically. After 10 days' incubation, the pale peach/ dirty yellowish brown cultures appeared. Only the supernatant part of culture was extracted by ethyl acetate by the method described in paragraphs 2.4 on page 33. The HPLC chromatogram of extract from culture broth of 20 L supernatant is seen in Figure 3-39.

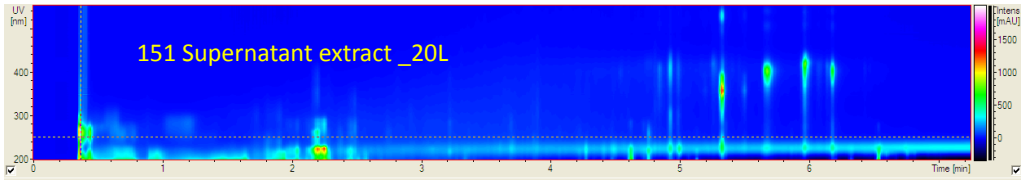

Figure 3-39. HPLC chromatogram of the 20 L supernatant extract of *Rubrivivax gelatinosus* strain 151 grown for 10 days.

A large number of UV absorption peaks were visible in the HPLC chromatogram (Figure 3-39) compared to extracts from 100 ml cultures (Figure 3-38). Especially between Rt 4.8-6.2 min, at least nine UV absorption peaks existed in the wavelength range of 200-550 nm which were indicated as pigments (Bchl *c* and/or carotenoids) (Pierson and Castenholz, 1974). 300 mg dried supernatant extract was obtained and then dissolved in MeOH and adjusted to 100 mg/ml. Fractionation was performed by semi-preparative HPLC, and 21 fractions were obtained (see in Figure 3-40).

All 21 fractions were collected and further analyzed by analytical HPLC-DAD/MS (Figure 3-41). As the weight of each fraction was too low (0.1-0.5 mg) to perform further NMR or bioassay tests, the bioactivities were not tested. A large volume of culture is required to obtain sufficient extract.

According to the results, it was concluded that *Rubrivivax gelatinosus* strain 151 may have the potential to produce bioactive secondary metabolites in AT medium, but the proof for this needs further studies.

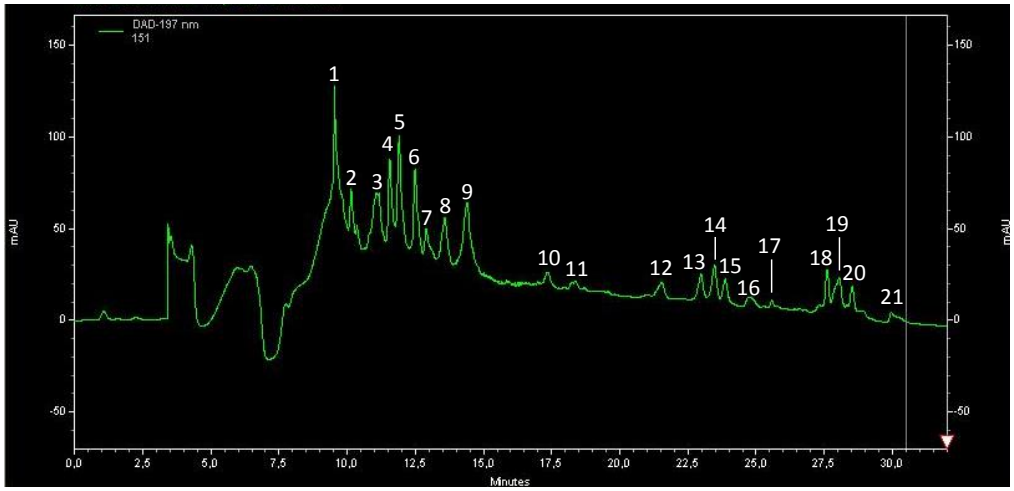

Figure 3-40. Semi-preparative HPLC chromatogram of extract of supernatant (20 L) of strain 151.

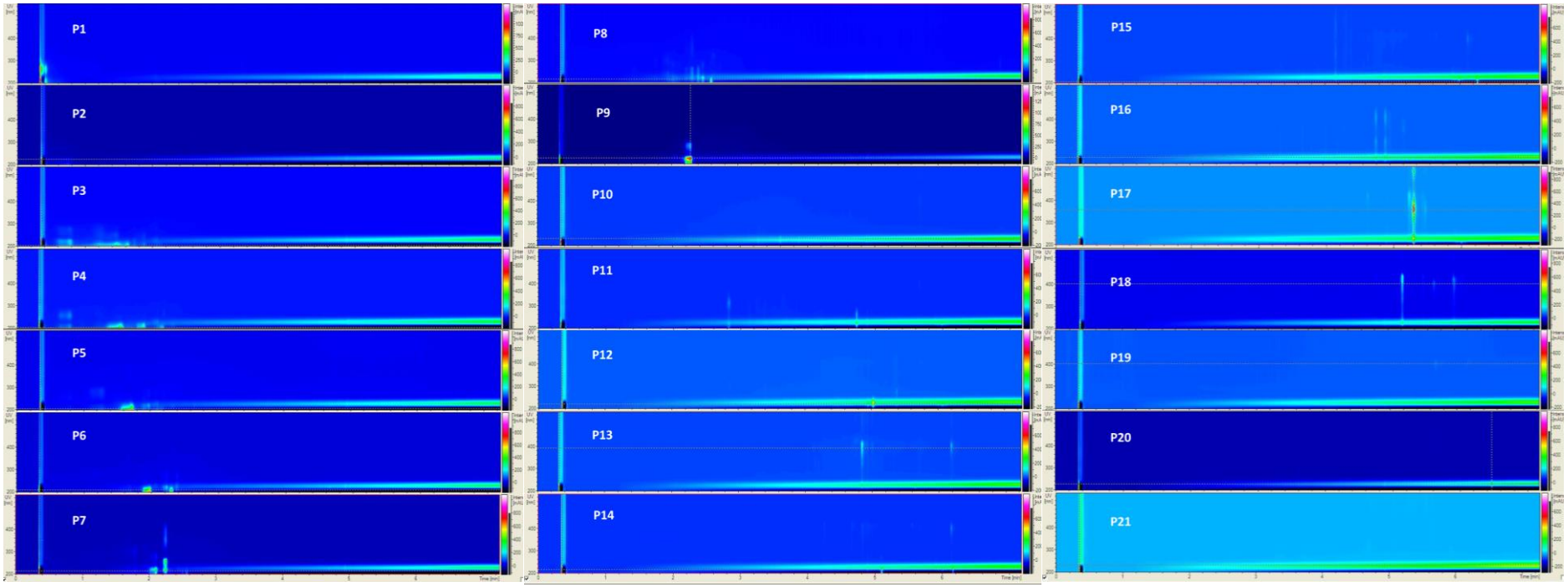

Figure 3-41. HPLC-DAD/MS chromatograms of 21 fractions from strain 151.

3.6 Genetic screening of selected anoxygenic phototrophic bacteria

Genetic screening includes the DNA extraction, PCR amplification, sequencing and BLASTn analysis of selected anoxygenic phototrophic bacteria, and the antiSMASH analysis of whole genome sequences of phototrophic bacteria available in database (NCBI).

3.6.1 DNA extraction of these bacteria

DNA was extracted from representative strains of green sulfur bacteria (*Chlorobium phaeobacteroides* strain 2360^T, *Chlorobium limicola* strain 2310^T, and *Prosthecochloris aestuarii* strain 2410^T), purple sulfur bacteria (*Marichromatium gracile* strain 5212^T, *Allochromatium vinosum* strain 5110^T, *Thiocystis violascens* strain 5410, and *Allchromatium vinosum* strain MT86) and purple nonsulfur bacteria (*Rhodopseudomonas palustris* strain 120/1, *Rhodobacter capsulatus* strain 182, and *Rubrivivax gelatinosus* stain 151). DNA could be successfully extracted from all strains as is shown by gel electrophoresis by the method described in paragraph 2.6.3 (on page 45) (Figure 3-42). The bands of each lane were clear and the concentrations of all DNA extracts were sufficient for further PCR amplification.

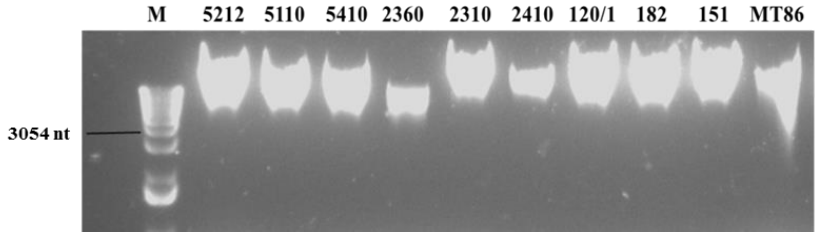

M: Marker X

Figure 3-42. DNA extraction of ten representative strains.

3.6.2 PCR amplifications and sequences analyses

PCR amplifications and sequences analyses of *pks* I, *pks* II, *nrps*, *phz*E fragments of selected phototrophic bacteria were done according to the paragraph 2.6.2, on page 42.

3.6.2.1 Classification of strains by 16S rRNA analysis

The fragments of 16S rRNA genes are approximately 1500 nt, and these are shown in the results of the gel electrophoresis (Figure 3-43) performed as described in paragraph 2.6.3 (on page 45). With the exception of *Rhodopseudomonas palustris* strain 120/1, all strains were pure isolates as demonstrated by the BLASTn results (Table 3-26) and the microscopic observation. For strain 120/1, only 679 nt of the sequence were assembled and 45% of query cover with partial sequence of *Rhodopseudomonas palustris*, but 91% similarity. Strain MT86 was identified as *A. vinosum* strain MT86, because the sequence of the 16S rRNA gene showed 99.73% similarity with *A. vinosum* DSM180^T (GenBank

accession number NR_074584.1), and 99.72% sequence similarity with *A. vinosum* strain 5110 (GenBank accession number NR_044605.1).

Query cover (query coverage) indicates the percent of the query length that is included in the aligned segments how long piece of the sequences is covered by the amplified fragments (http://www.ncbi.nlm.nih.gov/Web/Newsltr/V15N2/BLView.html). By aligning query sequence against all sequences in a database, alignment can be used to search database for similar sequences.

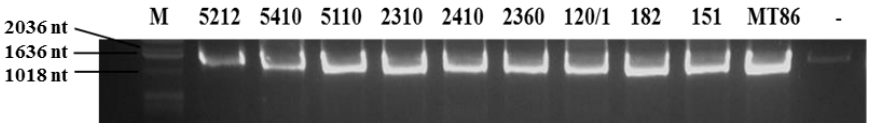

M: marker X; -: negative control (ddH_2O as PCR template)

Figure 3-43. 16S rRNA of ten strains.

From the microscopic, growth observations and 16S rRNA band in Figure 3-43, strain 5410 showed to be pure. However, the BLASTn result of 16S rRNA was 93% similar to an uncultured bacterium clone EMIRGE OUT s7t4e93, which was not the same species as the classification species as original collection and definition.

The remaining seven strains were identified according to origin and previous classification (Table 2-1).

Table 3-26. 16S rRNA analysis of selected anoxygenic phototrophic bacteria.

Sample	Length	Next related strains	Accession No.	Ident
5212	1492 nt	*Marichromatium gracile* strain DSM 203^T	NR_116468.1	99%
5410	1485 nt	Uncultured bacterium clone EMIRGE OUT s7t4e 93	JX224500.1	93%
5110	1434 nt	*Allochromatium vinosum* strain DSM 180 ^{T}	NR_074584.1	99%
2310	1466 nt	*Chlorobium limicola* strain DSM 245 ^{T}	NR_074355.1	99%
2410	1423 nt	*Prosthecochloris aestuarii* strain DSM 271 ^{T}	NR_074364.1	99%
2360	1462 nt	*Chlorobium phaeobacteroides* strain Glu	AM050128.1	99%
120/1	697 nt	*Rhodopseudomonas palustris* CGMCC:9632	KM875706.1	91%
182	1430 nt	*Rhodobacter capsulatus* SB 1003	NR_102927.1	99%
151	1495 nt	*Rubrivivax gelatinosus* IL144	NR_074794.1	99%
MT86	1495 nt	*Allochromatium vinosum* strain DSM 180 ^{T}	NR_074584.1	99.73%
		Allochromatium vinosum strain 5110 ^{T}	NR_044605.1	99.72%

3.6.2.2 PCR amplification of *pks* I fragments

The fragments of *pks* I were amplified from the genomic DNA of all the ten strains with the primers K1F and M6R as outlined in the methods (paragraph 2.6.2, on page 42). The lengths of the amplificates were controlled by gel electrophoresis as shown in Figure 3-44 and Figure 3-45.

The positive control showed one weak but clear band with about 1700 nt and one main band with 1500 nt. There was no PCR band of *pks* I from the DNA of strain MT86, and a very weak band of strain 5110. The other eight strains showed one clear band around 600 nt. Strain 120/1 and 151 showed an additional band around 1000 nt, and strain 2410 showed a clear band at 1700 nt which was the only band corresponding in length to the positive control.

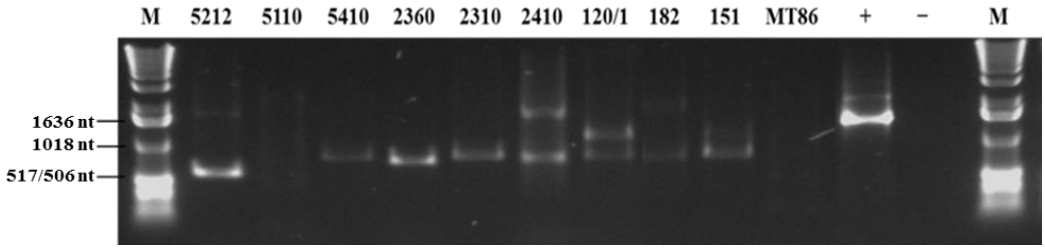

M: marker X; +: the extracted DNA of *Streptomyces clavuligerus* DSM 738 as the positive control; -: ddH_2O as the negative control

Figure 3-44. Gel electrophoresis of *pks* I amplified fragments.

PCR amplifications of *pks* I were re|peated from all other strains (except *A. vinosum* strain MT86). 25 µl of PCR (instead of 5 µl, Figure 3-44) of each amplificate was taken to the gel electrophoresis. The results of the gel separation are shown in Figure 3-45. Major bands were excised from the gel and purified by the method according to paragraph 2.6.4 (on page 45). The results of the sequence comparison and the detailed information for each band of PCR amplification is shown in Table 3-27, including the sequencing and BLASTn results.

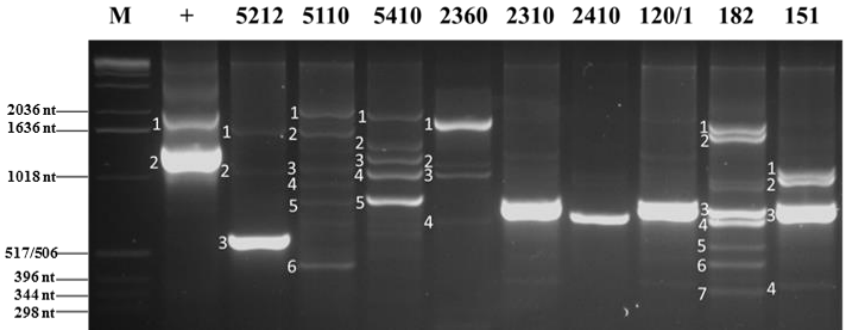

M: marker X; +: the extracted DNA of *Streptomyces clavuligerus* DSM 738 as the positive control; -: ddH_2O as the negative control

Figure 3-45. Gel electrophoresis of *pks* I amplified from nine strains and identification of purified bands.

Table 3-27. PCR amplification, sequencing results, and BLASTn results of *pks* I.

Stains	Expected length (nt)	Length (nt)	Next related sequences	Max score	Query cover	Ident	Accession	Features
Streptomyces clavuligerus DSM 738 (Positive Control)	①1636	ND	-	-	-	-	-	-
	②1200 -1400	1302	*Streptomyces neyagawaensis* **concanamycin A** biosynthetic gene cluster	220	41%	74%	DQ149987.1	NF
			Streptomyces sp. WAC5292 putative **PKS gene**, partial cds; and putative PKS gene, complete cds	167	26%	76%	JQ768039.1	NF
			Streptomyces amakusaensis gene for **polyketide synthase**, partial cds, strain: NBRC 12835, clone: amak12835m-N4	134	21%	76%	AB431358.1	NF
			Streptomyces cyaneogriseus subsp. *noncyanogenus* strain NMWT 1, complete genome	152	22%	77%	CP010849.1	3598 bp at 5' side: short-chain dehydrogenase; 4109 bp at 3' side: methyltransferase
			Streptomyces violaceusniger Tu 4113, complete genome	190	16%	75%	CP002994.1	①Acyl transferase ②Beta-ketoacyl synthase
			Streptomyces leeuwenhoekii genome assembly sleC34, chromosome : chromosome	80.5	14%	74%	LN831790.1	Polyketide synthase, type I, modules: 4, 5 and 6
			Streptomyces albulus strain NK660, complete genome	69.4	5%	85%	CP007574.1	25238 bp at 5' side: GDP-mannose 4,6-dehydratase 3396 bp at 3' side: type I modular polyketide synthase
5212	①1600	ND	-	-	-	-	-	-
	②1020	ND	-	-	-	-	-	-
	③600	520	*Marichromatium purpuratum* 984	344	98%	79%	CP007031.1	diguanylate cyclase
5110	①2036	ND	-	-	-	-	-	-
	②1600	ND	-	-	-	-	-	-
	③1020	ND	-	-	-	-	-	-
	④900	ND	-	-	-	-	-	-
	⑤800	ND	-	-	-	-	-	-
	⑥400	ND	-	-	-	-	-	-
5410	①2036	ND	-	-	-	-	-	-
	②1300	ND	-	-	-	-	-	-

	③1200	ND	-	-	-	-	-	-
	④1000	ND	-	-	-	-	-	-
	⑤800	760	*Thiocystis violascens* DSM 198	1382	99%	99%	CP003154.1	signal transduction histidine kinase
2410	①700	616	*Prosthecochloris aestuarii* DSM 271	1074	100%	98%	CP001108.1	NF
2310	①700-800	647	*Rhodopseudomonas palustris* CGA009 complete genome; segment 12/16	1066	96%	96%	BX572604.1	NF
			R. palustris TIE-1	647	96%	95%	CP001096.1	NF
			R. palustris DX-1	431	84%	87%	CP002418.1	NF
2360	①1636	ND	-	-	-	-	-	-
	②1020	ND	-	-	-	-	-	-
	③1000	ND	-	-	-	-	-	-
	④700	ND	-	-	-	-	-	-
120/1	①700-800	674	*R. palustris* CGA009	996	92%	95%	BX572604.1	NF
			R. palustris TIE-1	601	92%	92%	CP001096.1	NF
			R. palustris DX-1	412	81%	86%	CP002418.1	NF
			R. palustris BisB5	327	75%	84%	CP000283.1	NF
182	①1600	ND	-	-	-	-	-	-
	②1300	ND	-	-	-	-	-	-
	③700	703	*Rhodobacter capsulatus* SB 1003	431	51%	95%	CP001312.1	conserved hypothetical protein
			R. capsulatus strain SB1003	431	51%	95%	AF010496.1	transposase, IS3/IS911 family
	④650	ND	-	-	-	-	-	-
	⑤500	ND	-	-	-	-	-	-
	⑥400	ND	-	-	-	-	-	-
	⑦350	300	*R. capsulatus* SB 1003	327	84%	90%	CP001312.1	peptidase, M10 family
151	①1000	ND	-	-	-	-	-	-
	②900	ND	-	-	-	-	-	-
	③700-800	772	*R. palustris* CGA009	1347	97%	99%	BX572604.1	NF
			R. palustris TIE-1	811	97%	98%	CP001096.1	NF
			R. palustris DX-1	573	87%	91%	CP002418.1	NF
	④360	ND	-	-	-	-	-	-
MT86	×	×	×	×	×	×	×	×

ND: not detected; NF: no feature; NB: no BLASTn results; -: not available; ×: no results.

3.6.2.3 PCR amplification of *pks* II fragments

The fragments of *pks* II were amplified from the genomic DNA of all ten strains using primers 945f and 945r (refers to paragraph 2.6.2, and Table 2-12). The separation of the PCR products using gel electrophoresis (paragraph 2.6.3, on page 45) is shown in Figure 3-46.

The positive control (*Streptomyces achromogehes* DSM40789) showed three main bands; the upper two bands (ca. 1200 nt, and 900-1000 nt) were weaker than the brightest band with around 600 nt. The *pks* II amplification result of strain 5212 did not show any band. The other strains showed at least four bands in each lane, and the bands that were easier to cut off for purification were given numbers as seen in Figure 3-46. The sequencing results and BLASTn results are shown in Table 3-28.

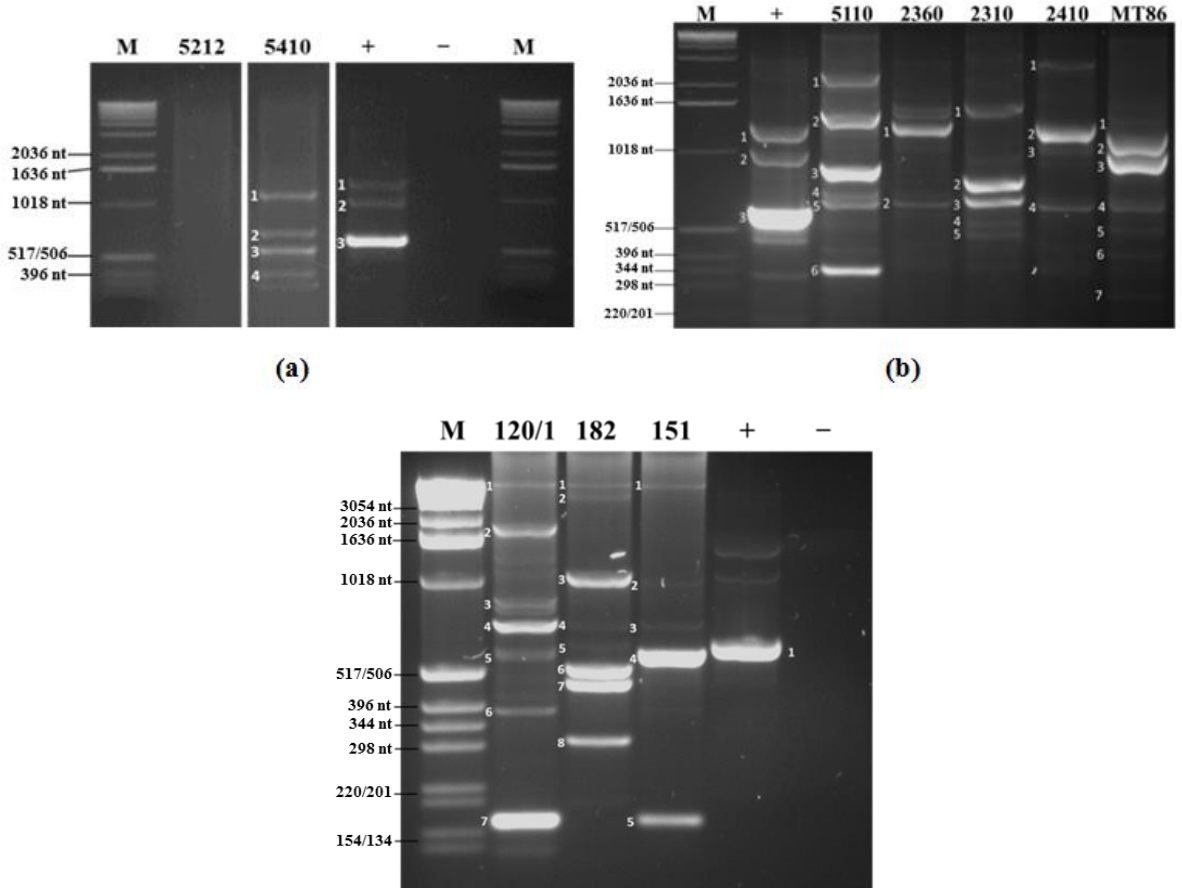

M: marker X; +: extracted DNA of *Streptomyces achromogehes* DSM 40789 as the positive control;-: ddH_2O as negative control.

Figure 3-46. Gel electrophoresis of PCR products amplified with primers 945f and 945r supposed to amplify *pks* II from nine strains and numbers of purified bands.

Table 3-28. PCR amplification, sequencing results, and BLASTn results of *pks* II.

Strains	Expected length (nt)	Length (nt)	Next related sequences	Max score	Query cover	Ident	Accession	
Streptomyces achromogehes **(Positive Control)**	①1200	ND	-	-	-	-	-	-
	②900-1000	ND	-	-	-	-	-	-
	③600	614	*Streptomyces* sp. PBH53 genome	893	99%	92%	CP011799.1	beta-ACP synthase
			Streptomyces hygroscopicus subsp. *jinggangensis* TL01	881	99%	92%	NC_020895.1	beta-ACP synthase
			Streptomyces hygroscopicus subsp. *jinggangensis* 5008	881	99%	92%	NC_017765.1	beta-ACP synthase
			Streptomyces lividans TK24	547	99%	82%	NZ_CP009124.1	beta-ACP synthase
5212	×	×	×	×	×	×	×	×
5110	①2036	ND	-	-	-	-	-	-
	②1300	ND	-	-	-	-	-	-
	③800	ND	-	-	-	-	-	-
	④700	ND	-	-	-	-	-	-
	⑤650	ND	-	-	-	-	-	-
	⑥350	351	*Allochromatium vinosum* DSM 180	518	92%	96%	CP001896.1	acriflavin resistance protein
			Rubrivivax gelatinosus IL144 DNA	244	79%	83%	AP012320.1	acriflavin resistance protein
			Variovorax paradoxus B4 chromosome 1	222	78%	81%	CP003911.1	putative multidrug efflux transporter, AcrB/AcrD/AcrF family
			Variovorax paradoxus EPS	222	78%	81%	CP002417.1	acriflavin resistance protein
			Leptothrix cholodnii SP-6	217	85%	80%	CP001013.1	acriflavin resistance protein
			Acidovorax citrulli AAC00-1	176	78%	78%	CP000512.1	acriflavin resistance protein
			Pseudoxanthomonas suwonensis 11-1	172	79%	78%	CP002446.1	acriflavin resistance protein
			Acidovorax avenae subsp. *avenae* ATCC 19860	171	78%	78%	CP002521.1	acriflavin resistance protein
			Stenotrophomonas rhizophila strain DSM14405	161	70%	79%	CP007597.1	ACR/RND family transmembrane transporter
5410	①1100	ND	-	-	-	-	-	-

	②700	ND	-	-	-	-	-	-
	③550	ND	-	-	-	-	-	-
	④400	ND	-	-	-	-	-	-
2410	①> 2360	ND	-	-	-	-	-	-
	②1200	518	NB	/	/	/	/	/
	③1000	ND	-	-	-	-	-	-
	④650	ND	-	-	-	-	-	-
2310	①1350	ND	-	-	-	-	-	-
	②750	437	*R palustris* CGA009; segment 12/16	800	100%	99%	BX572604.1	NF
			R. palustris TIE-1, complete genome	767	99%	98%	CP001096.1	urea ABC transporter, permease protein UrtC
			R. palustris DX-1, complete genome	540	92%	91%	CP002418.1	urea ABC transporter, permease protein UrtC
			R. palustris HaA2, complete genome	494	88%	90%	CP000250.1	inner-membrane translocator
			R. palustris BisB5, complete genome	431	88%	87%	CP000283.1	inner-membrane translocator
			Agromonas oligotrophica S58 DNA, complete genome	407	88%	86%	AP012603.1	putative branched-chain amino acid ABC transporter, permease protein
			Bradyrhizobium sp. ORS278,complete sequence	396	88%	85%	CU234118.1	Putative Branched-chain amino acid ABC transporter (permease protein)
			Bradyrhizobium sp. BTAi1, complete genome	385	88%	85%	CP000494.1	amino acid/amide ABC transporter membrane protein 2, HAAT family
			Bradyrhizobium japonicum USDA 6 DNA, complete genome	383	88%	85%	AP012206.1	ABC transporter permease protein
			R. palustris BisB18, complete genome	381	91%	84%	CP000301.1	inner-membrane translocator
	③650	156	NB	/	/	/	/	/
	④500	ND	-	-	-	-	-	-
	⑤450	ND	-	-	-	-	-	-
2360	①1200	ND	-	-	-	-	-	-
	②650	ND	-	-	-	-	-	-
120/1	①> 3054	ND	-	-	-	-	-	-

	②1800	ND	-	-	-	-	-	-
	③800	ND	-	-	-	-	-	-
	④750	575	*R. palustris* CGA009 complete genome; segment 10/16	1031	100%	99%	BX572602.1	NF
			R. palustris TIE-1, complete genome	970	100%	97%	CP001096.1	diguanylate cyclase/phosphodiesterase
	⑤600	496	*R. palustris* CGA009; segment 13/16	891	100%	99%	BX572605.1	NF
			R. palustris TIE-1, complete genome	857	100%	98%	CP001096.1	conserved hypothetical protein flagellar motor switch protein FliM
			R. palustris DX-1, complete genome	736	100%	93%	CP002418.1	flagellar motor switch protein FliM hypothetical protein
			R. palustris BisB5, complete genome	580	96%	89%	CP00283.1	NF
	⑥170	ND	-	-	-	-	-	-
	⑦170	169	*R palustris* TIE-1, complete genome	217	91%	92%	CP001096.1	ABC transporter substrate-binding protein
			R palustris CGA009; segment 1/16	217	91%	92%	BX572593.1	NF
			R palustris DX-1, complete genome	198	86%	91%	CP002418.1	ABC transporter substrate-binding protein
182	①>3054	ND	-	-	-	-	-	-
	②3054	ND	-	-	-	-	-	-
	③1000	974	*Paracoccus bengalensis* strain DSM 17099 insertion sequence ISPbe1 transposase genes, complete cds	220	16%	92%	GQ871936.1	NF
			Rhodobacter sphaeroides ATCC 17025 plasmid pRSPA01, complete sequence	174	12%	93%	CP000662.1	NF
			Rhodobacter sphaeroides ATCC 17025	174	24%	93%	CP000661.1	hypothetical protein
			Rhodobacter sphaeroides KD131 chromosome 1, complete sequence	167	12%	92%	CP001150.1	①D12 class N6 adenine-specific DNA methyltransferase ②4 bp at 5' side: Hypothetical Protein 516 bp at 3' side: Hypothetical Protein
			R. sphaeroides ATCC 17029 chromosome 2	165	11%	93%	CP000578.1	NF
			Octadecabacter arcticus 238, complete genome	84.2	8%	85%	CP003742.1	putative transposase

	④750	ND	-	-	-	-	-	-
	⑤600	436	NB	/	/	/	/	/
	⑥500	514	*Rhodobacter capsulatus* SB 1003	623	95%	90%	CP001312.1	NAD(+) kinase transcriptional regulatory protein ZraR
	⑦450	436	*R. capsulatus* SB 1003, complete genome	324	92%	81%	CP001312.1	methionine synthase, A subunit-2
	⑧300	307	NB	/	/	/	/	/
151	①>3054	ND	-	-	-	-	-	-
	②1000	ND	-	-	-	-	-	-
	③750	ND	-	-	-	-	-	-
	④580	572	*Ralstonia solanacearum* CFBP2957 plasmid RCFBPv3 mp	100	25%	80%	FP885907.1	NF
			R. solanacearum strain IPO1609 Genome Draft	100	25%	79%	CU914166.1	NF
			R. solanacearum Po82 megaplasmid	95.3	25%	79%	CP002820.1	NF
			R. solanacearum PSI07 megaplasmid mpPSI07	84.2	25%	78%	FP885891.2	NF
			Chromobacterium violaceum ATCC 12472	73.1	11%	86%	AE016825.1	nitrate reductase
	⑤170	169	*R palustris* TIE-1, complete genome	217	91%	92%	CP001096.1	ABC transporter substrate-binding protein
			R. palustris CGA009 complete genome; segment 1/16	217	91%	92%	BX572593.1	NF
			R. palustris DX-1, complete genome	198	86%	91%	CP002418.1	ABC transporter substrate-binding protein
MT86	①1200	ND	-	-	-	-	-	-
	②1000	ND	-	-	-	-	-	-
	③900	ND	-	-	-	-	-	-
	④650	366	*Allochromatium vinosum* DSM 180	351	97%	85%	CP001896.1	Glucose-1-phosphate adenylyl transferase
	⑤450	ND	-	-	-	-	-	-
	⑥400	ND	-	-	-	-	-	-
	⑦280	255	*Allochromatium vinosum* DSM 180	388	98%	94%	CP001896.1	multi-sensor signal transduction histidine kinase

ND: not detected; NF: no feature; NB: no BLASTn results; -: not available; /: no results, ×: no PCR results.

3.6.2.4 PCR amplification of *nrps* fragments

The fragments of *nrps* were amplified from the genomic DNA of all ten strains using the primers A2f and A3r. The gel electrophoresis of the PCR products is shown in Figure 3-47.

The positive control (*Pseudomonas* sp. DSM50117) showed only one band in the position of 250 nt. The *nrps* amplification results of all ten strains showed one or more (2-7) bands, and those bands that were cut off for purification and sequencing were given numbers as seen in Figure 3-47. The sequencing results and BLASTn results are shown in Table 3-29.

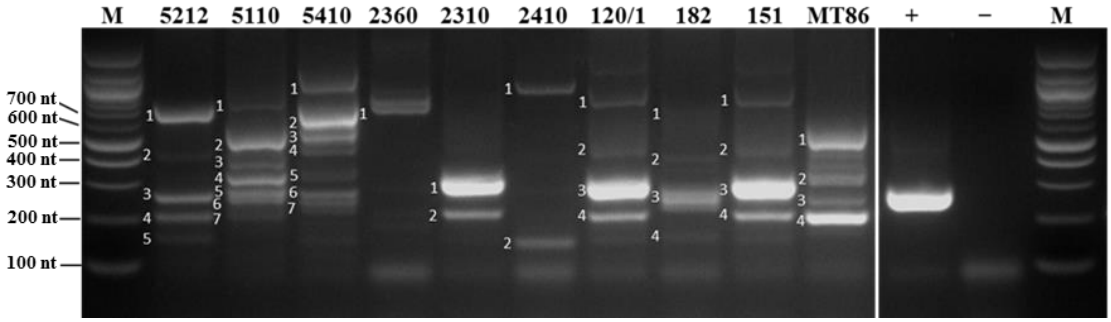

M: marker 100 bp ladder; +: extracted DNA of *Pseudomonas* sp. DSM 50117 as positive control; -: ddH_2O as negative control.

Figure 3-47. Gel electrophoresis of PCR products from amplification with primers designed for *nrps* gene fragments and identification by numbers of the bands purified.

Table 3-29. PCR amplification, sequencing results, and BLASTn results of *nrps*.

Strains	Expected length of band (nt)	Sequence length (nt)	Next related sequences	Max score	Query cover	Ident	Accession	Features
***Pseudomonas* sp. DSM50117 (Positive control)**	①250	218	*Streptomyces* sp. HB157 amino acid **adenylation domain**-containing protein-like gene, partial sequence	279	90%	92%	GQ863956.1	NF
			Streptomyces sp. HB102 putative amino acid **adenylation domain**-containing protein gene, partial cds	278	100%	90%	GQ863949.1	NF
			Streptomyces sp. HB272 amino acid **adenylation domain**-containing protein-like gene, partial sequence	265	90%	91%	GQ863961.1	NF
			Streptomyces sp. HB142 putative amino acid **adenylation domain**-containing protein gene, partial cds	265	90%	91%	GQ863953.1	NF
			Streptomyces sp. HB149 amino acid adenylation domain-containing protein-like gene, partial sequence	254	90%	90%	GQ863954.1	NF
5212	①700	328	NB	/	/	/	/	/
	②400	ND	-	-	-	-	-	-
	③280	155	NB					
	④200	ND	-	-	-	-	-	-
	⑤150	ND	-	-	-	-	-	-
5110	①800	ND	-	-	-	-	-	-
	②500	241	*Allochromatium vinosum* DSM 180, complete genome	355	99%	93%	CP001896.1	1289 bp at 5' side: hypothetical protein 560 bp at 3' side: glutamate-1-semialdehyde-2,1-aminomutase
	③350	ND	-	-	-	-	-	-
	④300	244	*A. vinosum* DSM 180, complete genome	252	99%	87%	CP001896.1	**acyl-CoA ligase (AMP-forming), exosortase system type 1 associated**
	⑤290	135	*A. vinosum* DSM 180, complete genome	174	85%	93%	CP001896.1	Di-heme cytochrome c peroxidase
	⑥280	ND	-	-	-	-	-	-
	⑦200	ND	-	-	-	-	-	-
5410	①1000	ND	-	-	-	-	-	-
	②600	ND	-	-	-	-	-	-

	③550	ND	-	-	-	-	-	-
	④450	ND	-	-	-	-	-	-
	⑤300	261	NB	/	/	/	/	/
	⑥290	157	NB	/	/	/	/	/
	⑦280	ND	-	-	-	-	-	-
2410	①1000	ND	-	-	-	-	-	-
	②150	ND	-	-	-	-	-	-
2310	①300	190	*R palustris* TIE-1, complete genome	270	97%	93%	CP001096.1	AMP-dependent synthetase and ligase
			R. palustris CGA009 complete genome; segment 1/16	237	91%	91%	BX572593.1	NF
	②200	140	*R. palustris* TIE-1, complete genome	132	97%	84%	CP001096.1	urea ABC transporter, permease protein UrtC
			R. palustris CGA009 complete genome; segment 12/16	132	87%	86%	BX572604.1	NF
			R. palustris DX-1, complete genome	115	89%	83%	CP002418.1	urea ABC transporter, permease protein UrtC
			Bradyrhizobium japonicum USDA 110 DNA, complete genome	111	79%	85%	BA000040.2	ABC transporter permease protein
			Burkholderia thailandensis MSMB121 chromosome 1, complete sequence	110	82%	84%	CP004095.1	urea ABC transporter, permease protein UrtC
			Bradyrhizobium sp. S23321 DNA, complete genome	106	81%	84%	AP012279.1	ABC transporter permease protein
2360	①800	559	*Chlorobium phaeobacteroides* DSM 266, complete genome	905	97%	97%	CP000492.1	①conserved hypothetical protein, protein of unknown function DUF1568 ②199 bp at 5' side: conserved hypothetical protein 80 bp at 3' side: protein of unknown function DUF1568 ③246 bp at 5' side: conserved hypothetical protein 33 bp at 3' side: protein of unknown function DUF1568
120/1	①800	ND	-	-	-	-	-	-
	②500	ND	-	-	-	-	-	-
	③300	290	*R. palustris* TIE-1, complete genome	481	99%	97%	CP001096.1	AMP-dependent synthetase

								and ligase
			R. palustris CGA009 complete genome; segment 1/16	394	99%	91%	BX572593.1	NF
			R. palustris DX-1, complete genome	372	99%	90%	CP002418.1	AMP-dependent synthetase and ligase
			R. palustris BisB5, complete genome	259	97%	83%	CP000283.1	AMP-dependent synthetase and ligase
			R. palustris BisA53, complete genome	211	99%	80%	CP000463.1	AMP-dependent synthetase and ligase
	④200	132	*R. palustris* CGA009 complete genome; segment 12/16	156	86%	91%	BX572604.1	urea ABC transporter, permease protein UrtC
			R. palustris TIE-1, complete genome	145	97%	87%	CP001096.1	NF
			R. palustris DX-1, complete genome	124	89%	86%	CP002418.1	urea ABC transporter, permease protein UrtC
			Agromonas oligotrophica S58 DNA, complete genome	122	72%	90%	AP012603.1	putative branched-chain amino acid ABC transporter permease protein
			Bradyrhizobium japonicum USDA 110 DNA, complete genome	122	86%	86%	BA000040.2	ABC transporter permease protein
			Bradyrhizobium sp. S23321 DNA, complete genome	117	88%	85%	AP012279.1	ABC transporter permease protein
			Burkholderia thailandensis MSMB121 chromosome 1, complete sequence	106	88%	83%	CP004095.1	urea ABC transporter, permease protein UrtC
182	①700	ND	-	-	-	-	-	-
	②400	ND	-	-	-	-	-	-
	③250	266	*R. palustris* CGA009 complete genome; segment 2/16	261	83%	88%	BX572594.1	NF
	④150	ND	-	-	-	-	-	-
151	①800	ND	-	-	-	-	-	-
	②500	245	*R. palustris* TIE-1, complete genome	361	93%	94%	CP001096.1	AMP-dependent synthetase and ligase
			R. palustris CGA009 complete genome; segment 1/16	283	91%	88%	BX572593.1	NF
			R. palustris BisB5, complete genome	195	75%	85%	CP000283.1	AMP-dependent synthetase and ligase
	③300	138	*R. palustris* TIE-1, complete genome	150	95%	87%	CP001096.1	urea ABC transporter, permease protein UrtC
			R. palustris CGA009 complete genome; segment 12/16	145	84%	89%	BX572604.1	NF

			R. palustris DX-1, complete genome	124	87%	85%	CP002418.1	urea ABC transporter, permease protein UrtC
			Bradyrhizobium japonicum USDA 110 DNA, complete genome	121	84%	86%	BA000040.2	ABC transporter permease protein
			Bradyrhizobium sp. S23321 DNA, complete genome	115	86%	84%	AP012279.1	ABC transporter permease protein
	④200	173	NB	/	/	/	/	/
MT86	①500	281	*A. vinosum* DSM 180, complete genome	318	85%	90%	CP001896.1	1466 bp at 5' side: hypothetical protein 378 bp at 3' side: glutamate-1-semialdehyde-2,1-aminomutase
			Thioalkalivibrio sulfidophilus HL-EbGr7, complete genome	122	51%	82%	CP001339.1	**propionate--CoA ligase**
			Leisingera methylohalidivorans DSM 14336 strain MB2, DSM 14336, complete genome	106	57%	79%	CP006773.1	**acyl-CoA synthetase**
			Azotobacter vinelandii CA6, complete genome	104	54%	79%	CP005095.1	**acetyl-CoA synthetase**
	②300	ND	-	-	-	-	-	-
	③250	191	*A. vinosum* DSM 180, complete genome	291	96%	95%	CP001896.1	**acetate/CoA ligase**
	④200	149	NB	/	/	/	/	/

ND: not detected; NF: no feature; NB: no BLASTn results; -: not available; /: no results.

3.6.2.5 PCR amplification of *phz*E fragments

The fragments of *phz*E were amplified from the genomic DNA of all ten strains by using the primers *phz*Ef and *phz*Er. Separation of the PCR products by gel electrophoresis (paragraph 2.6.3, on page 45) is shown in Figure 3-48.

The positive control (*Pseudomonas* sp. DSM50117) showed one band in the position of 400-450 nt. The *phz*E amplification results of all strains showed one clear band (ca. 420 nt) at the position of the positive control (no band was seen in strain 2360). The bands were cut off and purified for sequencing. The sequencing results and BLASTn results are shown in Table 3-30.

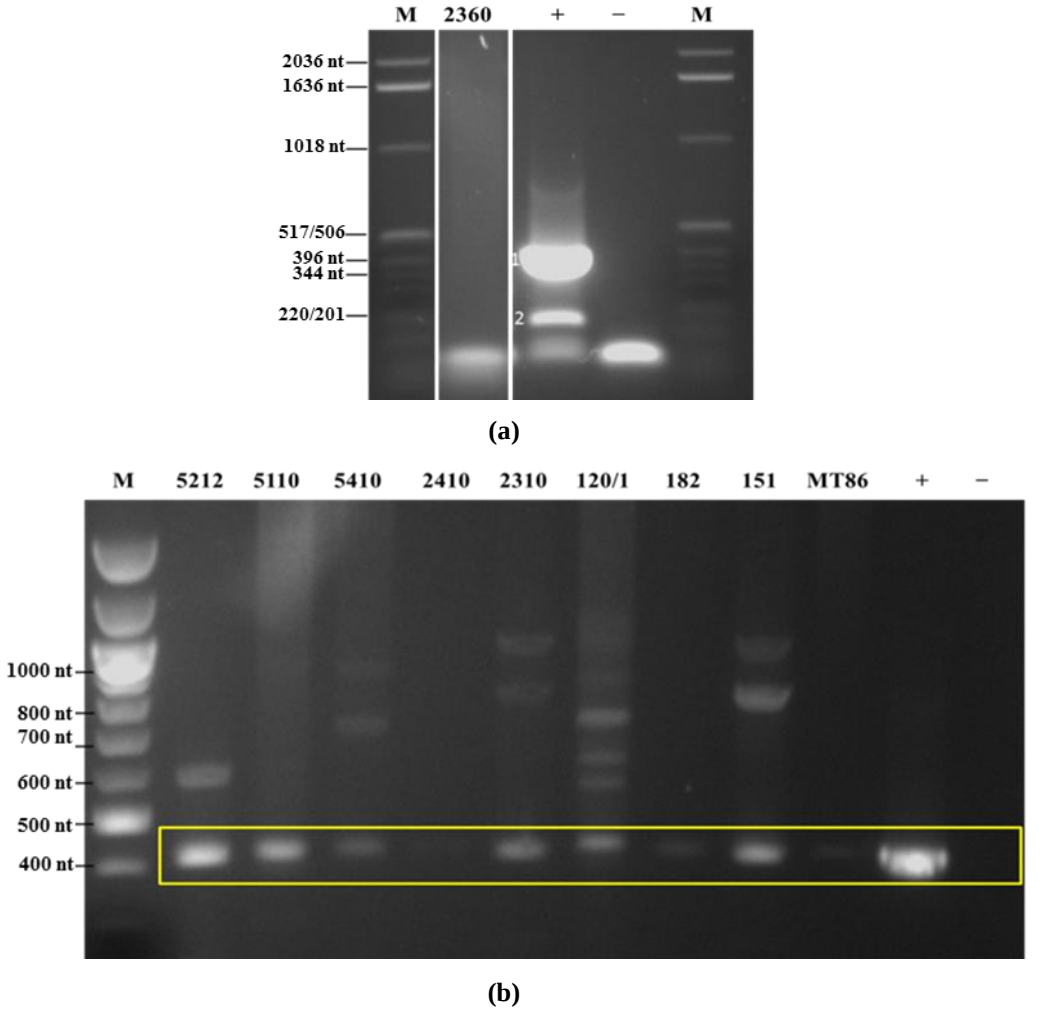

M: marker X (a) and marker 100 bp ladder (b);
+: extracted DNA of *Pseudomonas* sp. DSM50117 as positive control; -: ddH_2O as negative control.

Figure 3-48. Gel electrophoresis of PCR products from amplification with primers designed for *phz*E gene fragments and identification by numbers of the bands purified.

Table 3-30. PCR amplification, sequencing results, and BLASTn results of *phz*E.

Strains	Expected length (nt)	Length (nt)	Next related sequences	Max score	Query cover	Ident	Accession	Features
Pseudomonas sp. DSM50117 (Positive control)	①400-450	425	*Pseudomonas chlororaphis* subsp. *aurantiaca* strain JD37	682	99%	96%	CP009290.1	anthranilate*
			P. chlororaphis subsp. *aurantiaca* DNA, ***phz* gene cluster**, complete cds, strain: StFRB508	682	99%	96%	AB794886.1	NF
			P. chlororaphis strain GP72 **phenazine biosynthesis gene cluster**	676	99%	95%	HM594285.1	NF
			P. chlororaphis strain PA23	671	99%	95%	CP008696.1	anthranilate*
			P. chlororaphis **partial *phz*E gene for Phenazine E**, isolate Toza7	634	88%	97%	HG800017.1	NF
			Pseudomonas fluorescens strain LBUM223	538	99%	89%	CP011117.1	PhzE*
5212	①420	418	*P. chlororaphis* subsp. *aurantiaca* strain JD37	715	99%	98%	CP009290.1	anthranilate*
			P. chlororaphis subsp. *aurantiaca* DNA, ***phz* gene cluster**, complete cds, strain: StFRB508	715	99%	98%	AB794886.1	NF
			P. chlororaphis strain GP72 **phenazine biosynthesis gene cluster**,	710	99%	97%	HM594285.1	NF
			P. chlororaphis strain PA23	704	99%	97%	CP008696.1	anthranilate*
			P. chlororaphis **partial *phz*E gene for Phenazine E**, isolate Toza7	645	89%	98%	HG800017.1	NF
			P. fluorescens strain LBUM223	571	99%	91%	CP011117.1	PhzE*
5110	①420	418	*P. chlororaphis* subsp. *aurantiaca* strain JD37	715	99%	98%	CP009290.1	anthranilate*
			P. chlororaphis subsp. *aurantiaca* DNA, ***phz* gene cluster**, complete cds, strain: StFRB508	715	99%	98%	AB794886.1	NF
			P. chlororaphis strain GP72 **phenazine biosynthesis gene cluster**	710	99%	97%	HM594285.1	NF
			P. chlororaphis strain PA23	704	99%	97%	CP008696.1	anthranilate*
			P. chlororaphis **partial *phz*E gene for Phenazine E**, isolate Toza7	645	89%	98%	HG800017.1	NF
			P. fluorescens strain LBUM223	571	99%	91%	CP011117.1	PhzE*
			P. fluorescens strain S2P5 **phenazine biosynthetic gene locus**,	544	99%	90%	AY960782.1	NF
5410	①420	425	*P. chlororaphis* subsp. *aurantiaca* strain JD37	723	99%	97%	CP009290.1	anthranilate*
			P. chlororaphis subsp. *aurantiaca* DNA, ***phz* gene cluster**, complete cds, strain: StFRB508	723	99%	97%	AB794886.1	NF

			P. chlororaphis strain GP72 **phenazine biosynthesis gene cluster**	717	99%	97%	HM594285.1	NF
			P. chlororaphis strain PA23	712	99%	97%	CP008696.1	anthranilate*
			P. chlororaphis **partial *phz*E gene for Phenazine E**, isolate Toza7	645	88%	98%	HG800017.1	NF
			P. fluorescens strain LBUM223	579	99%	91%	CP011117.1	PhzE*
2410	①420	421	*P. chlororaphis* subsp. *aurantiaca* strain JD37	723	99%	97%	CP009290.1	anthranilate*
			P. chlororaphis subsp. *aurantiaca* DNA, ***phz* gene cluster**, complete cds, strain: StFRB508	723	99%	97%	AB794886.1	NF
			P. chlororaphis strain GP72 **phenazine biosynthesis gene cluster**	717	99%	97%	HM594285.1	NF
			P. chlororaphis strain PA23	712	99%	97%	CP008696.1	anthranilate*
			P. chlororaphis **partial *phz*E gene for Phenazine E**, isolate Toza7	645	88%	98%	HG800017.1	NF
			P. fluorescens strain LBUM223	579	99%	91%	CP011117.1	PhzE*
			Pseudomonas fluorescens strain S2P5 **phenazine biosynthetic gene locus**, complete sequence	551	99%	90%	AY960782.1	NF
			P. fluorescens autoinducer synthase **(*phz*I) gene, positive regulator protein (*phz*R), *phz*ABCDEFG genes**, complete cds	551	99%	90%	L48616.1	NF
2310	①420	414	*P. chlororaphis* subsp. *aurantiaca* strain JD37	710	100%	98%	CP009290.1	anthranilate*
			P. chlororaphis subsp. *aurantiaca* DNA, ***phz* gene cluster**, complete cds, strain: StFRB508	710	100%	98%	AB794886.1	NF
			P. chlororaphis strain GP72 **phenazine biosynthesis gene cluster**	704	100%	97%	HM594285.1	NF
			P. chlororaphis strain PA23	699	100%	97%	CP008696.1	anthranilate*
			P. chlororaphis **partial *phz*E gene for Phenazine E**, isolate Toza7	645	90%	98%	HG800017.1	NF
			P. fluorescens strain LBUM223,	566	100%	91%	CP011117.1	PhzE*
			P. fluorescens strain S2P5 **phenazine biosynthetic gene locus**	538	100%	90%	AY960782.1	NF
			P. fluorescens autoinducer synthase **(*phz*I) gene, positive regulator protein (*phz*R), *phz*ABCDEFG genes**, complete cds	538	100%	90%	L48616.1	NF
2360	/	/	/	/	/	/	/	/
120/1	①420	425	*P. chlororaphis* subsp. *aurantiaca* strain JD37	728	99%	98%	CP009290.1	anthranilate*
			P. chlororaphis subsp. *aurantiaca* DNA, ***phz* gene cluster**, complete cds, strain: StFRB508	728	99%	98%	AB794886.1	NF

			***P. chlororaphis* strain GP72 phenazine biosynthesis gene cluster**	723	99%	97%	HM594285.1	NF
			P. chlororaphis strain PA23	717	99%	97%	CP008696.1	anthranilate*
			P. chlororaphis subsp. *aurantiaca* strain Pcho10 **phenazine-1-carboxamide product biosynthetic and regulatory gene cluster**, partial sequence	712	99%	97%	KJ457347.1	NF
			P. fluorescens strain LBUM223	584	99%	92%	CP011117.1	PhzE*
182	①420	429	*P. chlororaphis* subsp. *aurantiaca* strain JD37	623	98%	93%	CP009290.1	anthranilate*
			P. chlororaphis subsp. *aurantiaca* DNA, ***phz* gene cluster**, complete cds, strain: StFRB508	623	98%	93%	AB794886.1	NF
			P. chlororaphis strain GP72 **phenazine biosynthesis gene cluster**	623	98%	93%	HM594285.1	NF
			P. chlororaphis strain PA23	617	98%	92%	CP008696.1	anthranilate*
			P. chlororaphis subsp. *aurantiaca* strain Pcho10 **phenazine-1-carboxamide product biosynthetic and regulatory gene cluster**, partial sequence	606	98%	92%	KJ457347.1	NF
			P. chlororaphis **partial *phz*E gene for Phenazine E**, isolate Toza7	580	87%	94%	HG800017.1	NF
			P. fluorescens strain LBUM223	488	98%	87%	CP011117.1	PhzE*
151	①420	215	NB	/	/	/	/	/
MT86	①420	424	*P. chlororaphis* subsp. *aurantiaca* strain JD37	721	99%	97%	CP009290.1	anthranilate*
			P. chlororaphis subsp. *aurantiaca* DNA, ***phz* gene cluster**, complete cds, strain: StFRB508	721	99%	97%	AB794886.1	NF
			P. chlororaphis strain GP72 **phenazine biosynthesis gene cluster**	715	99%	97%	HM594285.1	NF
			P. chlororaphis strain PA23	710	99%	97%	CP008696.1	anthranilate*
			P. chlororaphis subsp. *aurantiaca* strain Pcho10 **phenazine-1-carboxamide product biosynthetic and regulatory gene cluster**, partial sequence	704	99%	97%	KJ457347.1	NF
			P. chlororaphis **partial *phz*E gene for Phenazine E**, isolate Toza7	645	88%	98%	HG800017.1	NF
			P. fluorescens strain LBUM223	577	99%	91%	CP011117.1	PhzE
			P. fluorescens strain S2P5 **phenazine biosynthetic gene locus**	549	99%	90%	AY960782.1	NF

ND: not detected; NF: no feature; NB: no BLASTn results; -: not available; ×: no results. PhzE*: Phenazine biosynthesis protein/PhzE 2-Amino-2-deoxy-isochorismate synthase; anthranilate*: anthranilate synthase

3.6.2.6 Sequences analysis

From the Table 3-27, Table 3-28, Table 3-29, and Table 3-30, a summary can be obtained and is shown in Table 3-31.

BLASTn results of *pks* I sequences (column 1 of Table 3-31) demonstrated the following:

1) The *pks* I fragment of *Streptomyces clavuligetus* DSM 738 (the positive control) had a 1302 nt sequence and showed 74% similarity to a concanamycin A biosynthetic gene cluster (41% query cover) of *Streptomyces neyagawaensis*, 76% similarity to a putative PKS gene cluster (26% query cover) of *Streptomyces* sp. WAC5292 and other PKSs related features of other *Streptomyces* species. This indicates that the primers, PCR system and program for *pks* I were well functioning.

2) The BLASTn results of the sequences from *pks* I fragment of all ten strains revealed similar features to deposited sequences of the databases. However, relatedness was obtained to several other functional genes, but not to the polyketide synthase systems. There is no proof for a type I *pks* gene in the tested phototrophic bacteria by the methods used in the present study.

3) Although the 16S rRNA result showed the next related strain to *Thiocystis violascens* 5410 was an uncultured bacterium (clone EMIRGE OUT s7t4e93), the *pks* I result of strain 5410 showed that the 760 nt fragment was 99% similar to a signal transduction histidine kinase gene cluster of *Thiocystis violascens* DSM 198 (which should be the same strain as 5410). The discrepancies between the type strains of *Thiocystis violascens* from different sources, respectively of the sequences assigned to this strain, cannot be explained.

The BLASTn results of fragments of *pks* II demonstrated that the desired genes of the positive control *Streptomyces arehromogenes* DSM 40789 were amplified with a fragment size of 614 nt. This fragment sequence was 92% similar (99% query cover) to the corresponding sequence of the genomes of *Streptomyces* sp. PBH53, *Streptomyces hygroscopicus* subsp. *jinggangensis* TL01, and *Streptomyces hygroscopicus* subsp. *jinggangensis* 5008. All the features can be found as β-ACP synthase (EC 2.3.1.41, an enzyme involved in PKS system and results in the formation of acetoacetyl ACP). The positive control demonstrated the functionality of the primers and PCR system, but there was no indication of a type II *pks* gene in any of the bacteria analyzed in the present study.

From the *nrps* amplification and BLASTn results, some interesting features were found. As the positive control *Pseudomonas* sp. DSM 50117 was used, a 218 nt fragment was 90% similar (100% query cover) to the gene of a putative amino acid adenylation domain-containing protein of *Streptomyces* sp. HB102. The amplified *nrps* fragment from strain 5110 was 244 nt and 87% similar, with 99% query cover, to an exosortase system type 2 associated AMP-forming acyl-CoA ligase gene

cluster of *A. vinosum* DSM 180^T. The 281 nt fragment of *nrps* from MT86 showed 85% similarity (90% query cover) to a glutamate-1-semialdehyde-2,1-aminomutase gene cluster of *A. vinosum* DSM 180^T; 82% similarity (51% query cover) to a propionate-CoA ligase gene cluster of *Thioalkalivibrio sulfidophilus* HL-EbGr7; 79% (57% query cover) similarity to a feature of acyl-CoA synthase gene cluster of *Leisingera methylohalidivorans* DSM 14336 strain MB2; and 79% (54% query cover) similarity to an acetyl-CoA synthase gene cluster of *Azotobacter vinelandii* CA6. Another shorter 191 nt fragment, which was 95% similar (96% query cover) to an acetate/CoA ligase gene cluster of *A. vinosum* DSM 180^T, was amplified and assembled successfully from MT86.

The positive control for *phz*E amplification was the anthralinate synthase gene of *Psedomonas* sp. DSM50117 (425 nt). The *phz*E gene sequence from *Pseudomonas* sp. DSM50117, according to BLASTn analysis, was 95-97% similar (99% query cover) to this gene from *P. chlororaphis* subsp. *aurantiaca* strain JD37; *P. chlororaphis* subsp. *aurantiaca* StFRB508; *P. chlororaphis* strain GP72; 97% similar (88% query cover) to a partial *phz*E sequence of *P. chlororaphis* Toza7 isolate; 89% similar (99% query cover) to a *phz*E gene cluster of *P. fluorescens* strain LBUM223.

The lengths of *phz*E fragments from eight strains were between 414 and 430 nt, and showed almost the same results of BLASTn analyses and indicated features as the positive control. Two strains gave negative results: *Chlorobium phaeobacteroides* strain 2360 yielded no *phz*E amplification product and *Rubrivivax gelatinosus* strain 151 yielded a 215 nt fragment but did not give positive results with BLASTn analysis. The used *phz*E amplification primers, PCR system and program were useful in *phz*E gene screening and allowed identification of putative PhzE synthases in eight strains (including *A. vinosum* strain MT86) of the studied phototrophic bacteria.

Table 3-31. Summary of gene screening of representative phototrophic bacteria.

Strain No.	*pks* I		*pks* II		*nrps*		*phz*E	
	Length	Features	Length	Features	Length	Features	Length	Features
Pos.	1302 nt	concanamycin A; short-chain dehydrogenase; Acyl transferase, β-ketoacyl synthase, type I modular polyketide synthase	614 nt	β-ACP synthase	218 nt	Adenylation domain	425 nt	anthranilate; biosynthesis protein PhzE (2-amino-2-deoxy-isochrimate synthase
5212	520 nt	diguanylate cyclase	×	×	328 nt	(NB)	418 nt	anthranilate; biosynthesis protein PhzE
					155 nt	(NB)		
5110	ND	-	351 nt	acriflavin resistance protein; putative multidrug efflux transporter, AcrB/AcrD/AcrF family	241 nt	glutamate-1-semialdehyde-2,1-aminomutase	418 nt	anthranilate; biosynthesis protein PhzE
					244 nt	acyl-CoA ligase (AMP-forming), exosortase system type 1 associated		
					135 nt	Di-heme cytochrome c peroxidase		
5410	760 nt	signal transduction histidine kinase	ND	-	261 nt	NB	425 nt	anthranilate; biosynthesis protein PhzE
					157 nt	NB		
2310	647 nt	NF	437 nt	Putative Branched-chain amino acid ABC transporter (permease protein)	190 nt	AMP-dependent synthetase and ligase	414 nt	anthranilate; biosynthesis protein PhzE
			146 nt	NB	140 nt	urea ABC transporter, permease protein UrtC		
2360	ND	-	ND	-	559 nt	conserved hypothetical protein, protein of unknown function DUF1568	×	-
2410	616 nt	NF	518 nt	NB	ND	-	421 nt	anthranilate; biosynthesis protein PhzE
120/1	674 nt	NF	575 nt	diguanylate cyclase/	290 nt	AMP-dependent synthetase and	425 nt	anthranilate;

				phosphodiesterase		ligase		biosynthesis protein PhzE
			496 nt	conserved hypothetical protein flagellar motor switch protein FliM	132 nt	urea ABC transporter, permease protein UrtC		
			169 nt	ABC transporter substrate-binding protein				
182	703 nt	conserved hypothetical protein; transposase, IS3/IS911 family	974 nt	D12 class N6 adenine-specific DNA methyltransferase; putative transposase	260 nt	NF	429 nt	anthranilate; biosynthesis protein PhzE (2-amino-2-deoxy-isochrimate synthase
			514 nt	NAD(+) kinase transcriptional regulatory protein ZraR				
	300 nt	peptidase, M10 family	436 nt	methionine synthase, A subunit-2				
			307 nt	NB				
151	772 nt	NF	572 nt	nitrate reductase	245 nt	AMP-dependent synthetase and ligase	215 nt	NB
			169 nt	ABC transporter substrate-binding protein	148 nt	urea ABC transporter, permease protein UrtC		
					173 nt	(NB)		
MT86	×	×	366 nt	Glucose-1-phosphate adenylyl transferase	281 nt	glutamate-1-semialdehyde-2,1-aminomutase; propionate--CoA ligase; acyl-CoA synthetase; acetyl-CoA synthetase	424 nt	anthranilate; biosynthesis protein PhzE (2-amino-2-deoxy-isochrimate synthase
			255 nt	multi-sensor signal transduction histidine kinase	191 nt	acetate/CoA ligase=acetyl-CoA synthase		
					149 nt	(NB)		

ND: bands existed but not detected; NF: no feature; NB: no BLASTn results; -: not available; ×: No PCR results.

3.7 Genome evaluation of phototrophic bacteria from databases

Because anoxygenic phototrophic bacteria are not known as producers of secondary metabolites with bioactivity, a genome-based screening by using antiSMASH was applied in this study to predetermine the potential of bioactive compound biosynthesis of these bacteria.

Whole genome sequences of a number of phototrophic bacteria are available from NCBI database and accession numbers of 32 complete genome sequences were submitted to online antiSMASH and functional annotated for detection of biosynthetic clusters of secondary metabolites. Table 3-32 shows the results of the antiSMASH search of the type strains or the next related strains of the ten phototrophic bacteria of this study. The complete genome sequences are available and the analysis showed that all ten genome sequences predicted at least one terpene biosynthetic gene cluster. Especially *Rubrivivax gelatinosus* IL144 (related to strain 151) showed two terpene clusters and *R: palustris* CGA009 (related to strain 120/1) showed three terpene clusters (one of them showed very poor similarity to the malleobactin biosynthetic cluster).

Marichromatium purpuratum 984 (complete genome available in the genus *Marichromatium* related to *Marichromatium gracile* strain 5212) showed two *nrps* biosynthesis gene clusters, *Chlorobium phaeobacteroides* DSM 266^T (complete genome available of *Chlorobium phaeobacteroides* strain 2360 = DSM 266) showed one *nrps* biosynthesis gene cluster, *Rhodopseudomonas palustris* CGA009 (complete genome available in the genus *Rhodopseudomonas* related to *Rhodopseudomomnas palustris* strain 120/1) showed one *nrps*-T1pks biosynthesis gene cluster, and *Rubrivivax gelatinosus* IL144 (next related to *Rubrivivax gelatinosus* strain 151) showed one T1pks-other biosynthesis gene cluster which was only 4% similar to the azinomycin B biosynthesis gene.

Rubrivivax gelatinosus IL144 showed one lassopeptide biosynthesis gene cluster which was 80% similar to the most similar known biosynthetic gene cluster rubrivinodin.

A. vinosum DSM 180^T (identical to strain 5110 and next related strain to MT86) showed one terpene cluster, which was 100% similar to a carotenoid biosynthesis cluster.

Thiocystis violascens DSM 198 (complete genome available in the genus *Thiocystis*, strain should be identical to our strain designed 5410) showed an arylpolyene cluster that was 14% similar to a xanthomonadin cluster. Xanthomonadins are a class of carotenoid-like pigments produced by genus *Xanthomonas*. Xanthomonadin may serve to protect the bacterial membrane from oxidative damage (Rajagopal *et al.*, 1997). *Xanthomonas maltophilia* produces aryl-polyene (xanthomonadin) pigments.

Bacteriocin clusters account for 7 out of 39 in the strains of *Marichromatium purpuratum* 984, *Chlorobium phaeobacteroides* DSM 266, *Chlorobium limicola* DSM 245^T (strain identical to strain

2310), *Prosthecochloris aestuarii* DSM 271^{T} (strain identical to strain 2410) (three bacteriocin clusters), and *Rubrivivax gelatinosus* IL144.

There are six homoserine lactone clusters (abbreviation: hserlactone cluster) account from strain *Allochromatium vinosum* DSM 180^{T}, *Thiocystis violascens* DSM 198 (2 clusters), *Rhodopseudomonas palustris* CGA009, and *Rhodobacter capsulatus* SB1003 (complete genome available in the genus *Rhodobacter* related to *Rhodobacter capsulatus* strain 182) (2 clusters). Three *nrps* clusters exist in *Marichromatium purpuratum* 984 (2 *nrps* clusters) and *Chlorobium phaeobacteroides* DSM 266. *Rubrivivax gelatinosus* IL144 owns the only two peptide clusters, namely lantipeptide cluster and lassopeptide cluster. *Rhodopseudomonas palustris* CGA009 contains the only Nrps-T1pks cluster and one siderophore cluster.

.

Table 3-32. AntiSMASH results of the whole genome sequences of the strains from database related to the 10 strains in this study.

Strains	Submitter	BioProject	Length (Mb)	GC%	NCBI Reference Sequence	AntiSMASH		
						Cluster	Most similar known biosynthetic gene cluster and genes similarity	MIBiG BGC-ID
***Marichromatium purpuratum* 984**	JGI	PRJNA72575 PRJNA224116 PRJNA62513	3.78	67.9	NZ_CP007031.1	Cluster 1=Nrps	-	-
						Cluster 2=Nrps	-	-
						Cluster 3=Other	-	-
						Cluster 4=Bacteriocin	-	-
						Cluster 5=Terpene	-	-
***Allochromatium vinosum* DSM 180^T = 5110 (next related to MT86)**	JGI	PRJNA46083	3.53	64.4	NC_013851.1	Cluster 1=Hserlactone	-	-
						Cluster 2=Other	-	-
						Cluster 3=Terpene	Carotenoid (100%)	BGC0000647_c1
***Thiocystis violascens* DSM 198 = 5410**	JGI	PRJNA74025 PRJNA60641	5.02	62.6	NC_018012.1	Cluster 1=Other	-	-
						Cluster 2=Terpene	-	-
						Cluster 3=Arylpolyene	Xanthomonadin (14%)	BGC0000840_c1
						Cluster 4=Hserlactone	-	-
						Cluster 5=Hserlactone	-	-
***Chlorobium phaeobacteroides* DSM 266 = 2360**	JGI	PRJNA58133 PRJNA12609	3.13	48.4	NC_008639.1	Cluster 1=Bacteriocin	-	-
						Cluster 2=Nrps	-	-
						Cluster 3=Terpene	-	-
						Cluster 4=Butyrolactone	-	-
***Chlorobium limicola* DSM 245^T**	JGI	PRJNA12606, 58127	2.76	51.3	NC_010803.1	Cluster 1=Butyrolactone	-	-
						Cluster 2=Terpene	-	-
						Cluster 3=Bacteriocin	-	-
***Prosthecochloris aestuarii* DSM 271^T = 2410**	JGI	PRJNA12749, 58151	2.51	50.1	NC_011059.1	Cluster 1= Bacteriocin	-	-
						Cluster 2= Bacteriocin	-	-
						Cluster 3= Bacteriocin	-	-
						Cluster 4= Terpene	-	-
Rhodopseudo-monas palustris	JGI	PRJNA62901 PRJNA57	5.46	65.0	NC_005296.1	Cluster 1=Hserlactone	-	-
						Cluster 2=Terpene	-	-

CGA009 = 120/1						Cluster 3=Siderophore	-	-
						Cluster 4=Terpene	-	-
						Cluster 5=Nrps-T1pks	-	-
						Cluster 6=Terpene	Malleobactin (7%)	BGC0000386_c1
***Rhodobacter capsulatus* SB1003 = 182**	Univ. Chicago	PRJNA47509PRJNA55	3.74	66.6	NC_014034.1	Cluster 1=Hserlactone	-	-
						Cluster 2=Terpene	-	-
						Cluster 3=Hserlactone	-	-
***Rubrivivax gelatinosus* IL144 = 151**	National Institute of Technology and Evaluation NBRC 100245	PRJNA158163PRJNA62703	5.04	71.2	NC_017075.1	Cluster 1=Lassopeptide	Rubrivinodin (80%)	BGC0000576_c1
						Cluster 2=Lantipeptide	-	-
						Cluster 3=Terpene	-	-
						Cluster 4=T1pks-other	Azinomycin B (4%)	BGC0000960_c1
						Cluster 5=Terpene	-	-
						Cluster 6=Bacterioncin	-	-

JGI = US DOE Joint Genome Institute; **t1pks =** Type I PKS cluster; **arylpolyene** = Aryl polyene cluster; **nrps =** Nonribosomal peptide synthetase cluster**; terpen e=** Terpene cluster**; lantipeptide =** Lanthipeptide cluster**; bacteriocin =** Bacteriocin or other unspecified ribosomally synthesized and post-translationally modified peptide product (RiPP) cluster**; lassopeptide =** Lassopeptide cluster**; bottromycin =** Bottromycin cluster**; siderophore=**Siderophore cluster**; ectoine=**Ectoine cluster**; butyrolactone=**Butyrolactone cluster**; indole=**Indole cluster**; oligosaccharide=**Oligosaccharide cluster**; hserlactone=**Homoserine lactone cluster**; phosphonate=**Phosphonate cluster**; other=**Cluster containing a secondary metabolite-related protein that does not fit into any other category

-: no results;
*: not the next related strain; they are the strains with complete genome sequence available in the Genus.
**: not the next related strain; it is the original classification from our database.

Secondary metabolite biosynthetic gene clusters were identified from a total 32 genome sequences available strains from NCBI database by the online antiSMASH tool. The detailed information is seen in Table 8-1 in Appendix.

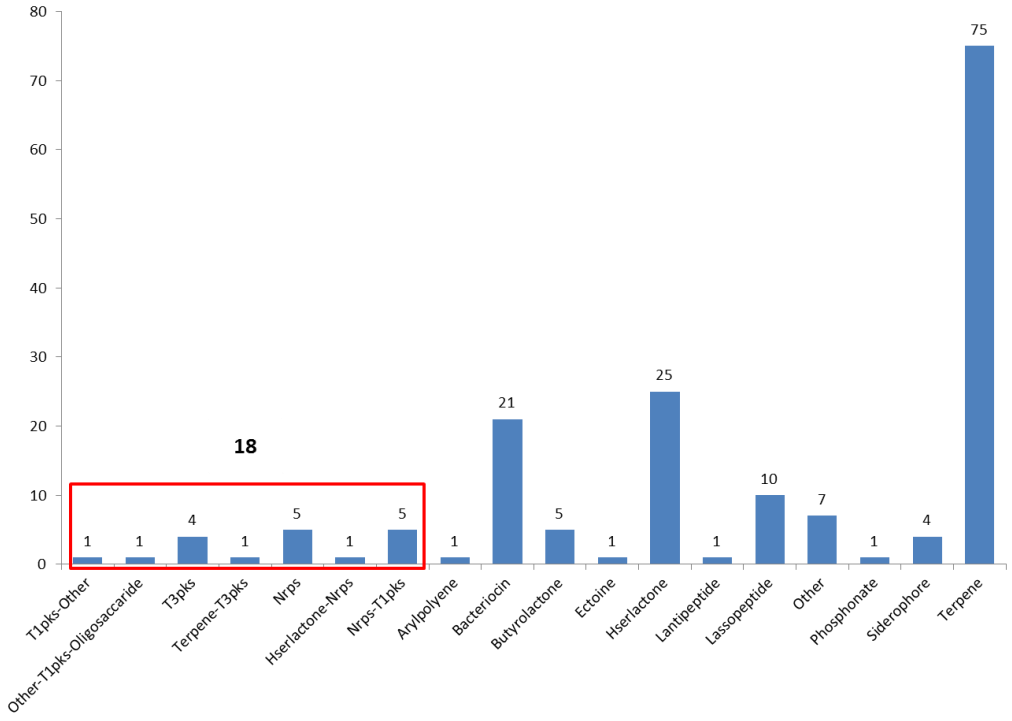

T1pks-Other = Type I PKS and other cluster (mixed); **Other-T1pks-Oligosaccaride** = other, Type I PKS and oligosaccharide cluster; T3pks = Type III PKS cluster; **Terpene-T3pks** = terpene and Type III pks cluster; **Nrps** = Nonribosomal peptide synthetase cluster**; Hserlactone-Nrps** = homoserine lactone and nonribosomal peptide synthetase cluster**; Nrps-T1pks** = nonribosimal peptide synthetase and Type I PKS cluster**; Arylpolyene** = Aryl polyene cluster; **Bacteriocin** = Bacteriocin or other unspecified ribosomally synthesized and post-translationally modified peptide product (RiPP) cluster**; Butyrolactone** = Butyrolactone cluster**; Ectoine** = Ectoine cluster**; Hserlactone** = Homoserine lactone cluster**; Lantipeptide** = Lanthipeptide cluster**; Lassopeptide** = Lassopeptide cluster**; Other** = Cluster containing a secondary metabolite-related protein that does not fit into any other category; **Phosphonate** = Phosphonate cluster**; Siderophore** = Siderophore cluster; **Terpene** = Terpene cluster

Figure 3-49. The numbers of gene clusters obtained from online antiSMASH tool.

Based on the analysis of the antiSMASH program, 169 gene clusters (Figure 3-49) were found to match to one of the indicated functions of secondary metabolites biosynthesis among 31 species of anoxygenic phototrophic bacteria (*Rhodobacter sphaeroides* KD131 showed no matching cluster in the whole genome). There are 1 mixed T1pks-other, 1 mixed other-T1pks-oligosaccaride, 4 T3pks, 1 mixed terpene-T3pks, 5 NRPS, 1 mixed homoserine lactone-NRPS, 5 mixed NRPS-T1pks, 1 aryl polyene, 21 bacteriocins, 5 butyrolactones, 1 ectoine, 25 homoserine lactones, 1 lanthipeptide, 10 lassopeptides, 1 phosphonate, 4 siderophores, 75 terpenes, and 7 other clusters containing a secondary metabolite-related gene that does not fit into any other category.

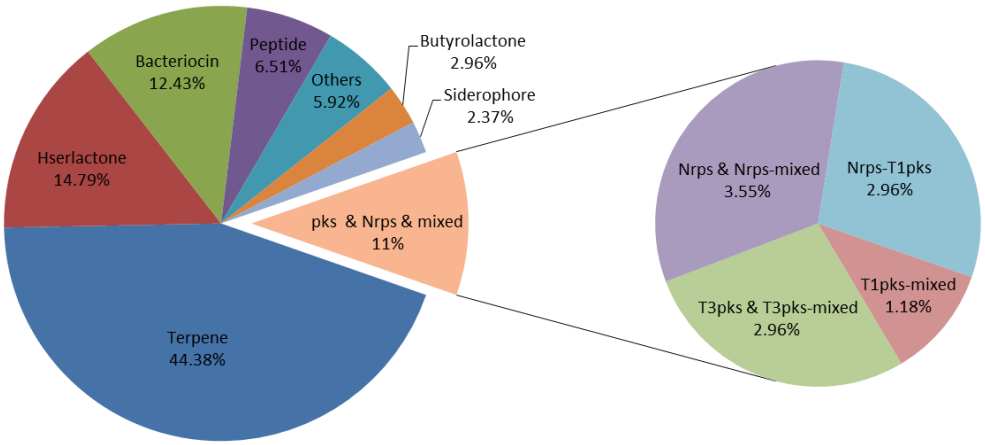

Terpene = Terpene cluster; **Hserlactone** = Homoserine lactone cluster**; Bacteriocin** = Bacteriocin or other unspecified ribosomally synthesized and post-translationally modified peptide product (RiPP) cluster**; Peptide** = Lanthipeptide cluster (lantipeptide) and Lassopeptide cluster (Lassopeptide); **Butyrolactone** = Butyrolactone cluster**; Siderophore** = Siderophore cluster; **Other** = Cluster containing a secondary metabolite-related protein that does not fit into any other category; T1pks-mixed: Type I PKS and other cluster (T1pks-Other**),** other, Type I PKS and oligosaccharide cluster (Other-T1pks-Oligosaccaride); **T3pks & T3pks-mixed** = Type III PKS cluster, terpene and Type III PKS cluster (Terpene-T3pks); Nrps & Nrps-mixed: Nonribosomal peptide synthetase cluster, homoserine lactone and nonribosomal peptide synthetase cluster (Hserlactone-Nrps); **Nrps-T1pks** = nonribosimal peptide synthetase and Type I PKS cluster

Figure 3-50. Pie chart of the distribution of biosynthesis gene clusters of anoxygenic phototrophic bacteria.

All types of gene clusters can be categorized to eight different groups and the relative contribution of the different functional gene groups is depicted in Figure 3-50 and Table 3-33, namely terpenes (44.38%), hserlactones (homoserine lactone cluster) (14.79%), bacteriocins (12.43%), peptides (lassopeptide and lantipeptide, 6.51%), siderophores (2.37%), butyrolactones (2.96%), PKS/NRPS/mixed clusters (11%), and others (5.92%).

The most frequently seen biosynthesis gene cluster is the terpene cluster that accounts for 44.38% (75 of 169) of the identified genes. Among them, a total of 12 terpene clusters are related to the biosynthesis of carotenoids (3 clusters, 66%-100% similarity), malleobactin (5 clusters, 7%-11% similarity), and hopenes (4 clusters, 15% similarity).

Table 3-33. Summary of the secondary metabolite clusters and the most similar compounds.

Name of cluster from antiSMASH	No. of cluster	No. of most similar compound	Strains	Cluster position	Most similar compounds	%
Arylpolyene	1	1	*Thiocystis violascens* DSM 198	Cluster 3	Xanthomonadin	14%
Bacteriocin	21	-	-	-	-	-
Butyrolactone	5	-	-	-	-	-
Ectoine	1	1	*Halorhodospira halophila* SL1	Cluster 4	Ectoine	66%
Hserlactone	25	4	*Rhodobacter sphaeroides* 2.4.1	Cluster 3	Streptomycin	2%
			Rhodobacter sphaeroides ATCC 17029	Cluster 3	Streptomycin	2%
			Rhodopseudomonas palustris DX-1	Cluster 1	Bottromycin A2	6%
				Cluster 5	Lipopolysaccharide	16%
Hserlactone-Nrps	1	-	-	-	-	-
Lantipeptide	1	-	-	-	-	-
Lassopeptide	10	1	*Rubrivivax gelatinosus* IL144	Cluster 1	Rubrivinodin	80%
Phosphonate	1	-	-	-	-	-
Siderophore	4	-	-	-	-	-
Nrps	5	-	-	-	-	-
Nrps-T1pks	5	1	*Rhodopseudomonas palustris* BisB18	Cluster 6	Pyoluteorin	15%
T1pks-Other	1	1	*Rubrivivax gelatinosus* IL144	Cluster 4	Azinomycin B	4%
Other-T1pks-Oligosaccaride	1	-	-	-	-	-
T3pks	4	-	-	-	-	-
Terpene-T3pks	1	1	*Rhodomicrobium vannielii* ATCC 17100	Cluster 1	Carotenoid	66%
Terpene	75	12	*Allochromatium vinosum* DSM 180^T	Cluster 3	Carotenoid	100 %
			Thioflavicocus mobilis 8321	Cluster 5	Carotenoid	100 %
			Rhodospirillum rubrum ATCC 11170	Cluster 1	Malleobactin	1%
			Rhodospirillum photometricum DSM 122	Cluster 2	Carotenoid	100 %
			Rhodomicrobium vannielii ATCC 17100	Cluster 5	Malleobactin	7%
			Rhodopseudomonas palustris CGA009	Cluster 6	Malleobactin	7%
			Rhodopseudomonas palustris DX-1	Cluster 3	Hopene	5%
			Rhodopseudomonas palustris HaA2	Cluster 2	Hopene	5%
			Rhodopseudomonas palustris BisB5	Cluster 3	Malleobactin	7%
			Rhodopseudomonas palustris BisB18	Cluster 3	Hopene	5%
			Rhodopseudomonas palustris BisA53	Cluster 2	Hopene	5%
			Rhodopseudomonas palustris TIE-1	Cluster 7	Malleobactin	7%
Other	7	-	-	-	-	-
Sum	169	22				

The PKS/NRPS/mixed group is the combination of four parts (accounts together for 17%), namely T1pks-mixed (1.18%), T3pks & T3pks-mixed (2.96%), Nrps-T1pks (2.96%), and Nrps & Nrps-mixed (3.55%).

① The T1pks-mixed part contains 1 T1pks-other cluster (only 4% similar to azinomycin B in *Rubrivivax gelatinosus* IL144) and 1 other-T1pks-oligosaccaride cluster in *Thioflavicoccus mobilis* 8321.

> Azinomycin B ($C_{31}H_{33}N_3O_{11}$) produced by *Streptomyces griseofuscus* S42227 (FERM P-8443) is active against Gram-positive bacteria, Gram-negative bacteria and L5178Y cells in tissue culture (Nagaoka *et al.*, 1986). The cloning and sequence analysis of *azi* gene cluster revealed a type I polyketide synthase (PKS)/nonribosomal peptide synthetase (NRPS) hybrid system for the azinomycin B production (Zhao *et al.*, 2008). It is an effective antitumor compound active against the intraperitoneally inoculated tumors such as P388 leukemia, B-16 melanoma and Ehrlich carcinoma (Ishizeki *et al.*, 1987).

② The T3pks & T3pks-mixed part contains one terpene-T3pks cluster which is 66% similar to a carotenoid cluster in *Rhodomicrobium vannielii* ATCC 17100, and four T3pks clusters in *Rhodospirillum centenum* SW, *Rhodobacter capsulatus* SB1003, *Rhodobacter sphaeroides* ATCC 17029, and *Heliobacterium modesticaldum* Ice1.

> Carotenoids are organic pigments that are found in plants and some other photosynthetic organisms (bacteria and fungi). In plants and algae, carotenoids serve in photosynthesis (light absorption for use), and protection of chlorophyll from photodamage (Armstrong and Hearst, 1996). Carotenoids produced by bacteria protect themselves from oxidative attack (Liu *et al.*, 2005).

③ The Nrps-T1pks part contains 5 hybrid Nrps-T1pks clusters in four strains belonging to *Rhodopseudomonas palustris*, namely *R. palustris* CGA009, *R. palustris* DX-1, *R. palustris* BiB18, and *R. palustris* TIE-1. There are two Nrps-T1pks clusters in *R. palustris* BiB18, and one of them is annotated 15% similar to a pyoluteorin biosynthesis gene cluster.

> Pyoluteorin (4,5-dichloro-1*H*-pyrrol-2-yl-2,6-dihydroxyphenyl ketone) is an antifungal compound composed of a bichlorinated pyrrole linked to a resorcinol moiety (Howell and Stipanovic, 1980; Nowak-Thompson *et al.*, 1999). Pyoluteorin is composed of a resorcinol ring, derived via polyketide biosynthesis (Cuppels *et al.*, 1986; Nowak-Thompson *et al.*, 1997).

④ The Nrps & Nrps-mixed part includes 1 hserlactone-Nrps cluster in *R. palustris* BisB18 and 5 Nrps clusters in the purple sulfur bacterium *Marichromatium purpuratum* (2 clusters), the purple nonsulfur bacteria *Rhodospirillum rubrum* ATCC11170 and F11, and the green sulfur bacterium *Chlorobium phaeobacteroides*.

The other groups are mostly ribosomal peptide products. 25 hserlactone (homoserine lactone) cluster accounts for 14.79% and 4 clusters of them are predicted to the biosynthesis of two streptomycins

(only 2% similarity) in *Rhodobacter sphaeroides* 2.4.1 and *Rhodobacter sphaeroides* ATCC17029 (see Appendix, Table 8-1), one bottromycin A2 (only 6% similarity) and one lipopolysaccharide (only 16% similarity) in *Rhodopseudomonas palustris* DX-1.

> Streptomycin is a useful broad-spectrum antibiotic drug derived from *Streptomyces griseus*, and it was used for the first effective treatment for tuberculosis (Schatz *et al.*, 1944).
>
> Ribosomal bottromycins represent a promising class of peptides binding to the therapeutically unexploited aminoacyl-*t*RNA binding site (A site) on the 50S ribosome of the bacterial ribosome (Otaka and Kaji, 1976). Bottromycin A2 inhibited MS2 phage RNA-dependent protein synthesis and was discovered from the fermentation broth of *Streptomyces bottropensis* as antibacterial with promising activity against Gram-positive bacteria and mycoplasma (Waisvisz *et al.*, 1957; Tanaka *et al.*, 1968).
>
> Lipopolysaccharides (LPS) typically consist of a lipid A (or endotoxin), an oligosaccharide, and an O-antigen (Raetz and Whitfield, 2002). They are found in the outer membrane of Gram-negative bacteria and elicit immune responses in animals (Schumann *et al.*, 1990). LPS-activated $CD4^+CD25^+$ T regulatory (Treg) cells inhibit neutrophil function and promote their apoptosis and death (Lewkowicz *et al.*, 2006).

1 lanthipeptide and 10 lassopeptide clusters account for 6.51%. There is only one lasso pepetide cluster with 80% similarity to a rubrivinodin biosynthesis gene cluster in *Rubrivivax gelatinosus* IL144. Bioactive peptides, which are driven by ribosome-independent processes, are called NRP (assembled by NRPS). However, lanthipeptides (Zhang *et al.*, 2012) and lassopeptides belong to a superfamily of ribosomally-synthesized and post-translationally modified natural products (peptides) with diverse bioactivities. This strategy seems to be widely distributed in all kingdoms of life. Lassopeptides produced from bacteria were first described in 1991, and showed an array of potential therapeutic functions as general receptor antagonists, enzyme inhibitors and antibacterial or antiviral (anti-HIV) agents (Li *et al.*, 2015; Maksimov *et al.*, 2012). Rubrivinodin is a lassopeptide and was detected by Hegemann *et al.* (2013).

Bacteriocin, butyrolactone, and siderophore gene clusters occupy 21 (12.43%), 5 (2.96%) and 4 clusters (2.37%), respectively. However, there is no predicted compounds of this type gene clusters.

> Bacteriocins are ribosomally assembled and post-translationally modified peptides (RiPPs). They are antimicrobial peptides produced by certain bacteria, and exhibit significant potency against other bacteria with a stable property and can have narrow or broad activity spectra (Cotter *et al.*, 2013).
>
> Gamma-butyrolactones and acyl homoserine lactones (AHLs or N/AHLs) are signalling molecules which regulate antibiotic production and morphological differentiation, and many physiological aspects like biofilm formation, respectively (Horinouchi, 2002). They have been shown to be important mainly in *Streptomyces* species (Hughes and Sperandio, 2008). Takano *et al.* (2005) showed that a gamma-butyrolactone-binding protein directly regulates a secondary metabolite pathway-specific regulatory gene in *Streptomyces*. AHLs are involved in prokaryotic function of virulence, T3SS regulation, biofilm formation, motility, antibiotic production and in

eukaryotic function of immunomodulation, intracellular calcium signalling and apoptosis (Hughes and Sperandio, 2008).

A siderophore is a natural compound with a high affinity to ferric ion which is secreted by microorganisms (Reid *et al.*, 1993). Siderophores are applicated as antibiotics in the treatment of iron diseases (Hider and Kong, 2010) as response to iron deficienty.

The group named "other" (5.92%) includes arylpolyene (1 cluster, 14% similarity to xanthomonadin in *Thiocystics violascens* DSM198), ectoine (1 cluster, 66% similarity to ectoine in *Halorhodospira halophila* SL1), phosphonate (1 cluster), and other clusters (7 clusters, secondary metabolite-related proteins that do not fit into any other category).

The yellow pigments (xanthomonadins) produced by the phytopathogenic bacterium *Xanthomonas* are unimportant during pathogenesis but may be important for protection against photobiological damage (Poplawsky *et al.*, 2000).

Ectoine (1,4,5,6-tetrahydro-2-methyl-4-pyrimidine carboxylic acid) is a natural product found in some bacteria. It serves as an osmolyte and thus helps organisms to survive extreme osmotic stress. Ectoine is found in high concentrations in halophilic microorganisms and confers resistance towards salt and temperature stress. it was first identified in the phototrophic purple sulfur bacteria (PSB) *Halorhodospira halochloris* (previously known as *Ectothiorhodospira halophila*) (Peters *et al.*, 1990).

Phosphonates are organophosphorus compounds and are commonly used as inhibitors of enzymes which utilize phosphates as substrates in medicine (Wiemer *et al.*, 2009).

There are no Type II PKS (T2pks) and phenazine related clusters detected in any of the 32 anoxygenic phototrophic bacteria by antiSMASH.

4 DISCUSSION

Drug discovery from marine sources becomes more and more significant because the huge potential of new chemical structures isolated from the ocean. Hundreds to thousands of new compounds are reported every year (Molinski *et al.*, 2009; Blunt *et al.*, 2014). However, as far as we know, anoxygenic phototrophic bacteria were never screened for the secondary metabolites. From the work of Dr. Marcus Tank, strain MT86 was similar to the type strain of *Allochromatium vinosum* DSM180^T. In this present thesis, the 16S rRNA gene sequence of strain MT86 was confirmed to be 99.73% and 99.72% similar to *A. vinosum* DSM180^T and *A. vinosum* 5110^T and thereby identified as a strain of this species.

4.1 Metabolite profiles of *A. vinosum* strain MT86

One main aim of the present Ph.D. thesis was to screen for the secondary metabolites of *A. vinosum* MT86. For this purpose, different approaches approved for natural product discovery were used (variation of culture conditions for growth, salt stress and stimulating effects by salts). In addition, the genetic potential according to *pks* I, *pks* II, *nrps*, and *phz*E gene sequences was analyzed.

Cultivation of *A. vinosum* MT86 under different conditions and fractionation of the supernatant extract of MT86 was performed to get the first insights into the production of bioactive compounds.

It is known that thiosulfate acts as electron donor in the photolithoautotrophic growth of *A. vinosum* DSM180^T, and acetate is a carbon source of photolithoheterotrophic growth (Weissgerber *et al.*, 2011). In consideration of the utilisation of thiosulfate and acetate, Pfennigs medium with $MgCl_2$, supplemented with thiosulfate and acetate was experimentally supported to be the optimal cultivation condition for growth of *A. vinosum* MT86. This also made the cultivation much easier because addition of sulfide solution every two days was not necessary.

Compound F13 was considered as the most interesting one for further studies and was produced under various culture conditions by strain MT86 (Table 4-1). In the first chromatograms it was designated as P10, which was shown to be identical to F13 of the later HPLC separations, according to NMR spectra.

A. vinosum DSM180^T does not require salts but can tolerate low concentrations (Weissgerber *et al.*, 2011). Comparison of cultures of *A. vinosum* MT86 grown at different salt concentrations revealed that the strain could tolerant up to 3.33% salts. This result is in accord with those from Weissgerber *et al.* (2011). The preferred cultivation conditions were 0.67% salts for 10 days and 2.5% salts for 15 days. The production of compound F13 was reproducible under the different conditions and showed some antimicrobial properties.

Table 4-1. Comparison of F13 produced in different cultivation.

	20 L	36L	50 L (45 L)	50 L (50 L)
Salt concentration	0%	0%	0.67%	2.5%
Thiosulfate and acetate	-	1%	1%	1%
Mg^{2+}	$MgSO_4 \cdot 7H_2O$	$MgCl_2 \cdot 6H_2O$	$MgCl_2 \cdot 6H_2O$	$MgCl_2 \cdot 6H_2O$
Trace element solution	SL-12	SLA	SLA	SLA
Adding sulfide solution	1%, every 2 days	-	-	-
Incubationn time	in twice 16 d + 17 d	11 d	10 d	15 d
Light intensity (lux)	1000	1000	1000	1000
Temperature (°C)	28-30	28-30	28-30	28-30
Dried weight of supernatant crude extract	82.7 mg	283 mg *	318 mg	570 mg
Fractionations	Peak 1-10	F1-F18	F1-F18	P1-P18 (Polar column) C1-C18 (C18 column)
F13 exist or not	+ (P10)	+ (F13)	+ (F13)	+ (P13=C13)
Summary	F13 = P10 = P13 = F13			

+: existed; -: no adding sulfide solution; *: oil-gel liked

4.2 Metabolite profiles of other anoxygenic phototrophic bacteria

Metabolite production of *Rhodopseudomonas palustris* strain120/1, *Rhodobacter capsulatus* strain 182, and *Rubrivivax gelatinosus* strain 151 were studied. These bacteria were the most interesting regarding potential secondary metabolite production. With all strains, the metabolite profiles according to the HPLC-DAD/MS chromatograms, indicated increased metabolite production at prolonged cultivation for 10 (instead of 7) days.

The antiSMASH search of the genome of *Rubrivivax gelatinosus* IL144 revealed the potential for biosynthesis of terpenes and also a T1pks-other gene cluster was identified, although the later showed only 4% similarity to the gene for biosynthesis of zainomycin.

Rubrivivax gelatinosus strain 151 was an interesting bacterium because of its bioactivity and the metabolite profile revealed by HPLC analysis. Extracts of strain 151 showed good inhibition of *Staphylococcus lentus* and *Septoria tritici* (82% and 80% inhibition). In the HPLC chromatograms several well separated peaks appeared, which indicated that they could probably be easily purified. In conclusion, *Rubrivivax gelatinosus* strain 151 is a candidate for further studies on secondary metabolites.

4.3 Classification and identification of strains

16S rRNA alignment results showed that strain 5410 used in this study was next related to an uncultured bacterium clone EMIRGE OUT s7t4e 93. This is different classification from the original strain offered at the beginning. However, the *pks* I result of strain 5410 showed a 760 nt fragment that was 99% similar to a signal transduction histidine kinase gene cluster of *Thiocystis violascens* DSM 198 (which should be identical to strain 5410).

Strain MT86 showed 99.73% and 99.72% similarity to *Allochromatium vinosum* DSM180^T and *A. vinosum* strain 5110^T, respectively. Strain 5110 in this study is 99% similar to *A. vinosum* DSM180^T. In conclusion, stain MT86 should belong to the same species as a new strain of *A. vinosum*.

4.4 PCR amplification of strains and sequences BLASTn analysis

BLASTn results of *pks* I, *pks* II, *nrps*, and *phz*E sequences from control strains demonstrated that the primers, PCR systems and programs amplification were well functioning. The results of the sequences of *pks* I and *pks* II fragments of all ten strains revealed similar features to deposited sequences of NCBI database. However, relatedness was obtained to several other functional genes, but not to the polyketide synthase systems. There was no indication of a type II *pks* gene in any of the bacteria analysed in present study.

The *nrps* amplification and BLASTn results showed an adenylation (A) domain could be found in positive control strain. "A domain" is capable of substrate recognition and formation of the corresponding acyl-adenylate-monophosphate by consumption of ATP to PCP. It is an important domain in the modules of NRPS systems. Acyl-CoA synthases (synonymous name is acetate-CoA ligases, EC 6.2.1.1) played important functional roles in coenzymes formation, such as active in acetyl-CoA biosynthetic process from acetate (ATP + acetate + CoA = AMP + diphosphate + acetyl-CoA). From Weissgerber *et al.* (2011), acetate is utilized by *A. vinosum* DSM180^T by converting to acetyl-CoA via acetate-CoA-ligase or the successive reactions of acetate kinase and phosphate acetyltransferase. In addition, the CoAs are the basic units for chain elongation, and CoA-ligase is necessary in PKS, NRPS-PKS and also in fatty acid synthases. In conclusion, there is no direct relationship to the NRPS-PKSs in *A. vinosum* MT86 and all other tested strains.

The *phz*E amplification and BLASTn results showed an anthranilate synthase gene of positive control *Pseudomonas* sp. DSM50117 (425 nt) and also in eight strains (with exception of strains 2360, 414 nt and 151, 430 nt). Anthranilate synthase (ID GO: 0004049 = EC 4.1.3.27) belongs to the enzymes of phenazine biosynthesis. PhzE (synonymous name is 2-amino-2-deoxy-isochorismate synthase, EC 4.1.3.-) is a phenazine biosynthesis specific protein (from databases of ExPASy and UniProtKB). It catalyses the reaction chorismate + L-glutamine = anthranilate + pyruvate + L-glutamate, or chorismate + L-glutamine = 2-amino-4-deoxyisochorismate + L-glutamate (see in Figure 4-1).

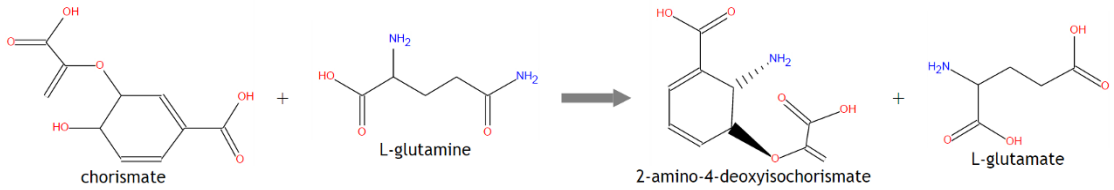

Figure cited from:
http://www.pseudomonas.com:1555/PSEUDO/NEW-IMAGE?type=REACTION&object=RXNB-5661

Figure 4-1. A PhzE pathway for *Pseudomonas aeruginosa* PAO1.

In conclusion, from the results of PCR amplification of *pks* I, *pks* II, *nrps*, and *phz*E fragments of ten phototrophic bacteria, type I and type II *pks* could not be amplified in these bacteria by the methods used in this study. Moreover, with the exception of *C. phaeobacteroides* strain 2360 (no *phz*E amplification product) and *Rubrivivax gelatinosus* strain 151 (a 215 nt fragment without BLASTn result), the lengths of all *phz*E fragments from eight strains are between 414 and 430 nt, which are similar to the size of the positive control. The *phz*E amplification system and PCR program were useful in *phz*E gene screening of those ten phototrophic bacteria. In addition, eight strains including strain MT86, showed the possibility of phenazine biosynthesis.

4.5 Genome evaluation of phototrophic bacteria from database

Genome mining of gene clusters encoding the biosynthetic pathways for these metabolites has become a significant methodology for novel compound discovery. Since 2008, genome mining approaches allowed the targeted isolation and characterization of such molecules and helped to better understand these compounds classes and their biosyntheses (Hegemann *et al.*, 2015). AntiSMASH is a comprehensive resource for the genome mining of biosynthetic gene clusters (Weber *et al.*, 2015). By comparison of BLASTn results with PCR amplificates and the antiSMASH-based analyses (see Figure 3-49, Figure 3-50 and Table 3-33) of the results, some interesting conclusions can be obtained.

In genome sequences available anoxygenic phototrophic bacteria, clusters of terpene biosynthesis occupy the most significant part of the antiSMASH results. In the genome of *A. vinosum* 180^T, hserlactone, terpene (100% similar to carotenoid) and other clusters are the representatives of secondary metabolites biosynthesis genes. While terpenes are the major class of secondary metabolites discovered in anoxygenic phototrophic bacteria, polyketides and nonribosomal peptides are also identified, as were ribosomally assembled and post-translationally modified peptides (RiPPs).

According to antiSMASH, no phenazine E gene clusters are predicted from the 32 genome sequences of anaerobic anoxygenic phototrophic bacteria. However, the PCR amplification and BLASTn results showed that except for *C. phaeobacteroides* stain 2360 and *Rubrivivax gelatinosus* strain 151, the lengths of *phz*E fragments from other eight strains were between 414 and 430 nt. When a bacterial

genome sequence (by accession number) is uploaded to antiSMASH, the program identifies putative gene clusters by comparing all predicted gene products to models that in database. It is speculated that the differences of results between PCR, BLASTn and antiSMASH analysis showed that not all classes of secondary metabolites could be predicted to gene products, and vice versa. This hypothesis is consilient to Zeilinger *et al.* (2015) that, while antiSMASH is extremely powerful, it still has some limitations in its ability to correctly predict genes and their encoded proteins and identify full biosynthetic pathways. It can easily miss some individual biosynthetic genes and the rules for defining the boundaries of secondary metabolic clusters are not yet entirely clear.

Comparison of the primer sequences with whole or partial genome sequences was in consideration. Unfortunately, by using the Primer-BLAST, there is a limitation of the gene size of no more than 50000 bp and the predicted genes of secondary metabolites by antiSMASH showed always more than this size. Therefore, the sequence matches of the primers used for amplification of the desired genes within strains investigated in this study could not be demonstrated.

Genome mining has revealed the diversity, abundance and complex nature of secondary metabolite potential of anoxygenic phototrophic bacteria. Secondary metabolic pathways and their corresponding products are predicted from a genome sequence and a chemo type is linked to its biosynthetic gene cluster (genotype) based on information derived from the prediction (Zerikly and Challis, 2009). In current genome mining approaches, the “prediction step” has started to be automated by use of computational tools such as antiSMASH to rapidly characterize biosynthetic gene clusters in microbial genome sequences (Medema *et al.*, 2011).

5 SUMMARY

This thesis is the first detailed study on secondary metabolites produced by anoxygenic phototrophic bacteria. The main purpose of the work was the isolation of bioactive natural products from anoxygenic phototrophic bacteria, using cultivation-based, chemical and molecular approaches.

Much of the work focussed on the purple sulfur bacterium *Allochromatium vinosum* strain MT86. This strain was shown previously to produce antibiotic substances. For this strain, the optimal culture conditions were determined to be Pfennigs medium (containing $MgCl_2$) with the addition of thiosulfate and acetate. By comparison of metabolite profiles in HPLC-DAD/MS chromatograms of extracts from cultures grown under different conditions, it was shown that this medium well suited suitable for proper production of secondary metabolites by *A. vinosum* strain MT86. This was in particular the case for interesting compound F13, which was found under a variety of culture conditions. The structure of compound F13 was established using HPLC-DAD/MS, NMR-, IR-, and CD-analyses. Bioactivity tests showed that F13 was inhibitory against *Bacillus subtilis* and *Staphylococcus lentus* (IC_{50} = 70.5 µM (± 2.9) and 57.0 µM (± 3.3)).

In addition, the production of secondary metabolites, respectively the potential thereof, was studied in a number of other anoxygenic phototrophic bacteria, including purple sulfur bacteria, purple nonsulfur bacteria and green sulfur bacteria. Among several purple nonsulfur bacteria, extracts of *Rubrivivax gelatinosus* strain 151 showed antibiotic activities against *Staphylococcus lentus* and *Septoria tritici*. Identification of bioactive metabolites was not possible.

Genome-based search for genes for secondary metabolite biosynthesis revealed that *Allochromatium vinosum* MT86 has no *pks* I, *pks* II and *nrps* genes, but *phz*E gene exists. Within ten representative anoxygenic phototrophic bacteria (including strain MT86), type I and type II *pks* could not be identified. Moreover, there were no genes with direct relationship to *nrps* genes, with the exception of genes of CoA ligase in *Allochromatium vinosum* MT86 and 5110, which maybe relevant to the synthesis of NRPS.

The *phz*E amplification system and PCR program resulted in products of the expected sequence length in eight from ten strains, with the exception of *Chlorobium phaeobacteroides* strain 2360 and *Rubrivivax gelatinosus* strain 151. These strains included *Allochromatium vinosum* strain MT86. The sequence comparison yielded a clear relationship to the relevant *phzE* genes.

The complete genome-based bioinformatics screening of anoxygenic phototrophic bacteria clearly indicates the uncertainty in determining the potential of the synthesis of bioactive compounds by these bacteria. Terpene biosynthesis clusters occupied the most significant fraction in the antiSMASH results of 62 complete genomes of anoxygenic phototrophic bacteria. These analyses showed that

terpene, homoserine lactones and other synthesis gene clusters for secondary metabolites were present in the genome of *A. vinosum* 180^T. However, the antiSMASH results showed that there was no phenazine gene clusters predicted from 32 whole genome sequences. The results enlighten the knowledge about the natural products potential of anoxygenic phototrophic bacteria.

6 ZUSAMMENFASSUNG

Dies ist die erste detaillierte Untersuchung zur Sekundärmetabolitproduktion durch anoxygene phototrophe Bakterien. Das Hauptziel der Arbeit war die Isolierung von Wirkstoffen aus anoxygenen phototrophen Bakterien durch kultur-abhängige Methoden sowie chemische und molekulare Analysen.

Ein Großteil der Arbeit konzentrierte sich auf das Schwefelpurpurbakterium *Allochromatium vinosum* Stamm MT86. Von diesem Stamm war bekannt, dass er antibiotische Substanzen produziert. Als optimal für die Kultur dieses Stammes erwies sich Pfennigs Medium (mit $MgCl_2$) mit Zusatz von Thiosulfate und Acetat. Durch Vergleich der Metabolitprofile in HLPC-DAD/MS Chromatogrammen von Extrakten aus Kulturen, die unter verschiedenen Bedingungen angezogen wurden, zeigte sich, dass es für die Metabolitproduktion durch *A. vinosum* Stamm MT86 gut geeignet war. Dies galt insbesondere für die interessante Verbindung F13, die unter verschiedenen Kulturbedingungen gebildet wurde. Die Struktur der Substanz F13 wurde aufgeklärt durch HPLC-DAD/MS-, NMR-, IR-, und CD-Analysen. Bioaktivitätstests mit F13 zeigten, dass sie gegen *Bacillus subtilis* und *Staphylococcus lentus* (IC_{50} = 70.5 µM (± 2.9) und 57.0 µM (± 3.3) aktiv war).

Zusätzlich wurde die Produktion von Sekundärmetaboliten bzw. das Potential hierzu in einer Auswahl weiterer anoxygener phototropher Bakterien, einschließlich Schwefelpurpurbakterien, Nichtschwefel-Purpurbakterien und grüner Schwefelbakterien, untersucht. Unter den Nicht-Schwefel Purpurbakterien zeigten Extrakte von *Rubrivivax gelatinosus* Stamm 151 antibiotische Aktivitäten gegen *Staphylococcus lentus* and *Septoria tritici*. Eine Identifizierung der bioaktiven Metabolite war nicht möglich. Genom-basierte Suche nach Genen für die Sekundärmetabolitsynthese machte deutlich, dass in *Allochromatium vinosum* MT86 *pks* I, *pks* II und *nrps* Gene nicht vorhanden sind, wohl aber *phz*E Gene.. Als repräsentativ für Sekundärmetabolit-Biosynthesewege wurden *pks* I, *pks* II, *nrps*, and *phz*E Gene durch PCR Amplifikation mittels für diese Gene spezifischer Primer analysiert. In zehn repräsentativen anoxygenen phototrophen Bakterien (einschließlich Stamm MT86) konnten), Type I und Typ II *pks* nicht identifiziert werden. Zudem wurden keine Gene gefunden, die einen direkten Bezug zu *nrps* Genen haben gefunden. Eine Ausnahme machen Gene der CoA-ligase in *Allochromatium vinosum* MT86 and 5110, die in Bezug zur Bildung NRPS stehen.

Die Amplifikation von *phz*E und das PCR Programm ergaben Amplifikate in der erwarteten Sequenzlänge in acht von zehn untersuchten Stämmen, mit Ausnahme von *Chlorobium phaeobacteroides* Stamm 2360 und *Rubrivivax gelatinosus* Stamm 151. Dies schließt *Allochromatium vinosum* Stamm MT86 mit ein. Ein Sequenzvergleich gibt klaren Bezug zu den relevanten *phz*E Genen.

Die gesamte Information der verfügbaren Genome von anoxygenen phototrophen Bakterien zeigt die Unsicherheit auf, die bei der Bestimmung des Potentials zur Biosynthese von bioaktiven Substanzen durch diese Bakterien besteht. Biosynthesecluster für Terpene hatten den größten Teil der Ergebnisse

aus 62 Genomen anoxygener phototropher Bakterien unter den Ergebnissen mit antiSMASH. Es wurden Gene zur Biosynthese von Terpenen, Homoserinlacton und anderen Sekundärmetaboliten im Genom von *A. vinosum* 180^T gefunden. Allerdings wurden mittels antiSMASH keine Hinweise auf Phenazin-Biosynthesegene in einem der 32 untersuchten Genome gefunden.

Die Ergebnisse beleuchten unseren Kenntnisstand zum Potential der Wirkstoffsynthese durch anoxygene phototrophe Bakterien.

7 REFERENCES

Alfano, J. R. and Collmer, A. (1996) Bacterial pathogens in plants: life up against the wall. The Plant Cell, 8, 1683.

Anand, S., Prasad, M. R., Yadav, G., Kumar, N., Shehara, J., Ansari, M. Z. and Mohanty, D. (2010) SBSPKS: structure based sequence analysis of polyketide synthases. Nucleic Acids Research, 1-10.

Arbiser, J. L. and Moschella, S. L. (1995) Clofazimine: a review of its medical uses and mechanisms of action. Journal of the American Academy of Dermatology, 32, 241-247.

Armstrong, G. A. and Hearst, J. E. (1996) Carotenoids 2: Genetics and molecular biology of carotenoid pigment biosynthesis. The Journal of the Federation of American Societies for Experimental Biology, 10, 228-237.

Asao, M. and Madigan, M. T. (2009) Family IV Heliobacteriaceae *In* Bergey's Manual of Systematic Bacteriology, 2nd Ed., Vol. III (Eds, Paul, D. V., Garrity, G. M., D., J., Krieg, N. R., Ludwig, W., Rainey, F. A., K.-H., S. and Whitman, W. B.) Springer Science & Business Media, New York, pp. 913-916.

Augustin, J. M., Kuzina, V., Andersen, S. B. and Bak, S. (2011) Molecular activities, biosynthesis and evolution of triterpenoid saponins. Phytochemistry, 72, 435-457.

Ayuso-Sacido, A. and Genilloud, O. (2005) New PCR primers for the screening of NRPS and PKS-I systems in Actinomycetes: detection and distribution of these biosynthetic gene sequences in major taxonomic groups. Microbial Ecology, 49, 10-24.

Baki, A., Bielik, A., Molnár, L., Szendrei, G. and Keserü, G. M. (2007) A high throughput luminescent assay for glycogen synthase kinase-3β inhibitors. Assay and Drug Development Technologies, 5, 75-84.

Bhadury, P., Mohammad, B. T. and Wright, P. C. (2006) The current status of natural products from marine fungi and their potential as anti-infective agents. Journal of Industrial Microbiology and Biotechnology, 33, 325-337.

Blunt, J. W., Copp, B. R., Keyzers, R. A., Munro, M. H. and Prinsep, M. R. (2014) Marine natural products. Natural Product Reports, 31, 160-258.

Bolognesi, M. L., Minarini, A., Rosini, M., Tumiatti, V. and Melchiorre, C. (2008) From dual binding site acetylcholinesterase inhibitors to multi-target-directed ligands (MTDLs): a step forward in the treatment of Alzheimer's disease. Mini Reviews in Medicinal Chemistry, 8, 960-967.

Brosius, J., Palmer, M. L., Kennedy, P. J. and Noller, H. F. (1978) Complete nucleotide sequence of a 16S ribosomal RNA gene from *Escherichia coli*. Proceedings of the National Academy of Sciences, 75, 4801-4805.

Bryant, D. A. and Frigaard, N.-U. (2006) Prokaryotic photosynthesis and phototrophy illuminated. Trends in Microbiology, 14, 488-496.

Bull, A. T. and Stach, J. E. (2007) Marine actinobacteria: new opportunities for natural product search and discovery. Trends in Microbiology, 15, 491-499.

Bumpus, S. B., Evans, B. S., Thomas, P. M., Ntai, I. and Kelleher, N. L. (2009) A proteomics approach to discovering natural products and their biosynthetic pathways. Nature Biotechnology, 27, 951-956.

Buss, A. D. and Butler, M. S. (2010) Natural product chemistry for drug discovery, Royal Society of Chemistry, Cambridge.

Castoe, T. A., Stephens, T., Noonan, B. P. and Calestani, C. (2007) A novel group of type I polyketide synthases (PKS) in animals and the complex phylogenomics of PKSs. Gene, 392, 47-58.

Chakraborty, C., Hsu, C.-H., Wen, Z.-H. and Lin, C.-S. (2009) Anticancer drugs discovery and development from marine organisms. Current Topics in Medicinal Chemistry, 9, 1536-1545.

Chapman, H. (2012) Dictionary of Natural Products on DVD (23: 1). CRC Press, Taylor & Francis Group, URL: http://dnp. chemnetbase. com.

Chin, Y.-W., Balunas, M. J., Chai, H. B. and Kinghorn, A. D. (2006) Drug discovery from natural sources. The The American Association of Pharmaceutical Scientists (AAPS) Journal, 8, E239-E253.

Cooper, E. L. (2004) Drug discovery, CAM and natural products. Evidence-Based Complementary and Alternative Medicine, 1, 215-217.

Cotter, P. D., Ross, R. P. and Hill, C. (2013) Bacteriocins-a viable alternative to antibiotics? Nature Reviews Microbiology, 11, 95-105.

Cuppels, D., Howell, C., Stipanovic, R., Stoessl, A. and Stothers, J. (1986) Biosynthesis of pyoluteorin: a mixed polyketide-tricarboxylic acid cycle origin demonstrated by [1, 2-$^{13}C_2$] acetate incorporation. Zeitschrift für Naturforschung C, 41, 532-536.

Danila, D. C., Szmulewitz, R. Z., Baron, A. D., Higano, C. S., Scher, H. I., Morris, M. J., Gilbert, H., Brunstein, F., Lemahieu, V. and Kabbarah, O. (2014) A phase I study of DSTP3086S, an antibody-drug conjugate (ADC) targeting STEAP-1, in patients (pts) with metastatic castration-resistant prostate cancer (CRPC). In ASCO Annual Meeting Proceedings, Vol. 32, pp. 5024.

Doekel, S. and Marahiel, M. A. (2001) Biosynthesis of natural products on modular peptide synthetases. Metabolic Engineering, 3, 64-77.

Donadio, S., Monciardini, P. and Sosio, M. (2007) Polyketide synthases and nonribosomal peptide synthetases: the emerging view from bacterial genomics. Natural Product Reports, 24, 1073-1109.

Eichler, B. and Pfennig, N. (1988) A new purple sulfur bacterium from stratified freshwater lakes, *Amoebobacter purpureus* sp. nov. Archives Microbiology, 149, 395-400.

Esquenazi, E., Coates, C., Simmons, L., Gonzalez, D., Gerwick, W. H. and Dorrestein, P. C. (2008) Visualizing the spatial distribution of secondary metabolites produced by marine cyanobacteria and sponges via MALDI-TOF imaging. Molecular BioSystems, 4, 562-570.

Feling, R. H., Buchanan, G. O., Mincer, T. J., Kauffman, C. A., Jensen, P. R. and Fenical, W. (2003) Salinosporamide A: a highly cytotoxic proteasome inhibitor from a novel microbial source, a marine bacterium of the new genus *Salinospora*. Angewandte Chemie International Edition, 42, 355-357.

Finking, R. and Marahiel, M. A. (2004) Biosynthesis of nonribosomal peptides. Annual Review of Microbiology, 58, 453-488.

Forrest, R. D. (1982) Early history of wound treatment. Journal of the Royal Society of Medicine, 75, 198-205.

Garrity, G. M. and Holt, J. G. (2001) Phylum BVI. Chloroflexi phy. nov. *In* Bergey's Manual of Systematic Bacteriology, 2nd Ed., Vol. I (Eds, Boone, D. R. and Castenholz, R. W.) Springer-Verlag New York, New York, pp. 427-444.

Gerwick, W. H. and Fenner, A. M. (2013) Drug discovery from marine microbes. Microbial Ecology, 65, 800-806.

Gerwick, W. H. and Moore, B. S. (2012) Lessons from the past and charting the future of marine natural products drug discovery and chemical biology. Chemistry & Biology, 19, 85-98.

Gest, H. and Favinger, J. L. (1983) *Heliobacterium chlorum*, an anoxygenic brownish-green photosynthetic bacterium containing a "new" form of bacteriochlorophyll. Archieve Microbiology, 136, 11-16.

Glöckner, F. O. and Joint, I. (2010) Marine microbial genomics in Europe: current status and perspectives. Microbial Biotechnology, 3, 523-530.

Guirouilh-Barbat, J., Antony, S. and Pommier, Y. (2009) Zalypsis (PM00104) is a potent inducer of γ-H2AX foci and reveals the importance of the C ring of trabectedin for transcription-coupled repair inhibition. Molecular Cancer Therapeutics, 8, 2007-2014.

Gulder, T. A. and Moore, B. S. (2009) Chasing the treasures of the sea - bacterial marine natural products. Current Opinion in Microbiology, 12, 252-260.

Haefner, B. (2003) Drugs from the deep: marine natural products as drug candidates. Drug Discovery Today, 8, 536-544.

Hanada, S., Takaichi, S., Matsuura, K. and Nakamura, K. (2002) *Roseiflexus castenholzii* gen. nov., sp. nov., a thermophilic, filamentous, photosynthetic bacterium that lacks chlorosomes. International Journal of Systematic and Evolutionary Microbiology, 52, 187-193.

Hashimoto, M., Nonaka, T. and Fujii, I. (2014) Fungal type III polyketide synthases. Natural Product Reports, 31, 1306-1317.

Hegemann, J. D., Zimmermann, M., Xie, X. and Marahiel, M. A. (2015) Lassopeptides: an intriguing class of bacterial natural products. Accounts of Chemical Research, 48, 1909-1919.

Hegemann, J. D., Zimmermann, M., Zhu, S., Klug, D. and Marahiel, M. A. (2013) Lassopeptides from proteobacteria: genome mining employing heterologous expression and mass spectrometry. Peptide Science, 100, 527-542.

Helaly, S., Schneider, K., Nachtigall, J., Vikineswary, S., Tan, G. Y. A., Zinecker, H., Imhoff, J. F., Süssmuth, R. D. and Fiedler, H.-P. (2009) Gombapyrones, new α-pyrone metabolites produced by *Streptomyces griseoruber* Acta 3662*. The Journal of Antibiotics, 62, 445-452.

Hider, R. C. and Kong, X. (2010) Chemistry and biology of siderophores. Natural Product Reports, 27, 637-657.

Horinouchi, S. (2002) A microbial hormone, A-factor, as a master switch for morphological differentiation and secondary metabolism in *Streptomyces griseus*. Frontiers in Bioscience: A Journal and Virtual Library, 7, d2045-2057.

Houslay, M. and Adams, D. (2003) PDE4 cAMP phosphodiesterases: modular enzymes that orchestrate signalling cross-talk, desensitization and compartmentalization. Biochemical Journal, 370, 1-18.

Howell, C. and Stipanovic, R. (1980) Suppression of *Pythium ultimium* induced damping off of cotton seedlings by *Pseudomonas fluorescens* and its antibiotic pyoluterin. Phytopathology, 70, 712-715.

Hu, Y., Chen, J., Hu, G., Yu, J., Zhu, X., Lin, Y., Chen, S. and Yuan, J. (2015) Statistical research on the bioactivity of new marine natural products discovered during the 28 years from 1985 to 2012. Marine Drugs, 13, 202-221.

Hughes, D. T. and Sperandio, V. (2008) Inter-kingdom signalling: communication between bacteria and their hosts. Nature Reviews Microbiolgy, 6, 111-120.

Imhoff, J. (2014) The family Chromatiaceae. *In* The Prokaryotes, 4th Ed. (Eds, Rosenberg, E., DeLong, E., Lory, S., Stackebrandt, E. and Thompson, F.) Springer-Verlag Berlin Heidelberg, New York, pp. 151-178.

Imhoff, J., Trüper, H. and Pfennig, N. (1984) Rearrangement of the species and genera of the phototrophic "purple nonsulfur bacteria". International Journal of Systematic Bacteriology, 34, 340-343.

Imhoff, J. F. (2002) Phototrophic purple and green bacteria in marine and hypersaline environments, *In* Encyclopedia of Environmental Microbiology. John Wiley & Sons, New York.

Imhoff, J. F. (2005a) Family Chromatiaceae. *In* Bergey's Manual of Systematic Bacteriology, 2nd Ed., Vol. II (Ed, Garrity, G. M.) Springer Science & Business Media, New York, pp. 3-14.

Imhoff, J. F. (2005b) Genus *Allochromatium*. *In* Bergey's Manual of Systematic Bacteriology, 2nd Ed., Vol. II, Part B (Eds, Brenner, D. J., Krieg, N. R. and Staley, J. T.) Springer Science + Business Media, New York, pp. 12-14.

Imhoff, J. F. (2006) The phototrophic Alpha-Proteobacteria. *In* The Prokaryotes, 3rd Ed., Vol. V (Eds, M., D., S., F., Rosenberg, E., K.-H., S. and Stackebrandt, E.) Springer, New York, pp. 41-64.

Imhoff, J. F. (2008) Systematics of anoxygenic phototrophic bacteria. *In* Sulfur metabolism in phototrophic organisms. Advances in Photosynthesis and Respiration, Vol. 27 (Eds, Hell, R., Dahl C., Knaff, D. and Leustek T.) Springer Science & Business Media, pp. 269-287.

Imhoff, J. F. and Trüper, H. (1989) The purple nonsulfur bacteria. *In* Bergey's Manual of Systematic Bacteriology, 1st Ed., Vol. III (Eds, Staley, J. T., P., B. M., Pfennig, N. and Holt, J. G.) The Williams & Wilkins Co., Baltimore, pp. 1658-1661.

Infante, J. R., Sandhu, S. K., McNeil, C. M., Kabbarah, O., Li, C., Zhong, W., Asundi, J., Wood, K., Chu, Y.-W. and Hamid, O. (2014) Abstract CT233: A first-in-human phase I study of the safety and pharmacokinetic (PK) activity of DEDN6526A, an anti-endothelin B receptor (ETBR) antibody-drug conjugate (ADC), in patients with metastatic or unresectable melanoma. Cancer Research, 74, CT233-CT233.

Ishizeki, S., Ohtsuka, M., Irinoda, K., Kukita, K.-i., Nagaoka, K. and Nakashima, T. (1987) Azinomycins A and B, new antitumor antibiotics. III. Antitumor activity. The Journal of Antibiotics, 40, 60-65.

Jain, N., Smith, S. W., Ghone, S. and Tomczuk, B. (2015) Current ADC linker chemistry. Pharmaceutical Research, 1-15.

Jansen, N., Ohlendorf, B., Erhard, A., Bruhn, T., Bringmann, G. and Imhoff, J. F. (2013) Helicusin E, isochromophilone X and isochromophilone XI: new chloroazaphilones produced by the fungus *Bartalinia robillardoides* strain LF550. Marine Drugs, 11, 800-816.

Jenke-Kodama, H., Sandmann, A., Müller, R. and Dittmann, E. (2005) Evolutionary implications of bacterial polyketide synthases. Molecular Biology and Evolution, 22, 2027-2039.

Jimeno, J., Faircloth, G., Sousa-Faro, J., Scheuer, P. and Rinehart, K. (2004) New Marine Derived Anticancer Therapeutics - A Journey from the Sea to Clinical Trials. Marine Drugs, 2, 14-29.

Jones, A. C., Gu, L., Sorrels, C. M., Sherman, D. H. and Gerwick, W. H. (2009) New tricks from ancient algae: natural products biosynthesis in marine cyanobacteria. Current Opinion in Chemical Biology, 13, 216-223.

Karlovsky, P. (2008) Secondary metabolites in soil ecology. *In* Soil Biology. Secondary Metabolites in Soil Ecology, Vol. 14 (Ed, Karlovsky, P.) Springer-Verlag Berlin Heidelberg, Berlin Heidelberg, pp. 1-19.

Katsuyama, Y. and Ohnishi, Y. (2012) Type III polyketide synthases in microorganisms. *In* Methods in Enzymology, Vol. 515 (Ed, David, A. H.) Elsevier Inc., Oxford, UK, pp. 359-377.

Katz, J., Janik, J. E. and Younes, A. (2011) Brentuximab vedotin (SGN-35). Clinical Cancer Research, 17, 6428-6436.

Khosla, C., Gokhale, R. S., Jacobsen, J. R. and Cane, D. E. (1999) Tolerance and specificity of polyketide synthases. Annual Review of Biochemistry, 68, 219-253.

Kliebenstein, D. J. (2004) Secondary metabolites and plant/environment interactions: a view through Arabidopsis thaliana tinged glasses. Plant, Cell & Environment, 27, 675-684.

Koehn, F. E. and Carter, G. T. (2005) The evolving role of natural products in drug discovery. Nature Reviews Drug Discovery, 4, 206-220.

Laatsch, H. (2014) AntiBase 2014: The natural compound identifier. John Wiley & Sons, Inc.

Lewkowicz, P., Lewkowicz, N., Sasiak, A. and Tchórzewski, H. (2006) Lipopolysaccharide-activated CD4+ CD25+ T regulatory cells inhibit neutrophil function and promote their apoptosis and death. The Journal of Immunology, 177, 7155-7163.

Li, M. H., Ung, P. M., Zajkowski, J., Garneau-Tsodikova, S. and Sherman, D. H. (2009) Automated genome mining for natural products. BMC Bioinformatics, 10, 185.

Li, Y., Zirah, S. and Rebuffat, S. (2015) Lassopeptides. Bacterial strategies to make and maintain bioactive entangled scaffolds. Springer-Verlag New York, New York.

Lin, K., Sukumaran, S., Xu, J., Zhang, C., Choi, Y., Yu, S., Polakis, P. and Maslyar, D. (2014) Translational PKPD of DNIB0600A, an anti-NaPi2b-VC-MMAE ADC in ovarian and NSCLC cancers. Annals of Oncology, 25, iv554-iv554.

Lindblad, W. J. (2008) Review paper: considerations for determining if a natural product is an effective wound-healing agent. The International Journal of Lower Extremity Wounds, 7, 75-81.

Liu, G. Y., Essex, A., Buchanan, J. T., Datta, V., Hoffman, H. M., Bastian, J. F., Fierer, J. and Nizet, V. (2005) *Staphylococcus aureus* golden pigment impairs neutrophil killing and promotes virulence through its antioxidant activity. The Journal of Experimental Medicine, 202, 209-215.

Liu, J., Hu, Y., Waller, D. L., Wang, J. and Liu, Q. (2012) Natural products as kinase inhibitors. Natural Product Reports, 29, 392-403.

Liu, J., Moore, K., Birrer, M., Berlin, S., Matulonis, U., Infante, J., Xi, J., Kahn, R., Wang, Y. and Wood, K. (2013) Targeting MUC16 with the antibody-drug conjugate (ADC) DMUC5754A in patients with platinum-resistant ovarian cancer: A phase I study of safety and pharmacokinetics. *In* Cancer Research, Vol. 73 (8) Amer Assoc Cancer Research 615 Chestnut st. 17th floor, Philadelphia, PA 19106-4404 USA.

Maksimov, M. O., Pan, S. J. and Link, A. J. (2012) Lassopeptides: structure, function, biosynthesis, and engineering. Natural Product Reports, 29, 996-1006.

Martin, D. M., Gershenzon, J. and Bohlmann, J. (2003) Induction of volatile terpene biosynthesis and diurnal emission by methyl jasmonate in foliage of Norway spruce. Plant Physiology, 132, 1586-1599.

Martinez, A., Alonso, M., Castro, A., Pérez, C. and Moreno, F. J. (2002) First non-ATP competitive glycogen synthase kinase 3 β (GSK-3β) inhibitors: thiadiazolidinones (TDZD) as potential drugs for the treatment of Alzheimer's disease. Journal of Medicinal Chemistry, 45, 1292-1299.

Mayer, A., Rodríguez, A. D., Taglialatela-Scafati, O. and Fusetani, N. (2013) Marine pharmacology in 2009–2011: Marine compounds with antibacterial, antidiabetic, antifungal, anti-inflammatory, antiprotozoal, antituberculosis, and antiviral activities; affecting the immune and nervous systems, and other miscellaneous mechanisms of action. Marine Drugs, 11, 2510-2573.

Mayer, A. M., Glaser, K. B., Cuevas, C., Jacobs, R. S., Kem, W., Little, R. D., McIntosh, J. M., Newman, D. J., Potts, B. C. and Shuster, D. E. (2010a) The odyssey of marine pharmaceuticals: a current pipeline perspective. Trends in Pharmacological Sciences, 31, 255-265.

Mayer, A. M., Rodríguez, A. D., Berlinck, R. G. and Fusetani, N. (2011) Marine pharmacology in 2007–8: Marine compounds with antibacterial, anticoagulant, antifungal, anti-inflammatory, antimalarial, antiprotozoal, antituberculosis, and antiviral activities; affecting the immune and nervous system, and other miscellaneous mechanisms of action. Comparative Biochemistry and Physiology Part C: Toxicology & Pharmacology, 153, 191-222.

Mayer, A. M. S., Glaser, K. B., Cuevas, C., Jacobs, R. S., Kem, W., Little, R. D., McIntosh, J. M., Newman, D. J., Potts, B. C. and Shuster, D. E. (2010b) The odyssey of marine pharmaceuticals: a current pipeline perspective. Trends in Pharmacological Sciences, 31, 255-265.

McDonald, M., Mavrodi, D. V., Thomashow, L. S. and Floss, H. G. (2001) Phenazine Biosynthesis in Pseudomonas f luorescens: Branchpoint from the Primary Shikimate Biosynthetic Pathway and Role of Phenazine-1,6-dicarboxylic Acid. Journal of the American Chemical Society, 123, 9459-9460.

Medema, M. H., Blin, K., Cimermancic, P., de Jager, V., Zakrzewski, P., Fischbach, M. A., Weber, T., Takano, E. and Breitling, R. (2011) antiSMASH: Rapid identification, annotation and analysis of secondary metabolite biosynthesis gene clusters in bacterial and fungal genome sequences. Nucleic Acids Research, 39, W339-W346.

Metsä-Ketelä, M., Salo, V., Halo, L., Hautala, A., Hakala, J., Mäntsälä, P. and Ylihonko, K. (1999) An efficient approach for screening minimal PKS genes from Streptomyces. Federation of European Microbiological Societies (FEMS) Microbiology Letters, 180, 1-6.

Mitchell, R. E. and Teh, K. L. (2005) Antibacterial iminopyrrolidines from *Burkholderia plantarii*, a bacterial pathogen of rice. Organic & biomolecular chemistry, 3, 3540-3543.

Molinski, T. F., Dalisay, D. S., Lievens, S. L. and Saludes, J. P. (2009) Drug development from marine natural products. Nature Reviews Drug Discovery, 8, 69-85.

Munro, M. H., Blunt, J. W., Dumdei, E. J., Hickford, S. J., Lill, R. E., Li, S., Battershill, C. N. and Duckworth, A. R. (1999) The discovery and development of marine compounds with pharmaceutical potential. Journal of Biotechnology, 70, 15-25.

Muyzer, G., De Waal, E. C. and Uitterlinden, A. G. (1993) Profiling of complex microbial populations by denaturing gradient gel electrophoresis analysis of polymerase chain reaction-amplified genes coding for 16S rRNA. Applied and Environmental Microbiology, 59, 695-700.

Nagaoka, K., Matsumoto, M., Oono, J., Yokoi, K., Ishizeki, S. and Nakashima, T. (1986) Azinomycins A and B, new antitumor antibiotics. I Producing organism, fermentation, isolation, and characterization. The Journal of Antibiotics, 39, 1527-1532.

Nastrucci, C., Cesario, A. and Russo, P. (2012) Anticancer drug discovery from the marine environment. Recent Patents on Anti-cancer Drug Discovery, 7, 218-232.

Natsume, T., Watanabe, J. i., Tamaoki, S., Fujio, N., Miyasaka, K. and Kobayashi, M. (2000) Characterization of the interaction of TZT-1027, a potent antitumor agent, with tubulin. Japanese Journal of Cancer Research, 91, 737-747.

Naumovski, L. and Junutula, J. R. (2010) Glembatumumab vedotin, a conjugate of an anti-glycoprotein non-metastatic melanoma protein B mAb and monomethyl auristatin E for the treatment of melanoma and breast cancer. Current Opinion in Molecular Therapeutics, 12, 248-257.

Newman, D. J. and Cragg, G. M. (2004) Advanced preclinical and clinical trials of natural products and related compounds from marine sources. Current Medicinal Chemistry, 11, 1693-1713.

Newman, D. J. and Cragg, G. M. (2007) Natural products as sources of new drugs over the last 25 years. Journal of Natural Products, 70, 461-477.

Newman, D. J. and Cragg, G. M. (2012) Natural products as sources of new drugs over the 30 years from 1981 to 2010. Journal of Natural Products, 75, 311-335.

Newman, D. J. and Cragg, G. M. (2014) Marine-sourced anti-cancer and cancer pain control agents in clinical and late preclinical development. Marine Drugs, 12, 255-278.

Newman, D. J., Cragg, G. M. and Snader, K. M. (2000) The influence of natural products upon drug discovery. Natural Product Reports, 17, 215-234.

Newman, D. J., Cragg, G. M. and Snader, K. M. (2003) Natural products as sources of new drugs over the period 1981-2002. Journal of Natural Products, 66, 1022-1037.

Niewerth, D., Jansen, G., Riethoff, L. F., van Meerloo, J., Kale, A. J., Moore, B. S., Assaraf, Y. G., Anderl, J. L., Zweegman, S. and Kaspers, G. J. (2014) Antileukemic activity and mechanism of drug resistance to the marine *Salinispora tropica* proteasome inhibitor salinosporamide A (marizomib). Molecular Pharmacology, 86, 12-19.

Nowak-Thompson, B., Chaney, N., Wing, J. S., Gould, S. J. and Loper, J. E. (1999) Characterization of the pyoluteorin biosynthetic gene cluster of *Pseudomonas fluorescens* Pf-5. Journal of Bacteriology, 181, 2166-2174.

Nowak-Thompson, B., Gould, S. J. and Loper, J. E. (1997) Identification and sequence analysis of the genes encoding a polyketide synthase required for pyoluteorin biosynthesis in *Pseudomonas fluorescens* Pf-5. Gene, 204, 17-24.

Ohlendorf, B., Schulz, D., Erhard, A., Nagel, K. and Imhoff, J. F. (2012) Geranylphenazinediol, an acetylcholinesterase inhibitor produced by a *Streptomyces* species. Journal of Natural Products, 75, 1400-1404.

Otaka, T. and Kaji, A. (1976) Mode of action of bottromycin A2. Release of aminoacyl-or peptidyl-tRNA from ribosomes. Journal of Biological Chemistry, 251, 2299-2306.

Overmann, J. (2008) Green nonsulfur bacteria. eLS.

Overmann, J. and Garcia-Pichel, F. (2013) The phototrophic way of life. *In* The Prokaryotes, 4th Ed., Vol. II (Eds, Rosenberg, E., DeLong, E., Lory, S., Stackebrandt, E. and Thompson, F.) Springer-Verlag Berlin Heidelberg, Berlin Heidelberg, pp. 203-257.

Paddon, C. J. and Keasling, J. D. (2014) Semi-synthetic artemisinin: a model for the use of synthetic biology in pharmaceutical development. Nature Reviews Microbiology, 12, 355-367.

Paterson, I. and Anderson, E. A. (2005) The renaissance of natural products as drug candidates. Science, 310, 451.

Pereira, D. S., Guevara, C. I., Jin, L., Mbong, N., Verlinsky, A., Hsu, S. J., Avina, H., Karki, S., Abad, J. D. and Yang, P. (2015) AGS67E, an anti-CD37 monomethyl auristatin E antibody drug conjugate as a potential therapeutic for B/T-cell malignancies and AML: a new role for CD37 in AML. Molecular Cancer Therapeutics, 1650-1660.

Peters, P., Galinski, E. and Trüper, H. (1990) The biosynthesis of ectoine. Federation of European Microbiological Societies (FEMS) Microbiology Letters, 71, 157-162.

Petrylak, D. P., Smith, D. C., Appleman, L. J., Fleming, M. T., Hussain, A., Dreicer, R., Sartor, A. O., Shore, N. D., Vogelzang, N. J. and Youssoufian, H. (2014) A phase 2 trial of prostate-specific membrane antigen antibody drug conjugate (PSMA ADC) in taxane-refractory metastatic castration-resistant prostate cancer (mCRPC). *In* ASCO Annual Meeting Proceedings, Vol. 32, pp. 5023.

Pfeifer, M., Zheng, B., Erdmann, T., Koeppen, H., McCord, R., Grau, M., Staiger, A., Chai, A., Sandmann, T. and Madle, H. (2015) Anti-CD22 and anti-CD79B antibody drug conjugates are active in different molecular diffuse large B-cell lymphoma subtypes. Leukemia, 1578-1586.

Pfennig, N. (1965) Anreicherungskulturen für rote und grüne Schwefelbakterien. Zb. Bakt., 1. Abt. Orig. Suppl., 1, 503-504.

Pfennig, N. and Trüper, H. G. (1981) Isolation of members of the families Chromatiaceae and Chlorobiaceae. *In* The prokaryotes (Eds, Starr, M., Stolp, H., G., T. H. and Schlegel, H.) Springer-Verlag Berlin Heidelberg, Berlin Heidelberg, pp. 279-289.

Pfennig, N. and Trüper, H. G. (1992) The family Chromatiaceae. *In* The Prokaryotes (Eds, Balows, A., G., T. H., M., D., W., H. and K.-H., S.) Springer Science & Business Media, New York, pp. 3200-3221.

Phillips, A. C., Boghaert, E. R., Vaidya, K. S., Ansell, P. J., Shalinsky, D. R., Zhang, Y., Voorbach, M. J., Mudd, S., Holen, K. D. and Humerickhouse, R. A. (2013) Abstract A250: ABT-414: An anti-EGFR antibody-drug conjugate as a potential therapeutic for the treatment of patients with squamous cell tumors. Molecular Cancer Therapeutics, 12, A250-A250.

Pichersky, E., Noel, J. P. and Dudareva, N. (2006) Biosynthesis of plant volatiles: nature's diversity and ingenuity. Science, 311, 808-811.

Piel, J. (2004) Metabolites from symbiotic bacteria. Natural Product Reports, 21, 519-538.

Pierson, B. K. and Castenholz, R. W. (1974) Studies of pigments and growth in Chloroflexus aurantiacus, a phototrophic filamentous bacterium. Archives Microbiololgy, 100, 283-305.

Poplawsky, A., Urban, S. and Chun, W. (2000) Biological role of xanthomonadin pigments in *Xanthomonas campestris* pv. campestris. Applied and Environmental Microbiology, 66, 5123-5127.

Porter, N. (1913) Webster's revised unabridged dictionary of the English. G. & C. Merriam Company.

Proctor, L. M. (1997) Nitrogen-fixing, photosynthetic, anaerobic bacteria associated with pelagic copepods. Aquatic Microbial Ecology, 12, 105-113.

Raetz, C. R. H. and Whitfield, C. (2002) Lipopolysaccharide endotoxins. Annual Review of Biochemistry, 71, 635-700.

Rajagopal, L., Sundari, C. S., Balasubramanian, D. and Sonti, R. V. (1997) The bacterial pigment xanthomonadin offers protection against photodamage. Federation of European Biochemical Societies (FEBS) Letters, 415, 125-128.

Reid, R. T., Livet, D. H., Faulkner, D. J. and Butler, A. (1993) A siderophore from a marine bacterium with an exceptional ferric ion affinity constant. Nature, 366, 455-458.

Ridley, C. P., Lee, H. Y. and Khosla, C. (2008) Evolution of polyketide synthases in bacteria. Proceedings of the National Academy of Sciences, 105, 4595-4600.

Salomon, C. E., Magarvey, N. A. and Sherman, D. H. (2004) Merging the potential of microbial genetics with biological and chemical diversity: an even brighter future for marine natural product drug discovery. Natural Product Reports, 21, 105-121.

Sattley, W. M. and Madigan, M. T. (2014) The family Heliobacteriaceae. *In* The Prokaryotes (Eds, Rosenberg, E., DeLong, E., Lory, S., Stackebrandt, E. and Thompson, F.) Springer-Verlag Berlin Heidelberg, Berlin Heidelberg, pp. 185-196.

Schatz, A., Bugle, E. and Waksman, S. A. (1944) Streptomycin, a substance exhibiting antibiotic activity against Gram-positive and Gram-negative bacteria.∗†. Experimental Biology and Medicine, 55, 66-69.

Schneemann, I., Kajahn, I., Ohlendorf, B., Zinecker, H., Erhard, A., Nagel, K., Wiese, J. and Imhoff, J. F. (2010) Mayamycin, a cytotoxic polyketide from a Streptomyces strain isolated from the marine sponge Halichondria panicea. Journal of Natural Products, 73, 1309-1312.

Schneemann, I., Wiese, J., Kunz, A. L. and Imhoff, J. F. (2011) Genetic approach for the fast discovery of phenazine producing bacteria. Marine Drugs, 9, 772-789.

Schoenafinger, G. and Marahiel, M. A. (2009) Nonribosomal peptide: biosynthesis. *In* Wiley Encyclopedia of Chemical Biology, Vol. III (Ed, Begley, T. P.) John Wiely & sons, Inc., Hoboken, New Jersey, pp. 432-440.

Schulz, D., Beese, P., Ohlendorf, B., Erhard, A., Zinecker, H., Dorador, C. and Imhoff, J. F. (2011) Abenquines A–D: Aminoquinone derivatives produced by *Streptomyces* sp. strain DB634. The Journal of Antibiotics, 64, 763-768.

Schumann, R. R., Flaggs, G., Gray, P., Wright, S., Mathison, J., Tobias, P. and Ulevitch, R. (1990) Structure and function of lipopolysaccharide binding protein. Science, 249, 1429-1431.

Shah, J. B. (2011) The history of wound care. The Journal of the American College of Certified Wound Specialists, 3, 65-66.

Shen, B. (2000) Biosynthesis of aromatic polyketides. *In* Biosynthesis-Aromatic Polyketides, Isoprenoides, Alkaloides. , Vol. 209 (Eds, Leeper, F. J. and Vederas, J. C.) Springer-Verlag Berlin Heidelberg, Germany, pp. 1-51.

Siegl, A., Kamke, J., Hochmuth, T., Piel, J., Richter, M., Liang, C., Dandekar, T. and Hentschel, U. (2011) Single-cell genomics reveals the lifestyle of Poribacteria, a candidate phylum symbiotically associated with marine sponges. International Society for Microbial Ecology (ISME) 5, 61-70.

Siezen, R. J. and Khayatt, B. I. (2008) Natural products genomics. Microbial Biotechnology, 1, 275-282.

Silber, J., Ohlendorf, B., Labes, A., Erhard, A. and Imhoff, J. F. (2013) Calcarides A-E, antibacterial macrocyclic and linear polyesters from a *Calcarisporium* strain. Marine Drugs, 11, 3309-3323.

Skropeta, D. (2008) Deep-sea natural products. Natural Product Reports, 25, 1131-1166.

Stackebrandt, E. and Goodfellow, M. (1991) Nucleic acid techniques in bacterial systematics, John Wiley & Sons.

Starcevic, A., Zucko, J., Simunkovic, J., Long, P. F., Cullum, J. and Hranueli, D. (2008) ClustScan: an integrated program package for the semi-automatic annotation of modular biosynthetic gene clusters and in silico prediction of novel chemical structures. Nucleic Acids Research, 36, 6882-6892.

Strobel, G. and Daisy, B. (2003) Bioprospecting for microbial endophytes and their natural products. Microbiology and Molecular Biology Reviews, 67, 491-502.

Suzuki, M. T. and Giovannoni, S. J. (1996) Bias caused by template annealing in the amplification of mixtures of 16S rRNA genes by PCR. Applied and Environmental Microbiology, 62, 625-630.

Takano, E., Kinoshita, H., Mersinias, V., Bucca, G., Hotchkiss, G., Nihira, T., Smith, C. P., Bibb, M., Wohlleben, W. and Chater, K. (2005) A bacterial hormone (the SCB1) directly controls the expression of a pathway-specific regulatory gene in the cryptic type I polyketide biosynthetic gene cluster of *Streptomyces coelicolor*. Molecular Microbiology, 56, 465-479.

Tanaka, N., Nishimura, T., Nakamura, S., Umezawa, H. and Hayami, T. (1968) Activity of bottromycin against Mycoplasma gallisepticum. The Journal of Antibiotics, 21, 75-76.

Tank, M. (2010) Ecological and phylogenetic studies on purple sulfur bacteria based on their *puf*LM genes of the photosynthetic reaction center. Kiel University, Dissertation, 2010.

Thiel, V., Tank, M., Neulinger, S. C., Gehrmann, L., Dorador, C. and Imhoff, J. F. (2010) Unique communities of anoxygenic phototrophic bacteria in saline lakes of Salar de Atacama (Chile): evidence for a new phylogenetic lineage of phototrophic Gammaproteobacteria from *puf*LM gene analyses. Federation of European Microbiological Societies (FEMS) Microbiology Ecology, 74, 510-522.

Thimmappa, R., Geisler, K., Louveau, T., O'Maille, P. and Osbourn, A. (2014) Triterpene biosynthesis in plants. Annual Review of Plant Biology, 65, 225-257.

Thompson, J. A., Motzer, R., Molina, A. M., Choueiri, T. K., Heath, E. I., Kollmannsberger, C. K., Redman, B. G., Sangha, R. S., Ernst, D. S. and Pili, R. (2015) Phase I studies of anti-ENPP3 antibody drug conjugates (ADCs) in advanced refractory renal cell carcinomas (RRCC). *In* ASCO Annual Meeting Proceedings, Vol. 33, pp. 2503.

Tonia J. Buchholz, Jeffrey D. Kittendorf and Sherman, D. H. (2009) Polyketide biosynthesis: modular polyketide synthases. *In* Wiely Encyclopedia of Chemical Biology, Vol. III (Ed, Begley, T. P.) John Wiely & Sons, Inc., Hoboken, New Jersey, pp. 746-759.

Tulp, M. and Bohlin, L. (2005) Rediscovery of known natural compounds: nuisance or goldmine? Bioorganic & Medicinal Chemistry, 13, 5274-5282.

Van Gemerden, H. and Mas, J. (1995) Ecology of phototrophic sulfur bacteria. *In* Anoxygenic photosynthetic bacteria (Eds, Blankenship, R. E., Madigan, M. T. and E., B. C.) Springer Netherlands, pp. 49-85.

Villa, F. A. and Gerwick, L. (2010) Marine natural product drug discovery: Leads for treatment of inflammation, cancer, infections, and neurological disorders. Immunopharmacology and Immunotoxicology, 32, 228-237.

Vuorela, P., Leinonen, M., Saikku, P., Tammela, P., Rauha, J.-P., Wennberg, T. and Vuorela, H. (2004) Natural products in the process of finding new drug candidates. Current Medicinal Chemistry, 11, 1375-1389.

Wainwright, M. (1989) Moulds in ancient and more recent medicine. Mycologist, 3, 21-23.

Waisvisz, J., Van Der Hoeven, M., Van Peppen, J. and Zwennis, W. (1957) Bottromycin. I. A new sulfur-containing antibiotic. Journal of the American Chemical Society, 79, 4520-4521.

Waters, A. L., Hill, R. T., Place, A. R. and Hamann, M. T. (2010) The expanding role of marine microbes in pharmaceutical development. Current Opinion in Biotechnology, 21, 780-786.

Wawrik, B., Kerkhof, L., Zylstra, G. J. and Kukor, J. J. (2005) Identification of unique type II polyketide synthase genes in soil. Applied and Environmental Microbiology, 71, 2232-2238.

Weber, T., Blin, K., Duddela, S., Krug, D., Kim, H. U., Bruccoleri, R., Lee, S. Y., Fischbach, M. A., Müller, R., Wohlleben, W., Breitling, R., Takano, E. and Medema, M. H. (2015) AntiSMASH 3.0 - a comprehensive resource for the genome mining of biosynthetic gene clusters. Nucleic Acids Research, 43, W237-W243.

Weber, T. and Marahiel, M. A. (2001) Exploring the domain structure of modular nonribosomal peptide synthetases. Structure, 9, R3-R9.

Webster, M. (2006) Merriam-Webster online dictionary.

Weissgerber, T., Zigann, R., Bruce, D., Chang, Y.-J., Detter, J. C., Han, C., Hauser, L., Jeffries, C. D., Land, M. and Munk, A. C. (2011) Complete genome sequence of *Allochromatium vinosum* DSM 180^{T}. Standards in Genomic Sciences, 5, 311.

Whittaker, R. H. and Likens, G. E. (1975) The biosphere and man. *In* Primary productivity of the biosphere (Eds, H., L. and Whittaker, R. H.) Springer-Verlag Berlin Heidelberg New York Inc., pp. 305-328.

Wiemer, A. J., Hohl, R. J. and Wiemer, D. F. (2009) The intermediate enzymes of isoprenoid metabolism as anticancer targets. Anti-Cancer Agents in Medicinal Chemistry (Formerly Current Medicinal Chemistry-Anti-Cancer Agents), 9, 526-542.

Williams, P. G. (2009) Panning for chemical gold: marine bacteria as a source of new therapeutics. Trends in Biotechnology, 27, 45-52.

Woese, C., Weisburg, W., Paster, B., Hahn, C., Tanner, R., Krieg, N., Koops, H.-P., Harms, H. and Stackebrandt, E. (1984) The phylogeny of purple bacteria: the beta subdivision. Systematic and Applied Microbiology, 5, 327-336.

Woese, C. R. (1987) Bacterial evolution. Microbiological Reviews, 51, 221-271.

Yin, H., Yi, Y., Luo, K., Kuang, C. and Deng, Z. (2004) Identification and biocontrol test of tobacco endophytic bacteria against Ralstonia solanacearum. Chinese Journal of Biological Control, 20, 219-220.

Yurkov, V. V. and Beatty, J. T. (1998) Aerobic anoxygenic phototrophic bacteria. Microbiology and Molecular Biology Reviews, 62, 695-724.

Zeilinger, S., Martín, J.-F. and García-Estrada, C. (2015) Biosynthesis and molecular genetics of fungal secondary metabolites, Springer Science & Business Media, New York.

Zerikly, M. and Challis, G. L. (2009) Strategies for the discovery of new natural products by genome mining. ChemBioChem, 10, 625-633.

Zhang, Q., Yu, Y., Vélasquez, J. E. and van der Donk, W. A. (2012) Evolution of lanthipeptide synthetases. Proceedings of the National Academy of Sciences, 109, 18361-18366.

Zhao, Q., He, Q., Ding, W., Tang, M., Kang, Q., Yu, Y., Deng, W., Zhang, Q., Fang, J. and Tang, G. (2008) Characterization of the azinomycin B biosynthetic gene cluster revealing a different iterative type I polyketide synthase for naphthoate biosynthesis. Chemistry & Biology, 15, 693-705.

8 APPENDIX

Table 8-1. AntiSMSAH results of whole genome sequences of 62 anoxygenic phototrophic bacteria.

Taxnomy	Species	Submitter	BioProject	Length (Mb)	NCBI Reference Sequence	Clusters	Most similar known biosynthetic gene cluster and genes similarity	MIBiG BGC-ID
PSB Chromatiaceae Gamma-proteobacteria	***Allochromatium***							
	A.vinosum DSM 180	JGI	PRJNA46083	3.53	NC_013851.1	Cluster 1=Hserlactone	/	/
						Cluster 2=Other	/	/
						Cluster 3=Terpene	Carotenoid (100%)	BGC0000647_c1
	Marichromatium							
	M. purpuratum 984	JGI	PRJNA72575 PRJNA224116 PRJNA62513	3.78	NZ_CP007031 .1	Cluster 1=Nrps	/	/
						Cluster 2=Nrps	/	/
						Cluster 3=Other	/	/
						Cluster 4=Bacteriocin	/	/
						Cluster 5=Terpene	/	/
	Thiocystis							
	T. biolascens DSM 198	JGI	PRJNA74025 PRJNA60641	5.02	NC_018012.1	Cluster 1=Other	/	/
						Cluster 2=Terpene	/	/
						Cluster 3=Arylpolyene	Xanthomonadin (14%)	BGC0000840_c1
						Cluster 4=Hserlactone	/	/
						Cluster 5=Hserlactone	/	/
	Thioflavicoccus							
	T. mobilis 8321	JGI	PRJNA184343 PRJNA60883	4.05	NC_019940.1	Cluster 1=Bacteriocin	/	/
						Cluster 2=Other-T1pks-Oligosaccaride	/	/
						Cluster 3=Terpene	/	/
						Cluster 4=Terpene	/	/
						Cluster 5=Terpene	Carotenoid (100%)	BGC0000647_c1
PSB Ectothiorhodospiracea Gamma-proteobacteria	***Halorhodospira***							
	H. halophile SL1	JGI	PRJNA58473, PRJNA15767	2.68 nt	NC_008789.1	Cluster 1=Other	/	/
						Cluster 2=Terpene	/	/
						Cluster 3=Terpene	/	/
						Cluster 4=Ectoine	Ectoine (66%)	BGC0000852_c1
						Cluster 5=Terpene	/	/

PNSB Alpha-proteobacteria	***Rhodospirillum***							
	R. centenum SW	TGen	PRJNA58805 PRJNA18307	4.36 nt	NC_011420.2	Cluster 1=Terpene	/	/
						Cluster 2=T3pks	/	/
						Cluster 3=Terpene	/	/
	R. rubrum ATCC11170	JGI	PRJNA57655 PRJNA58	4.35 nt	NC_007643.1	Cluster 1=Terpene	Malleobactin (11%)	BGC0000386_c1
						Cluster 2=Terpene	/	/
						Cluster 3=Lassopeptide	/	/
						Cluster 4=Bacteriocin	/	/
						Cluster 5=Terpene	/	/
						Cluster 6=Lassopeptide	/	/
						Cluster 7=Nrps	/	/
						Cluster 8=Hserlactone	/	/
	R. rubrum F11	Gonzaga University	PRJNA162149 PRJNA67413	4.35	NC_017584.1	Cluster 1=Terpene	/	/
						Cluster 2=Terpene	/	/
						Cluster 3=Lassopeptide	/	/
						Cluster 4=Lassopeptide	/	/
						Cluster 5=Bacteriocin	/	/
						Cluster 6=Lassopeptide	/	/
						Cluster 7=Terpene	/	/
						Cluster 8=Lassopeptide	/	/
						Cluster 9=Nrps	/	/
						Cluster 10=Hserlactone	/	/
	R. photometricum DSM122	CNRS	PRJEA81611, 159003	3.88	NC_017059.1	Cluster 1=Terpene	/	/
						Cluster 2=Terpene	Carotenoid (100%)	BGC0000647_c1
						Cluster 3=Hserlactone	/	/
	Rhodobacter							
	R. capsulatus SB1003	Univ. Chicago	PRJNA47509, PRJNA55	3.74	NC_014034.1	Cluster 1=Hserlactone	/	/
						Cluster 2=Terpene	/	/
						Cluster 3=Hserlactone	/	/
	R. sphaeroides 2.4.1	JGI	PRJNA57653, PRJNA56	3.19	NC_007493.2	Cluster 1=Lassopeptide	/	/
						Cluster 2=Terpene	/	/
						Cluster 3=Hserlactone	Streptomycin (2%)	BGC0000717_c1
						Cluster 4=T3pks	/	/
						Cluster 5=Terpene	/	/
	R. sphaeroides ATCC 17025	JGI	PRJNA58451, PRJNA15755	3.22	NC_009428.1	Cluster 1=Terpene		
						Cluster 2=Hserlactone		
						Cluster 3=Hserlactone		

						Cluster 4=Lassopeptide		
						Cluster 5=Terpene		
	R. sphaeroides ATCC 17029	JGI	PRJNA58449, PRJNA15754	3.15	NC_009049.1	Cluster 1=Lassopeptide	/	/
						Cluster 2=Terpene	/	/
						Cluster 3=Hserlactone	Streptomycin (2%)	BGC0000717_c1
						Cluster 4=T3pks	/	/
						Cluster 5=Terpene	/	/
	R. sphaeroides KD131	GenoTech corp.	PRJNA59277, PRJNA31111	4.71	NC_011960.1	No	/	/
	Rhodomicrobium							
	R. vannielii ATCC 17100	JGI	PRJNA38253, 43247	4.01	NC_014664.1	Cluster 1=Terpene - T3pks	Carotenoid (66%)	BGC0000641_c1
						Cluster 2=Bacteriocin	/	/
						Cluster 3=Terpene	/	/
						Cluster 4=Hserlactone	/	/
						Cluster 5=Terpene	Malleobactin (7%)	BGC0000386_c1
						Cluster 6=Other	/	/
	Rhodopseudomonas							
	R. palustris CGA009	JGI	PRJNA62901 PRJNA57	5.46	NC_005296.1	Cluster 1=Hserlactone	/	/
						Cluster 2=Terpene	/	/
						Cluster 3=Siderophore	/	/
						Cluster 4=Terpene	/	/
						Cluster 5=Nrps-T1pks	/	/
						Cluster 6=Terpene	Malleobactin (7%)	BGC0000386_c1
	R. palustris DX-1	JGI	PRJNA43327, PRJNA38503	5.40	NC_014834.1	Cluster 1=Hserlactone	Bottromycin A2 (6%)	BGC0000469_c1
						Cluster 2=Hserlactone	/	/
						Cluster 3=Terpene	Hopene (15%)	BGC0000663_c1
						Cluster 4=Nrps-T1pks	/	/
						Cluster 5=Hserlactone	Lipopolysaccharide (16%)	BGC0000772_c1
						Cluster 6=Terpene	/	/
						Cluster 7=Siderophore	/	/
						Cluster 8=Terpene	/	/
	R. palustris HaA2	JGI	PRJNA58439, PRJNA15747	5.33	NC_007778.1	Cluster 1=Hserlactone	/	/
						Cluster 2=Terpene	Hopene (15%)	BGC0000663_c1
						Cluster 3=Terpene	/	/
						Cluster 4=Hserlactone	/	/

						Cluster 5=Terpene	/	/
						Cluster 6=Siderophore	/	/
	R. palustris BisB5	JGI	PRJNA58441, PRJNA15749	4.89	NC_007958.1	Cluster 1=Hserlactone	/	/
						Cluster 2=Hserlactone	/	/
						Cluster 3=Terpene	Malleobactin (7%)	BGC0000386_c1
						Cluster 4=Terpene	/	/
						Cluster 5=Terpene	/	/
	R. palustris BisB18	JGI	PRJNA58443, PRJNA15750	5.51	NC_007925.1	Cluster 1=Hserlactone	/	/
						Cluster 2=Terpene	/	/
						Cluster 3=Terpene	Hopene (15%)	BGC0000663_c1
						Cluster 4=Hserlactone-Nrps	/	/
						Cluster 5=Terpene	/	/
						Cluster 6=Nrps-T1pks	Pyoluteorin (15%)	BGC0000128_c1
						Cluster 7=Nrps-T1pks	/	/
						Cluster 8=Phosphonate	/	/
	R. palustris BisA53	JGI.	PRJNA58445, PRJNA15751	5.51	NC_008435.1	Cluster 1=Terpene	/	/
						Cluster 2=Terpene	Hopene (15%)	BGC0000663_c1
						Cluster 3=Bacteriocin	/	/
						Cluster 4=Hserlactone	/	/
						Cluster 5=Terpene	/	/
						Cluster 6=Terpene	/	/
	R. palustris TIE-1	JGI	PRJNA58995, PRJNA20167	5.74	NC_011004.1	Cluster 1=Hserlactone	/	/
						Cluster 2=Terpene	/	/
						Cluster 3=Hserlactone	/	/
						Cluster 4=Siderophore	/	/
						Cluster 5=Terpene	/	/
						Cluster 6=Nrps-T1pks	/	/
						Cluster 7=Terpene	Malleobactin (7%)	BGC0000386_c1
PNSB Beta-proteobacteria	***Rubrivivax***							
	R. gelatinosus IL144	National Institute of Technology and Evaluation NBRC 100245	PRJNA158163, PRJNA62703	5.04	NC_017075.1	Cluster 1=Lassopeptide	Rubrivinodin (80%)	BGC0000576_c1
						Cluster 2=Lantipeptide	/	/
						Cluster 3=Terpene	/	/
						Cluster 4=T1pks-Other	Azinomycin B (4%)	BGC0000960_c1
						Cluster 5=Terpene	/	/
						Cluster 6=Bacteriocin	/	/

GSB Chlorobiaceae	***Chlorobium***							
	C. phaeovibrioides DSM 265	JGI	PRJNA12607 PRJNA58129	1.97	NC_009337.1	Cluster 1=Terpene	/	/
	C. phaeobacteroides DSM 266	JGI	PRJNA58133, PRJNA12609	3.13	NC_008639.1	Cluster 1=Bacteriocin	/	/
						Cluster 2=Nrps	/	/
						Cluster 3=Terpene	/	/
						Cluster 4=Butyrolactone	/	/
	C. limicola DSM 245	JGI	PRJNA12606, 58127	2.76	NC_010803.1	Cluster 1=Butyrolactone	/	/
						Cluster 2=Terpene	/	/
						Cluster 3=Bacteriocin	/	/
	C. tepidum TLS	TIGR	PRJNA57897, PRJNA302	2.15	NC_002932.3	Cluster 1=Butyrolactone	/	/
						Cluster 2=Terpene	/	/
	C. chlorochromatii CaD3	JGI	PRJNA13921, 58375	2.57	NC_007514.1	Cluster 1=Terpene	/	/
	C. luteolum DSM 273	JGI	PRJNA13012, 58175	2.36	NC_007512.1	Cluster 1=Bacteriocin	/	/
						Cluster 2 =Terpene	/	/
	C. phaeobacteroides BS1	JGI	PRJNA58131, PRJNA12608	2.74	NC_010831.1	Cluster 1=Bacteriocin	/	/
						Cluster 2=Bacteriocin	/	/
						Cluster 3=Bacteriocin	/	/
						Cluster 4=Butyrolactone	/	/
						Cluster 5=Terpene	/	/
						Cluster 6=Bacteriocin	/	/
						Cluster 7=Bacteriocin	/	/
	Chloroherpeton							
	C. thalassium ATCC35110	JGI	PRJNA29215, 59187	3.29	NC_011026.1	Cluster 1=Terpene	/	/
						Cluster 2=Bacteriocin	/	/
	Pelodictyon**							
	P. phaeoclathratiforme BU-1	JGI	PRJNA13011, 58173	3.02	NC_011060.1	Cluster 1=Terpene	/	/
						Cluster 2=Bacteriocin	/	/
	Prosthecochloris							
	P. aestuarii DSM 271	JGI	PRJNA12749, 58151	2.51	NC_011059.1	Cluster 1=Bacteriocin	/	/
						Cluster 2=Bacteriocin	/	/
						Cluster 3=Bacteriocin	/	/
						Cluster 4 =Terpene	/	/
	Chlorobaculum ***							
	C. parvum NCIB 8327	JGI	PRJNA29213,	2.29	NC_011027.1	Cluster 1=Terpene	/	/

			59185			Cluster 2=Butyrolactone	/	/
						Cluster 3=Bacteriocin	/	/
	Chloroflexus							
	C.aggregans DSM 9485	JGI	PRJNA16708, 58621	4.68	NC_011831.1	Cluster 1=Terpene	/	/
						Cluster 2=Terpene	/	/
	Chloroflexus. sp. Y-400-fl	JGI	PRJNA59085, PRJNA21119	5.27	NC_012032.1	Cluster 1=Terpene	/	/
						Cluster 2=Terpene	/	/
	C. aurantiacus J-10-f1	JGI	PRJNA57657 PRJNA59	5.26	NC_010175.1	Cluster 1=Terpene	/	/
						Cluster 2=Terpene	/	/
GNSB Chloro-flexaceae	***Roseiflexus****							
	R. castenholzii DSM 13941	JGI	PRJNA13462, 58287	5.72	NC_009767.1	Cluster 1=Terpene	/	/
						Cluster 2=Terpene	/	/
						Cluster 3=Terpene	/	/
						Cluster 4=Other	/	/
	Roseiflexus RS-1	JGI	PRJNA58523, PRJNA16190	5.80	NC_009523.1	Cluster 1=Terpene	/	/
						Cluster 2=Terpene	/	/
						Cluster 3=Other	/	/
						Cluster 4=Terpene	/	/
Helio-bacteria	***Heliobacterium***							
	H. modesticaldum Ice1	Arizona State University	PRJNA13427, 58279	3.08	NC_010337.2	Cluster 1=T3pks	/	/

JGI= US DOE Joint Genome Institute; **t1pks=**Type I PKS cluster; **t2pks=**Type II PKS cluster; **t3pks=**Type III PKS cluster; **otherks=**Other types of PKS cluster; **arylpolyene**=Aryl polyene cluster; **resorcinol=**Resorcinol cluster; **ladderane=**Ladderane cluster; **PUFA=**Polyunsaturated fatty acid cluster; **nrps=**Nonribosomal peptide synthetase cluster**; terpene=Terpene**cluster**; lantipeptide=**Lanthipeptide cluster**; bacteriocin=**Bacteriocin or other unspecified ribosomally synthesized and post-translationally modified peptide product (RiPP) cluster**; lassopeptide=**Lassopeptide cluster**; bottromycin=**Bottromycin cluster**; siderophore=**Siderophore cluster**; ectoine=**Ectoine cluster**; butyrolactone=**Butyrolactone cluster**; indole=**Indole cluster**; oligosaccharide=**Oligosaccharide cluster**; hserlactone=**Homoserine lactone cluster**; phosphonate=**Phosphonate cluster**; other=**Cluster containing a secondary metabolite-related protein that does not fit into any other category

Poster in ISPP conference, Tübingen, 2015

New antibiotic compound produced from the anoxygenic phototrophic sulfur bacterium *Allochromatium vinosum*. MT86.

Min Sun[1], Jutta Wiese[1], Marcus Tank[2], Johannes F. Imhoff[1]

1 GEOMAR Helmholtz-Zentrum für Ozeanforschung, 24105 Kiel, Germany 2 The Pennsylvania State University, University Park 16802, PA, United States

Key words: anoxygenic phototrophic bacteria (APB), *Allochromatium* sp., bioactive compound

Background

In certain aquatic environments, anoxygenic phototrophic bacteria are important primary producers. Strain MT86 was isolated from coastal sediments of the Indian Ocean. Phylogenetic analyses revealed the type strain *Allochromatium vinosum* DSM 180^T to be the closest relative. *Allochromatium vinosum* MT86 is an anoxygenic phototrophic sulfur bacterium. As far as known this is the first report on the production of bioactive compounds by purple sulfur bacteria.

Methods

45 L of modified Pfennig medium with 0.67% salts was prepared and strain MT86 was incubated for 10 days at 28°C and 1000 lux. After centrifugation, the supernatant of the culture broth was extracted by ethyl acetate (1:1). HPLC-DAD/MS, semi-preparative HPLC, and NMR analyses were used for fractionation and compound identification, respectively. Antibiotic activities were determined with the crude extract, the fractions, and isolated compounds.

Results & Discussion

In this study, we discovered the new bioactive compound F13 from *A. vinosum* MT86. 5.2 mg of pure compound was obtained. The m/z of F13 is 300 corresponds to the molecular formula $C_{20}H_{28}O_2$. From the NMR chromatography, the structure was obtained. IC_{50} values for F13 against *Bacillus subtilis,* and *Staphylococcus lentus* were 70.5 µM (± 2.9) and 57.0 µM (± 3.3), respectively. Compound F13 is the first antibiotic substance isolated from phototrophic bacteria. Chemical structure and biological activities are presented.

Reference

Imhoff J.F., Hiraishi A., and Süling J. (2005). Anoxygenic Phototrophic Purple Bacteria. *Bergey's Manual of Systematic Bacteriology (2nd Edition)*, Vol. 2 (Part 2): pp. 119-132.

9 ACKNOWLEDGEMENTS

I would like to give my deepest appreciation and heartfelt respect to my supervisor Prof. Dr. Johannes F. Imhoff for giving me so many advices and patient guidance during my doctoral study. I cannot express how lucky I am getting the chance to continue scientific research in my life. Under the supervisor of Prof. Imhoff, he gave all efforts to help me get the scholarship and help me face to the difficulties. Without his untiring encouragement and sincere trust, I cannot image how I could come here now and grow up so fast.

I especially thank Dr. Jutta Wiese, who gave me the most useful suggestions and valuable guidance on my research work and my personal life in Kiel, a wonderful city.

I am very grateful to Bettina, who gave me a huge hug when the first time I arrived at Kiel and helped me adapt the first step of life in Germany and prepare many essential documents for me.

I want to thank all MI-FB3 members, including the previous and present workers. I appreciate the time stay with all of you in GEOMAR.

Many thanks to Dr. Vera Thiel and Dr. Marcus Tank, who paved the way of phototrophic bacteria strains for me. I would like to appreciate Dr. Mien Pham. We shared one office room for three years and we had a great time helping each other in scientific career and personal life.

Many thanks to Regine, Katrin, Tanja, Maren, Arlette, Susann, Jan, Dr. R. Schmaljohann, Dr. A. Labes, Dr. J. Silber, Dr. A. Kramer, and Dr. N. Jansen for new ideas of culture preparation, processes of experimental equipment, chemical analysis and so on. Thank other Ph.D. students, Apurva, Alvaro, and Ignacio, for good communication and scientific ideas sharing.

I sincerely thank Dr. Cristina Dorador and the members of her team for offering me a wonderful experience in Antofagasta University in Chile about the molecular work and fieldwork in the amazing desert. Thank Dr. Bin Wu from Zhejiang University, who helped me understand the chemical analysis and push the process of my chemical work. Moreover, thanks to Prof. Dr. Alex Zeeck, I obtained the structure of the precious target compound.

I am full of gratitude to my parents who financially and emotionally supported me so much not only during Ph.D. work, but also during my master life in Shanghai. Without their understanding and support, I cannot pursue my scientific career over the past eight years. I love all my family members especially Xiaobai and my dear uncle.

Thanks to Dr. Hui Zhang, I got two years CSC scholarship from China.

I would like to thank my friends Wolf Sun, Ivy Yang, Min Geng, Jirong Wang, Yao Zhang, Zizi, Circle Wei, Dr. Linwei Li, Dr. Peng Huang, Dr. Qiang Shi and Dr. Teng Huang Dr. Li Wang in all over the world. Even I am so far from them in different countries, I still feel the best friendship and support without reservation in my life forever.

Thanks to Shasha, Dr. Si Li, I had a wonderful time in 2015. Thank all my friends in Kiel.